

## Nutrients release and melanoidins formation during thermal hydrolysis of waste activated sludge and implications in downstream processes

Pavez Jara, J.A.

**DOI**

[10.4233/uuid:ea925fae-be33-4f62-a5c8-a1ca4d520456](https://doi.org/10.4233/uuid:ea925fae-be33-4f62-a5c8-a1ca4d520456)

**Publication date**

2024

**Document Version**

Final published version

**Citation (APA)**

Pavez Jara, J. A. (2024). *Nutrients release and melanoidins formation during thermal hydrolysis of waste activated sludge and implications in downstream processes*. [Dissertation (TU Delft), Delft University of Technology]. <https://doi.org/10.4233/uuid:ea925fae-be33-4f62-a5c8-a1ca4d520456>

**Important note**

To cite this publication, please use the final published version (if applicable).  
Please check the document version above.

**Copyright**

Other than for strictly personal use, it is not permitted to download, forward or distribute the text or part of it, without the consent of the author(s) and/or copyright holder(s), unless the work is under an open content license such as Creative Commons.

**Takedown policy**

Please contact us and provide details if you believe this document breaches copyrights.  
We will remove access to the work immediately and investigate your claim.

**Nutrients release and melanoidins formation during thermal hydrolysis of waste activated sludge  
and implications in downstream processes**

**Javier Andrés Pavez Jara**



**Nutrients release and formation of melanoidins during thermal hydrolysis of waste activated sludge, and implications in downstream processes**

**DISSERTATION**

For the purpose of obtaining the degree of doctor

at Delft University of Technology

by the authority of the Rector Magnificus Prof.dr.ir. T.H.J.J. van der Hagen

chair of the Board for Doctorates

to be defended publicly on

Wednesday 08 May 2024 at 10:00 o'clock

by

**Javier Andrés PAVEZ JARA**

Master of Science in Engineering Science in Biotechnology,

Universidad de La Frontera, Chile

Born in Lautaro, Chile

**This dissertation has been approved by the promotor.**

***Composition of the doctoral committee:***

Rector Magnificus,	chairperson
Prof.dr.ir. M. K. de Kreuk	Delft University of Technology, promotor
Prof.dr.ir. J. B. van Lier	Delft University of Technology, promotor

***Independent Members***

Prof.dr. H. Carrere	INRAE, France
Prof.dr.ir. R. Dewil	KU Leuven, Belgium
Prof.dr. D.A Jeison Nuñez	PUCV, Chile
Prof.dr. A. Soares	Cranfield University, UK
Prof.dr.ir. W. de Jong	Delft University of Technology
Prof.dr. D. Brdjanovic	Delft University of Technology/IHE Delft, reserve member

The research presented in this thesis was performed at the Sanitary Section, Department of Water Management, Faculty of Civil Engineering and Geosciences, Delft University of Technology, The Netherlands. The research was financially supported by ANID PFCHA/DOCEXT 72170548, TU Delft, STOWA, Paques BV, Water Authorities from The Netherlands (Waterschap de Dommel, Waterschap Vechtstromen, Waterschap Vallei en Veluwe and Waterschap Limburg).

*To all those who contributed in one way or another to making this book possible.*

## Table of contents

1. Chapter 1. General introduction .....	13
1.1. Introduction .....	14
1.2. Effects of THP on WAS characteristics.....	17
1.3. THP use and implications on AD.....	29
1.4. Effect of THP on the downstream processes after AD .....	38
1.5. Research aims and thesis outline.....	43
1.6. List of abbreviations.....	45
1.7. References .....	46
2. Chapter 2. Accumulating ammoniacal nitrogen instead of melanoidins determines the anaerobic digestibility of thermally hydrolysed waste-activated sludge. ....	59
2.1. Introduction .....	61
2.2. Materials and methods .....	64
2.3. Results and discussion.....	72
2.4. Conclusions .....	84
2.5. List of abbreviations.....	85
2.6. References .....	87
2.7. Appendix chapter 2 .....	92
3. Chapter 3. Increased solubilisation of multivalent cations decreases soluble orthophosphate concentration during anaerobic digestion of thermally hydrolysed bio-P waste-activated sludge.....	97
3.1. Introduction .....	99
3.2. Materials and methods .....	101
3.3. Results and discussion.....	106
3.4. Concussions.....	115
3.5. List of abbreviations.....	116
3.6. References .....	117

4. Chapter 4. Role of the composition of humic substances formed during thermal hydrolysis process on struvite precipitation in reject water from anaerobic digestion .....	123
4.1. Introduction .....	125
4.2. Materials and methods .....	128
4.3. Results and discussion.....	132
4.4. Conclusions .....	147
4.1. List of abbreviations.....	148
4.2. References .....	149
4.3. Appendix chapter 4 .....	154
5. Chapter 5. Effects of thermal hydrolysis process-generated melanoidins on partial nitrification/anammox in full-scale installations treating waste activated sludge. ....	159
5.1. Introduction .....	161
5.2. Methodology .....	164
5.3. Results and discussion.....	170
5.4. Conclusions .....	186
5.5. List of abbreviations.....	187
5.6. References .....	189
5.7. Appendix chapter 5 .....	194
6. Chapter 6. Outlook and perspectives. ....	203
6.1. Side reactions during THP of WAS .....	204
6.2. AD (semi-)recalcitrant melanoidins formation and total ammoniacal nitrogen (TAN) release during THP.....	204
6.3. Release and precipitation of nutrients during THP and AD.....	206
6.4. Effects of different humic substances released during THP on struvite precipitation	206
6.5. Effects of the increased TAN concentrations and melanoidins on the PN/A process	208
6.6. Effect on the WWTPs final effluent quality.....	209



6.7.	Overall conclusions .....	210
6.8.	Recommendations .....	210
6.9.	List of abbreviations.....	212
6.10.	References .....	213
7.	Acknowledgements .....	217
8.	About the applicant.....	220
9.	List of publications .....	221

## Summary

This thesis research investigated the dynamics of nutrient release and the formation of melanoidins during thermal hydrolysis processes (THP) of waste activated sludge (WAS) preceding mesophilic anaerobic digestion (AD). In Chapter 2, a fractionation of THP-sludge allowed for researching the distribution of nutrients and melanoidins over the liquid and solid fraction of the sludge matrix during AD. The soluble melanoidins formed during THP were found to be partially biodegradable during subsequent AD, particularly those with a molecular weight under 1.1 kDa, associated with protein-like substances. In addition, total ammoniacal nitrogen (TAN) concentrations exhibited a modest increase during THP, but a substantial increase was observed during AD, negatively impacting acetotrophic methanogenesis.

In Chapter 3, the influence of THP on  $\text{PO}_4^{3-}\text{-P}$  release and precipitation during AD is described. The dynamics in soluble  $\text{PO}_4^{3-}\text{-P}$  concentrations were most pronounced in WAS from enhanced biological phosphorus removal (EBPR) plants. The results indicated an increment in TAN and  $\text{PO}_4^{3-}\text{-P}$  release with THP temperature, while varying soluble concentrations were observed during AD. Full-scale samples provided insights into the precipitation of multivalent cations with  $\text{PO}_4^{3-}\text{-P}$ . The results showed that precipitation reactions during AD governed the concentration of soluble nutrients during THP-AD.

In this thesis, also the impact of THP on downstream processes was researched, particularly reject water treatment after AD. The research focused on the potential consequences of elevated concentrations of humic substances (HSs) and nutrients in the reject water from digestate dewatering. In Chapter 4, research is described on the effects of THP pre-treatment on the struvite precipitation efficiency, considering the chemical characteristics of HSs. Batch experiments revealed the influence of melanoidins and humic acids on struvite precipitation at different pH levels. The intrinsic characteristics of HSs emerged as critical factors affecting struvite yield, morphology, and colour of the formed precipitates.

In Chapter 5, six full-scale partial nitrification and anammox (PN/A) influents and effluents were sampled, with four wastewater treatment plants (WWTPs) using THP and two without. Characterization of the samples revealed that THP increased concentrations of TAN, and aromatic organics, which is an indication of melanoidins occurrence. Additionally, THP decreased stoichiometric  $\text{NO}_3^- \text{-N}$  concentrations in effluents from the PN/A reactors. This study also emphasizes the importance of considering increased  $\text{O}_2$  consumption and possible

limited trace element availability during PN/A process operation, when utilizing THP-AD to optimize overall system performance.

In summary, the results of this thesis provide an understanding of the interactions and consequences of THP in full-scale scenarios, focusing on the dynamics in nutrient release and the effects of melanoidins formation, in THP, AD, and downstream processes for nutrient removal (PN/A and struvite precipitation).





**1.**

**General introduction**

## 1.1. Introduction

Anaerobic digestion (AD) is a process that stabilizes organic compounds in absence of oxygen by utilizing these same organics as a source and sink of electrons. AD's main end-products are biogas, a mixture of the most reduced and most oxidised form of carbon, i.e., CH<sub>4</sub>, CO<sub>2</sub>, as well as trace gases and microbial biomass (Appels et al., 2011; Kelleher et al., 2002). The biogas can be upgraded and used as a source of energy, owing to its high percentage of CH<sub>4</sub> (Qian et al., 2017; Stürmer, 2017; Zhang et al., 2016a). Additionally, the digestate produced during AD can be used as a soil conditioner/fertilizer (Bratina et al., 2016; Sahlström, 2003; Weiland, 2010), landfilled or incinerated (Dou et al., 2017), depending on the presence of heavy metals, microbial activity, pathogens, and local legislation.

AD has been widely adopted and integrated into society over the past century, with numerous full-scale plants currently operational worldwide (Sawatdeenarunat et al., 2015). In Europe, the REPowerEU plan, launched in May 2022, has set a target of producing 35 billion cubic meters (bcm) of bio-CH<sub>4</sub> per year by 2030. Figure 1.1 shows the combined biomethane and biogas production in Europe in the last few years. To achieve the 2030 target of 35 bcm, the Biomethane Industrial Partnership has been initiated (BIP-europe, 2023). Among other objectives, the BIP-Europe partnership aims to establish the conditions for setting higher targets by 2050.

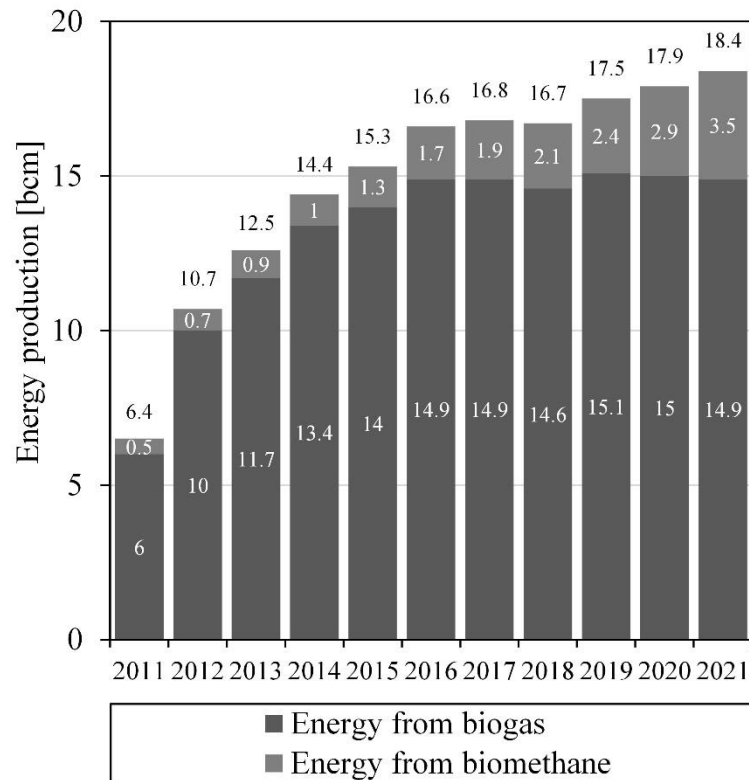


**Figure 1.1.** Combined bio CH<sub>4</sub> and biogas production in Europe in the decade 2011-2021. Adapted from (Association, 2022)

Wide-spread and important applications of AD can be observed in municipal wastewater treatment plants (WWTPs), where it serves as a technology for reducing, stabilizing, and recovering energy from primary and secondary sludges, generated during sewage treatment (Appels et al., 2008). The handling and management of these sludges are fundamental concerns for modern WWTPs and can account from approximately 19-50% of the total costs of sewage treatment (Ozgun et al., 2021; Pastore et al., 2013; Scrinzi et al., 2023). The production of biogas is likely to increase along with the production of sludge, which exceeded 7.5 million tons (in dry basis) in the 27 EU Member States in 2019 (Ronda et al., 2023).

Due to the continuous increase in sludge production, research efforts have focused on strategies that enhance the conversion of organics into CH<sub>4</sub> and thus minimize ultimate sludge disposal (Semblante et al., 2014). The bioconversion of organic matter into biogas involves four steps, i.e., hydrolysis of particulates, acidogenesis, acetogenesis, and methanogenesis (Appels et al., 2008). These processes occur in parallel and in series, and the overall conversion rate in the AD process is governed by the slowest step, known as the rate-limiting step. Hydrolysis of particulate matter and complex polymers into soluble substrates is considered the rate-limiting



step in AD of sewage sludge (Dohányos et al., 1997; Eastman and Ferguson, 1981; Pavlostathis, 1991). To enhance the hydrolysis rate and to improve the bioconversion of organics into biogas, various amendments to the conventional AD process have been developed, including pre-treatments of waste activated sludge (WAS), process operation under thermophilic regimes, sequential AD, separation of hydraulic retention time (HRT) and solids retention time (SRT), among others (Gonzalez et al., 2022; Neumann et al., 2016). Various pre-treatment methods for WAS prior to AD have been developed at laboratory scale, which include mechanical, thermal, chemical, biological, or integrated approaches (Zhen et al., 2017). Figure 1.2 shows the location of pre-treatment in a conventional WWTP scheme.

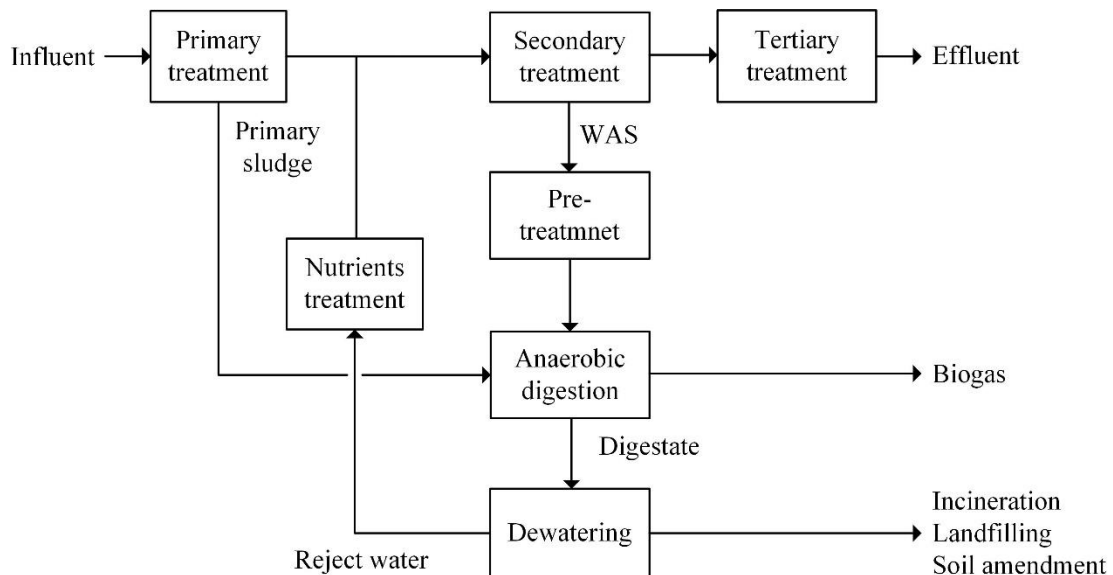


**Figure 1.2.** Schematic set-up of a WWTP including WAS pre-treatment and AD (modified from Cano et al. (2015)).

## 1.2. Effects of THP on WAS characteristics.

The composition of WAS can be influenced by various operational parameters, seasonal variations, and the chemical properties of the organic substrates present during secondary treatment. However, regardless of these factors, WAS primarily consists of microbial cells which are composed of specific organic compounds. These compounds are either structural components e.g., cell walls, or EPS matrix, or are involved in metabolic processes e.g., cytoplasmic material. The organic fraction of WAS is primarily composed of proteins, humic substances, carbohydrates, uronic acids, and nucleic acids (mainly DNA) (Mottet et al., 2010; Wilén et al., 2003). In addition, ashes, which account for approximately 30% of WAS, originate from all (earth)-alkali metals present in the biomass (Hupka et al., 2002). Table 1.1 shows an overview of the composition of WAS.

During the thermal hydrolysis process (THP), the composition of WAS undergoes changes, and certain constituents may undergo chemical transformations due to exposure to high temperatures. For instance, physical changes, such as protein denaturation or solubilization are well documented (Barber, 2016; Farno et al., 2014).

**Table 1.1.** Composition of activated sludge from a municipal WWTP.

Component	Amount in WAS	Reference
Volatile suspended solids	71-80% of TSS	(Wilén et al., 2003)
Ashes	20-29% of TSS	
Proteins	224-353 mg/g TSS	
Humic Substances	111-191 mg/g TSS	
Carbohydrates	61-93 mg/g TSS	
Uronic acids	3.4-6.2 mg/g TSS	
Nucleic acids (mainly DNA)	15-28 mg/g TSS	
Lipids	0-5 mg/g TSS *	(Mottet et al., 2010)

\*Considering VS/TS=64% and TSS/TS=90%

Table 1.1 shows that the organic fraction of WAS primarily consists of proteins, humic substances, and carbohydrates, which are largely biodegradable and can be converted into biogas during AD. However, during THP, the organic constituents present in WAS are released into the liquid phase and may undergo chemical interactions, leading to the formation of new products. These interactions are influenced by the operational conditions during THP, such as

temperature, pressure, pH, reaction time, amongst others. The subsequent section elaborates on the modifications observed in the constituents of WAS during THP.

### **1.2.1. Humic substances (HSs)**

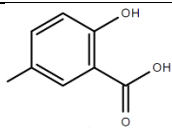
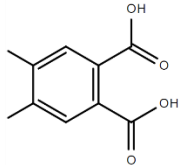
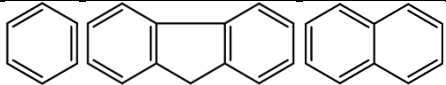


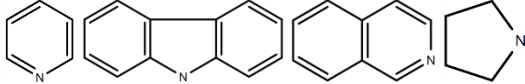
HSs are complex organic compounds, and there is no single worldwide accepted definition or formula for HSs, which are widely spread across our planet (Sutton and Sposito, 2005). According to Stevenson (1994), HSs can be defined as “a series of relatively high molecular weight, brown to black coloured substances, formed by secondary synthesis reactions”. Additionally, Aiken (1985) defines HSs as “a general category of naturally occurring, biogenic, heterogeneous organic substances that can be characterized as being yellow to black in colour, of high molecular weight, and refractory”. Both definitions highlight that HSs are coloured, heterogeneous, high molecular weight (MW) compounds that are refractory, but they do not specify their origin.

The heterogeneity of HSs results in an unclear molecular structure, and therefore, they can only be characterized based on physicochemical properties such as light absorbance, MW, colour, aromaticity, (low) biodegradability, pH dependent solubility, and others.

HSs can be classified into three main categories: humic acids (HAs), fulvic acids (FAs), and humins, based on their solubility in acid-alkali conditions, typically determined by passing through a 0.45  $\mu\text{m}$  filter (Klavins et al., 1999). HAs are the fractions of HSs that are soluble under alkaline and mildly acidic conditions but insoluble at pH lower than 2. Conventionally, the HA fraction comprises molecules with MW between 1.5-5 kDa in water streams and 50-500 kDa in soils. FAs, on the other hand, are soluble at any pH and have MW ranging from 0.6-1 kDa in water streams and 1-5 kDa in soils. Humins represent the insoluble portion of HSs under all pH values (McDonald et al., 2004; Sutton and Sposito, 2005).

Although the pH-solubility-based classification provides insights into the solubility of HSs, it does not classify them based on their moieties and functional groups present in their structure, which potentially can interact during AD. HSs are formed by the condensation of building blocks and functional groups. Table 1.2 shows the building blocks that constitute HSs. The interactions of HSs with the surrounding medium depend on their structure, leading to a wide range of possibilities based on characteristics such as functional groups, aromaticity, hydrophobicity, molecular weight, and others.

**Table 1.2.** Main functional groups found in HSs including functional groups and building blocks (Klavins et al., 1999).

Constituents in the HS	
Loosely bound substances.	
<ul style="list-style-type: none"> <li>• Metal ions chelated to inorganic particulate materials; low molecular weight organic substances.</li> </ul>	
Functional groups	
<ul style="list-style-type: none"> <li>• R-COOH (Carboxyl groups).</li> <li>• R-OH (Hydroxyl groups).</li> <li>• R&gt;C=O (Carbonyl groups).</li> <li>• R-O-R (Ether groups).</li> <li>• R-O-CH<sub>3</sub> (Methoxyl groups).</li> <li>• R-CH<sub>3</sub> (Methyl groups).</li> <li>• R-C≡N (Cyano groups).</li> <li>• R-SH, R-SO<sub>3</sub>H (Sulphur containing groups).</li> <li>• R-NH<sub>2</sub>, R&gt;N-R' (Amino groups).</li> </ul>	
Major molecular structures present in the moieties of HSs	
Pentoses and hexoses	Carbohydrates
-CH <sub>2</sub> -CH <sub>2</sub> -, -CH=CH-, -CH <sub>2</sub> -NH <sub>2</sub>	Aliphatic structures
	Phenols, phenolcarboxylic acids
	Benzene-carboxylic acids
	Aromatic and polyaromatic structures
	Quinones
	Oxygen-containing heterocycles
	Nitrogen-containing heterocycles

	Sulphur containing heterocycles
---	---------------------------------

HSs are widely recognized for their effectiveness as soil amendments due to their ability to slowly release nutrients, high cation exchange capacity, and interaction with micro-nutritive and micro-toxic chemicals, such as micronutrients and xenobiotics (Kobyas and Gengec, 2012; Senesi et al., 1996). The chelation of cations by HSs, including melanoidins, is attributed to the presence of negatively charged moieties in their structure (Hedges, 1978; Kobyas and Gengec, 2012; Morales et al., 2012). HSs can chelate various cations, including  $\text{Fe}^{2+}$ ,  $\text{Fe}^{3+}$ ,  $\text{Al}^{3+}$ ,  $\text{Cu}^{2+}$ ,  $\text{Cr}^{3+}$ ,  $\text{Fe}^{3+}$ ,  $\text{Zn}^{2+}$ ,  $\text{Pb}^{2+}$ , and others (Anita Rani and Nater Pal, 2013; Migo et al., 1997; Tagliazucchi et al., 2010). HSs can also bind cations and chelate  $\text{PO}_4^{3-}$  in solution, forming organo-metallic compounds (Sinha, 1971). However, the origin of HSs and the specific cations involved play a significant role in their complexing capacity. Generally, cations with higher oxidation states have stronger interactions with HSs, such as  $\text{Al}^{3+}$  or  $\text{Fe}^{3+}$ , interacting more strongly than alkaline earth metals, such as  $\text{Ca}^{2+}$  or  $\text{Mg}^{2+}$ , and monovalent cations, such as  $\text{Na}^+$  or  $\text{K}^+$ . For divalent cations, the cation binding capacity of HSs typically follows the Irving–Williams series, which is independent of the ligand (Irving and Williams, 1948; Irving and Williams, 1953; Miličević et al., 2011).

On the one hand, the complexation of metals by humic substances may have a negative impact on the nutrients' treatment removal efficiencies, because the HSs-chelated nutrients are less accessible for removal. On the other hand, in countries where AD digestate is utilized in agricultural fields, the HSs produced during THP can have positive effects contributing to soil amendment. HSs can increase soil stability (Piccolo and Mbagwu, 1990), provide benefits in plant physiology (Trevisan et al., 2010) and can adsorb pollutants and heavy metals (Cattani et al., 2009; Celano et al., 2008; Luo and Gu, 2009; Martin-Neto et al., 2001; Tan and Binger, 1986; Wang and Mulligan, 2009). Table 1.3 shows some properties of HSs and their effects on the soil.

**Table 1.3.** General characteristics of HSs and associated effects in the soil (modified from Stevenson (1994)).

Characteristic	Remarks	Effect on soil
----------------	---------	----------------

Colour	The typical dark colour of many soils is caused by organic matter.	May facilitate warming
Water retaining capacity	Organic matter can hold up to 20 times its weight in water.	Help prevent drying and shrinking. Improves moisture-retaining properties of sandy soils
Interacts with clay minerals	Cements soil particles into structural units called aggregates.	Permits exchange of gasses and stabilizes structure
Chelating properties	Forms stable complexes with $\text{Cu}^{2+}$ , $\text{Mn}^{2+}$ , $\text{Zn}^{2+}$ , and others polyvalent cations.	Increases the availability of micronutrients to higher plants
Limited solubility in water	Insolubility of organic matter is due to its association with clay. Also, salts of divalent and trivalent cations with organic matter are insoluble.	Little organic matter is lost by leaching.
pH buffering capacity	Exhibits buffering capacity in slightly acid, neutral, and alkaline pH ranges.	Helps to maintain a uniform reaction conditions in the soil.
Cation exchange capacity	Total acidities of isolated fractions of humus range from 300 to 1400 cmoles/kg .	Increases cation exchange capacity (CEC) of the soil. Humic matter contributes from 20 to 70% to the CEC of many soils.
Limitedly biodegradable	Decomposition of organic matter yields $\text{CO}_2$ , $\text{NH}_4^+$ , $\text{NO}_3^-$ , $\text{PO}_4^{3+}$ , and $\text{SO}_4^{2-}$ .	Source of nutrients for plant growth.*
Interacts with xenobiotics	Affects bioactivity, persistence, and biodegradability of pesticides	Modifies application rate of pesticides for effective control.

---

\* Measured as [sum of  $\text{COOH}$  + acidic (phenolic)  $\text{OH}$ ] Schnitzer, M. and Gupta, U.C. 1965. Determination of Acidity in Soil Organic Matter. Soil Science Society of America Journal 29(3), 274-277.

### 1.2.2. Melanoidins

Melanoidins are a particular type of HSs formed during THP due to the reaction of reducing sugars and proteins presents in WAS. Melanoidins are a group of high molecular weight, dark-coloured, and recalcitrant compounds formed as end products of the Maillard reactions (Arimi et al., 2015; Satori and Kawase, 2014). The Maillard reactions were first described by Louis C. Maillard in 1912 and play a crucial role in the food industry as they can modify the sensory and nutritional properties of food products. The Maillard reaction is propitiated by aldoses, in which the carbonyl group is able to react with the amine group present in amino-compounds such as an amino acids. This initial reaction triggers the formation of a series of intermediate steps ending in the formation of various types of compounds.

The formation of melanoidins involves seven different types of reactions divided into three steps, as depicted in Figure 1.4 (Hodge, 1953):

I Initial stage: in this stage there is no colour appearing, and there is no near UV absorption by the reactants or products.

i) Sugar-amine condensation: this concerns the reaction between the carbonyl group present in aldoses and the amine group present in nitrogenated compounds, resulting in the formation of an N-substituted glycosylamine.

ii) Amadori rearrangement: in this step, the N-substituted glycosyl-amine rearranges to form a 1-amino-1-deoxy-2-ketose and is catalysed by an acidic medium. Despite the formed products may undergo browning in an alkaline medium in the presence of amino compounds.

II Intermediate stage: this stage is characterized by a colourless or yellowish reaction matrix, with strong absorption in the near UV region due to the formation of aromatic rings.

iii) Sugar dehydration: depending on the pH of the medium, two reaction pathways can be distinguished. In an acidic medium, furfural and hydroxymethylfurfural are produced, while in the presence of amines and in a dry state or non-aqueous solvents, 6-carbon reductones are formed.

iv) Sugar fragmentation: this reaction occurs through dealdolisation, where amino products can catalyse the reaction into trioses and other fission products.

v) Amino acids degradation: the so-called Strecker degradation (Schonberg and Moubacher, 1952) converts  $\alpha$ -amino acids to an aldehyde, releasing one carbon as  $\text{CO}_2$ .

III Final stage: in this stage a dark colour is appearing.

vii) Aldol condensation: Enols with a carbonyl group react to form a  $\beta$ -hydroxy aldehyde or  $\beta$ -hydroxy ketone, sometimes followed by the loss of one molecule of water. Amino compounds catalyse this reaction.

vii) Aldehyde-amine polymerisation: the aldehydes and moieties from the previously described processes react and increase their molecular size, leading to the formation of heterocyclic nitrogenated compounds known as melanoidins, a group of polyheterocyclic highly coloured and refractory molecules.

Figure 1.3 shows the pathways described above, starting from aldoses and amino compounds present in WAS and culminating in the formation of melanoidins. It is important to note that the term "melanoidins" refers to a group of compounds that exhibit similar behaviour and does not represent the behaviour of a single compound.



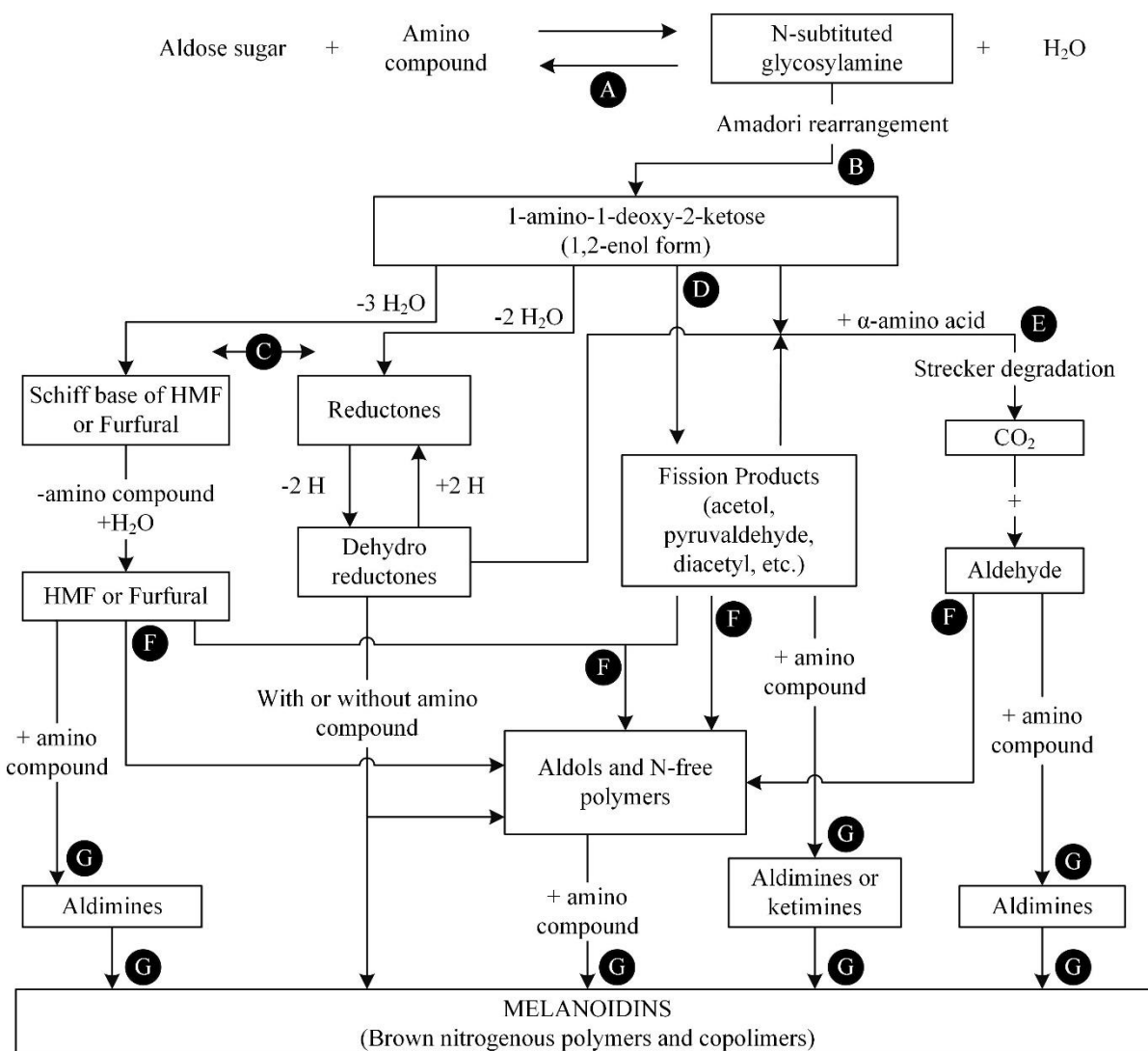


**Figure 1.3.** Formation of melanoidins based on the Maillard reactions and the subsequent interactions between the products formed (adapted from (Hodge, 1953)).

As mentioned previously, the structural composition of WAS primarily consists of proteins and carbohydrates, making the occurrence of the Maillard reaction likely during THP of WAS. The Maillard reactions can be influenced by various parameters, such as pH, temperature, the presence of heavy metals, and sulphur compounds (sulphites and mercaptans) (Erbaş et al., 2012; Ma et al., 2017; Martins and Van Boekel, 2005; Mohsin et al., 2018; Ramonaityte et al., 2009).

Inhibiting the Maillard reactions by modifying operational parameters is an interesting approach to prevent the formation of melanoidins. However, the addition of chemicals may not be economically feasible on a full-scale basis due to their costs and possible environmental impact. To the best knowledge of the authors, reducing the THP temperature and reaction time

appears to be a feasible method to decrease melanoidin formation. Dwyer (2008) demonstrated that reducing the THP temperature by 20°C (from 160°C to 140°C) resulted in a reduction in melanoidins formation without compromising the overall biodegradability of WAS. However, further research is needed to develop full-scale technologies for inhibiting Maillard reactions.

### **1.2.3. Caramelisation reactions**

Caramelization is a term used to describe a group of reactions that cause non-enzymatic browning of carbohydrates when exposed to high temperature. The main difference between caramelization and the Maillard reaction is the presence of amine groups in the Maillard reaction producing N-containing melanoidins (Quintas et al., 2007). Since caramelization reactions do not involve amino groups, the resulting aromatic compounds do not contain organic nitrogen in their structure. Caramelization of carbohydrates can be divided into two steps: depolymerization of complex carbohydrates (Ciesielski et al., 1997) and decomposition of monosaccharides leading to the formation of HMF (hydroxymethylfurfural) and other degradation products (Gurgel et al., 2012; Pilath et al., 2010). Various parameters can influence carbohydrate decomposition, including temperature, pH, and water content (Ajandouz and Puigserver, 1999; Buera et al., 1987; Wilson and Novak, 2009). Additionally, the decomposition of monosaccharides can be strongly influenced by sugar concentration, temperature, and the presence of metal ions (Lu and Lü, 2009; Yu and Wu, 2011). Moreau et al. (2011) found that the presence of specific ions such as Na<sup>+</sup>, K<sup>+</sup>, Mg<sup>2+</sup> and Ca<sup>2+</sup> in the liquid phase may enhance caramelisation and subsequent browning of starch. Both caramelisation and the Maillard reactions are predominantly temperature-driven (Ajandouz et al., 2008). However, since some intermediates, such as furfural or HMF, are common to both reactions, it is difficult to attribute the end products solely to one particular reaction.

Both caramelization and the Maillard reaction produce aromatic, coloured, highly polymerized compounds that absorb UV light (Ajandouz et al., 2001; Hrynets et al., 2015; Nagai et al., 2018). Wilson and Novak (2009) found that cellulose and starch can be hydrolysed to mono and disaccharides at 220 °C. Sugars degradation was confirmed by Pineda-Gómez et al. (2014) who found that starch decomposition begins at temperatures above 240 °C in a dry medium, and by Shogren (1992), who also observed starch decomposition at 230°C. However, the decomposition of monosaccharides occurs within the same temperature range as the decomposition of polysaccharides, suggesting that both processes likely occur simultaneously. Considering the composition of WAS and the typical temperature range of THP (140-160 °C),

the main contributor to browning during THP is expected to be the Maillard reaction rather than caramelization. Nonetheless, localized high temperatures resulting from poor mixing can lead to local browning due to caramelization reactions during THP.

#### **1.2.4. Lipids hydrolysis**

Lipids found in WAS can originate from two sources: either from the influent of the secondary treatment or they can be produced by the microbial biomass during the secondary treatment process (Chipasa and Mdrzycka, 2008). The fraction of lipids produced by the biomass is associated with microbial growth (phospholipids), release of metabolites, cell lysis products, and lipids adsorbed onto the biomass (Siddiquee and Rohani, 2011). Lipids adsorbed to the biomass come from the influent of the secondary treatment and are associated with colloidal materials that cannot be retained in the primary treatment due to their low density and size. While the lipids content in the analysed wastewater is generally a small fraction of WAS by weight, the low carbon oxidation state in lipids results in a relatively large contribution of lipids to the total chemical oxygen demand (COD) in WAS, i.e. accounting for 30-40% of the total COD (Chipasa and Mędrzycka, 2006).

During THP, both triacylglycerides and long-chain fatty acids (LCFAs) undergo degradation through similar mechanisms. The degradation mechanism for fatty acids involves their peroxidation into volatile fatty acids (VFAs) and other reaction products due to the high temperature and the hydrolytic capacity of water (Brunner, 2009; Farhoosh, 2022). The peroxidation of lipids depends on various factors such as temperature, fatty acid saturation, trace metals, peroxides, oxidized compounds, and the presence of antioxidants (Silvagni et al., 2012; Wilson and Novak, 2009). Lipid peroxidation reactions can result in the production of volatile compounds such as alcohols and free fatty acids, both LCFAs and VFAs (Porter, 1984). LCFAs are partially biodegradable under anaerobic conditions through  $\beta$ -oxidation, which leads to the production of VFAs (Elsamadony et al., 2021; Holohan et al., 2022; Rinzema et al., 1994). Unless the VFA concentrations reach inhibitory levels, they are biodegradable under anaerobic conditions, resulting in the production of biogas (Holohan et al., 2022; Stafford, 1982; Wang et al., 1999)

#### **1.2.5. Proteins deamination and total ammoniacal nitrogen (TAN) release**

The degradation of proteins and the subsequent release of TAN have been identified as major factors contributing to the inhibition of AD when THP is employed (Barber, 2016; Chen et al.,

2008; Pavez-Jara et al., 2023). Proteins are biopolymers composed of amino acid chains, and their structure undergoes denaturation and deamination with increasing temperature (He et al., 2015; Mulvihill and Donovan, 1987). Denaturation of proteins occurs in a wide range of temperatures depending on the protein structure (Bischof and He, 2006; Sohn, 1996). It is expected that after THP, most proteins in WAS lose their biological activity since the majority irreversibly denatures at temperatures above 100°C (Matsuura et al., 2015).

. Once WAS surpasses the denaturation temperature during THP, the primary structure may breakdown with the subsequent release of free amino acids, VFAs, and TAN as by-products through deamination (Somero, 1995; Wilson and Novak, 2009). Deamination caused solely by the temperature increase has been observed during hydrothermal processes (Sato et al., 2004; Toor et al., 2011). Moreover, the increased TAN concentration can also raise the costs of centrate deammonification processes, as they are dependent on the TAN concentration that needs to be removed (Bowden et al., 2016). Furthermore, the degradation of proteins during AD mostly follows the so-called Stickland reactions (Nisman, 1954), to be methanised with the rest of the organic substrates.

#### 1.2.6. Ashes

Ashes are defined by Metcalf et al. (2003) as the non-volatile residue remaining after a sample is burned to a constant weight at 550°C. In the context of WAS, ashes represent the inorganic fraction (Wilén et al., 2003). The composition of WAS ashes may vary depending on the geographical location and the specific treatment methods employed. Chemically, these ashes consist of phosphorous oxides,  $\text{Ca}^{2+}$  oxides,  $\text{Mg}^{2+}$  oxides, sulphates, and various trace elements or heavy metals (Dewil et al., 2007; Hong et al., 2005). In addition, if enhanced biological phosphorus removal (EBPR) is utilized, the ashes of WAS may contain a notable amount of phosphorus (P). Increased P occurs, because phosphate-accumulating organisms (PAOs) in EBPR systems can accumulate up to 12% P on a dry basis, in contrast to the 1%-3% typically found in conventional WAS (Van Loosdrecht et al., 1997). Table 1.4 shows a typical composition of the ashes in WAS.

**Table 1.4.** Composition of ashes in WAS, adapted from Willems et al. (1976))

Component	Concentration
Sand and clay	37-39%

Ca <sup>2+</sup> and Mg <sup>2+</sup> phosphates, CaCO <sub>3</sub> , CaSO <sub>4</sub> , and oxides of Ca <sup>2+</sup> , Al <sup>3+</sup> and Fe <sup>2+/3+</sup> .	23-32%
Zn <sup>2+</sup>	0.9
Cu <sup>+2+</sup>	0.2
Pb	0.1
Cr	0.07
Ni	0.02
Cd	0.006

\*Also, Ar, Co and Hg were found to be present in low concentrations.

During THP the disruption of cells and subsequent release of cytoplasmic contents result in the solubilization of the inorganic fraction into the bulk liquid. Cations released during THP interact with the solubilized organic matter, particularly with HSs and melanoidins, forming complexes. The interaction between cations such as Fe<sup>2+/3+</sup> and Al<sup>3+</sup> with HSs has been well documented, and these cations can also complex PO<sub>4</sub><sup>3-</sup> ions (Bedrock et al., 1997; Levesque and Schnitzer, 1967; Weir and Soper, 1963). Furthermore, the increased release of PO<sub>4</sub><sup>3-</sup> due to EBPR use and cations can promote the precipitation of minerals based on PO<sub>4</sub><sup>3-</sup> such as amorphous Ca-P, hydroxyapatite, and struvite during AD (Langerak et al., 1999; Soler-Cabezas et al., 2018). Uncontrolled precipitation can even lead to additional maintenance costs due to pipe and anaerobic reactor incrustation (Barat et al., 2009; Parsons and Doyle, 2004).

### 1.3. THP use and implications on AD

THP was initially developed in the 1940s as a sludge conditioning technology, operating at temperatures ranging from 180-220°C (Øegaard, 2004). In the 1970s, research focused on improving sludge dewaterability to reduce disposal costs (Everett, 1972; Haug, 1977; Haug et al., 1983). Currently, many countries require AD digestate to meet the "EPA class A" standard, which necessitates low pathogen and microbial activity levels. Consequently, THP has become a tool to achieve this goal (Lukicheva et al., 2009; Pérez-Elvira and Fdz-Polanco, 2012; Pérez-Elvira et al., 2008). Furthermore, THP has facilitated a reduction in HRT in AD reactors, increasing treatment capacity.

THP combines two effects to enhance sludge biodegradability and dewaterability. Firstly, it exposes the sludge to high temperatures and pressure for a defined period, altering the chemical structure and breaking down complex molecules. Secondly, a rapid decompression stage causes the cellular content in the sludge to explode, releasing the cytoplasmic material (Donoso-Bravo et al., 2011). This phenomenon, known as "steam explosion," occurs when the overheated intracellular liquid transforms into steam due to a sudden decrease in pressure, significantly increasing its volume and thus cell breakage.

Researchers have extensively investigated the implications of THP on AD, focusing primarily on CH<sub>4</sub> production, organic compound solubilization, and increased nutrient release. Numerous studies have aimed to optimize the process for maximizing CH<sub>4</sub> production. Most of these studies agree that a pre-treatment temperature range of approximately 160-180°C and a duration of 20-40 minutes yields the highest CH<sub>4</sub> production (Bougrier et al., 2006; Fdz-Polanco, 2008; Sapkaite et al., 2017; Stuckey and McCarty, 1984). Temperature has been identified as the primary parameter driving the process, with inadequate hydrolysis observed below the optimal temperature range and excessive formation of recalcitrant or inhibitory compounds observed at higher temperatures. Despite its limitations, THP has proven to be a reliable technique, significantly improving sludge dewaterability, increasing CH<sub>4</sub> production, and reducing the organic solids content in the digestate (Cano et al., 2015).

Several THP technologies are commercially available at an industrial scale. Table 1.5 provides a comparison of these technologies and their key features.

**Table 1.5.** Comparison among most common THP pre-treatment technologies used at full-scale.

Brand name	Amount treated	Number of installations	Main THP parameters			Reference
			Time	Temperature	Regime	
Cambi® (Cambi)	1.426.400 (tDS/year) 1.570.471 (US tons/year)	62	Above 30 min	150-180°C	Batch	(Armstrong et al., 2017; AS, 2017)
Biothelys® (Veolia)	80.800 (tDS/year)	7	30 min	165°C	Batch	(Veolia, 2017a)
Exelys® (Veolia)	30.446 (tDS/year)	3	30 min approx.	165°C	Continuous	(Veolia, 2017b; c)
THP® (Fraunhofer UMSICHT)	30.000-40.000 (ton/year)	2	Not available	Above 200°C	Not specified	(UMSICHT, 2013)
LysoTherm® (ELIQUO STULZ)	3.500 (kg DS/d) 1.277,5(tDS/year)	2	30-60min	150-175°C	Continuous	(GMBH, 2015a; b)
Turbotec® (Sustec B.V.)	20.000 tDS/year (full-scale plants)	6 Pilot plants + 2 full scale	30-70min	140-175°C	Continuous	(B.V., 2015; 2017)

As shown in Table 1.5, CAMBI® (Norway) leads the market. However, other companies offer products with diverse configurations to cater to specific customer demands. Additionally, Table 1.1 indicates that all full-scale processes operate within the optimal range mentioned earlier (temperature: 160-180°C and time: 20-40 minutes). Manufacturers also report a significant level of hydrolysis, a 30-50% increase in biogas production, and the formation of refractory materials without compromising CH<sub>4</sub> production.

Numerous authors have investigated the formation of refractory compounds in THP, but a clear consensus regarding their origin and nature has not yet been reached. Table 1.6 provides a summary of studies that highlight the inhibition of AD resulting from THP treatments and the most plausible explanations for this phenomenon.

**Table 1.6:** Comparison of inhibition of AD in different studies and the causes of it, in THP pre-treatments.

Possible inhibitor	Pre-treatment conditions	Substrate	Effect	Reference
HMF and Furfural (in HCl + autoclaving) High lignin solubilisation (in NaOH + autoclaving)	121°C for 60 min. HCl + 121°C for 60 min. NaOH + 121 °C for 60 min.	Wheat straw and sugarcane bagasse.	Inactivity or death of the anaerobic inoculum with all three heating strategies	(Bolado-Rodríguez et al., 2016)
Compounds produced by Maillard reactions	70°C for 60 min 133°C and 3 bars for 20 min.	Poultry and piggery slaughterhouse wastes.	Increase in soluble COD without an increase in BMP in sludge with a high percentage of carbohydrates.	(Rodríguez-Abalde et al., 2011)
Possible formation of inhibitory substances.	100-225°C and 0-120 min., no steam explosion.	Primary sludge, activated sludge and blend of both.	Reduction in methane production at pre-treatment over 175°C	(Haug et al., 1978)
Possible production of	150-225°C for 60 min	WAS, N-based compounds	Reduced bio-convertibility to	(Stuckey and



melanoidins and humic acids.	150-225°C for 60 min + NaOH. Mesophilic and thermophilic digestion regimes were tested.	mixture and pure carbohydrates.	CH <sub>4</sub> of individual N-based compounds under identical treatment conditions.	McCarty, 1984)
Possible formation of inhibitory substances. (expressed as refractory compounds).	62-175°C for 15-120 min.	WAS.	Low digestibility of proteins* and decreased methane production over 170°C.	(Li and Noike, 1992)
Refractory compounds formed by polymerization.	130-170°C and 60 min KOH and Fenton reagent dosage	WAS.	No increment in biodegradability over 170°C.	(Valo et al., 2004)
Possible production of melanoidins.	130-180°C for 5–50 min and decompression mode (slow or steam-explosion effect).	WAS.	Increase in soluble COD without an increase in BMP over 163°C.	(Sapkaite et al., 2017)
Possible formation of inhibitory substances. (Probably	120-180°C for 15-180 min.	Dewatered/high solid sludge	Increase in soluble COD, with poor degradability, and decrease in	(Xue et al., 2015)

because of the production of melanoidins)			biogas production.	
Melanoidins	175 °C for 60 min.	Kitchen waste, vegetable/fruit residue, and WAS.	Decrease in anaerobic biodegradability.	(Liu et al., 2012)
Increase in $\text{NH}_4^+$ and non-biodegradable materials that are created by carbohydrate and proteins at high temperature.	100-220°C for 30 min	WAS.	Decrease in methane production over 160-180°C	(Jeong et al., 2016)
De-ammonification of proteins.	130-220°C and two hours	WAS and primary sludge.	Breakdown of proteins over 150 °C	(Wilson and Novak, 2009)
Melanoidins	140-165°C and 30 minutes	WAS.	Increase along with the temperature in colour, UVA 254, dissolved organic carbon, and humic acid-like substances.	(Dwyer et al., 2008)
Maillard reaction products	140°C, pH 12, for 30 min	Soluble part of spent microbial biomass from an industrial plant.	Formation of high-molecular-weight compounds which are involved in the	(Penaud et al., 2000a)

			poor biodegradability and bio-toxicity.	
Possible formation of inhibitory substances., expressed as refractory or inhibitory compounds	120-200°C pH 8-13 for 15-60 min	Spent microbial biomass obtained from an industrial plant	Not increasing in biodegradability with more severe condition of pretreatment (longer time, high temperature and not neutral pH).	(Penaud et al., 2000b)
TAN and free ammoniacal nitrogen (FAN).	160 °C and a treatment time per batch of 30 min	WAS.	Inhibited methanogenic activity.	(Pavez-Jara et al., 2023)

\*Proteins possibly measured as HSs because the used method does not distinguish between those two components.

From Table 1.6 it can be observed that the formation of refractory compounds during THP is reported at different temperatures, process times, and substrates composition. Although numerous studies have demonstrated the presence of compounds that can adversely affect the AD process, the mechanism of inhibition or the fate of these compounds in subsequent steps of water/sludge treatment remains poorly understood.

In addition to the solubilization/formation of recalcitrant organic matter during THP, the solubilization of nutrients after THP also has been reported in the literature (Barber, 2016; Devos et al., 2023; Ekpo et al., 2016). Nutrients, mainly present as TAN and  $\text{PO}_4^{3-}$ , are mineralized end-products of organic matter degradation under anaerobic conditions (Appels et al., 2008; Holm-Nielsen et al., 2009). These nutrients remain in the digestate and reach the dewatering step, where the soluble fraction is retained in the reject water, while the solids are sent to the final sludge disposal location.

The release of  $\text{PO}_4^{3-}$  occurs due to the degradation of phospholipids, nucleic acids, and polyphosphates present in the AD substrates. As previously mentioned, the release of  $\text{PO}_4^{3-}$  is

particularly significant when the WAS originates from facilities using EBPR (Wild et al., 1997), and thus contains PAOs. Also, the release of  $\text{PO}_4^{3-}$  from PAOs during AD can occur through the degradation and release of polyphosphate in the presence of VFA (Flores-Alsina et al., 2016) or via direct release from the cytoplasm. Additionally,  $\text{PO}_4^{3-}$  is a reactive species and can precipitate with cations present in the digestion broth (Latif et al., 2018). These precipitates generated during AD can lead to issues such as pipe clogging or increased maintenance in the AD reactors. Table 1.7 shows precipitates that can be formed during AD of WAS, which can cause operational problems during the process.

**Table 1.7.** Precipitates that are reported to be formed during of after AD.

Precipitation	System	Reference
$\text{Mg}^{2+}$ and $\text{NH}_4^+$ based precipitates (struvite) $\text{Ca}^{2+}$ -based precipitates ( $\text{CaCO}_3$ , $(\text{Ca})_3(\text{PO}_4)_2$ , hydroxyapatite).	Continuous pilot scale reactor fed with EBPR sludge and primary pre-fermented sludge	(Marti et al., 2008)
$\text{Mg}^{2+}$ and $\text{NH}_4^+$ based precipitates (struvite).	Pilot anaerobic reactors fed with primary and secondary sludge under mesophilic conditions.	(Sánchez-Ramírez et al., 2021)
Struvite	Anaerobic sludge from mechanical-biological treatment	(Fricke et al., 2007)
$\text{PO}_4^{3-}$ $\text{Ca}^{2+}$ and $\text{Mg}^{2+}$ precipitates	AD of dried fish sludge	(Estevez et al., 2022)
$\text{Ca}^{2+}$ precipitates	High salinity full-scale inoculum. $\text{Ca}^{2+}$ was added on purpose to assess its effect on the microbial community	(Gagliano et al., 2020)
$\text{PO}_4^{3-}$ $\text{Ca}^{2+}$ and $\text{Mg}^{2+}$ precipitates	Full-scale anaerobic digester processing primary sludge	(Barat et al., 2009)

	and WAS from an EBPR system.	
Struvite ( $\text{MgNH}_4\text{PO}_4$ ), newberyite ( $\text{MgHPO}_4$ ), amorphous calcium phosphate, $\text{CaCO}_3$ and $\text{MgCO}_3$	Supernatant from a UASB digester treating wine distillery waste	(Musvoto et al., 2000)
Mg and Ca-phosphates	Supernatants from manure digestion	(Brown et al., 2018)
Struvite	Precipitates from a full-scale sludge pipes at a municipal WWTP applying EBPR with $\text{Fe}_2(\text{SO}_4)_3$ and $\text{Al}_2(\text{SO}_4)_3$ dosage.	(Kecskéssová et al., 2020)
$\text{CaCO}_3$ and $\text{PO}_4^{3-}$ precipitates	Expanded granular sludge bed reactors with synthetic medium containing $\text{Ca}(\text{OH})_2$ and $\text{KH}_2\text{PO}_4$ .	(Langerak et al., 1999)
Struvite, amorphous $\text{Ca-PO}_4^{3-}$ , and calcite.	Centrates obtained after centrifugation of anaerobically digested sludge and supernatants from the thickener of an AD pilot plant	(Pastor et al., 2010)
Struvite and Ca-phosphates	AD pilot plant fed with pre-fermented primary sludge and WAS from an EBPR pilot-scale.	(Marti et al., 2008)

TAN is typically used as an indicator of ammoniacal nitrogen levels, as the  $\text{NH}_4^+/\text{NH}_3$  ratio can vary depending on factors such as solution pH, temperature, and ionic strength (Astals et al., 2018). TAN is released during AD primarily as a result of protein degradation, as previously mentioned. Once TAN is produced, it cannot be oxidized due to the reducing conditions present

during AD, leading to its accumulation as an end-product. The elevated TAN concentration in the digestate can lead to AD biomass inhibition. TAN and FAN inhibition is pH and temperature-dependent, with FAN being the primary contributor (Jin et al., 2012; Rajagopal et al., 2013; Van Hulle et al., 2010; Van Hulle et al., 2007; Yenigün and Demirel, 2013). TAN, and particularly FAN, can exhibit toxicity during AD. The threshold concentration for TAN inhibition is not clearly defined in the literature due to the adaptive capacity of anaerobic biomass to the increased TAN concentrations (Capson-Tojo et al., 2020). It is typically assumed that the primary AD inhibitor is the non-ionized species, FAN; however, Astals et al. (2018) found that the inhibition caused by both, FAN and  $\text{NH}_4^+$  cannot be isolated.

#### 1.4. Effect of THP on the downstream processes after AD

Following AD, the resulting digestate is subjected to dewatering, commonly performed by decanters, belt presses or other types of mechanical or physicochemical techniques (Tsang and Vesilind, 1990). The resulting solids fraction is transported for incineration, landfilling, or is utilized as a soil amendment, depending on local conditions and regulations. The liquid fraction, known as centrate or reject water, is recycled to the primary or secondary treatment processes. In the Netherlands, the solid fraction is typically incinerated, and therefore, a very low water content is pursued to decrease the transportation and incineration costs (Hao et al., 2020). THP providers claim that their pre-treatment improves the dewaterability of the digestate (Neyens and Baeyens, 2003). Furthermore, according some technology providers THP can also be implemented as an AD post-treatment, which is designed particularly to enhance dewaterability (Cai et al., 2021; Svensson et al., 2018)\*.

The reject water mainly contains nutrients (such as TAN and  $\text{PO}_4^{3-}$ ) and soluble AD-recalcitrant compounds. Various studies have reported an increased nutrients concentration following THP and AD (Carrere et al., 2010), compared to AD alone. The elevated nutrients concentrations in the reject water may have an impact on downstream processes such as partial nitrification and anammox (PN/A) which removes TAN, or struvite precipitation, which removes  $\text{PO}_4^{3-}$  and to a lesser extent TAN.

Struvite precipitation is a chemical process that involves the addition of  $\text{Mg}^{2+}$ -containing salts to a nutrient-rich liquid stream, resulting in the precipitation of  $\text{NH}_4\text{MgPO}_4 \cdot 6\text{H}_2\text{O}$  (struvite) according to Equation 1.1. Once the precipitation is complete, the struvite crystals can be separated from the liquid through sedimentation. Struvite precipitation offers a dual benefit as it removes next to  $\text{PO}_4^{3-}$  also some TAN from the solution, while the generated mineral can be utilized in fertilizer production (Talboys et al., 2016). The driving force behind struvite precipitation is the oversaturation of the reagents (Kofina and Koutsoukos, 2005). The degree of oversaturation is evaluated using the saturation index (SI), which indicates the deviation from equilibrium for the reagents. Equation 1.2 represents the saturation index for struvite, where IAP represents the ion activity product, the brackets represent the activity of each ion in

---

\* The companies Cambi and Veolia have commercial processes of THP of the digestate to mainly enhance dewaterability.

<https://www.cambi.com/what-we-do/equipment/thp-after-anaerobic-digestion/>

<https://www.veoliawatertech.com/en/publications/articles/next-generation-thermal-hydrolysis-process-high-solids-thp>

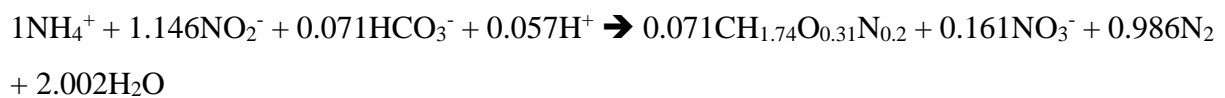
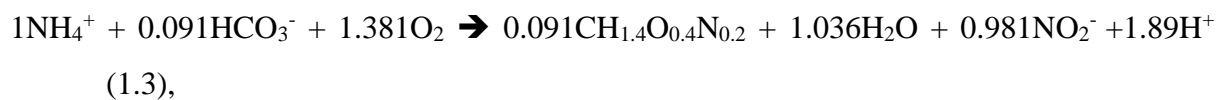
solution, and  $K_{sp}$  represents the solubility product of struvite, which typically ranges from  $3.89 \cdot 10^{-10}$  to  $5.37 \cdot 10^{-14}$  (Hanhoun et al., 2011).



$$\text{SI} = \log_{10} \left( \frac{\text{IAP}}{K_{sp}} \right) = \log_{10} \left( \frac{\{\text{Mg}^{2+}\}\{\text{NH}_4^+\}\{\text{PO}_4^{3-}\}}{K_{sp}} \right) \quad (1.2),$$

Several factors indirectly affect the SI of struvite, including pH (through the speciation of the reagents), reagent concentration, ionic strength, and temperature. Inadequate control of these operational parameters during struvite precipitation can lead to the formation of side precipitates containing phosphorus, such as newberyite ( $\text{MgHPO}_4 \cdot 3\text{H}_2\text{O}$ ), bobierite ( $\text{Mg}_3(\text{PO}_4)_2 \cdot 8\text{H}_2\text{O}$ ) or tri-magnesium phosphate ( $\text{Mg}_3(\text{PO}_4)_2 \cdot 22\text{H}_2\text{O}$ ) (Warmadewanthi and Liu, 2009). Moreover, precise pH control is crucial to induce the precipitation, since the reaction releases protons (Equation 1.1), which may require pH adjustment in certain cases.

As shown in Figure 1.2 nutrient removal before reject water recirculation to the water line, is advantageous for the effluent quality of the treatment plant. The PN/A process has gained interest in recent years due to its cost-effective removal of TAN compared to traditional nitrification-denitrification methods. The PN/A process consumes less oxygen and therefore requires less energy than conventional nitrification-denitrification, and it does not rely on organic matter as external electron donors. As the name suggests, the PN/A process consists of two main reactions: partial nitritation and anammox, as shown in Equations 1.3 and 1.4 (Lotti et al., 2014b). During the partial nitritation reaction,  $\text{NH}_4^+$  is oxidised using  $\text{O}_2$  as final electron acceptor resulting in the production of  $\text{NO}_2^-$ . During the anammox reaction,  $\text{NH}_4^+$  serves as electron donor, and  $\text{NO}_2^-$  acts as the final electron acceptor, producing  $\text{N}_2$  as final product. Once  $\text{N}_2$  reaches the saturation concentration, it is desorbed from the liquid phase and escapes into the atmosphere. Both partial nitritation and anammox utilize inorganic carbon as a carbon source (Lotti et al., 2014b; Strous et al., 1998).



(Modified from Hiet Wong et al. (2003) and Lotti et al. (2014a) (1.4),



In recent years, the PN/A process has been extensively implemented at full scale, particularly in Europe, North America, and Asia (Cao et al., 2017). Although PN/A is a well-established technology widely applied in full-scale operations, its performance can still be influenced by changes in operational conditions and influent composition. The factors that affect PN/A performance can be attributed to either the partial nitrification or anammox reaction. Regardless that in current installation partial nitrification and anammox reactions happen in the same reaction, both reactions need to work in series to ensure efficient nitrogen removal. Therefore, inhibition in one reaction may compromise the N-removal efficiency.

One noticeable effect of using THP is the increased oxygen requirements due to the treatment of reject water with elevated TAN concentrations. It has been well reported that the operational costs of the PN/A process are directly proportional to the TAN concentration. Additionally, the AD-recalcitrant organics present in the reject water may not necessarily exhibit recalcitrance under the anoxic/anaerobic conditions experienced during PN/A and may undergo oxidation reactions. The degradation of THP-produced organics during PN/A also contributes to increased oxygen consumption and can lead to the overgrowth of the anammox and nitrifying biomass by heterotrophic microorganisms. Heterotrophic microorganisms can compete with partial nitrifiers for oxygen at a usually higher growth rate, negatively affecting PN/A performance. Furthermore, the effects of the compounds generated during THP on anammox microorganisms are not yet fully understood. Table 1.8 provides an overview of some of the problems associated with the use of THP followed by PN/A processes as addressed in the literature.

**Table 1.8.** Observed effects of THP on PN/A process.

Factor	Conditions	Reference
The article states that no inhibition was observed. However, conversion rates were not measured and it is not clear how the inhibition was assessed.	Dewatering liquors originated from post THP/AD using three different PN/A systems	(Ochs et al., 2021)
Inhibition on AOB and anammox activity, which was mitigated by long acclimation periods.	Two stages PN/A and bath tests for activities	(Cao et al., 2021)

Very low effects of recalcitrant carbon on maximum specific anammox activity	Batch tests performed with laboratory enriched granular biomass.	(Hong et al., 2022)
Inhibition effect on AOB, potentially caused by particulate and colloidal organics	Sequencing batch reactors were studied treating conventional digestate and THP-AD digestate, respectively	(Zhang et al., 2016b)
Inhibition of THP-AD centrate in batch tests, which was alleviated with ozone oxidation.	THP-AD centrate was generated from a lab-scale anaerobic digester and used in batch experiments and two-step reactors.	(Cao et al., 2022)
Decrease in specific anammox activity.	Lab-scale sequencing batch reactors fed with THP-AD from a full-scale installation.	(Li et al., 2022)
Inhibition caused by flocculent sludge which consisted of suspended solids and heterotrophic bacteria and was characterised by a high conductivity.	Three reactors system, treating lab-produced THP-AD reject water.	(Wang et al., 2022)
Anammox activity was inhibited due to proliferation of heterotrophic microorganisms resulting from presence of biodegradable COD.	One-stage PN/A system for the treatment of reject water from high-solid-sludge THP-AD.	(Cui et al., 2022)
No adverse effects related to the THP-AD process was observed in the anammox reactor.	Lab scale two stages PN/A systems fed with THP-AD dewatering liquor from the municipal WWTP.	(Valenzuela-Heredia et al., 2022)
AOB were directly inhibited by dissolved organics, and indirectly, by particulate and colloidal fractions,	Semi-technical side stream deammonification sequencing batch reactor fed with lab-scale	(Zhang et al., 2018)

causing diffusion limitation of the substrate.	and full-scale produced THP-AD.	
THP pre-treated side stream had inhibitory effects on the activity of anammox bacteria. The inhibition was possibly due to the high carbon content which might have led to growth of heterotrophic bacteria.	Lab scale membrane bioreactors fed wit full-scale THP -AD sludge.	(Gu et al., 2018)

### 1.5. Research aims and thesis outline

To gain a comprehensive understanding of the transformations that occur in WAS during THP and their implications for process performance, it is essential to identify the specific components of WAS and analyse their modifications and interactions throughout the THP-AD process.

During THP and subsequent AD, multiple transformations mentioned earlier can occur simultaneously. However, the unique conditions of each THP-AD process and the specific, localised composition of WAS determine the characteristics of the THP sludge. Moreover, the impact of THP-treated WAS on AD and PN/A processes is influenced by either the products generated during THP, or the intermediates formed during AD. Figure 1.5 presents a schematic representation of the transformations that can take place during the THP process and illustrates the potential interactions among them. This figure highlights the intricate nature of the transformations occurring during THP and the diverse range of products that are likely to be formed throughout the process.

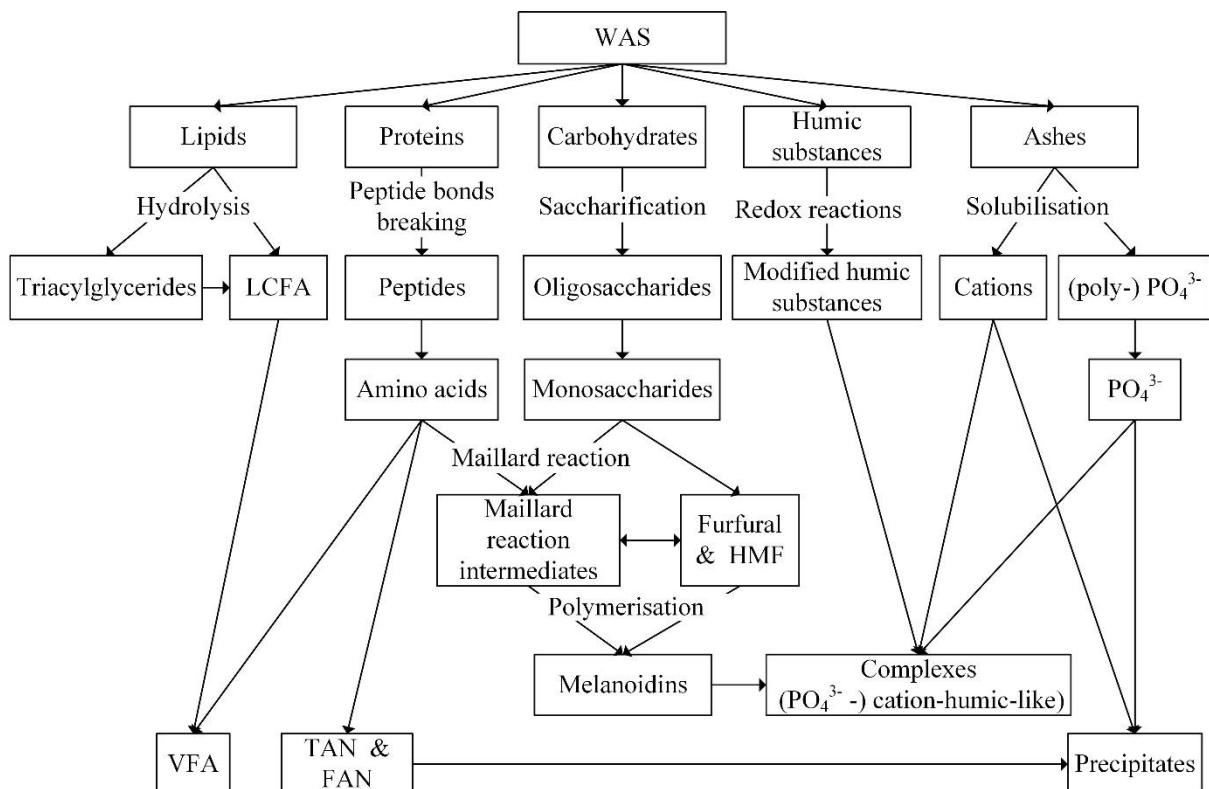


**Figure 1.5.** Interactions during the THP process of WAS.

To the best knowledge of the authors, there is not a comprehensive understanding of all side reactions and transformations suffered by WAS during THP, nor there is understanding of the effects and fate of the formed HSs in subsequent treatment units. Also, the effects of the (additional) nutrients released during THP on AD and subsequent treatment steps needs further research. After this introductory chapter, the thesis will follow the route of potential impacts of THP on subsequent treatment units in a WWTP.

Chapter 2 addressed the formation of recalcitrant compounds and the release of N from the different fractions of THP sludge and WAS. Also, the distribution of melanoidins and N between supernatants and sludge pellets of centrifuged THP sludge was studied and compared to WAS without pre-treatment in order to elucidate the origin and fate of N and melanoidins. An evaluation of the melanoidins' MW, aromaticity, and anaerobic biodegradability was also conducted, to determine their anaerobic biodegradability. In addition, acetoclastic toxicity tests were performed in order to assess the possible inhibition of the THP-generated compounds on methanogenesis.

Chapter 3 assessed the effect of THP on the release of nutrients during AD and the possible precipitation of TAN and  $\text{PO}_4^{3-}\text{-P}$  with metal ions in the AD broth. Also, simulations in PhreeqC were conducted to assess the precipitates formed during AD.

Chapter 4 researched the influence of HSs, including melanoidins and humic acids, on the struvite crystallisation process, evaluating the effects on the yields of precipitated nutrients, and the morphology of the produced crystals. The results were used to build a conceptual model, which considered the influence of particular characteristics of HSs on the struvite precipitation process.

Chapter 5 researched the changes in PN/A influents and effluents as a consequence of the use of THP-AD. Nutrients, organics, and cations are measured and compared in full-scale WWTPs, using either THP or without pre-treatment. Also, stoichiometric calculations were performed to assess the aerobic/anoxic biodegradability of the organics produced in THP using different final electron acceptors. Finally, trace elements complexation assays were conducted to investigate metals availability and possible microbial growth limitations of PN/A reactors in full-scale.

The final chapter addresses the main conclusions of the thesis. Also, perspectives are discussed in order to assess future research lines and the implications of the conducted work.

## **1.6. List of abbreviations**

AD: anaerobic digestion.

COD: chemical oxygen demand.

DS: Dry solids.

EBPR: enhanced biological phosphorus removal.

FAs: fulvic acids.

HAs: humic acids.

HMF: hydroxymethylfurfural.

HRT: hydraulic retention time.

HSs: Humic substances.

LCFAs: long-chain fatty acids.

MW: molecular weight.

PAOs: phosphate-accumulating organisms.

PN/A: partial nitrification and anammox.

SI: saturation index.

SRT: solids retention time.

TAN: total ammoniacal nitrogen.

THP: thermal hydrolysis process.

VFAs: volatile fatty acids.

WAS: waste activated sludge.

WWTPs: municipal wastewater treatment plants.

## 1.7. References

- Aiken, M. (1985) *Humic Substances In Soil, Sediment And Water*, New York.
- Ajandouz, E.H., Desseaux, V., Tazi, S. and Puigserver, A. 2008. Effects of temperature and pH on the kinetics of caramelisation, protein cross-linking and Maillard reactions in aqueous model systems. *Food Chemistry* 107(3), 1244-1252.
- Ajandouz, E.H. and Puigserver, A. 1999. Nonenzymatic browning reaction of essential amino acids: Effect of pH on caramelization and Maillard reaction kinetics. *Journal of Agricultural and Food Chemistry* 47(5), 1786-1793.
- Ajandouz, E.H., Tchiakpe, L.S., Ore, F.D., Benajiba, A. and Puigserver, A. 2001. Effects of pH on Caramelization and Maillard Reaction Kinetics in Fructose-Lysine Model Systems. *Journal of Food Science* 66(7), 926-931.
- Anita Rani, S. and Nater Pal, S. (2013) *Biodegradation of Hazardous and Special Products*. Rolando, C. and Francisca, R. (eds), p. Ch. 5, IntechOpen, Rijeka.
- Appels, L., Baeyens, J., Degrève, J. and Dewil, R. 2008. Principles and potential of the anaerobic digestion of waste-activated sludge. *Progress in Energy and Combustion Science* 34(6), 755-781.
- Appels, L., Lauwers, J., Degrève, J., Helsen, L., Lievens, B., Willems, K., Van Impe, J. and Dewil, R. 2011. Anaerobic digestion in global bio-energy production: Potential and research challenges. *Renewable and Sustainable Energy Reviews* 15(9), 4295-4301.
- Arimi, M.M., Zhang, Y., Götz, G. and Geißen, S.-U. 2015. Treatment of melanoidin wastewater by anaerobic digestion and coagulation. *Environmental Technology* 36(19), 2410-2418.
- Armstrong, D.L., Rice, C.P., Ramirez, M. and Torrents, A. 2017. Influence of thermal hydrolysis-anaerobic digestion treatment of wastewater solids on concentrations of triclosan, triclocarban, and their transformation products in biosolids. *Chemosphere* 171, 609-616.
- AS, C.G. 2017 CAMBI Web Page.
- Association, E.B. 2022 EBA Statistical Report 2022. Association, E.B. (ed), European Biogas Association, Brussels
- Astals, S., Peces, M., Batstone, D.J., Jensen, P.D. and Tait, S. 2018. Characterising and modelling free ammonia and ammonium inhibition in anaerobic systems. *Water Research* 143, 127-135.
- B.V., S. 2015 TurboTec® The cost effective Continuous Thermal Hydrolysis Process (cTHP).
- B.V., S. 2017 Sustec B.V. Sustainable technologies for a circular economy.
- Barat, R., Bouzas, A., Martí, N., Ferrer, J. and Seco, A. 2009. Precipitation assessment in wastewater treatment plants operated for biological nutrient removal: A case study in Murcia, Spain. *Journal of Environmental Management* 90(2), 850-857.
- Barber, W. 2016. Thermal hydrolysis for sewage treatment: A critical review. *Water research* 104, 53-71.
- Bedrock, C.N., Cheshire, M.V. and Shand, C.A. 1997. The involvement of iron and aluminum in the bonding of phosphorus to soil humic acid. *Communications in Soil Science and Plant Analysis* 28(11-12), 961-971.
- BIP-europe 2023 BIP europe, BIP-europe.
- Bischof, J.C. and He, X. 2006. Thermal Stability of Proteins. *Annals of the New York Academy of Sciences* 1066(1), 12-33.
- Bolado-Rodríguez, S., Toquero, C., Martín-Juárez, J., Travaini, R. and García-Encina, P.A. 2016. Effect of thermal, acid, alkaline and alkaline-peroxide pretreatments on the

- biochemical methane potential and kinetics of the anaerobic digestion of wheat straw and sugarcane bagasse. *Bioresource technology* 201, 182-190.
- Bougrier, C., Delgenès, J.P. and Carrère, H. 2006. Combination of Thermal Treatments and Anaerobic Digestion to Reduce Sewage Sludge Quantity and Improve Biogas Yield. *Process Safety and Environmental Protection* 84(4), 280-284.
- Bowden, G., Tsuchihashi, R. and Stensel, H.D. (2016) *Technologies for Sidestream Nitrogen Removal*, IWA Publishing.
- Bratina, B., Šorgo, A., Kramberger, J., Ajdnik, U., Zemljič, L.F., Ekart, J. and Šafarič, R. 2016. From municipal/industrial wastewater sludge and FOG to fertilizer: A proposal for economic sustainable sludge management. *Journal of Environmental Management* 183, Part 3, 1009-1025.
- Brown, K., Harrison, J. and Bowers, K. 2018. Struvite Precipitation from Anaerobically Digested Dairy Manure. *Water, Air, & Soil Pollution* 229(7), 217.
- Brunner, G. 2009. Near critical and supercritical water. Part I. Hydrolytic and hydrothermal processes. *The Journal of Supercritical Fluids* 47(3), 373-381.
- Buera, M.d.P., Chirife, J., Resnik, S.L. and Lozano, R.D. 1987. Nonenzymatic Browning in Liquid Model Systems of High Water Activity: Kinetics of Color Changes due to Caramelization of Various Single Sugars. *Journal of Food Science* 52(4), 1059-1062.
- Cai, C., Hu, C., Yang, W., Hua, Y., Li, L., Yang, D. and Dai, X. 2021. Sustainable disposal of excess sludge: Post-thermal hydrolysis for anaerobically digested sludge. *Journal of Cleaner Production* 321, 128893.
- Cano, R., Pérez-Elvira, S.I. and Fdz-Polanco, F. 2015. Energy feasibility study of sludge pretreatments: A review. *Applied Energy* 149, 176-185.
- Cao, S., Du, R., Yan, W. and Zhou, Y. 2022. Mitigation of inhibitory effect of THP-AD centrate on partial nitrification and anammox: Insights into ozone pretreatment. *Journal of Hazardous Materials* 431, 128599.
- Cao, S., Yan, W., Yu, L., Zhang, L., Lay, W. and Zhou, Y. 2021. Challenges of THP-AD centrate treatment using partial nitrification-anammox (PN/A) – inhibition, biomass washout, low alkalinity, recalcitrant and more. *Water Research* 203, 117555.
- Cao, Y., van Loosdrecht, M.C.M. and Daigger, G.T. 2017. Mainstream partial nitrification–anammox in municipal wastewater treatment: status, bottlenecks, and further studies. *Applied Microbiology and Biotechnology* 101(4), 1365-1383.
- Capson-Tojo, G., Moscoviz, R., Astals, S., Robles, Á. and Steyer, J.P. 2020. Unraveling the literature chaos around free ammonia inhibition in anaerobic digestion. *Renewable and Sustainable Energy Reviews* 117, 109487.
- Carrere, H., Dumas, C., Battimelli, A., Batstone, D.J., Delgenes, J.P., Steyer, J.P. and Ferrer, I. 2010. Pretreatment methods to improve sludge anaerobic degradability: A review. *J. Hazard. Mater.* 183(1-3), 1-15.
- Cattani, I., Zhang, H., Beone, G.M., Del Re, A.A.M., Boccelli, R. and Trevisan, M. 2009. The Role of Natural Purified Humic Acids in Modifying Mercury Accessibility in Water and Soil All rights reserved. No part of this periodical may be reproduced or transmitted in any form or by any means, electronic or mechanical, including photocopying, recording, or any information storage and retrieval system, without permission in writing from the publisher. *Journal of Environmental Quality* 38(2), 493-501.
- Celano, G., Šmejkalová, D., Spaccini, R. and Piccolo, A. 2008. Interactions of Three s-Triazines with Humic Acids of Different Structure. *Journal of Agricultural and Food Chemistry* 56(16), 7360-7366.
- Chen, Y., Cheng, J.J. and Creamer, K.S. 2008. Inhibition of anaerobic digestion process: A review. *Bioresource Technology* 99(10), 4044-4064.



- Chipasa, K.B. and Mdrzycka, K. 2008. Characterization of the fate of lipids in activated sludge. *Journal of Environmental Sciences* 20(5), 536-542.
- Chipasa, K.B. and Mędrzycka, K. 2006. Behavior of lipids in biological wastewater treatment processes. *Journal of Industrial Microbiology and Biotechnology* 33(8), 635-645.
- Ciesielski, W., Achremowicz, B., Tomasik, P., Baczkowicz, M. and Korus, J. 1997. Starch radicals. Part II: Cereals—native starch complexes. *Carbohydrate Polymers* 34(4), 303-308.
- Cui, R., Gong, H., Xu, Y., Xu, E., Yang, D., Gu, G. and Dai, X. 2022. One-stage partial nitrification-anammox treatment of reject water from high-solid-sludge anaerobic digestion with thermal hydrolysis pretreatment: Inhibition and system recovery. *Journal of Environmental Chemical Engineering* 10(3), 107958.
- Devos, P., Filali, A., Grau, P. and Gillot, S. 2023. Sidestream characteristics in water resource recovery facilities: a critical review. *Water Research*, 119620.
- Dewil, R., Baeyens, J. and Appels, L. 2007. Enhancing the use of waste activated sludge as bio-fuel through selectively reducing its heavy metal content. *Journal of Hazardous Materials* 144(3), 703-707.
- Dohányos, M., Zábranská, J. and Jeníček, P. 1997. Innovative technology for the improvement of the anaerobic methane fermentation. *Water Science and Technology* 36(6), 333-340.
- Donoso-Bravo, A., Pérez-Elvira, S., Aymerich, E. and Fdz-Polanco, F. 2011. Assessment of the influence of thermal pre-treatment time on the macromolecular composition and anaerobic biodegradability of sewage sludge. *Bioresource technology* 102(2), 660-666.
- Dou, X., Chen, D., Hu, Y., Feng, Y. and Dai, X. 2017. Carbonization of heavy metal impregnated sewage sludge oriented towards potential co-disposal. *Journal of Hazardous Materials* 321, 132-145.
- Dwyer, J., Starrenburg, D., Tait, S., Barr, K., Batstone, D.J. and Lant, P. 2008. Decreasing activated sludge thermal hydrolysis temperature reduces product colour, without decreasing degradability. *Water Research* 42(18), 4699-4709.
- Eastman, J.A. and Ferguson, J.F. 1981. Solubilization of Particulate Organic Carbon during the Acid Phase of Anaerobic Digestion. *Journal (Water Pollution Control Federation)* 53(3), 352-366.
- Ekpo, U., Ross, A.B., Camargo-Valero, M.A. and Williams, P.T. 2016. A comparison of product yields and inorganic content in process streams following thermal hydrolysis and hydrothermal processing of microalgae, manure and digestate. *Bioresource Technology* 200, 951-960.
- Elsamadony, M., Mostafa, A., Fujii, M., Tawfik, A. and Pant, D. 2021. Advances towards understanding long chain fatty acids-induced inhibition and overcoming strategies for efficient anaerobic digestion process. *Water Research* 190, 116732.
- Erbas, M., Sekerci, H., Arslan, S. and Durak, A.N. 2012. Effect of sodium metabisulfite addition and baking temperature on maillard reaction in bread. *Journal of Food Quality* 35(2), 144-151.
- Estevez, M.M., Tomczak-Wandzel, R. and Kvamme, K. 2022. Fish sludge as a co-substrate in the anaerobic digestion of municipal sewage sludge- maximizing the utilization of available organic resources. *EFB Bioeconomy Journal* 2, 100027.
- Everett, J.G. 1972. Dewatering of Wastewater Sludge by Heat Treatment. *Journal (Water Pollution Control Federation)* 44(1), 92-100.
- Farhoosh, R. 2022. New insights into the kinetic and thermodynamic evaluations of lipid peroxidation. *Food Chemistry* 375, 131659.
- Farno, E., Baudez, J.C., Parthasarathy, R. and Eshtiaghi, N. 2014. Rheological characterisation of thermally-treated anaerobic digested sludge: Impact of temperature and thermal history. *Water Research* 56, 156-161.

- Fdz-Polanco, F.F.F. 2008. Continuous thermal hydrolysis and energy integration in sludge anaerobic digestion plants. *Water Science and Technology* 57(8), 1221-1226.
- Flores-Alsina, X., Solon, K., Kazadi Mbamba, C., Tait, S., Gernaey, K.V., Jeppsson, U. and Batstone, D.J. 2016. Modelling phosphorus (P), sulfur (S) and iron (Fe) interactions for dynamic simulations of anaerobic digestion processes. *Water Research* 95, 370-382.
- Fricke, K., Santen, H., Wallmann, R., Hüttner, A. and Dichtl, N. 2007. Operating problems in anaerobic digestion plants resulting from nitrogen in MSW. *Waste Management* 27(1), 30-43.
- Gagliano, M.C., Sudmalis, D., Temmink, H. and Plugge, C.M. 2020. Calcium effect on microbial activity and biomass aggregation during anaerobic digestion at high salinity. *New Biotechnology* 56, 114-122.
- GMBH, E.S. 2015a ELIQUO STULZ LYSOTHERM Thermal sludge disintegration.
- GMBH, E.S. 2015b LYSOTHERM Maximise your sludge digestion.
- Gonzalez, A., van Lier, J.B. and de Kreuk, M.K. 2022. Effects of mild thermal pre-treatment combined with H<sub>2</sub>O<sub>2</sub> addition on waste activated sludge digestibility. *Waste Management* 141, 163-172.
- Gu, Z., Li, Y., Yang, Y., Xia, S., Hermanowicz, S.W. and Alvarez-Cohen, L. 2018. Inhibition of anammox by sludge thermal hydrolysis and metagenomic insights. *Bioresource Technology* 270, 46-54.
- Gurgel, L.V.A., Marabezi, K., Zambom, M.D. and Curvelo, A.A.d.S. 2012. Dilute Acid Hydrolysis of Sugar Cane Bagasse at High Temperatures: A Kinetic Study of Cellulose Saccharification and Glucose Decomposition. Part I: Sulfuric Acid as the Catalyst. *Industrial & Engineering Chemistry Research* 51(3), 1173-1185.
- Hanhoun, M., Montastruc, L., Azzaro-Pantel, C., Biscans, B., Frèche, M. and Pibouleau, L. 2011. Temperature impact assessment on struvite solubility product: A thermodynamic modeling approach. *Chemical Engineering Journal* 167(1), 50-58.
- Hao, X., Chen, Q., van Loosdrecht, M.C.M., Li, J. and Jiang, H. 2020. Sustainable disposal of excess sludge: Incineration without anaerobic digestion. *Water Research* 170, 115298.
- Haug, R.T. 1977. Sludge Processing to Optimize Digestibility and Energy Production. *Journal (Water Pollution Control Federation)* 49(7), 1713-1721.
- Haug, R.T., LeBrun, T.J. and Tortorici, L.D. 1983. Thermal pretreatment of sludges - a field demonstration. *Journal of the Water Pollution Control Federation* 55(1), 23-34.
- Haug, R.T., Stuckey, D.C., Gossett, J.M. and McCarty, P.L. 1978. Effect of thermal pretreatment on digestibility and dewaterability of organic sludges. *Journal of the Water Pollution Control Federation* 50(1), 73-85.
- He, C., Wang, K., Yang, Y., Amaniampong, P.N. and Wang, J.-Y. 2015. Effective Nitrogen Removal and Recovery from Dewatered Sewage Sludge Using a Novel Integrated System of Accelerated Hydrothermal Deamination and Air Stripping. *Environmental Science & Technology* 49(11), 6872-6880.
- Hedges, J.I. 1978. The formation and clay mineral reactions of melanoidins. *Geochimica et Cosmochimica Acta* 42(1), 69-76.
- Hiet Wong, C., Barton, G.W. and Barford, J.P. (2003) *Handbook of Water and Wastewater Microbiology*. Mara, D. and Horan, N. (eds), pp. 427-439, Academic Press, London.
- Hodge, J.E. 1953. Dehydrated foods, chemistry of browning reactions in model systems. *Journal of agricultural and food chemistry* 1(15), 928-943.
- Holm-Nielsen, J.B., Al Seadi, T. and Oleskowicz-Popiel, P. 2009. The future of anaerobic digestion and biogas utilization. *Bioresource Technology* 100(22), 5478-5484.
- Holohan, B.C., Duarte, M.S., Szabo-Corbacho, M.A., Cavaleiro, A.J., Salvador, A.F., Pereira, M.A., Ziels, R.M., Frijters, C.T.M.J., Pacheco-Ruiz, S., Carballa, M., Sousa, D.Z., Stams, A.J.M., O'Flaherty, V., van Lier, J.B. and Alves, M.M. 2022. Principles,

- Advances, and Perspectives of Anaerobic Digestion of Lipids. *Environmental Science & Technology* 56(8), 4749-4775.
- Hong, K.-J., Tarutani, N., Shinya, Y. and Kajiuchi, T. 2005. Study on the Recovery of Phosphorus from Waste-Activated Sludge Incinerator Ash. *Journal of Environmental Science and Health, Part A* 40(3), 617-631.
- Hong, S., De Clippeleir, H. and Goel, R. 2022. Response of mixed community anammox biomass against sulfide, nitrite and recalcitrant carbon in terms of inhibition coefficients and functional gene expressions. *Chemosphere* 308, 136232.
- Hrynets, Y., Ndagijimana, M. and Betti, M. 2015. Studies on the Formation of Maillard and Caramelization Products from Glucosamine Incubated at 37 °C. *Journal of Agricultural and Food Chemistry* 63(27), 6249-6261.
- Hupka, J., Rzechula, J. and Jędrzejewski, C. 2002. Ashes from activated sludge as potential raw materials. *Prace Naukowe Instytutu Górnictwa Politechniki Wrocławskiej* (101), 77-86.
- Irving, H. and Williams, R. 1948. Order of stability of metal complexes. *Nature* 162(4123), 746-747.
- Irving, H. and Williams, R. 1953. 637. The stability of transition-metal complexes. *Journal of the Chemical Society (Resumed)*, 3192-3210.
- Jeong, S., Jeung, J., Moon, D. and Chang, S. 2016 Enhancement of Anaerobic Biodegradability and Solubilization by Thermal Pre-Treatment of Waste Activated Sludge, pp. 68-74, World Scientific.
- Jin, R.-C., Yang, G.-F., Yu, J.-J. and Zheng, P. 2012. The inhibition of the Anammox process: A review. *Chemical Engineering Journal* 197(Supplement C), 67-79.
- Kecskésóvá, S., Imreová, Z., Martonka, M. and Drtil, M. 2020. Chemical dissolution of struvite precipitates in pipes from anaerobic sludge digestion. *Chemical Papers* 74(8), 2545-2552.
- Kelleher, B., Leahy, J., Henihan, A., O'dwyer, T., Sutton, D. and Leahy, M. 2002. Advances in poultry litter disposal technology—a review. *Bioresource technology* 83(1), 27-36.
- Klavins, M., Eglite, L. and Serzane, J. 1999. Methods for Analysis of Aquatic Humic Substances. *Critical Reviews in Analytical Chemistry* 29(3), 187-193.
- Kobya, M. and Gengec, E. 2012. Decolourization of melanoidins by a electrocoagulation process using aluminium electrodes. *Environmental Technology* 33(21), 2429-2438.
- Kofina, A.N. and Koutsoukos, P.G. 2005. Spontaneous Precipitation of Struvite from Synthetic Wastewater Solutions. *Crystal Growth & Design* 5(2), 489-496.
- Langerak, E.P.A.v., Beekmans, M.M.H., Beun, J.J., Hamelers, H.V.M. and Lettinga, G. 1999. Influence of phosphate and iron on the extent of calcium carbonate precipitation during anaerobic digestion. *Journal of Chemical Technology & Biotechnology* 74(11), 1030-1036.
- Latif, M.A., Mehta, C.M. and Batstone, D.J. 2018. Enhancing soluble phosphate concentration in sludge liquor by pressurised anaerobic digestion. *Water Research* 145, 660-666.
- Levesque, M. and Schnitzer, M. 1967. Organo-metallic interactions in soils: 6. Preparation and properties of fulvic acid-metal phosphates. *Soil Science* 103(3), 183-190.
- Li, X., Peng, Y., Zhang, J. and Du, R. 2022. Multiple roles of complex organics in polishing THP-AD filtrate with double-line anammox: Inhibitory relief and bacterial selection. *Water Research* 216, 118373.
- Li, Y.-Y. and Noike, T. 1992. Upgrading of Anaerobic Digestion of Waste Activated Sludge by Thermal Pretreatment. *Water Science and Technology* 26(3-4), 857-866.
- Liu, X., Wang, W., Gao, X., Zhou, Y. and Shen, R. 2012. Effect of thermal pretreatment on the physical and chemical properties of municipal biomass waste. *Waste Management* 32(2), 249-255.

- Lotti, T., Kleerebezem, R., Lubello, C. and van Loosdrecht, M.C.M. 2014a. Physiological and kinetic characterization of a suspended cell anammox culture. *Water Research* 60, 1-14.
- Lotti, T., Kleerebezem, R., Lubello, C. and van Loosdrecht, M.C.M. 2014b. Physiological and kinetic characterization of a suspended cell anammox culture. *Water Research* 60(Supplement C), 1-14.
- Lu, C. and Lü, X. 2009. Effect of metal chlorides on glucose decomposition kinetics in high temperature liquid water. *Huagong Xuebao/CIESC Journal* 60(12), 3035-3041.
- Lukicheva, I., Pagilla, K., Rohloff, G. and Kunetz, T. 2009. To Do Class A or Not? What To Do To Enhance Sludge Processing? *Proceedings of the Water Environment Federation* 2009(16), 1256-1273.
- Luo, W. and Gu, B. 2009. Dissolution and Mobilization of Uranium in a Reduced Sediment by Natural Humic Substances under Anaerobic Conditions. *Environmental Science & Technology* 43(1), 152-156.
- Ma, X.J., Gao, J.Y., Tong, P., Li, X. and Chen, H.B. 2017. Tracking the behavior of Maillard browning in lysine/arginine–sugar model systems under high hydrostatic pressure. *Journal of the Science of Food and Agriculture* 97(15), 5168-5175.
- Marti, N., Bouzas, A., Seco, A. and Ferrer, J. 2008. Struvite precipitation assessment in anaerobic digestion processes. *Chemical Engineering Journal* 141(1), 67-74.
- Martin-Neto, L., Traghetta, D.G., Vaz, C.M.P., Crestana, S. and Sposito, G. 2001. On the interaction mechanisms of atrazine and hydroxyatrazine with humic substances. *Journal of Environmental Quality* 30(2), 520-525.
- Martins, S.I.F.S. and Van Boekel, M.A.J.S. 2005. Kinetics of the glucose/glycine Maillard reaction pathways: influences of pH and reactant initial concentrations. *Food Chemistry* 92(3), 437-448.
- Matsuura, Y., Takehira, M., Joti, Y., Ogasahara, K., Tanaka, T., Ono, N., Kunishima, N. and Yutani, K. 2015. Thermodynamics of protein denaturation at temperatures over 100° C: CutA1 mutant proteins substituted with hydrophobic and charged residues. *Scientific reports* 5.
- McDonald, S., Bishop, A.G., Prenzler, P.D. and Robards, K. 2004. Analytical chemistry of freshwater humic substances. *Analytica Chimica Acta* 527(2), 105-124.
- Metcalf, Eddy, Burton, F.L., Stensel, H.D. and Tchobanoglous, G. (2003) *Wastewater engineering: treatment and reuse*, McGraw Hill.
- Migo, V.P., Del Rosario, E.J. and Matsumura, M. 1997. Flocculation of melanoidins induced by inorganic ions. *Journal of Fermentation and Bioengineering* 83(3), 287-291.
- Miličević, A., Branica, G. and Raos, N. 2011. Irving-Williams Order in the Framework of Connectivity Index  $3\chi_v$  Enables Simultaneous Prediction of Stability Constants of Bivalent Transition Metal Complexes. *Molecules* 16(2), 1103-1112.
- Mohsin, G.F., Schmitt, F.J., Kanzler, C., Dirk Epping, J., Flemig, S. and Hornemann, A. 2018. Structural characterization of melanoidin formed from D-glucose and L-alanine at different temperatures applying FTIR, NMR, EPR, and MALDI-ToF-MS. *Food Chemistry* 245, 761-767.
- Morales, F.J., Somoza, V. and Fogliano, V. 2012. Physiological relevance of dietary melanoidins. *Amino Acids* 42(4), 1097-1109.
- Moreau, L., Bindzus, W. and Hill, S. 2011. Influence of salts on starch degradation: Part II - Salt classification and caramelisation. *Starch/Staerke* 63(11), 676-682.
- Mottet, A., François, E., Latrille, E., Steyer, J.P., Déléris, S., Vedrenne, F. and Carrère, H. 2010. Estimating anaerobic biodegradability indicators for waste activated sludge. *Chemical Engineering Journal* 160(2), 488-496.

- Mulvihill, D.M. and Donovan, M. 1987. Whey Proteins and Their Thermal Denaturation - A Review. *Irish Journal of Food Science and Technology* 11(1), 43-75.
- Musvoto, E.V., Wentzel, M.C. and Ekama, G.A. 2000. Integrated chemical–physical processes modelling—II. simulating aeration treatment of anaerobic digester supernatants. *Water Research* 34(6), 1868-1880.
- Nagai, T., Kai, N., Tanoue, Y. and Suzuki, N. 2018. Chemical properties of commercially available honey species and the functional properties of caramelization and Maillard reaction products derived from these honey species. *Journal of Food Science and Technology* 55(2), 586-597.
- Neumann, P., Pesante, S., Venegas, M. and Vidal, G. 2016. Developments in pre-treatment methods to improve anaerobic digestion of sewage sludge. *Reviews in Environmental Science and Bio/Technology* 15(2), 173-211.
- Neyens, E. and Baeyens, J. 2003. A review of thermal sludge pre-treatment processes to improve dewaterability. *Journal of Hazardous Materials* 98(1), 51-67.
- Nisman, B. 1954. THE STICKLAND REACTION. *Bacteriological Reviews* 18(1), 16-42.
- Ochs, P., Martin, B.D., Germain, E., Stephenson, T., van Loosdrecht, M. and Soares, A. 2021. Ammonia removal from thermal hydrolysis dewatering liquors via three different deammonification technologies. *Science of The Total Environment* 755, 142684.
- Øegaard, H. 2004. Sludge minimization technologies - an overview. *Water Science and Technology* 49(10), 31-40.
- Ozgun, H., Cicekalan, B., Akdag, Y., Koyuncu, I. and Ozturk, I. 2021. Comparative evaluation of cost for preliminary and tertiary municipal wastewater treatment plants in Istanbul. *Science of The Total Environment* 778, 146258.
- Parsons, S.A. and Doyle, J.D. 2004. Struvite scale formation and control. *Water Science and Technology* 49(2), 177-182.
- Pastor, L., Mangin, D., Ferrer, J. and Seco, A. 2010. Struvite formation from the supernatants of an anaerobic digestion pilot plant. *Bioresource Technology* 101(1), 118-125.
- Pastore, C., Lopez, A., Lotito, V. and Mascolo, G. 2013. Biodiesel from dewatered wastewater sludge: A two-step process for a more advantageous production. *Chemosphere* 92(6), 667-673.
- Pavez-Jara, J.A., van Lier, J.B. and de Kreuk, M.K. 2023. Accumulating ammoniacal nitrogen instead of melanoidins determines the anaerobic digestibility of thermally hydrolyzed waste activated sludge. *Chemosphere* 332, 138896.
- Pavlostathis, S.G. 1991. Kinetics of anaerobic treatment: A critical review. *Critical Reviews in Environmental Control* 21(5-6), 411-490.
- Penaud, V., Delgenes, J.P. and Moletta, R. 2000a. Characterization of soluble molecules from thermochemically pretreated sludge. *Journal of Environmental Engineering* 126(5), 397-402.
- Penaud, V., Delgenes, J.P. and Moletta, R. 2000b. Influence of thermochemical pretreatment conditions on solubilization and anaerobic biodegradability of a microbial biomass. *Environmental Technology* 21(1), 87-96.
- Pérez-Elvira, S.I. and Fdz-Polanco, F. 2012. Continuous thermal hydrolysis and anaerobic digestion of sludge. Energy integration study. *Water Science and Technology* 65(10), 1839-1846.
- Pérez-Elvira, S.I., Fernández-Polanco, F., Fernández-Polanco, M., Rodríguez, P. and Rouge, P. 2008. Hydrothermal multivariable approach: Full-scale feasibility study. *Electronic Journal of Biotechnology* 11(4), 7-8.
- Piccolo, A. and Mbagwu, J.S.C. 1990. Effects of different organic waste amendments on soil microaggregates stability and molecular sizes of humic substances. *Plant and Soil* 123(1), 27-37.

- Pilath, H.M., Nimlos, M.R., Mittal, A., Himmel, M.E. and Johnson, D.K. 2010. Glucose Reversion Reaction Kinetics. *Journal of Agricultural and Food Chemistry* 58(10), 6131-6140.
- Pineda-Gómez, P., Angel-Gil, N.C., Valencia-Muñoz, C., Rosales-Rivera, A. and Rodríguez-García, M.E. 2014. Thermal degradation of starch sources: Green banana, potato, cassava, and corn - Kinetic study by non-isothermal procedures. *Starch/Staerke* 66(7-8), 691-699.
- Porter, N.A. (1984) *Methods in Enzymology*, pp. 273-282, Academic Press.
- Qian, Y., Sun, S., Ju, D., Shan, X. and Lu, X. 2017. Review of the state-of-the-art of biogas combustion mechanisms and applications in internal combustion engines. *Renewable and Sustainable Energy Reviews* 69, 50-58.
- Quintas, M., Guimarães, C., Baylina, J., Brandão, T.R.S. and Silva, C.L.M. 2007. Multiresponse modelling of the caramelisation reaction. *Innovative Food Science & Emerging Technologies* 8(2), 306-315.
- Rajagopal, R., Massé, D.I. and Singh, G. 2013. A critical review on inhibition of anaerobic digestion process by excess ammonia. *Bioresource Technology* 143(Supplement C), 632-641.
- Ramonaityte, D.T., Keršiene, M., Adams, A., Tehrani, K.A. and Kimpe, N.D. 2009. The interaction of metal ions with Maillard reaction products in a lactose-glycine model system. *Food Research International* 42(3), 331-336.
- Rinzema, A., Boone, M., van Knippenberg, K. and Lettinga, G. 1994. Bactericidal Effect of Long Chain Fatty Acids in Anaerobic Digestion. *Water Environment Research* 66(1), 40-49.
- Rodríguez-Abalde, A., Fernández, B., Silvestre, G. and Flotats, X. 2011. Effects of thermal pre-treatments on solid slaughterhouse waste methane potential. *Waste Management* 31(7), 1488-1493.
- Ronda, A., Haro, P. and Gómez-Barea, A. 2023. Sustainability assessment of alternative waste-to-energy technologies for the management of sewage sludge. *Waste Management* 159, 52-62.
- Sahlström, L. 2003. A review of survival of pathogenic bacteria in organic waste used in biogas plants. *Bioresource technology* 87(2), 161-166.
- Sánchez-Ramírez, J.E., Pastor, L., Martí, N., Claros, J., Doñate, S. and Bouzas, A. 2021. Analysis of uncontrolled phosphorus precipitation in anaerobic digesters under thermophilic and mesophilic conditions. *Environmental Technology* 42(12), 1836-1845.
- Sapkaite, I., Barrado, E., Fdz-Polanco, F. and Pérez-Elvira, S.I. 2017. Optimization of a thermal hydrolysis process for sludge pre-treatment. *Journal of Environmental Management* 192, 25-30.
- Sato, N., Quitain, A.T., Kang, K., Daimon, H. and Fujie, K. 2004. Reaction Kinetics of Amino Acid Decomposition in High-Temperature and High-Pressure Water. *Industrial & Engineering Chemistry Research* 43(13), 3217-3222.
- Satori, H. and Kawase, Y. 2014. Decolorization of dark brown colored coffee effluent using zinc oxide particles: The role of dissolved oxygen in degradation of colored compounds. *Journal of Environmental Management* 139, 172-179.
- Sawatdeenarunat, C., Surendra, K.C., Takara, D., Oechsner, H. and Khanal, S.K. 2015. Anaerobic digestion of lignocellulosic biomass: Challenges and opportunities. *Bioresource technology* 178, 178-186.
- Schnitzer, M. and Gupta, U.C. 1965. Determination of Acidity in Soil Organic Matter. *Soil Science Society of America Journal* 29(3), 274-277.

- Schonberg, A. and Moubacher, R. 1952. The Strecker degradation of  $\alpha$ -amino acids. *Chemical Reviews* 50(2), 261-277.
- Scrinzi, D., Ferrentino, R., Baù, E., Fiori, L. and Andreottola, G. 2023. Sewage Sludge Management at District Level: Reduction and Nutrients Recovery via Hydrothermal Carbonization. *Waste and Biomass Valorization* 14(8), 2505-2517.
- Semblante, G.U., Hai, F.I., Ngo, H.H., Guo, W., You, S.-J., Price, W.E. and Nghiem, L.D. 2014. Sludge cycling between aerobic, anoxic and anaerobic regimes to reduce sludge production during wastewater treatment: Performance, mechanisms, and implications. *Bioresource Technology* 155, 395-409.
- Senesi, N., Miano, T.M. and Brunetti, G. (1996) Humic Substances in Terrestrial Ecosystems. Piccolo, A. (ed), pp. 531-593, Elsevier Science B.V., Amsterdam.
- Shogren, R.L. 1992. Effect of moisture content on the melting and subsequent physical aging of cornstarch. *Carbohydrate Polymers* 19(2), 83-90.
- Siddiquee, M.N. and Rohani, S. 2011. Lipid extraction and biodiesel production from municipal sewage sludges: A review. *Renewable and Sustainable Energy Reviews* 15(2), 1067-1072.
- Silvagni, A., Franco, L., Bagno, A. and Rastrelli, F. 2012. Thermo-induced lipid oxidation of a culinary oil: The effect of materials used in common food processing on the evolution of oxidised species. *Food Chemistry* 133(3), 754-759.
- Sinha, M.K. 1971. Organo-metallic phosphates. *Plant and Soil* 35(1), 471-484.
- Sohn, M. (1996) Thermal deamination and deamidation of amino acids and their contribution to aroma generation, Rutgers The State University of New Jersey, School of Graduate Studies.
- Soler-Cabezas, J.L., Mendoza-Roca, J.A., Vincent-Vela, M.C., Luján-Facundo, M.J. and Pastor-Alcañiz, L. 2018. Simultaneous concentration of nutrients from anaerobically digested sludge centrate and pre-treatment of industrial effluents by forward osmosis. *Separation and Purification Technology* 193, 289-296.
- Somero, G.N. 1995. Proteins and temperature. *Annual review of physiology* 57(1), 43-68.
- Stafford, D.A. 1982. The effects of mixing and volatile fatty acid concentrations on anaerobic digester performance. *Biomass* 2(1), 43-55.
- Stevenson, F.J. (1994) Humus chemistry: genesis, composition, reactions, John Wiley & Sons.
- Strous, M., Heijnen, J.J., Kuenen, J.G. and Jetten, M.S.M. 1998. The sequencing batch reactor as a powerful tool for the study of slowly growing anaerobic ammonium-oxidizing microorganisms. *Applied Microbiology and Biotechnology* 50(5), 589-596.
- Stuckey, D.C. and McCarty, P.L. 1984. The effect of thermal pretreatment on the anaerobic biodegradability and toxicity of waste activated sludge. *Water Research* 18(11), 1343-1353.
- Stürmer, B. 2017. Feedstock change at biogas plants – Impact on production costs. *Biomass and Bioenergy* 98, 228-235.
- Sutton, R. and Sposito, G. 2005. Molecular structure in soil humic substances: The new view. *Environmental Science and Technology* 39(23), 9009-9015.
- Svensson, K., Kjølraug, O., Higgins, M.J., Linjordet, R. and Horn, S.J. 2018. Post-anaerobic digestion thermal hydrolysis of sewage sludge and food waste: Effect on methane yields, dewaterability and solids reduction. *Water Research* 132, 158-166.
- Tagliazucchi, D., Verzelloni, E. and Conte, A. 2010. Effect of Dietary Melanoidins on Lipid Peroxidation during Simulated Gastric Digestion: Their Possible Role in the Prevention of Oxidative Damage. *Journal of Agricultural and Food Chemistry* 58(4), 2513-2519.
- Talboys, P.J., Heppell, J., Roose, T., Healey, J.R., Jones, D.L. and Withers, P.J.A. 2016. Struvite: a slow-release fertiliser for sustainable phosphorus management? *Plant and Soil* 401(1), 109-123.

- Tan, K. and Binger, A. 1986. Effect of humic acid on aluminum toxicity in corn plants. *Soil Science* 141(1), 20-25.
- Toor, S.S., Rosendahl, L. and Rudolf, A. 2011. Hydrothermal liquefaction of biomass: A review of subcritical water technologies. *Energy* 36(5), 2328-2342.
- Trevisan, S., Francioso, O., Quaggiotti, S. and Nardi, S. 2010. Humic substances biological activity at the plant-soil interface: From environmental aspects to molecular factors. *Plant Signaling and Behavior* 5(6), 635-643.
- Tsang, K.R. and Vesilind, P.A. 1990. Moisture Distribution in Sludges. *Water Science and Technology* 22(12), 135-142.
- UMSICHT, F. 2013 Thermal Pressure Hydrolysis® Efficient pretreatment and digestion of biomass, sewage sludge and animal byproducts.
- Valenzuela-Heredia, D., Panatt, C., Belmonte, M., Franchi, O., Crutchik, D., Dumais, J., Vázquez-Padín, J.R., Lesty, Y., Pedrouso, A., Val del Río, Á., Mosquera-Corral, A. and Campos, J.L. 2022. Performance of a two-stage partial nitrification-anammox system treating the supernatant of a sludge anaerobic digester pretreated by a thermal hydrolysis process. *Chemical Engineering Journal* 429, 131301.
- Valo, A., Carrere, H. and Delgenes, J.P. 2004. Thermal, chemical and thermo-chemical pre-treatment of waste activated sludge for anaerobic digestion. *Journal of chemical technology and biotechnology* 79(11), 1197-1203.
- Van Hulle, S.W.H., Vandeweyer, H.J.P., Meesschaert, B.D., Vanrolleghem, P.A., Dejans, P. and Dumoulin, A. 2010. Engineering aspects and practical application of autotrophic nitrogen removal from nitrogen rich streams. *Chemical Engineering Journal* 162(1), 1-20.
- Van Hulle, S.W.H., Volcke, E.I.P., Teruel, J.L., Donckels, B., van Loosdrecht, M.C.M. and Vanrolleghem, P.A. 2007. Influence of temperature and pH on the kinetics of the Sharon nitrification process. *Journal of Chemical Technology & Biotechnology* 82(5), 471-480.
- Van Loosdrecht, M., Hooijmans, C., Brdjanovic, D. and Heijnen, J. 1997. Biological phosphate removal processes. *Applied microbiology and biotechnology* 48, 289-296.
- Veolia 2017a Bio Thelys™ batch thermal hydrolysis.
- Veolia 2017b Exelys™ Hidrólisis térmica en continuo.
- Veolia 2017c Exelys™ Technical Details
- Wang, G., Dai, X., Zhao, S. and Zhang, D. 2022. Research on Ammonia Removal from Reject Water Produced from Anaerobic Digestion of Thermally Hydrolyzed Sludge Through Partial Nitrification—Anammox. *Water, Air, & Soil Pollution* 233(4), 106.
- Wang, Q., Kuninobu, M., Ogawa, H.I. and Kato, Y. 1999. Degradation of volatile fatty acids in highly efficient anaerobic digestion. *Biomass and Bioenergy* 16(6), 407-416.
- Wang, S. and Mulligan, C.N. 2009. Enhanced mobilization of arsenic and heavy metals from mine tailings by humic acid. *Chemosphere* 74(2), 274-279.
- Warmadewanthi and Liu, J.C. 2009. Recovery of phosphate and ammonium as struvite from semiconductor wastewater. *Separation and Purification Technology* 64(3), 368-373.
- Weiland, P. 2010. Biogas production: Current state and perspectives. *Applied Microbiology and Biotechnology* 85(4), 849-860.
- Weir, C. and Soper, R. 1963. Interaction of phosphates with ferric organic complexes. *Canadian Journal of Soil Science* 43(2), 393-399.
- Wild, D., Kisliakova, A. and Siegrist, H. 1997. Prediction of recycle phosphorus loads from anaerobic digestion. *Water Research* 31(9), 2300-2308.
- Wilén, B.-M., Jin, B. and Lant, P. 2003. The influence of key chemical constituents in activated sludge on surface and flocculating properties. *Water Research* 37(9), 2127-2139.



- Willems, M., Pedersen, B., J., S.S., and Jørgensen 1976. Composition and Reactivity of Ash from Sewage Sludge. *Ambio* 5(1), 32-35.
- Wilson, C.A. and Novak, J.T. 2009. Hydrolysis of macromolecular components of primary and secondary wastewater sludge by thermal hydrolytic pretreatment. *Water research* 43(18), 4489-4498.
- Xue, Y., Liu, H., Chen, S., Dichtl, N., Dai, X. and Li, N. 2015. Effects of thermal hydrolysis on organic matter solubilization and anaerobic digestion of high solid sludge. *Chemical Engineering Journal* 264, 174-180.
- Yenigün, O. and Demirel, B. 2013. Ammonia inhibition in anaerobic digestion: A review. *Process Biochemistry* 48(5-6), 901-911.
- Yu, Y. and Wu, H. 2011. Kinetics and mechanism of glucose decomposition in hot-compressed water: Effect of initial glucose concentration. *Industrial and Engineering Chemistry Research* 50(18), 10500-10508.
- Zhang, G., Li, Y., Dai, Y.J. and Wang, R.Z. 2016a. Design and analysis of a biogas production system utilizing residual energy for a hybrid CSP and biogas power plant. *Applied Thermal Engineering* 109, Part A, 423-431.
- Zhang, Q., De Clippeleir, H., Su, C., Al-Omari, A., Wett, B., Vlaeminck, S.E. and Murthy, S. 2016b. Deammonification for digester supernatant pretreated with thermal hydrolysis: overcoming inhibition through process optimization. *Applied Microbiology and Biotechnology* 100(12), 5595-5606.
- Zhang, Q., Vlaeminck, S.E., DeBarbadillo, C., Su, C., Al-Omari, A., Wett, B., Pümpel, T., Shaw, A., Chandran, K., Murthy, S. and De Clippeleir, H. 2018. Supernatant organics from anaerobic digestion after thermal hydrolysis cause direct and/or diffusional activity loss for nitrification and anammox. *Water Research* 143, 270-281.
- Zhen, G., Lu, X., Kato, H., Zhao, Y. and Li, Y.-Y. 2017. Overview of pretreatment strategies for enhancing sewage sludge disintegration and subsequent anaerobic digestion: Current advances, full-scale application and future perspectives. *Renewable and Sustainable Energy Reviews* 69, 559-577.





## 2.

**Accumulating ammoniacal nitrogen instead of melanoidins  
determines the anaerobic digestibility of thermally hydrolysed  
waste-activated sludge\***

---

\* Based on Pavez-Jara, J.A., J.B. van Lier, and M.K. de Kreuk, Accumulating ammoniacal nitrogen instead of melanoidins determines the anaerobic digestibility of thermally hydrolyzed waste activated sludge. Chemosphere, 2023. 332: p. 138896.

## ABSTRACT

Full-scale thermal hydrolysis processes (THP) showed an increase in nutrients release and formation of melanoidins, which are believed to negatively impact methanogenesis during mesophilic anaerobic digestion (AD). In this research, fractionation of THP-sludge was performed to elucidate the distribution of nutrients and the formed melanoidins over the liquid and solid sludge matrix. Degradation of the different fractions in subsequent AD was assessed, and the results were compared with non-pre-treated waste-activated sludge (WAS). Results showed that the THP-formed soluble melanoidins were partially biodegradable under AD, especially the fraction with molecular weight under 1.1 kDa, which was related to protein-like substances. The use of THP in WAS increased the non-biodegradable soluble chemical oxygen demand (sCOD) after AD, from 1.1% to 4.9% of the total COD. The total ammoniacal nitrogen (TAN) concentration only slightly increased during THP without AD. However, after AD, TAN released was 34% higher in the THP-treated WAS compared to non-treated WAS, i.e.,  $36.7 \pm 0.7$  compared to  $27.4 \pm 0.4$  mgTANreleased/gCODsubstrate, respectively. Results from modified specific methanogenic activities (mSMAs) tests showed that the organics solubilised during THP, were not inhibitory for acetotrophic methanogens. However, after AD of THP-treated sludge and WAS, the mSMA showed that all analysed samples presented strong inhibition on methanogenesis due to the presence of TAN and associated free-ammonia nitrogen (FAN). In specific methanogenic activities (SMAs) tests with incremental concentration of TAN/FAN and melanoidins, TAN/FAN induced strong inhibition on methanogens, halving the SMA at around 2.5 gTAN/L and 100 mgFAN/L. Conversely, melanoidins did not show inhibition on the methanogens. Our present results revealed that when applying THP-AD in full-scale, the increase in TAN/FAN remarkably had a greater impact on AD than the formation of melanoidins.

## 2.1. Introduction

One of the most critical challenges for wastewater treatment facilities in many countries is the handling and disposal of waste-activated sludge (WAS) (Fytli and Zabaniotou, 2008; Kelessidis and Stasinakis, 2012; Yang et al., 2015). Among possibilities to stabilise WAS, anaerobic digestion (AD) is a well-established technology since it has shown, high system robustness, reduction of pathogens, and recovery of the biochemical energy as biogas (Appels et al., 2008; Lin et al., 1997). However, the conversion efficiency of organics present in WAS into biogas in a conventional AD process is still low, ranging between 20-50% (Kabouris et al., 2009; Luostarinen et al., 2009; Ohemeng-Ntiamoah and Datta, 2018). To improve the bioconversion rate and CH<sub>4</sub> yield, different pre-treatments for organic substrates have been proposed such as mechanical, thermal, chemical, and biological techniques, or integrations of these (Gonzalez et al., 2018; Zhen et al., 2017). Within full-scale installations using pre-treatment processes for WAS digestion, thermal hydrolysis process (THP) is the mainly applied technology, which is offered by different companies. Some THP brand names present in the market are Cambi®, Biothelys®, Exelys®, THP®, LysoTherm® and Turbotec®. THP suppliers claim to improve biogas production, dewaterability, and to reach a pathogens-free digestate (Kepp et al., 2000; Pérez-Elvira et al., 2010). THP follows a sequence of two steps. The first step consists of heating the product to be hydrolysed which may consist of secondary sludge, primary sludge or a mix of both, up to 140-180°C (at 4-10 bar) for a determined time. Commonly, 20-40 minutes is set by the manufacturer, depending on the offered technology. In the second step, the pressure is suddenly released, causing the pressurised-hot-water in the microbial biomass to evaporate, producing a violent expansion with the subsequent lysis, and release of the cytoplasmic content (Ringoot et al., 2012).

Despite the advantages of THP, several authors have reported the potential formation of recalcitrant and even inhibitory or toxic compounds due to the occurring side reactions during this process (Barber, 2016; Haug et al., 1978; Valo et al., 2004). The formation of recalcitrant and/or inhibitory compounds is reported to increase along with the THP pre-treatment time and temperature in the majority of the cases (Dwyer et al., 2008). Although different studies have found inconclusive results about the specific cause of possible inhibition of AD caused by THP, negative effects might be attributed to intermediates of Maillard and caramelisation reactions that are formed during the THP process (Balasundaram et al., 2022; Higgins et al., 2017; Ortega-Martínez et al., 2021; Penaud et al., 2000; Rahmani et al., 2023). Melanoidins can be formed during THP since organic compounds in WAS mainly consist of proteins,

carbohydrates, and small portions of lipids and humic substances (Gonzalez et al., 2018; Wilén et al., 2003), which react during THP in caramelisation and Maillard reactions. During the Maillard reaction, an amino group present in amino acids/peptides/proteins reacts with the “glycosidic” hydroxyl group present in sugars to produce an Amadori-rearrangement-product, which is a Maillard reaction precursor (Ellis, 1959). If the conditions are favourable, the products of the initial rearrangements continue reacting, leading to the formation of intermediates that suffer polymerization reactions, and will thus increase in molecular weight (MW). The reaction products will form a wide range of compounds called melanoidins (Hodge, 1953; Horvat and Jakas, 2004; Silván et al., 2006). Since the structure of melanoidins is not well defined and the environmental conditions can modify them, melanoidins refer to a group of molecules that behave similarly instead of to one specific compound. Melanoidins can be classified based on MW and solubility, in a similar way as the classification of humic substances in humic and fulvic acids and humins (Klavins et al., 1999; Migo et al., 1993). In literature, it is hypothesised that melanoidins might cause inhibition of the anaerobic process. However, the extent of this inhibition or the factors affecting inhibition are not fully understood (Brons et al., 1985; Gao et al., 2022; Li et al., 2019; Rufian-Henares and de la Cueva, 2009; Wang et al., 2022; Yin et al., 2019).

Besides the solubilisation of organics during THP, an increased nutrients release has also been observed (Ngo et al., 2021; Suárez-Iglesias et al., 2017). This (extra) solubilisation may cause operational problems in the subsequent steps of the reject water or sludge treatment. Additional maintenance may be required because of uncontrolled  $\text{NH}_4^+$ - $\text{PO}_4^{3-}$ -based minerals precipitation that causes pipe clogging or problems in the sludge dewatering installation. Furthermore, additional total ammoniacal nitrogen ( $\text{TAN} = \text{NH}_4^+ + \text{NH}_3$ ) release could lead to  $\text{NH}_4^+$  and free-ammonia nitrogen (FAN) inhibition of methanogenesis. The inhibition is mainly caused by FAN but the influence of TAN cannot be isolated (Astals et al., 2018). TAN/FAN are formed due to the breakdown of proteinaceous material (deamination) during AD and can cause inhibition of the process, especially in substrates with low C/N ratio (Akindele and Sartaj, 2018; Barber, 2016; Mata-Alvarez et al., 2014; Wilson and Novak, 2009). An elevated concentration of TAN/FAN may lead to an increased pH of the reactors since the  $\text{pK}_a$  of  $\text{NH}_4^+/\text{NH}_3 = 8.9$  at  $35^\circ\text{C}$ . Moreover, TAN/FAN exert a higher degree of inhibition on acetoclastic methanogens than hydrogenotrophic methanogens (Koster and Lettinga, 1984). The somewhat higher pH and temperature in AD reactors using THP as pre-treatment, i.e. around  $40^\circ\text{C}$  according to Barber (2016), increases the FAN concentration and thus the

potential inhibition. In addition to this inhibitory effect, high TAN concentrations might lead to an increase in the costs of reject water deammonification, either via nitrification/denitrification, partial nitrification/anammox, or physicochemical techniques (Deng et al., 2021; Fux and Siegrist, 2004; Ochs et al., 2023; Vineyard et al., 2020), since the costs are proportional to the mass of TAN to be removed.

In our present study, the formation of recalcitrant compounds and the release of N from the different fractions of THP sludge and WAS was monitored, and their effect on AD was determined. The distribution of melanoidins and N between supernatants and sludge pellets of centrifuged THP sludge was studied and compared to WAS without pre-treatment to elucidate the origin and fate of N and melanoidins. An evaluation of the melanoidins' MW, aromaticity, and anaerobic biodegradability was also conducted, to determine their recalcitrant character. In addition, acetotrophic toxicity tests were performed to assess the possible inhibition of the THP-generated compounds on methanogenesis.



## **2.2. Materials and methods**

### **2.2.1. Fractionation and characterisation of the substrates used for AD.**

Thickened WAS and THP-treated-WAS were collected immediately before and after a CAMBI® system from a municipal waste-water treatment plant (WWTP) located in Hengelo, The Netherlands. The sampling volume was 10 L, and only one sample of each sludge was taken. The WAS sample originated in an aerobic activated-sludge plant using enhanced biological phosphorus removal (EBPR) and nitrification/denitrification. THP sludge samples were collected after passing a CAMBI® installation, pre-treating only secondary sludge from the WWTP in Hengelo and surrounding small WWTPs. The CAMBI® installation comprised a pulper to pre-heat the sludge, a reactor with an operational temperature of 160°C and a treatment time per batch of 30 min, and a flash tank to perform the "steam explosion". The samples were stored at 4°C before analysis and fractionation.

THP sludge was homogenised and centrifuged at 12,000 rpm for 10 min in a centrifuge model Sorvall ST 16R (Thermo Fisher Scientific, USA) at 4°C, whereafter the pellet and supernatant were collected. The pellet of THP sludge was washed three times in a culture medium consisting of buffer, macronutrients, and micronutrients (Table 2.A1 in supplementary information), to remove the remnant soluble melanoidins. The washing was performed by doubling the pellet volume with culture medium and subsequently resuspending and centrifuging at 3,500 rpm for 10 min in a centrifuge model Heraeus Labofuge 400 (Thermo Fisher Scientific, USA). Four different samples were analysed: i) THP-liquid (THP<sub>l</sub>), comprising the centrifugation supernatant of THP sludge; ii) THP-solid (THP<sub>s</sub>), consisting of the buffer-washed pellet of THP sludge; iii) THP-total (THP<sub>t</sub>), comprising a homogenous sample of THP sludge; iv) WAS, comprising the non-pre-treated sample of thickened WAS. Note that iii) THP<sub>t</sub> and iv) WAS were not processed by centrifugation and washing. For clarification, a scheme of the fractionation is included in the supplementary material (Figure A1).

### **2.2.2. Chemical analysis**

Total solids (TS) and volatile solids (VS) were assessed according to Standard Methods for the examination of water and wastewater (Rice et al., 2012). Soluble and total chemical oxygen demand (sCOD and tCOD, respectively) and TAN, were measured with the kits LCK 114, APC 303, brand Hach Lange (Hach, USA). Carbohydrates were measured according to the

phenol–sulphuric acid method (Dubois et al., 1951). Proteins and humic substances were measured based on the Lowry method considering the interference of humic substances, according to Fr et al. (1995). Volatile fatty acids (VFA) were measured using an Agilent 19091F-112, 25 m × 320 µm × 0.5 µm column in an Agilent 7890A Gas Chromatograph (Agilent Technologies, USA) equipped with a flame ionisation detector. Helium was used as mobile phase with a total flow rate of 67 mL/min and a split ratio of 25:1, the sample injection volume was 1 µL. The gas chromatograph oven's temperature increased from 80 to 180°C in 10.5 min, and the temperatures of the injector and detector were 80 and 240°C, respectively. Free ammonia nitrogen (FAN) was calculated in each sample based on equation (2.1), according to Emerson et al. (1975).

$$FAN = \frac{TAN}{(10^{pK_a - pH} + 1)} = \frac{TAN}{\left(10^{\frac{(0.901821 + 2729.92)}{T_k} - pH} + 1\right)} \quad (2.1),$$

Where:

TAN=TAN concentration (NH<sub>4</sub><sup>+</sup>+NH<sub>3</sub> in gN/L).

FAN= FAN concentration gN/L.

pK<sub>a</sub>= NH<sub>4</sub><sup>+</sup>/NH<sub>3</sub> dissociation constant at the sample temperature (approximated as pK<sub>a</sub> =  $\frac{(0.901821 + 2729.92)}{T_k}$ ).

T<sub>k</sub>= Sample temperature in K.

### 2.2.3. Biochemical methane potential (BMP) and modified acetotrophic specific methanogenic activity (mSMA) tests

BMP and mSMA tests were conducted with the four fractions formerly mentioned using an AMPTS II system (Bioprocess Control, Sweden) at 35°C, considering the recommendations raised by Holliger et al. (2016). BMP tests were carried out in triplicate, using 500 mL bottles with a reaction volume of 300 mL. The BMP bottles comprising inoculum, substrate and culture medium were sampled for analysis at the beginning and the end of the AD. We obtained ten groups from the sampling: i) THP<sub>1</sub> and THP<sub>1</sub>+AD, comprising the THP<sub>1</sub> substrate at the beginning and end of the BMP, respectively; ii) THP<sub>s</sub> and THP<sub>s</sub>+AD, comprising the THP<sub>s</sub> substrate at the beginning and end of the BMP, respectively; iii) THP<sub>t</sub> and THP<sub>t</sub>+AD, comprising the THP<sub>t</sub> substrate at the beginning and end of the BMP, respectively; iv) WAS

and WAS+AD, comprising the WAS substrate at the beginning and end of the BMP, respectively; v) Blank and Blank+AD, comprising only inoculum and culture medium at the beginning and end of the BMP, respectively. The tests were conducted with a concentration of 19 grams of tCOD per litre of substrate and 28.5 grams of VS per litre of inoculum, having an inoculum/substrate ratio of 1.5 gVS/gCOD. In the blank bottles, the substrate was replaced by demineralized water, while the culture medium (Table 2.A1 in supplementary information) and inoculum remained in the same concentration as in the tests with substrates. Results were expressed in millilitres of normalised CH<sub>4</sub> (273.15 K and 1 atm) produced per gram of substrate COD. The percentage of biodegradability of the analysed samples was assessed considering that 100% corresponded to 350 NmL-CH<sub>4</sub>/gCOD.

The inoculum to perform the BMP and mSMA tests was collected from the digestate produced at municipal WWTP, Harnaschpolder operated by Delfluent Services (Den Hoorn, The Netherlands). These digesters treat a mixture of WAS and primary sludge without any pre-treatment, at a hydraulic retention time of 21-24 days and an operational temperature of 35°C. In preparatory tests (results not shown), microcrystalline cellulose (Sigma-Aldrich, USA) was used as the substrate in positive controls with the inoculum from the same provenance, ensuring that the inoculum was active and produced the stoichiometric amount of CH<sub>4</sub> according to the added substrate. The inoculum was pre-incubated at 35°C for seven days to consume the remaining substrate from the full-scale installation and was pre-concentrated 1.7 times by centrifugation 10 min at 3,500 rpm in a centrifuge model Heraeus Labofuge 400 (Thermo Fisher Scientific, USA) to reach the required concentration to perform the experiments.

To study the differences in acetotrophic methanogenic activity of the inoculum before and after the BMP test, two mSMAs tests were conducted with the mixed broth used for BMP tests at the beginning and the end. The mSMA tests were conducted under the same conditions as the BMP tests, using the automated methane potential test system (AMPTS) II (Bioprocess Control, Sweden) at 35°C, using the same culture media (Table 2.A1 in supplementary information), and recording CH<sub>4</sub> generation over time. The mSMA tests were conducted using 2 gCOD/L of sodium acetate, which was added to the BMP-substrates THP<sub>i</sub>, THP<sub>s</sub>, THP<sub>t</sub>, and WAS, using the same inoculum. The BMP-blank-bottle plus sodium acetate was considered as mSMA positive control in which no substrate for BMP was added. The reaction volume of mSMAs before and after the BMP test was 300 mL and 250 mL, respectively, since 50 mL of broths were taken for analysis once the BMP test was ended (symbolised in the figures as “+AD” samples). Both mSMAs were carried out in triplicate and the bars in the graphs

represent the standard deviation. The results were expressed in grams of COD as CH<sub>4</sub> produced per gram of VS inoculum per day, at the maximum CH<sub>4</sub> production rate.

Additionally, SMA tests with different concentrations of TAN/FAN and melanoidins were carried out, using the same inoculum as in the BMP and mSMA tests, in 500 mL bottles with 300 mL of reaction volume, and adding the same concentration of acetate and culture medium used for mSMAs. TAN was supplied as NH<sub>4</sub>Cl (CAS Number 12125-02-9, Sigma-Aldrich, USA). Resulting FAN concentrations were calculated according to equation (2.1) and plotted together with TAN. The pHs used to calculate FAN were measured at the beginning of the BMP test since it was close to the point when the maximum CH<sub>4</sub> rate was measured. At the end of the BMP test (day 23), the pH of the broth was measured again for the FAN calculation. Soluble melanoidins were prepared to resemble the humic substances formed during THP. Melanoidins were prepared according to Bernardo et al. (1997) and Dwyer et al. (2008): by reacting 0.25M glucose and 0.25M glycine using 0.5M NaHCO<sub>3</sub> as buffer, for three hours at 121°C, in an autoclave model FVA3/A1 (Fedegari Autoklaven AG, Switzerland). After the incubation, the synthetic melanoidins solution was anaerobically digested at 35°C using anaerobic inoculum in a proportion of 1 g VS<sub>inoculum</sub> /g COD<sub>melanoidins</sub> in order to reduce the amount of readily-biodegradable organics, such as short molecular weight melanoidins and non-reacted glucose and glycine. After the gas production stopped, the digested melanoidins supernatant was separated from the digestate using centrifugation at 3,500 rpm for 10 min in a centrifuge model Heraeus Labofuge 400 (Thermo Fisher Scientific, USA), characterised, and stored at 4 °C for further use. The inhibitory effect on SMA was modelled using equation (2.2), which is analogous to the equation used in ADM1 to model pH inhibition (Astals et al., 2018). Also, the half inhibition constant was calculated as (KI<sub>min</sub>+KI<sub>max</sub>)/2.

$$SMA = \begin{cases} SMA_{i, \max} , & \text{if } [S_i] \leq KI_{\min} \\ SMA_{i, \max} \cdot e^{-2.77259 \cdot \left( \frac{([S_i] - KI_{\min})}{(KI_{\max} - KI_{\min})} \right)^2} , & \text{if } [S_i] > KI_{\min} \end{cases} \quad (2.2),$$

Where:

$SMA_{i, \max}$  = SMA measured when inhibition starts.

$[S_i]$  : inhibitor concentration (i=TAN and FAN).

$KI_{\max}$ : inhibitor concentration at which the inhibition is almost complete (assumed as  $SMA = 0.06 \cdot SMA_{x, \max}$ ).

$KI_{min}$ =inhibitor concentration when inhibition starts.

#### **2.2.4. Size Exclusion Chromatography (SEC-HPLC)**

Employing SEC-HPLC we investigated the MW of the melanoidins formed during THP and their fate during AD. SEC-HPLC elutes the soluble molecules based on their hydrodynamic radius, which increases with the MW (Squire, 1985; Tarvers and Church, 1985). Absorbances at two wavelengths were used in the SEC-HPLC detector. One was measured at 254 nm, indicating the humic substances with a higher presence of phenolic groups (more condensed), and the other one was measured at 210 nm, which represented less condensed molecules associated with proteinaceous material (Her et al., 2008). Samples were taken before and after performing the BMP tests, filtered through 0.45  $\mu$ m with a CHROMAFIL Xtra PES-45/25 (Macherey-Nagel, Germany), and analysed by SEC-HPLC using a column model Yarra™ 3  $\mu$ m SEC-2000, LC Column 300  $\times$  7.8 mm, Ea (Phenomenex, USA) connected to an ultrafast liquid chromatography (UFLC) system (Prominence, Shimadzu, Japan). Acetonitrile and sodium  $PO_4^{3-}$  buffer of 10 mM, pH 7, prepared in ultrapure water in a proportion of 25% and 75%, respectively, were used as mobile phase. The eluent flow was 0.25 mL/min, and the separation was reached within one hour at 25°C. A UV detector was used at 254 nm and 210 nm to identify the analytes. Four Polystyrene sulfonate standards (Polymer standard service, Germany) of 0.1, 1.1, 3.6, and 29.1 kDa were used to correlate the elution time with the MW. The results were expressed as the area under the curve of the detector signal (in mV) in the timeframe that corresponds to the known MW defined in the standards. The UV absorbance ratio index (URI) describes the specific aromaticity of the soluble substances measured in SEC-HPLC. A high URI indicates the occurrence of protein-like moieties associated with carboxylic and hydroxyl groups, while a low value indicates phenolic groups occurrence and thus, aromaticity (Her et al., 2008). URI was calculated as the quotient of the averaged absorbances at 210 nm over 254 nm, in each MW interval.

#### **2.2.5. Fluorescence excitation emission matrix (FEEM)**

FEEM was conducted using a FluoroMax-3 spectrofluorometer (HORIBA Jobin Yvon, Japan) with a 1 cm path-length quartz cuvette. The samples were filtered through 0.45 $\mu$ m and diluted with ultrapure water to reach a concentration of 1 mgTOC/L. Emission and excitation spectra were analysed from 290 to 500 nm and 240 to 452 nm with 2 and 4 nm of interval, respectively. The Raman peaks were removed and the blank (ultrapure water) was subtracted. The integration of the fluorophores was performed based on the location of the maximum peak

method, according to Dwyer and Lant (2008). The FEEM was divided into three areas to perform normalised fluorescence regional integration (NFRI), as follows: protein-like substances ( $3,320 \text{ nm}^2$ ) comprised the polygon formed by the points (290 nm, 240 nm), (290 nm, 268 nm), (328 nm, 308 nm), (350 nm, 308 nm), and (350 nm, 240 nm); fulvic-like compounds ( $7,104 \text{ nm}^2$ ) comprised the polygon formed by the points (352 nm, 240 nm), (500 nm, 240 nm), (500 nm, 288 nm), and (352 nm, 288 nm); and humic-like compounds ( $16,472 \text{ nm}^2$ ) comprised the polygon formed by the points (352 nm, 288 nm), (500 nm, 288 nm), (500 nm, 452 nm), (472 nm, 452 nm), and (352 nm, 332 nm). The NFRI results comprised the volume under the FEEM in arbitrary units ( $\text{AU} \cdot \text{nm}^2$ ) in the three polygons analysed (protein-like, fulvic-like, and humic-like substances), over the area of the specific polygon in  $\text{nm}^2$  (Chen et al., 2003).

#### 2.2.6. True colour and UVA 254

True colour and UVA 254 were measured in the soluble fraction after filtration using  $0.45 \mu\text{m}$  syringe filters CHROMAFIL Xtra PES-45/25 (Macherey-Nagel, Germany). The true colour was measured at 475nm using a Platinum-Cobalt colour reference solution (Hazen 500, Certipur® Merck, Germany) with a concentration of 500 mgPt-Co/L in a Genesys 10S UV-Vis spectrophotometer (Thermo Scientific, USA) using 1cm pathway plastic cuvettes. UVA 254 was measured in the same spectrophotometer as the true colour measurement, at 254 nm with 1 cm pathway quartz cuvettes. The results are expressed in mg Pt-Co/L and 1/cm in the case of true colour and UVA 254, respectively.

#### 2.2.7. Analysis of results

The specific degree of solubilisation (SDOS) describes the solubilisation of specific compounds of interest (i-th compound) in a particular moment per unit of mass in the initial substrate (expressed as COD), and it is defined in equation (2.3). SDOS was calculated at the beginning and end of AD, discounting the blank sample at the same moment. For assessing this parameter, the soluble concentration of specific compounds in the blank sample (no substrate added) was subtracted from the soluble concentration before and after AD, and this was divided by the tCOD concentration in the initial substrate. The results are expressed in the mass of the i-th compound solubilised per mass of tCOD in the initial substrate.

$$i\text{-SDOS} = \frac{C_{i,j} - C_{i,\text{Blank}}}{\text{tCOD}_j} \bigg|_{t=0 \text{ and } t=23} \quad (2,3),$$

Where:

t= digestion time in days (t=0 is considered before AD t=23 after AD)

i-SDOS = Specific degree of solubilisation of the i-th parameter.

$C_{i,j}$ =Soluble concentration of the i-th parameter in the j-th sample.

$C_{i,Blank}$  = Soluble concentration of the i-th parameter blank sample (before and after AD, respectively).

tCOD<sub>j</sub> = Substrate tCOD concentration (homogenous) in the j-th sample, before AD (19 gCOD/L).

i=sCOD, T.colour, UVA 254, TAN, and soluble proteins.

j=THP<sub>1</sub>, THP<sub>s</sub>, THP<sub>t</sub>, and WAS.

To better understand the effect of THP conditions on the biodegradability of proteins in relation to the biodegraded organic matter during AD, the TAN<sub>released</sub>/ COD<sub>consumed</sub> ratio was calculated in all analysed fractions (COD balance in Figure 2.A2 of supplementary material). TAN released per unit of total COD consumed is defined in equation (2.4). This parameter shows the TAN released per unit of biodegradable COD in the analysed substrates.

$$\text{TAN}_{\text{released}}/\text{COD}_{\text{Consumed}} = \frac{\text{TAN-SDOS}_{+AD,j} - \text{TAN-SDOS}_{-AD,j}}{\left( \frac{(\text{tCOD}_{-AD,j} - \text{tCOD}_{-AD,Blank}) - (\text{tCOD}_{+AD,j} - \text{tCOD}_{+AD,Blank})}{\text{COD}_j} \right)} \quad (2.4),$$

Where:

TAN-SDOS<sub>+AD,j</sub>= TAN-SDOS after AD in the j-th sample.

TAN-SDOS<sub>-AD,j</sub>= TAN-SDOS before AD in the j-th sample.

tCOD<sub>+AD,j</sub>= tCOD concentration after AD in the j-th sample (tCOD<sub>+AD-Blank</sub>= tCOD concentration in the Blank after AD).

tCOD<sub>-AD,j</sub>= tCOD concentration before AD in the j-th sample (tCOD<sub>-AD,Blank</sub>= tCOD concentration in the Blank before AD).

Single-factor ANOVA with a confidence level of 95% was used to evaluate the significance of differences between the different samples. Also, mean difference tests with the same level of significance as ANOVA were used when comparing two samples' averages.



## 2.3. Results and discussion

### 2.3.1. Fractionation of THP sludge samples

The biochemical parameters of WAS and the different fractions of THP sludge are given in Table 2.1. After fractionation, about 40% of the THP sludge (THP<sub>t</sub>) consisted of THP<sub>i</sub>, while 60% of the mass was found as THP<sub>s</sub>. It is important to remark that the parameters measured in THP<sub>i</sub> and THP<sub>s</sub> corresponded to the concentrations reached after the fractionation that was performed in the laboratory and, therefore, do not represent values that can be found in a full-scale installation. The soluble biochemical parameters in the THP<sub>i</sub> fraction were similar to those of the THP<sub>t</sub> since both samples share the soluble portion of THP sludge. Measured VFAs in THP<sub>i</sub> and THP<sub>t</sub> could originate from the release of cytoplasmatic metabolites and/or physicochemical conversion of lipids, (long-chain) fatty acids and proteins present in WAS, which were solubilised. The increased TAN concentration in pre-treated samples was most likely produced by the physicochemical deamination of proteins during THP (Wilson and Novak, 2009). Melanoidins present in the THP sludge fractions caused the observed increase in UVA 254 and true colour compared to WAS. The percentage of solubilised organic matter after pre-treatment (sCOD/tCOD) increased from 0.5% in WAS to 32% in THP<sub>t</sub>, evidencing the capacity of the pre-treatment to solubilise the organic compounds present in the WAS. The soluble compounds present in the THP<sub>s</sub> fraction indicate that not all soluble substances were removed during the washing protocol, and some remained within the THP-treated sludge's solid matrix. In addition, true colour and UVA 254 were measured in the soluble phase only; the pre-treatment induced an increase of 650 and 300 times in true colour and UVA 254, respectively, compared to WAS. Elevated colour and UVA 254 during THP have been widely reported in the literature and have been attributed to the formation of melanoidins (Dwyer et al., 2008).

**Table 2.1.** Biochemical parameters in the fractionation of THP sludge and WAS.

Measurement	THP <sub>i</sub> fraction	THP <sub>s</sub> fraction	THP <sub>t</sub> sample	WAS sample
BMP (NmL-CH <sub>4</sub> /gCOD) [% of biodegradability]	230±23 [66±7]	119±35 [34±10]	165±24 [47±7]	122±22 [35±6]
sCOD (g/L)	54.9±0.9	9.76±0.06	52.9±0.2	0.95±0.05
tCOD (g/L)	75±2	238±9	172±1	212±7
Total solids (gTS/L)	57.5±0.1	187.3±0.7	136.3±0.5	166.8±0.4
Volatile solids (gVS/L)	50.5±0.4	131.1±0.5	105.2±0.1	130.6±0.3
TAN (mg TAN/L)	1,034±8	389±2	1,068±14	713±12

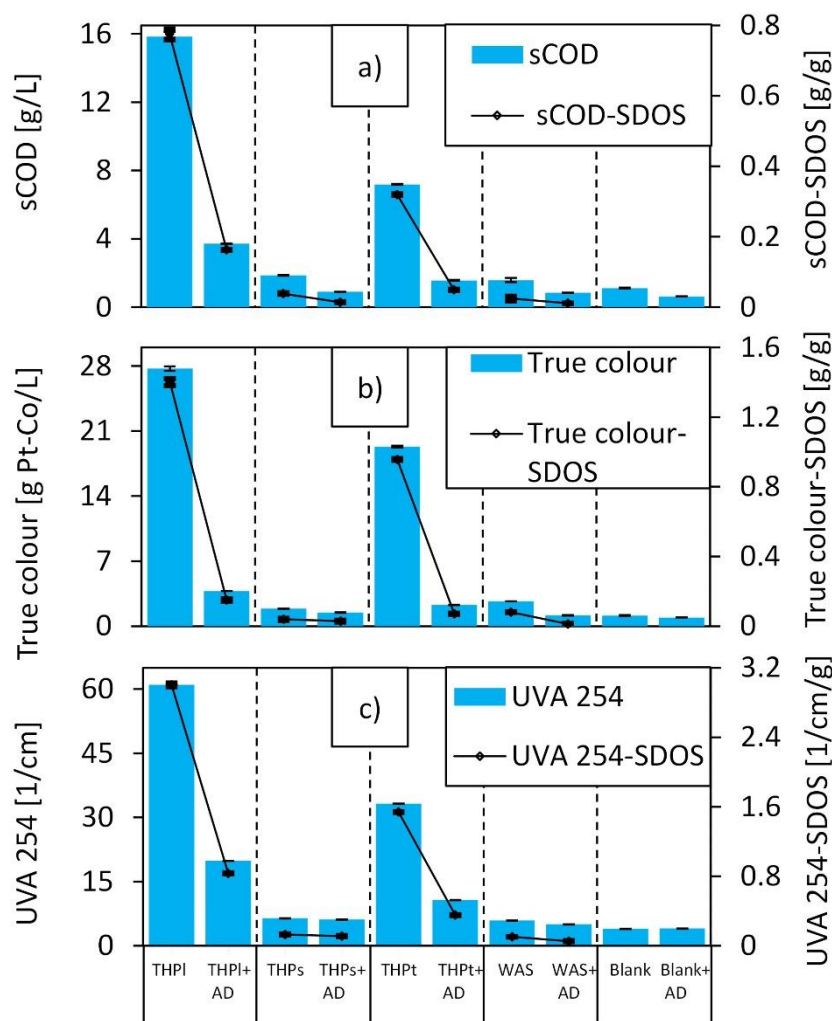
Soluble proteins (mgBSA/L)	16,993±1,480	2,406±231	17,578±896	Not detected.
Soluble carbohydrates (mg/L)	3,353±895	1,025±69	2,488±1,053	367±37
VFA mg (COD/L)	1,885±81	210±17	1,997±74	35.2±0.2
UVA 254 (1/cm)	207.2±0.2	41.93±0.05	207.6±0.2	0.688±0.001
True colour (g Pt-Co/L)	81.0±0.2	8.54±0.02	84.1±0.2	0.123±0.002

Table 2.1 also shows the BMPs of the analysed samples. Obtained values clearly indicate that the THP<sub>i</sub> fraction had the highest biodegradability, reaching 66% of the theoretical CH<sub>4</sub> production. Furthermore, THP<sub>s</sub> and WAS showed about 34% of biodegradability, indicating the low biodegradability of both substrates. The BMP of THP<sub>i</sub> corresponded to the weighted average of the BMPs of THP<sub>i</sub> and THP<sub>s</sub>, given a mass distribution of 40% in the supernatant and 60% in the pellet during the fractionation. The assessed biodegradability of WAS and THP<sub>i</sub> was slightly lower than the results obtained by Stuckey and McCarty (1984) and Jeong et al. (2019) at similar conditions. However, as suggested by Jeong et al. (2019), a high sludge concentration during THP may result in low BMP values of the pre-treated sludge due to mass transfer limitations. Notably, in our work, WAS was pre-treated at a concentration of 16.6% (166.8±0.4 gTS/L in Table 2.1), whereas in Jeong et al. (2019) the highest concentration reached was 7%. It is noteworthy that THP<sub>i</sub> was sampled before it was diluted to enter the anaerobic reactors, which explains the high TS concentration. Moreover, in the case of WAS and THP<sub>i</sub> the increment of about 35% in biodegradability (from 34% to 47%) due to pre-treatment is in accordance with the 25-27% increment that Jeong et al. (2019) found for mesophilic digestion and THP pre-treatment at 175°C. On the other hand, Haug et al. (1978) showed a biodegradability of WAS between 32.5 and 42.5% and an increment of 22.2%, i.e., from 32.5 to 39.7% after pre-treatment. While the biodegradability in their work was similar, the attained increment was lower than the one obtained in our present work, even though pre-treatment conditions were similar (175°C for 0.5 hours).

### 2.3.2. Occurrence and degradation of melanoidins

Figure 2.1-a shows the concentration of sCOD and its specific degree of solubilisation (sCOD-SDOS) in the studied samples before and after anaerobic digestion, (“+AD” indicates anaerobically digested samples). The sCOD-SDOS value relates the sCOD concentration at a specific moment to the initial substrate COD. This parameter is introduced to discount the

effect of the culture medium, and inoculum due to endogenous respiration. Besides, the concentrations shown were measured in the reaction broth, which includes the substrate, inoculum, and culture medium. The sCOD-SDOS decreased after AD in all analysed samples, showing that organic matter, which was solubilised during THP, was largely biodegraded under anaerobic conditions. Results showed a very high anaerobic biodegradability of the sCOD observed in the samples THP<sub>i</sub> and THP<sub>t</sub>. On the other hand, THP<sub>s</sub> and WAS showed less soluble organics before AD, which was a consequence of the particulate nature of the samples. The residual sCOD after AD was considered recalcitrant under anaerobic conditions, and accounted for 16.2, 1.4, 4.9 and 1.1% of the tCOD in THP<sub>i</sub>, THP<sub>s</sub>, THP<sub>t</sub>, and WAS, respectively. In practice, anaerobically recalcitrant sCOD will leave the anaerobic digester with the reject water and will be conveyed to any subsequent step after AD, such as struvite precipitation and/or partial nitrification/anammox processes, or will be directed toward the WWTP headworks. The sCOD in the analysed samples was correlated with true colour (Figure 2.1-b), UVA 254 (Figure 2.1-c) and soluble proteins (Figure 2.3-b), indicating that the solubilised organic matter contained proteins, aromatics, and coloured compounds such as melanoidins. The formation of soluble melanoidins in THP has been previously reported by Dwyer and Lant (2008), and colour and UVA 254 were used to estimate their concentration. Melanoidins, as well as humic substances, can be classified according to their acid/base solubility in i) fulvic acids (always soluble), ii) humic acids (insoluble at pH<2) and iii) insoluble humins (Sutton and Sposito, 2005). However, in our present work, sCOD, true colour, and UVA 254 only accounted for the fulvic and humic fractions that are soluble at the pH of the experiments, without distinction between humic and fulvic acid fractions.



**Figure 2.1.** Chemical analysis of the different THP-treated fractions and other sludge samples subjected to AD (indicated as +AD): a) Soluble COD concentration and sCOD-SDOS; b) True colour concentration and true colour-SDOS; c) UVA 254 concentration and UVA254-SCOD. The data consider the substrates dilution with inoculum and culture medium.

Figure 2.2-a and Figure 2.2-b show the MW distributions before and after AD as coloured bars in the soluble part of the analysed samples. The size of computed areas under the curve with 254 nm and 210 nm showed a similar trend as sCOD, true colour, UVA 254, and soluble proteins, in which THP<sub>I</sub> followed by THP<sub>t</sub> had the highest concentrations of humic substances, followed by THP<sub>s</sub> and WAS. The concentration of humic substances (254nm) decreased after AD. In addition, for both wavelengths, the MW of the humic substances before AD was mainly below 3.6 kDa, which according to MacCarthy (2001), corresponds to a fulvic acids fraction. The compounds measured in the Blank and WAS were very likely not melanoidins but

extracellular polymeric substances (EPS), which are commonly present in aerobic and anaerobic biomass (D'Abzac et al., 2010; Fr et al., 1995). The presence of EPS-like compounds was more evident in WAS, in which the fraction larger than 29.1 kDa was the highest in the measurements at 210 nm (Figure 2.2-b). After AD, the concentration of compounds measured at 254 nm and 210 nm decreased for all THP fractions, showing that the anaerobic microorganisms either consumed or adsorbed part of these substances, removing them from the soluble phase, as shown in Figure 2.2-b and Figure 2.2-c. For the pre-treated samples, the low MW molecules showed the highest biodegradability, and the fraction below 1.1 kDa, decreased in all samples analysed at 254 nm and 210 nm wavelengths. The low MW fraction may have consisted of furfural, hydroxymethylfurfural, and similar compounds, which have been identified as intermediates of Maillard reactions (Hodge, 1953). These compounds are reported to be biodegradable under anaerobic conditions (Boopathy, 2002; Huang et al., 2019; Park et al., 2012), which may explain our observed results (Figure 2.2 -a and Figure 2.2-b).

Figure 2.2-c shows URI per range of MW in each of the samples analysed before and after AD. As can be observed in all fractionated THP samples, compounds with a MW exceeding 3.6 kDa increased the URI values during AD. This URI increase indicated that in these MWs ranges, either the microorganisms converted the aromatic compounds or there was an increase in the non-aromatic substances. Non-aromatic substances increase can possibly be attributed to the excretion of soluble EPS during anaerobic biomass growth in the batch reactors, increasing the UV210 absorbance in these fractions. Moreover, within the pre-treated samples, compounds with a MW below 3.6 kDa increased their aromaticity after AD, which is indicated by decreasing URI values. This indicates that the low-MW-aromatic compounds (low URI) were biodegraded during AD as discussed before (Figure 2.2-b). In the case of the non-pre-treated samples, WAS and Blank samples, the fractions  $>29.1\text{ kDa}$  and  $\leq 0.1\text{ kDa}$  decreased their specific aromaticity, indicated by an increased URI. The rest of the MW fractions increased their aromaticity after AD. Since WAS and blank samples did not contain melanoidins, the changes in URI were most likely caused by changes in the EPS structure and the presence of degradation products of cell material in the case of WAS. The EPS spectrum has shown absorbance in the range 210-220 nm and 255-265 nm, which are related to protein and humic-like structures (Meng et al., 2016; Wang et al., 2018).

Figure 2.2-d shows the NFRI corresponding to humic-like, fulvic-like and protein-like substances in the FEEM. As observed in Figure 2.2-d NFRI decreased after AD showing a similar trend as sCOD (Figure 2.1-a) and total area in SEC-HPLC analysis (Figure 2.2-a and

Figure 2.2-b). Also, the pre-treated samples showed a higher degree of fluorescence compared to WAS, evidencing the presence of humic substances. Furthermore, it can be observed that after AD the humic-like and fulvic-like fractions remained at a similar level, indicating lower biodegradability in these fractions. On the other hand, the protein-like fraction decreased in all the samples after AD, indicating that this fraction can be degraded under anaerobic conditions. Overall, THP increased the solubilisation and formation of biodegradable and recalcitrant melanoidins. Among the aromatic compounds formed during THP, we observed anaerobic biodegradability in the low molecular weight fraction, which were associated with protein-like substances.

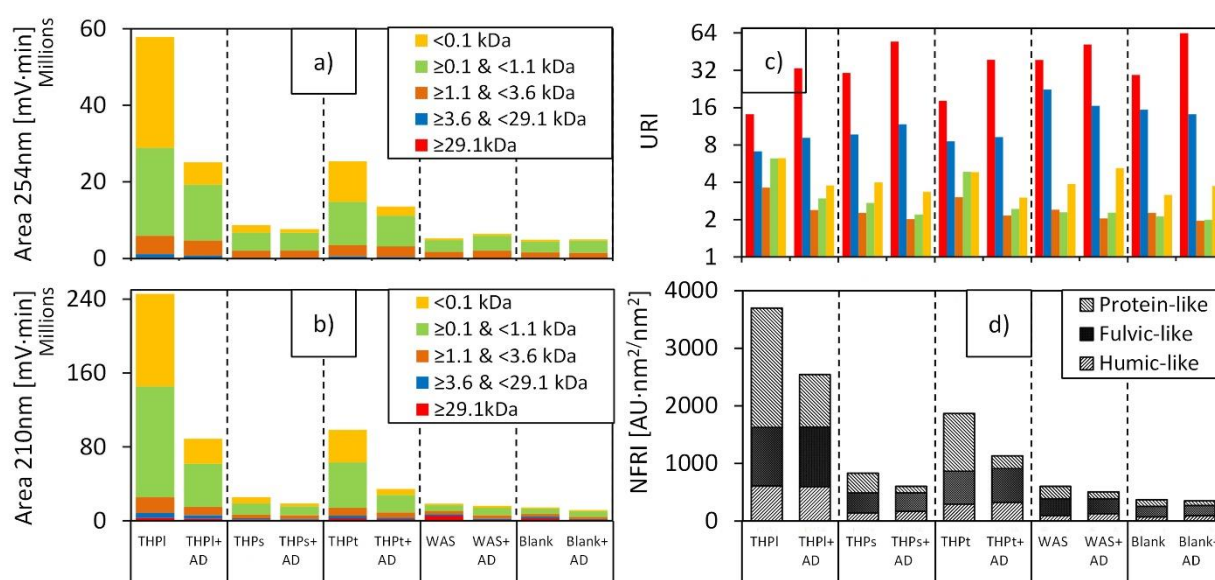


**Figure 2.2.** a) Distribution of MWs at 254 nm; b) Distribution of MWs at 210 nm; c) URI in each MW interval (logarithmic scale); d) Protein-like, fulvic-like and humic-like NFI in FEEM. Bars represent the samples before and after (+AD) anaerobic digestion.

### 2.3.3. TAN formation and release

TAN release was studied in the fractionated substrates before and after AD. Despite that FAN is considered the main inhibitor, TAN was chosen as determining parameter since TAN can be measured directly, and it was not possible to differentiate the inhibition caused by  $\text{NH}_4^+$  or FAN (Astals et al., 2018). Before AD, TAN originated from: TAN in the substrates, TAN present in the culture medium used in the BMP tests (Table 2.A1), and TAN in the inoculum. Moreover, TAN release after the BMP tests originated from TAN released from substrate digestion, and TAN released from the inoculum due to endogenous respiration. Figure 2.3

shows the concentration of TAN and soluble proteins, both before and after performing the BMP tests. The SDOSs of these compounds are shown in Figure 2.3 as well. Following the former reasoning, we choose TAN-SDOSs and soluble proteins-SDOS to assess the TAN and soluble COD release caused exclusively by the substrates added in the BMP bottles.

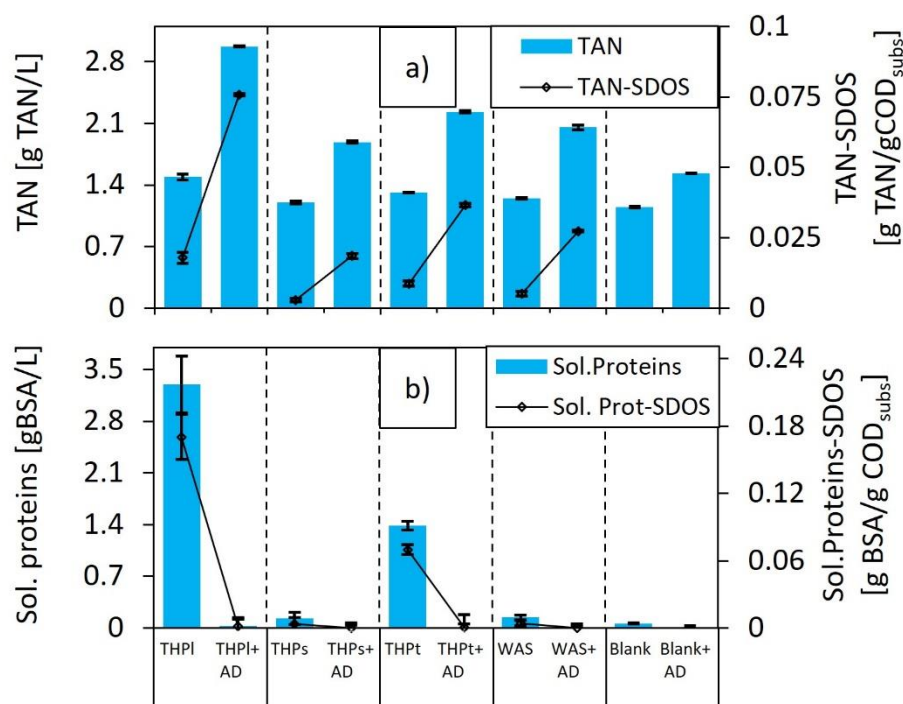


**Figure 2.3.** a) TAN concentration and TAN-SDOS; b) Soluble proteins concentration and soluble proteins-SDOS; in the samples before and after (+AD) BMP tests, in the analysed samples.

From Figure 2.3-a it can be observed that before AD, TAN-SDOSs of THPI and THPt showed values 3.5- and 1.7-times higher than WAS. The elevated TAN-SDOS concentration before AD indicated that the conditions during THP were such that they caused proteins deamination. The physicochemical breakdown of proteins to the extent of deamination during THP thermochemical reactions has already been reported by Wilson and Novak (2009). Conversely, before AD, TAN-SDOSs in WAS and THPs showed the lowest values, indicating that in these samples, N was contained in the particulate organics. In addition to the TAN solubilisation/formation during pre-treatment, AD resulted in a TAN-SDOS increase of at least four times in all samples analyzed.

Figure 2.3-a and b show that THPI rendered the highest TAN-SDOS increase during AD showing that most of the biodegradable proteins were in the soluble fraction of THP-treated sludge. Strikingly, THPs showed the lowest increase in TAN-SDOS during AD, i.e., from 2.8

to 19 mgTAN/gCOD<sub>subs</sub>, indicating a lower concentration of biodegradable proteins in THP. Guo et al. (2020) showed the presence of structural proteins in WAS pellet being part of the non-soluble EPS matrix, which confirms our present finding. Figure 2.3-b shows that the soluble proteins-SDOS before AD showed a similar tendency as TAN, rendering the highest values in the sample THP<sub>i</sub> followed by THP<sub>s</sub>. Figure 2.3-b also shows that in all the cases the solubilized proteins are biodegradable during AD, which resulted in accumulating TAN in the digester broth.

The TAN<sub>released</sub>/COD<sub>consumed</sub> ratios for the THP fractions were  $99 \pm 17$ ,  $46 \pm 9$  and  $56 \pm 15$  mgTAN/gCOD in THP<sub>i</sub>, THP<sub>s</sub> and THP<sub>t</sub>, and  $64 \pm 10$  mgTAN/gCOD for WAS, respectively. Comparing TAN<sub>released</sub>/COD<sub>consumed</sub>, it can be inferred that THP<sub>i</sub> consisted to a large extent of biodegradable proteins, considering 121 mgTAN/gCOD as the stoichiometric maximum from serum albumin digestion (C<sub>123</sub>H<sub>193</sub>O<sub>37</sub>N<sub>35</sub>, CAS 98420-25-8). The opposite was observed in THP<sub>s</sub>, in which the biodegradable solid fraction released about half of the TAN that was released in total by THP<sub>i</sub> during AD. The low TAN<sub>released</sub>/COD<sub>consumed</sub> in THP<sub>s</sub> indicated that the biodegradable solid fraction of THP<sub>t</sub> contained less biodegradable proteins. Moreover, the THP<sub>t</sub> sample released less TAN per biodegradable substrate than WAS. Considering that the BMP value of THP<sub>t</sub> was higher than that of WAS, THP increased the biodegradability of other organics too (not just proteins). At the same time, the decrease in TAN<sub>released</sub>/COD<sub>consumed</sub> in THP<sub>t</sub> compared to WAS was likely caused by the Maillard reaction, which rendered AD-recalcitrant melanoidins (Dwyer et al., 2008; Martins and van Boekel, 2003). Overall, THP increased the solubilisation of biodegradable organic matter (shown as THP<sub>i</sub>) and increased the BMP and TAN release, specifically from the soluble fraction. However, the use of THP reduced the TAN<sub>released</sub>/COD<sub>consumed</sub> ratio, due to the formation of melanoidins and deamination during THP (Wilson and Novak, 2009; Wilson et al., 2011).

#### **2.3.4. Acute inhibition of the methanogenic biomass**

By assessing the mSMA at the beginning of the BMP tests, using fresh inoculum and the fractionated substrates, we were able to determine any possible inhibitory effect on the methanogenic biomass caused by compounds that were present in the initial substrate, such as the organic matter released during pre-treatment. Additionally, the mSMA results obtained after the BMP tests (+AD) provided information about possible metabolites that were formed during AD, affecting the digestion process.



Figure 2.4-a shows that the mSMAs of inoculum with the addition of the THP-pre-treated samples were  $84.2 \pm 1.3$ ,  $87.1 \pm 1.7$  and  $87.0 \pm 0.2$  mgCOD/gVS/day for THP<sub>i</sub>, THP<sub>s</sub> and THP<sub>t</sub> respectively. Results showed that none of them was statistically different from the blank sample (inoculum only), using mean differences t-test (p-values of 0.36, 0.08 and 0.1, respectively). The equal mSMA compared to the Blank in the pre-treated samples before BMP indicated that there was no (acute) inhibition of methanogens that could have been caused by compounds formed or solubilised during THP. On the other hand, mSMA of WAS was 39% higher compared to the blank test, which was significantly different with a p-value = 0.001 in a mean difference t-test. The difference in mSMA between the Blank and WAS addition might be explained by the storage of WAS in a “sludge-buffer-tank” at the WWTP for approximately two weeks. This storage period might have led to an accumulation of methanogenic microorganisms that increased the acetotrophic activity in this sample. The CAMBI® system at the WWTP was fed from the same sludge buffer, but any microbial activity would have been destroyed during the THP pre-treatment. Therefore, the mSMA in the samples with addition of the pre-treated fractions was not affected.

Figure 2.4-a also shows the severe decrease in the microbial activity that was observed in all the samples analysed after the BMP tests (samples +AD). Results indicated that one or more compounds produced during AD decreased the acetotrophic activity of the anaerobic inoculum. The samples after AD were statistically indifferent with p-values of 0.628 in a single factor ANOVA, with 95% of confidence. Among the studied parameters, the increased concentrations of TAN and FAN possibly explained the decrease in acetotrophic activity after AD (Astals et al., 2018). Figure 2.3-a and Figure 2.4-b show the concentrations TAN and FAN, respectively, in the studied samples before and after the BMP tests. FAN increased in all the samples after AD, which was a consequence of the increased TAN concentration, plus a slight increase in the pH during the incubations. To the authors' knowledge, there is not a clear threshold in the literature for inhibition of acetotrophic methanogenic activity due to the presence of TAN and FAN (Capson-Tojo et al., 2020). Different authors reported different ranges of inhibition for TAN and FAN in AD, e.g. Bhattacharya and Parkin (1989) found that 55 mg FAN/L was the maximum tolerable concentration, while Calli et al. (2005) found a reduction in COD conversion in UASB reactors of 78-98%, with a concentration of 800 mgFAN/L. Literature results indicate that TAN and FAN inhibition thresholds, are inoculum-dependent and might vary depending on the operational conditions and acclimation of the microorganisms to these inhibitors (Chen et al., 2008; Lee et al., 2021; Moerland et al., 2021).

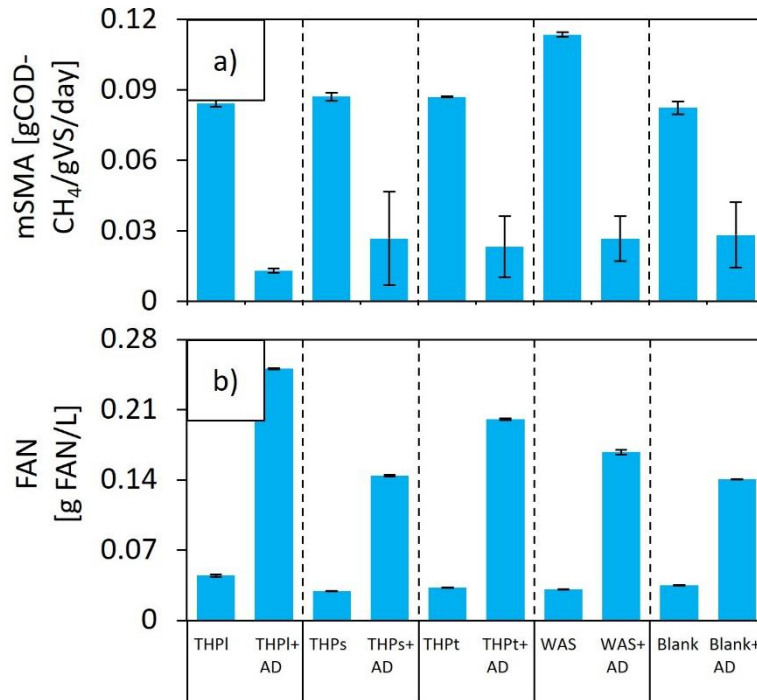


**Figure 2.4.** a) mSMA before and after BMP tests (+AD) in all substrates; b) FAN concentration before and after BMP tests in all substrates.

The influence of possible inhibitors in the samples was further assessed, using the same inoculum as in the mSMA test and applying incremental concentrations of TAN/FAN and melanoidins. Figures 2.5-a and b show the relative SMA values as a percentage of the positive control (without inhibitor) at different TAN/FAN, and melanoidins concentrations. Both TAN and FAN distinctly decreased the SMAs (Figure 2.5-a), and SMAs halved their maximum values at about 2.5 g TAN/L and 100 mg FAN/L. These half-inhibition concentrations were within the range that was observed in the studied samples after BMP (+AD). Moreover, the inoculum that was used in both (m)SMA and BMP was likely not well acclimated to increased concentrations of TAN and FAN, since the full-scale digester from where the inoculum was obtained contained around 789 mgTAN/L and 41 mgFAN/L. The mentioned full-scale digester was not equipped with any sludge pre-treatment technique.

Contrary to the observed TAN and FAN inhibition of the SMA, the SMAs at incremental concentrations of melanoidins showed no evidence of inhibition of the methanogenic activity, even at COD concentrations as high as 20 gCOD/L, when, conversely, higher activity was observed (Figure 2.5-b). The increased activity can possibly be attributed to some methanogens that might have been contained in the melanoidins stock solution due to the anaerobic pre-digestion process with anaerobic digestate. Our current findings agree with the results of

Rodríguez-Abalde et al. (2011) who did not find evidence that melanoidins can cause inhibition on methanogens. In contrast, Penaud et al. (2000) posed that there are recalcitrant compounds that may cause a decrease in anaerobic activity. However, in their study, TAN/FAN were not measured, although both compounds are expected to be present in ranges that might have led to process inhibition. Other studies also reported inhibition of methanogens by humic substances; however, the diversity of the microorganisms present in a full-scale inoculum might have helped to mitigate this effect (Khadem et al., 2017; Yap et al., 2018; Zhang et al., 2022). TAN/FAN are well-known inhibitors of AD. However, in literature, it is well described that anaerobic biomass can be acclimated to high TAN/FAN concentrations (Yan et al., 2019). The expected effect of increased TAN/FAN is especially high during the transition phase, when an AD reactor with no pre-treatment starts using THP. Under such conditions, the sudden increase in TAN/FAN concentrations might lead to instabilities in the process before the anaerobic biomass is acclimated to the new regime.

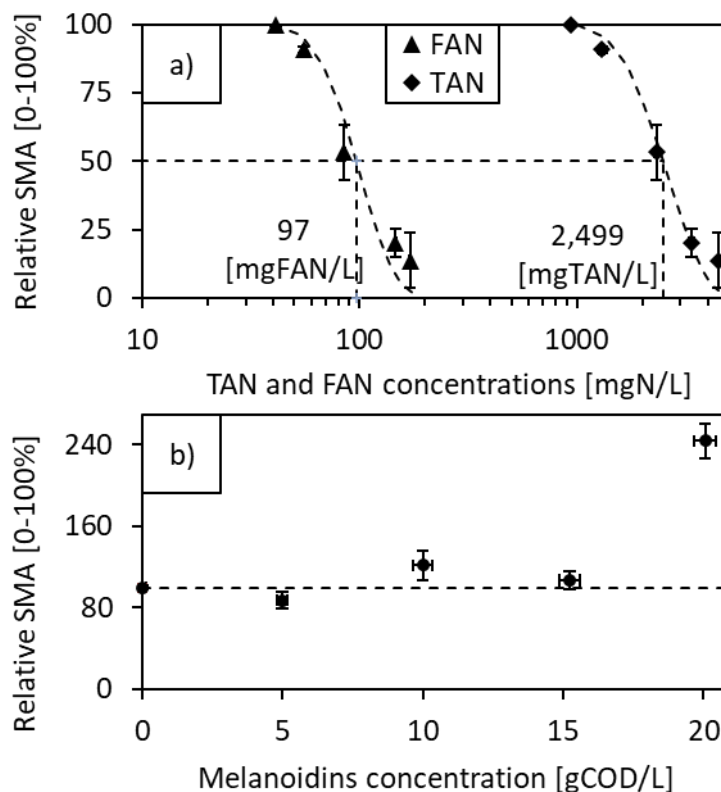


**Figure 2.5.** a) Relative SMA values of the inoculum used in the mSMA and BMP tests at different concentrations TAN and FAN; 100% agrees with an SMA of  $96 \pm 1$  mg COD/gVS/day. Note: X-axis is a log-scale. b) Relative SMA values at incremental melanoidins concentrations

of the inoculum used in the SMA and BMP tests; 100% agrees with an SMA of  $64 \pm 1$  mg COD/gVS/day.

## 2.4. Conclusions

From our present study the following conclusions can be drawn:

- THP of WAS released digestible organics and increased the concentration of aromatic compounds, which were partially biodegradable under anaerobic conditions. Especially, the aromatic fractions with a MW under 1.1 kDa that were related to protein-like compounds were partially biodegradable.
- TAN was limitedly released during THP solely, but TAN concentrations increased drastically during subsequent AD.
- THP increased the solubilisation and biodegradability of organic matter which increased the BMPs. However, the ratio  $\text{TAN}_{\text{released}}/\text{COD}_{\text{consumed}}$  decreased, due to THP-related deamination and the Maillard reaction of proteinaceous material that forms partially AD-recalcitrant melanoidins.
- Melanoidins that were formed during THP of WAS did not cause acute inhibition on acetotrophic methanogenesis of a full-scale inoculum sample.
- Inhibition of methanogens, while digesting THP-treated sludge, was likely a consequence of the released TAN (and FAN formation) from an increased amount of biodegradable proteins.

## **2.5. List of abbreviations**

+AD: samples taken after the BMP was performed.

AD: anaerobic digestion.

AMPTS: automated methane potential test system.

BMP: biochemical methane potential.

BSA: bovine serum albumin.

EBPR: enhanced biological phosphorus removal.

EPS: extracellular polymeric substances.

FAN: free ammonia nitrogen.

FEEM: Fluorescence excitation emission matrix.

mSMA: modified specific methanogenic activity.

MW: molecular weight.

NFRI: normalised fluorescence regional integration.

sCOD: soluble chemical oxygen demand.

SDOS: specific degree of solubilisation.

SEC-HPLC: size exclusion chromatography.

SMA: specific methanogenic activity.

TAN: total ammoniacal nitrogen.

tCOD: total chemical oxygen demand.

THP: thermal hydrolysis process.

THP<sub>l</sub>: THP-liquid.

THP<sub>s</sub>: THP-solid.

THP<sub>t</sub>: THP-total.

TS: total solids.

UFLC: ultrafast liquid chromatography.

URI: ultraviolet absorbance ratio index.

UVA 254: ultraviolet absorbance at 254 nm.

VFA: volatile fatty acids.

VS: volatile solids.

WAS: waste activated sludge.

WWTP: wastewater treatment plant.

## 2.6. References

- Akindele, A.A. and Sartaj, M. 2018. The toxicity effects of ammonia on anaerobic digestion of organic fraction of municipal solid waste. *Waste Management* 71, 757-766.
- Appels, L., Baeyens, J., Degreè, J. and Dewil, R. 2008. Principles and potential of the anaerobic digestion of waste-activated sludge. *Progress in Energy and Combustion Science* 34(6), 755-781.
- Astals, S., Peces, M., Batstone, D.J., Jensen, P.D. and Tait, S. 2018. Characterising and modelling free ammonia and ammonium inhibition in anaerobic systems. *Water Research* 143, 127-135.
- Balasundaram, G., Banu, R., Varjani, S., Kazmi, A.A. and Tyagi, V.K. 2022. Recalcitrant compounds formation, their toxicity, and mitigation: Key issues in biomass pretreatment and anaerobic digestion. *Chemosphere* 291, 132930.
- Barber, W.P.F. 2016. Thermal hydrolysis for sewage treatment: A critical review. *Water Research* 104, 53-71.
- Bernardo, E.C., Egashira, R. and Kawasaki, J. 1997. Decolorization of molasses' wastewater using activated carbon prepared from cane bagasse. *Carbon* 35(9), 1217-1221.
- Bhattacharya, S.K. and Parkin, G.F. 1989. The effect of ammonia on methane fermentation processes. *Journal (Water Pollution Control Federation)*, 55-59.
- Boopathy, R. 2002. Methanogenesis from Furfural by Defined Mixed Cultures. *Current Microbiology* 44(6), 406-410.
- Brons, H.J., Field, J.A., Lexmond, W.A.C. and Lettinga, G. 1985. Influence of humic acids on the hydrolysis of potato protein during anaerobic digestion. *Agricultural Wastes* 13(2), 105-114.
- Calli, B., Mertoglu, B., Inanc, B. and Yenigun, O. 2005. Effects of high free ammonia concentrations on the performances of anaerobic bioreactors. *Process Biochemistry* 40(3), 1285-1292.
- Capson-Tojo, G., Moscoviz, R., Astals, S., Robles, Á. and Steyer, J.P. 2020. Unraveling the literature chaos around free ammonia inhibition in anaerobic digestion. *Renewable and Sustainable Energy Reviews* 117, 109487.
- Chen, W., Westerhoff, P., Leenheer, J.A. and Booksh, K. 2003. Fluorescence Excitation–Emission Matrix Regional Integration to Quantify Spectra for Dissolved Organic Matter. *Environmental Science & Technology* 37(24), 5701-5710.
- Chen, Y., Cheng, J.J. and Creamer, K.S. 2008. Inhibition of anaerobic digestion process: A review. *Bioresource Technology* 99(10), 4044-4064.
- D'Abzac, P., Bordas, F., Van Hullebusch, E., Lens, P.N.L. and Guibaud, G. 2010. Extraction of extracellular polymeric substances (EPS) from anaerobic granular sludges: comparison of chemical and physical extraction protocols. *Applied Microbiology and Biotechnology* 85(5), 1589-1599.
- Deng, Z., van Linden, N., Guillen, E., Spanjers, H. and van Lier, J.B. 2021. Recovery and applications of ammoniacal nitrogen from nitrogen-loaded residual streams: A review. *Journal of Environmental Management* 295, 113096.
- Dubois, M., Gilles, K., Hamilton, J.K., Rebers, P.A. and Smith, F. 1951. A Colorimetric Method for the Determination of Sugars. *Nature* 168(4265), 167-167.
- Dwyer, J. and Lant, P. 2008. Biodegradability of DOC and DON for UV/H<sub>2</sub>O<sub>2</sub> pre-treated melanoidin based wastewater. *Biochemical Engineering Journal* 42(1), 47-54.
- Dwyer, J., Starrenburg, D., Tait, S., Barr, K., Batstone, D.J. and Lant, P. 2008. Decreasing activated sludge thermal hydrolysis temperature reduces product colour, without decreasing degradability. *Water Research* 42(18), 4699-4709.



- Ellis, G.P. (1959) *Advances in Carbohydrate Chemistry*. Wolfrom, M.L. (ed), pp. 63-134, Academic Press.
- Emerson, K., Russo, R.C., Lund, R.E. and Thurston, R.V. 1975. Aqueous ammonia equilibrium calculations: effect of pH and temperature. *Journal of the Fisheries Board of Canada* 32(12), 2379-2383.
- Fr, B., Griebe, T. and Nielsen, P. 1995. Enzymatic activity in the activated-sludge floc matrix. *Applied microbiology and biotechnology* 43(4), 755-761.
- Fux, C. and Siegrist, H. 2004. Nitrogen removal from sludge digester liquids by nitrification/denitrification or partial nitritation/anammox: environmental and economical considerations. *Water Science and Technology* 50(10), 19-26.
- Fytli, D. and Zabaniotou, A. 2008. Utilization of sewage sludge in EU application of old and new methods—A review. *Renewable and Sustainable Energy Reviews* 12(1), 116-140.
- Gao, J., Li, L., Yuan, S., Chen, S. and Dong, B. 2022. The neglected effects of polysaccharide transformation on sludge humification during anaerobic digestion with thermal hydrolysis pretreatment. *Water Research* 226, 119249.
- Gonzalez, A., Hendriks, A.T.W.M., van Lier, J.B. and de Kreuk, M. 2018. Pre-treatments to enhance the biodegradability of waste activated sludge: Elucidating the rate limiting step. *Biotechnology Advances* 36(5), 1434-1469.
- Guo, H., Felz, S., Lin, Y., van Lier, J.B. and de Kreuk, M. 2020. Structural extracellular polymeric substances determine the difference in digestibility between waste activated sludge and aerobic granules. *Water Research* 181, 115924.
- Haug, R.T., Stuckey, D.C., Gossett, J.M. and McCarty, P.L. 1978. Effect of thermal pretreatment on digestibility and dewaterability of organic sludges. *Journal (Water Pollution Control Federation)*, 73-85.
- Her, N., Amy, G., Sohn, J. and Gunten, U. 2008. UV absorbance ratio index with size exclusion chromatography (URI-SEC) as an NOM property indicator. *Journal of Water Supply: Research and Technology-Aqua* 57(1), 35-44.
- Higgins, M.J., Beightol, S., Mandahar, U., Suzuki, R., Xiao, S., Lu, H.-W., Le, T., Mah, J., Pathak, B., DeClippeleir, H., Novak, J.T., Al-Omari, A. and Murthy, S.N. 2017. Pretreatment of a primary and secondary sludge blend at different thermal hydrolysis temperatures: Impacts on anaerobic digestion, dewatering and filtrate characteristics. *Water Research* 122, 557-569.
- Hodge, J.E. 1953. Dehydrated foods, chemistry of browning reactions in model systems. *J. Agric. Food Chem.* 1(15), 928-943.
- Holliger, C., Alves, M., Andrade, D., Angelidaki, I., Astals, S., Baier, U., Bougrier, C., Buffière, P., Carballa, M. and De Wilde, V. 2016. Towards a standardization of biomethane potential tests. *Water Science and Technology*, wst2016336.
- Horvat, Š. and Jakas, A. 2004. Peptide and amino acid glycation: New insights into the maillard reaction. *J. Pept. Sci.* 10(3), 119-137.
- Huang, C., Xiong, L., Guo, H.-J., Li, H.-L., Wang, C., Chen, X.-F., Zhao, C. and Chen, X.-D. 2019. Anaerobic digestion of elephant grass hydrolysate: Biogas production, substrate metabolism and outlet effluent treatment. *Bioresource Technology* 283, 191-197.
- Jeong, S.Y., Chang, S.W., Ngo, H.H., Guo, W., Nghiem, L.D., Banu, J.R., Jeon, B.-H. and Nguyen, D.D. 2019. Influence of thermal hydrolysis pretreatment on physicochemical properties and anaerobic biodegradability of waste activated sludge with different solids content. *Waste Management* 85, 214-221.
- Kabouris, J.C., Tezel, U., Pavlostathis, S.G., Engelmann, M., Dulaney, J., Gillette, R.A. and Todd, A.C. 2009. Methane recovery from the anaerobic codigestion of municipal sludge and FOG. *Bioresource Technology* 100(15), 3701-3705.

- Kelessidis, A. and Stasinakis, A.S. 2012. Comparative study of the methods used for treatment and final disposal of sewage sludge in European countries. *Waste Management* 32(6), 1186-1195.
- Kepp, U., Machenbach, I., Weisz, N. and Solheim, O.E. 2000. Enhanced stabilisation of sewage sludge through thermal hydrolysis - three years of experience with full scale plant. *Water Science and Technology* 42(9), 89-96.
- Khadem, A.F., Azman, S., Plugge, C.M., Zeeman, G., van Lier, J.B. and Stams, A.J.M. 2017. Effect of humic acids on the activity of pure and mixed methanogenic cultures. *Biomass and Bioenergy* 99, 21-30.
- Klavins, M., Eglite, L. and Serzane, J. 1999. Methods for Analysis of Aquatic Humic Substances. *Critical Reviews in Analytical Chemistry* 29(3), 187-193.
- Koster, I.W. and Lettinga, G. 1984. The influence of ammonium-nitrogen on the specific activity of pelletized methanogenic sludge. *Agricultural Wastes* 9(3), 205-216.
- Lee, J., Kim, E. and Hwang, S. 2021. Effects of inhibitions by sodium ion and ammonia and different inocula on acetate-utilizing methanogenesis: Methanogenic activity and succession of methanogens. *Bioresource Technology* 334, 125202.
- Li, J., Hao, X., van Loosdrecht, M.C.M., Luo, Y. and Cao, D. 2019. Effect of humic acids on batch anaerobic digestion of excess sludge. *Water Research* 155, 431-443.
- Lin, J.-G., Chang, C.-N. and Chang, S.-C. 1997. Enhancement of anaerobic digestion of waste activated sludge by alkaline solubilization. *Bioresource Technology* 62(3), 85-90.
- Luostarinen, S., Luste, S. and Sillanpää, M. 2009. Increased biogas production at wastewater treatment plants through co-digestion of sewage sludge with grease trap sludge from a meat processing plant. *Bioresource Technology* 100(1), 79-85.
- MacCarthy, P. 2001. The principles of humic substances. *Soil Science* 166(11), 738-751.
- Martins, S.I.F.S. and van Boekel, M.A.J.S. 2003. Melanoidins extinction coefficient in the glucose/glycine Maillard reaction. *Food Chemistry* 83(1), 135-142.
- Mata-Alvarez, J., Dosta, J., Romero-Güiza, M.S., Fonoll, X., Peces, M. and Astals, S. 2014. A critical review on anaerobic co-digestion achievements between 2010 and 2013. *Renewable and Sustainable Energy Reviews* 36(Supplement C), 412-427.
- Meng, L., Xi, J. and Yeung, M. 2016. Degradation of extracellular polymeric substances (EPS) extracted from activated sludge by low-concentration ozonation. *Chemosphere* 147, 248-255.
- Migo, V.P., Matsumura, M., Del Rosario, E.J. and Kataoka, H. 1993. The effect of pH and calcium ions on the destabilization of melanoidin. *Journal of Fermentation and Bioengineering* 76(1), 29-32.
- Moerland, M.J., Bruning, H., Buisman, C.J.N. and van Eekert, M.H.A. 2021. Advanced modelling to determine free ammonia concentrations during (hyper-)thermophilic anaerobic digestion in high strength wastewaters. *Journal of Environmental Chemical Engineering* 9(6), 106724.
- Ngo, P.L., Udugama, I.A., Gernaey, K.V., Young, B.R. and Baroutian, S. 2021. Mechanisms, status, and challenges of thermal hydrolysis and advanced thermal hydrolysis processes in sewage sludge treatment. *Chemosphere* 281, 130890.
- Ochs, P., Martin, B., Germain-Cripps, E., Stephenson, T., van Loosdrecht, M. and Soares, A. 2023. Techno-economic analysis of sidestream ammonia removal technologies: Biological options versus thermal stripping. *Environmental Science and Ecotechnology* 13, 100220.
- Ohemeng-Ntiamoah, J. and Datta, T. 2018. Evaluating analytical methods for the characterization of lipids, proteins and carbohydrates in organic substrates for anaerobic co-digestion. *Bioresource Technology* 247(Supplement C), 697-704.

- Ortega-Martínez, E., Chamy, R. and Jeison, D. 2021. Thermal pre-treatment: Getting some insights on the formation of recalcitrant compounds and their effects on anaerobic digestion. *Journal of Environmental Management* 282, 111940.
- Park, J.-H., Yoon, J.-J., Park, H.-D., Lim, D.J. and Kim, S.-H. 2012. Anaerobic digestibility of algal bioethanol residue. *Bioresource Technology* 113, 78-82.
- Penaud, V., Delgenès, J.-P. and Moletta, R. 2000. Characterization of soluble molecules from thermochemically pretreated sludge. *Journal of Environmental Engineering* 126(5), 397-402.
- Pérez-Elvira, S., Fdz-Polanco, M. and Fdz-Polanco, F. 2010. Increasing the performance of anaerobic digestion: pilot scale experimental study for thermal hydrolysis of mixed sludge. *Frontiers of Environmental Science & Engineering in China* 4(2), 135-141.
- Rahmani, A.M., Tyagi, V.K., Gunjyal, N., Kazmi, A.A., Ojha, C.S.P. and Moustakas, K. 2023. Hydrothermal and thermal-alkali pretreatments of wheat straw: Co-digestion, substrate solubilization, biogas yield and kinetic study. *Environmental Research* 216, 114436.
- Rice, E.W., Baird, R.B., Eaton, A.D. and Clesceri, L.S. (2012) Standard methods for the examination of water and wastewater, American Public Health Association Washington, DC.
- Ringoot, D., Kleiven, H. and Panter, K. 2012 Energy efficient thermal hydrolysis with steam explosion, pp. 1-8.
- Rodríguez-Abalde, Á., Fernández, B., Silvestre, G. and Flotats, X. 2011. Effects of thermal pre-treatments on solid slaughterhouse waste methane potential. *Waste management* 31(7), 1488-1493.
- Rufian-Henares, J.A. and de la Cueva, S.P. 2009. Antimicrobial Activity of Coffee Melanoidins□ A Study of Their Metal-Chelating Properties. *J. Agric. Food Chem.* 57(2), 432-438.
- Silván, J.M., van de Lagemaat, J., Olano, A. and del Castillo, M.D. 2006. Analysis and biological properties of amino acid derivatives formed by Maillard reaction in foods. *Journal of Pharmaceutical and Biomedical Analysis* 41(5), 1543-1551.
- Squire, P.G. (1985) *Methods in Enzymology*, pp. 142-153, Academic Press.
- Stuckey, D.C. and McCarty, P.L. 1984. The effect of thermal pretreatment on the anaerobic biodegradability and toxicity of waste activated sludge. *Water Research* 18(11), 1343-1353.
- Suárez-Iglesias, O., Urrea, J.L., Oulego, P., Collado, S. and Díaz, M. 2017. Valuable compounds from sewage sludge by thermal hydrolysis and wet oxidation. A review. *Science of The Total Environment* 584-585, 921-934.
- Sutton, R. and Sposito, G. 2005. Molecular structure in soil humic substances: the new view. *Environmental science & technology* 39(23), 9009-9015.
- Tarvers, R.C. and Church, F.C. 1985. Use of high-performance size-exclusion chromatography to measure protein molecular weight and hydrodynamic radius. An investigation of the properties of the TSK 3000 SW column. *Int J Pept Protein Res* 26(5), 539-549.
- Valo, A., Carrère, H. and Delgenès, J.P. 2004. Thermal, chemical and thermo-chemical pre-treatment of waste activated sludge for anaerobic digestion. *Journal of Chemical Technology & Biotechnology* 79(11), 1197-1203.
- Vineyard, D., Hicks, A., Karthikeyan, K.G. and Barak, P. 2020. Economic analysis of electrodialysis, denitrification, and anammox for nitrogen removal in municipal wastewater treatment. *Journal of Cleaner Production* 262, 121145.
- Wang, B.-B., Liu, X.-T., Chen, J.-M., Peng, D.-C. and He, F. 2018. Composition and functional group characterization of extracellular polymeric substances (EPS) in activated sludge: the impacts of polymerization degree of proteinaceous substrates. *Water Research* 129, 133-142.

- Wang, S., Hu, Z.-Y., Geng, Z.-Q., Tian, Y.-C., Ji, W.-X., Li, W.-T., Dai, K., Zeng, R.J. and Zhang, F. 2022. Elucidating the production and inhibition of melanoidins products on anaerobic digestion after thermal-alkaline pretreatment. *Journal of Hazardous Materials* 424, 127377.
- Wilén, B.-M., Jin, B. and Lant, P. 2003. The influence of key chemical constituents in activated sludge on surface and flocculating properties. *Water Research* 37(9), 2127-2139.
- Wilson, C.A. and Novak, J.T. 2009. Hydrolysis of macromolecular components of primary and secondary wastewater sludge by thermal hydrolytic pretreatment. *Water Research* 43(18), 4489-4498.
- Wilson, C.A., Tanneru, C.T., Banjade, S., Murthy, S.N. and Novak, J.T. 2011. Anaerobic digestion of raw and thermally hydrolyzed wastewater solids under various operational conditions. *Water Environ Res* 83(9), 815-825.
- Yan, M., Fotidis, I.A., Tian, H., Khoshnevisan, B., Treu, L., Tsapekos, P. and Angelidaki, I. 2019. Acclimatization contributes to stable anaerobic digestion of organic fraction of municipal solid waste under extreme ammonia levels: Focusing on microbial community dynamics. *Bioresource Technology* 286, 121376.
- Yang, G., Zhang, G. and Wang, H. 2015. Current state of sludge production, management, treatment and disposal in China. *Water Research* 78(Supplement C), 60-73.
- Yap, S.D., Astals, S., Lu, Y., Peces, M., Jensen, P.D., Batstone, D.J. and Tait, S. 2018. Humic acid inhibition of hydrolysis and methanogenesis with different anaerobic inocula. *Waste Management* 80, 130-136.
- Yin, J., Liu, J., Chen, T., Long, Y. and Shen, D. 2019. Influence of melanoidins on acidogenic fermentation of food waste to produce volatility fatty acids. *Bioresource Technology* 284, 121-127.
- Zhang, L., Gong, X., Xu, R., Guo, K., Wang, L. and Zhou, Y. 2022. Responses of mesophilic anaerobic sludge microbiota to thermophilic conditions: Implications for start-up and operation of thermophilic THP-AD systems. *Water Research* 216, 118332.
- Zhen, G., Lu, X., Kato, H., Zhao, Y. and Li, Y.-Y. 2017. Overview of pretreatment strategies for enhancing sewage sludge disintegration and subsequent anaerobic digestion: Current advances, full-scale application and future perspectives. *Renewable and Sustainable Energy Reviews* 69(Supplement C), 559-577.

## 2.7. Appendix chapter 2

**Table A2.1.** Culture medium for BMP, mSMA, and SMA tests.

Constituent	Concentration in the medium	Unit
Substrates	19	gCOD/L
Inoculum	28.5	gVS/L
Substrate (only for mSMA and SMA)		
CH <sub>3</sub> COONa	2	gCOD/L
Buffer		
NaHCO <sub>3</sub>	1,000	mg/L
Macronutrients		
NH <sub>4</sub> Cl	1,020	mg/L
CaCl <sub>2</sub> ·2H <sub>2</sub> O	48	mg/L
MgSO <sub>4</sub> ·7H <sub>2</sub> O	54	mg/L
Micronutrients		
FeCl <sub>3</sub> ·4H <sub>2</sub> O	1.2	mg/L
CoCl <sub>2</sub> ·6H <sub>2</sub> O	1.2	mg/L
MnCl <sub>2</sub> ·4H <sub>2</sub> O	0.3	mg/L
CuCl <sub>2</sub> ·2H <sub>2</sub> O	18	μg/L
Na <sub>2</sub> SeO <sub>3</sub> ·5H <sub>2</sub> O	60	μg/L
NiCl <sub>2</sub> ·6H <sub>2</sub> O	30	μg/L
EDTA	0.6	mg/L
HCl 36%	0.6	μL/L
ZnCl <sub>2</sub>	30	μg/L
HBO <sub>3</sub>	30	μg/L
(NH <sub>4</sub> ) <sub>6</sub> Mo <sub>7</sub> O <sub>2</sub> ·4H <sub>2</sub> O	54	μg/L
Resazurin	0.3	mg/L
Yeast extract	1.2	mg/L

**Table A2.2.** Volumes and concentrations used to prepare the BMP tests.

Constituent	THP <sub>i</sub>	THP <sub>s</sub>	THP <sub>t</sub>	WAS	Blank
Reaction Volume (mL)	300	300	300	300	300
ISR (gVS/gCOD)	1.5	1.5	1.5	1.5	1.5

Inoculum concentration (raw measured)(gVS/L)	72.3	72.3	72.3	72.3	72.3
Substrates concentration (raw measured) (gCOD/L)	75	238	172	212	No substrate
Final substrate concentration in the medium (gVS/L)	19	19	19	19	19
<b>Volume of a constituent to be added per bottle</b>	<b>Volume</b>	<b>Volume</b>	<b>Volume</b>	<b>Volume</b>	<b>Volume</b>
Substrate volume (mL)	76.0	23.9	33.1	26.9	No substrate
Inoculum volume (mL)	118.2	118.2	118.2	118.2	118.2
Carbonate Buffer (100 g/L) volume (mL)	3.0	3.0	3.0	3.0	3.0
Macronutrients volume (mL)	1.8	1.8	1.8	1.8	1.8
Micronutrients volume (mL)	0.2	0.2	0.2	0.2	0.2
Demineralised water volume (mL)	100.8	152.9	143.7	149.9	176.8

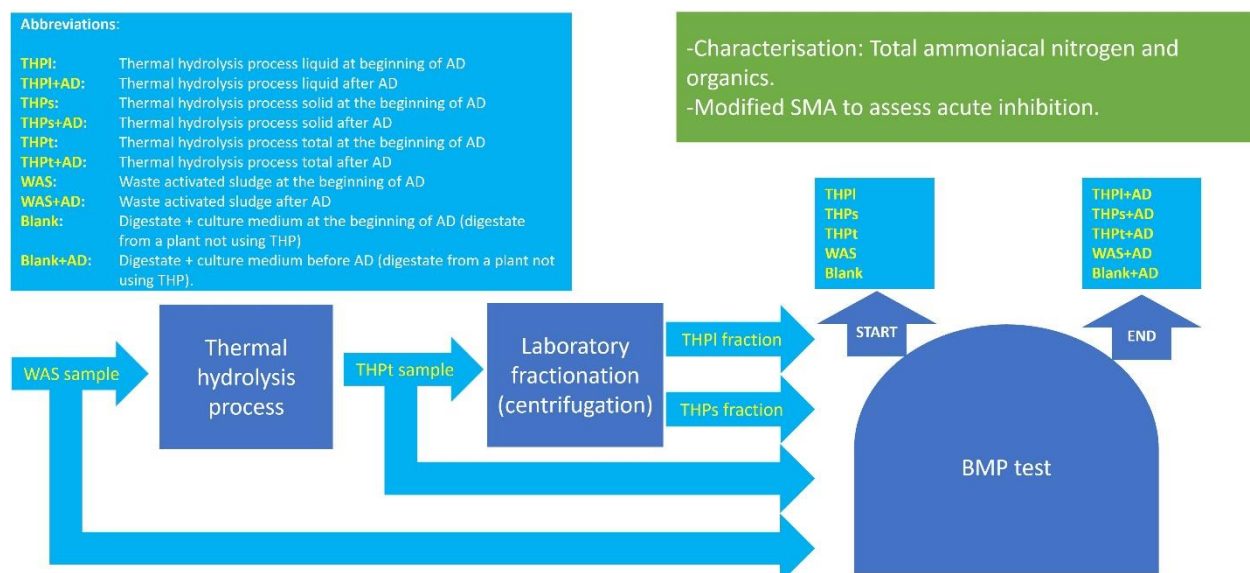


**Figure A2.1.** Scheme of the samples (in yellow) and the laboratory fractionation of the samples used in our present study.

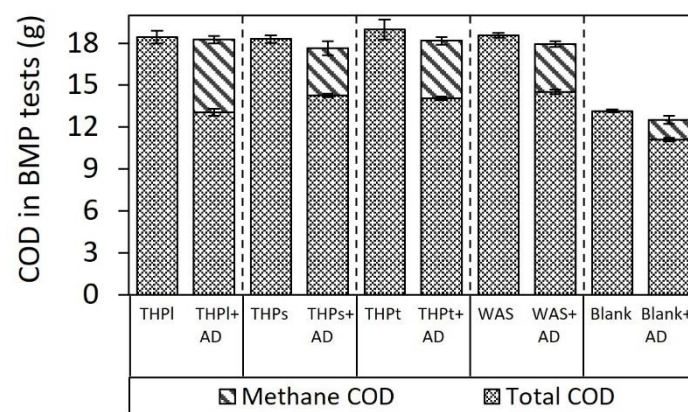


**Figure A2.2.** COD balance considering the tCOD measured within the analysed samples and the COD produced as  $\text{CH}_4$  in the BMP tests.

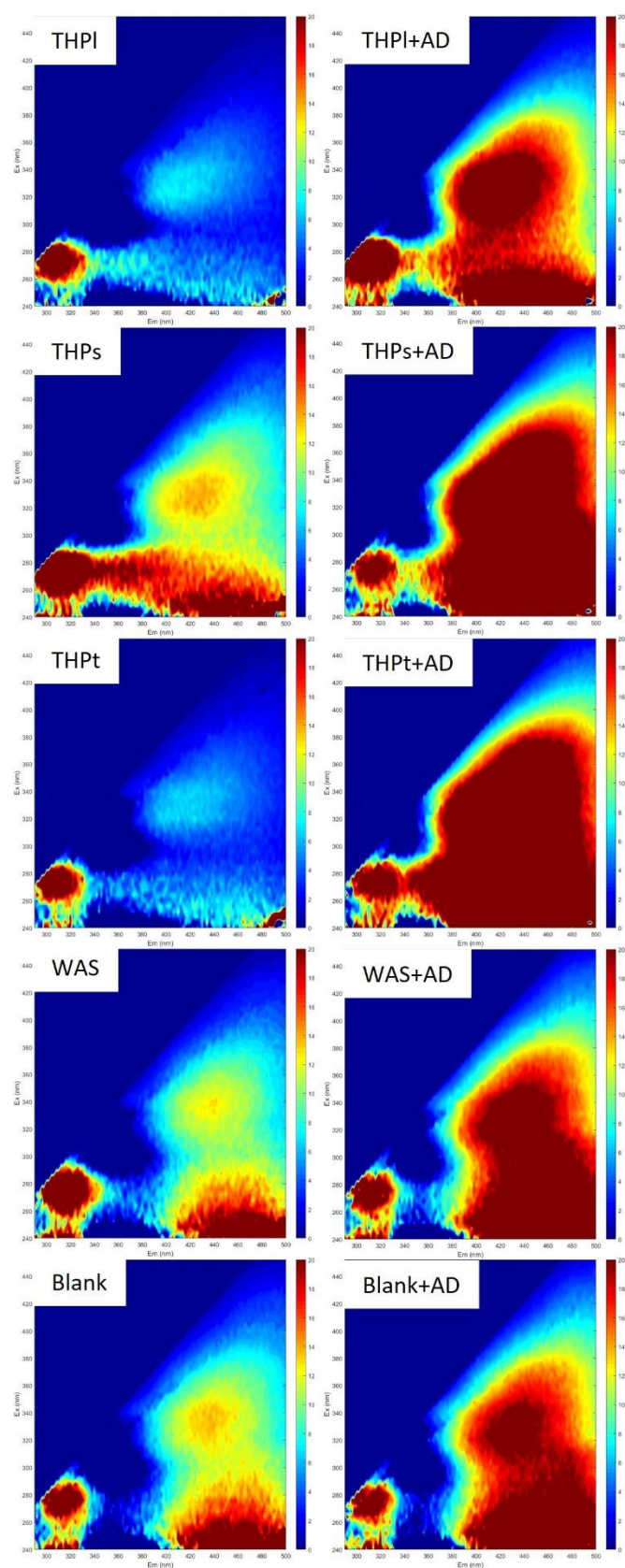


**Figure 2.A3.** FEEM samples used to calculate the NFRI shown in Figure 2-d.





# 3.

**Increased solubilisation of multivalent cations decreases soluble orthophosphate concentration during anaerobic digestion of thermally hydrolysed bio-P waste-activated sludge**

## Abstract

Nutrient treatment in reject water after anaerobic digestion (AD) avoids an extra burden in the main waste-water treatment system upon returning this flow, and also prevents spontaneous precipitation. In addition, the use of thermal hydrolysis process (THP) increases total ammoniacal nitrogen (TAN) concentrations during AD and thus in the reject water too. However, the effect of THP on  $\text{PO}_4^{3-}\text{-P}$  production release during AD has not been fully addressed in literature, particularly in the case of waste-activated sludge (WAS) used in enhanced biological phosphorous removal (EBPR). EBPR-WAS contains phosphate-accumulating organisms (PAOs), which store polyphosphate and release it as  $\text{PO}_4^{3-}\text{-P}$  during THP and/or AD. In our present study we researched the kinetic release of nutrients during AD in lab-scale samples at different THP temperatures and also in full-scale THP-treated samples. WAS lab-scale THP conducted at 120°C 160°C, and 200°C for 30 minutes; while full-scale samples of WAS and THP-WAS were obtained from Hengelo, WWTP, The Netherlands. The results showed that THP temperature increments increased TAN and  $\text{PO}_4^{3-}\text{-P}$  release (before AD) due to deamination and dephosphorylation. The soluble concentration of nutrients behaved differently in the case of TAN and  $\text{PO}_4^{3-}\text{-P}$ . TAN revealed an increasing concentration with AD time, while the  $\text{PO}_4^{3-}\text{-P}$  concentration increased during the first days, followed by a concentration decrease with time. TAN and  $\text{PO}_4^{3-}\text{-P}$  release were weakly correlated. The full-scale samples showed that the concentration of  $\text{PO}_4^{3-}\text{-P}$  decreased at the end of AD, concurrently with the concentration of THP solubilised  $\text{Ca}^{2+}$ ,  $\text{Mg}^{2+}$  and  $\text{Fe}^{2+/3+}$ , which likely precipitated with  $\text{PO}_4^{3-}\text{-P}$ . These results were confirmed by an equilibrium model which showed that THP increased the saturation indexes of multivalent cations- $\text{PO}_4^{3-}\text{-P}$  precipitates. Overall, the results showed that THP increases the release of nutrients and cations, but the kinetic is governed by precipitation reactions over digestion time.

### 3.1. Introduction

Anaerobic digestion (AD) is a common process used in wastewater treatment plants (WWTPs) to stabilise primary and secondary sludges (Appels et al., 2008), and to produce biogas, which can be used as a source of energy (Holm-Nielsen et al., 2009; van Lier et al., 2001). During AD, organically bound N and P is transformed into soluble total ammoniacal nitrogen (TAN) and  $\text{PO}_4^{3-}$ -P. Moreover, when waste activated sludge (WAS) of an enhanced biological phosphate removal (EBPR) plant is digested, cell internally stored poly-phosphate will also be released under anaerobic conditions, as well as due to decay: WAS from installations using EBPR contain up to 12% of P on a dry basis, in contrast to the 1%-3% found in conventional WAS (Van Loosdrecht et al., 1997). As a consequence of this nutrients solubilisation during AD, an important extent of the soluble nutrients present in the AD-digestate reach the liquid fraction (reject water) after digestate's dewatering. Preferably, the nutrients in the reject water are removed before this stream is returned to the secondary treatment or to the headworks. Nutrients can be removed by several methods such as nitrification/denitrification or partial nitrification/anammox for TAN removal (Baeten et al., 2019; Figdore et al., 2018; Joss et al., 2009; Lackner et al., 2014; Ochs et al., 2023); and precipitation with  $\text{Mg}^{2+}$  (struvite),  $\text{Fe}^{2+}$  (vivianite) or  $\text{Ca}^{2+}$  (hydroxyapatite) for simultaneous  $\text{PO}_4^{3-}$  and the corresponding TAN removal (Abel-Denee et al., 2018; Abma et al., 2010; Cichy et al., 2019; Ghosh et al., 2019; Monballiu et al., 2018).

Thermal hydrolysis process (THP) is the most commonly used full-scale pre-treatment for AD. THP has proven to increase AD biogas production, dewaterability, and decrease the pathogens in anaerobic digestate (Barber, 2016b). Several THP commercial processes are available in the market with different operational parameters and configurations. However, most of the THP technologies expose WAS to elevated temperatures (140-160°C) for around 20-30 minutes (Dwyer et al., 2008). The use of THP changes both, the physical and chemical structure of WAS: physically, THP denatures proteins and disrupts the cell's structures solubilising the cytoplasmic content. Chemically, THP causes protein deamination, lipids peroxidation and sugars dehydration (Barber, 2016a; Bougrier et al., 2007; Brunner, 2009; Devos et al., 2023; Farhoosh, 2022; Pavez-Jara et al., 2023; Wilson and Novak, 2009). Also, the elevated temperatures reached during THP promote Maillard and caramelisation reactions (Devos et al., 2021). Despite the advantages of THP it has also been reported that the process increases the concentration of recalcitrant compounds and nutrients in the AD digestates (Ortega-Martínez et al., 2021). The elevated nutrient concentrations may cause spontaneous precipitation during

AD, causing operational problems, and could increase the cost of downstream treatments (Krishnamoorthy et al., 2021).

Precipitation occurs when the concentration of a solute exceeds the saturation concentration in the equilibrium. Mathematically it is considered that precipitation occurs when the concentration of the reagents of certain specific compounds exceed the saturation index (SI) (Rahman et al., 2014). SI is shown in Equation 3.1 where  $IAP$  represents the ion activity product of the species involved in a particular reaction and  $K_{sp}$  is the product solubility, which depends on the thermodynamic characteristic of the precipitate formed.

$$SI = \log \frac{IAP}{K_{sp}} \quad (3.1),$$

During AD,  $PO_4^{3-}$ -P, TAN, and/or other cations can react and form precipitates (Barat et al., 2009; Kecskésová et al., 2020b; Marti et al., 2008; Musvoto et al., 2000). Most literature related to elevated nutrient concentrations due to THP focus on TAN release. However, the influence of THP on  $PO_4^{3-}$ -P release and precipitation during AD has not been well addressed. In our present work, we assessed the effect of THP on the release of nutrients during AD and the possible precipitation of TAN and  $PO_4^{3-}$ -P with metal ions in the AD broth. Also, simulations were conducted to assess the precipitate formed during AD.

## 3.2. Materials and methods

### 3.2.1. Laboratory and full-scale THP of WAS.

To measure the influence of THP on nutrients release and precipitation during AD, two experiments were conducted: a preliminary screening increasing THP temperature and a secondary experiment using full-scale samples. In the preliminary screening biochemical methane potentials (BMPs) were conducted using non-pre-treated WAS and laboratory THP-treated WAS at 120, 160 and 200 °C for 30 minutes (BMP1). The THP pre-treatment was conducted in a laboratory autoclave model Parr-series 4570 HP/HT (Parr Instrument Company, USA), and the steam explosion was reached by rapidly releasing the autoclave pressure at the end of the reaction time. The samples of the preliminary experiments were named after the temperature at which the laboratory pre-treatment was conducted, as follows: i) WAS<sub>l</sub> for non-treated WAS; ii) THP120<sub>l</sub> to THP-treated WAS at 120 °C and 30 minutes; iii) THP160<sub>l</sub> to THP-treated WAS at 160 °C and 30 minutes, and; iv) THP200<sub>l</sub> to THP-treated WAS at 200 °C and 30 minutes. The subscript “l” stands for lab-conducted THP. WAS<sub>l</sub> samples were collected from the municipal WWTP, Harnaschpolder operated by Delfluent Services, Den Hoorn, The Netherlands. In the second experiment, samples from full-scale WAS (WAS<sub>f</sub>) and THP-WAS (THP-WAS<sub>f</sub>) from a CAMBI® system were sampled and another BMP was conducted (BMP2). The full-scale CAMBI® installation treated exclusively secondary sludge from the WWTP in Hengelo, The Netherlands, and surrounding smaller WWTPs. Both WASs contained PAOs since both plants used EBPR in the secondary treatment besides nitrification/denitrification for N-removal. WAS samples were stored at 4°C before analysis to prevent degradation. The THP-treated samples were stored at room temperature to minimise phosphate precipitation that may occur if stored at 4°C.

### 3.2.2. BMP tests using THP pre-treated sludge

As mentioned in the previous section, two BMP tests were conducted to measure the release of nutrients during AD (BMP1 and BMP2). During BMP1 the release of TAN and PO<sub>4</sub><sup>3-</sup>P over time were measured. During the BMP2, samples of the mixed broths were taken only on the initial and final days, and nutrients and soluble cations were measured. A summary of the conditions in which the BMPs were measured is shown in Table 3.1. Both BMP tests were carried out in 500 mL bottles with a reaction volume of 300 mL using an AMPTS II system (Bioprocess Control, Sweden) at 35°C, taking into account the recommendations raised by Holliger et al. (2016). In the Blank samples, the substrate was replaced by demineralized water;

the culture medium and inoculum remained in the same concentrations as in the bottles containing substrates. The cumulative  $\text{CH}_4$  production was expressed in mL of normalised  $\text{CH}_4$  ( $\text{N-CH}_4$  at 273.15 K and 1 atm) produced per gram of volatile solids (VS) in the substrates. The percentage of biodegradability of the analysed substrates was assessed considering that 100% corresponded to 350 NmL- $\text{CH}_4$ /g COD.

The inocula to perform both BMP tests were sampled from the digestate produced at the municipal WWTP Harnaschpolder, operated by Delfluent Services (Den Hoorn, The Netherlands). The AD reactors from which the inoculum was sampled treat a mixture of WAS and primary sludge without any pre-treatment, at a hydraulic retention time of 21-24 days and an operational temperature of 35°C. After sampled, the inocula were incubated at 35°C for seven days to consume the remaining non-digested organic matter from the full-scale installation. The inoculum for the second BMP was pre-concentrated 1.7 times, centrifuging 10 min at 3,500 rpm in a centrifuge model Heraeus Labofuge 400 (Thermo Fisher Scientific, USA) to reach the required VS concentration in the test. Positive controls using microcrystalline cellulose (Sigma-Aldrich, USA), were conducted to ensure the inoculum was active and renders the stoichiometric  $\text{CH}_4$ .

**Table 3.1.** Experimental conditions and culture medium for BMPs.

Constituent	Concentration in the medium	Unit
Substrates	19 (BMP1) and 7 (BMP2)	g COD/L
Inoculum	28.5 (BMP2) and 14 (BMP2)	g VS/L
<b>Buffer</b>		
$\text{NaHCO}_3$	1,000	mg/L
<b>Macronutrients</b>		
$\text{NH}_4\text{Cl}$	1,020 (267mgTAN/L)	mg/L
$\text{CaCl}_2 \cdot 2\text{H}_2\text{O}$	48	mg/L
$\text{MgSO}_4 \cdot 7\text{H}_2\text{O}$	54	mg/L
<b>Micronutrients</b>		
$\text{FeCl}_3 \cdot 4\text{H}_2\text{O}$	1.2	mg/L
$\text{CoCl}_2 \cdot 6\text{H}_2\text{O}$	1.2	mg/L
$\text{MnCl}_2 \cdot 4\text{H}_2\text{O}$	0.3	mg/L
$\text{CuCl}_2 \cdot 2\text{H}_2\text{O}$	18	$\mu\text{g/L}$
$\text{Na}_2\text{SeO}_3 \cdot 5\text{H}_2\text{O}$	60	$\mu\text{g/L}$
$\text{NiCl}_2 \cdot 6\text{H}_2\text{O}$	30	$\mu\text{g/L}$
EDTA	0.6	mg/L
HCl 36%	0.6	$\mu\text{L/L}$
$\text{ZnCl}_2$	30	$\mu\text{g/L}$

HBO <sub>3</sub>	30	µg/L
(NH <sub>4</sub> ) <sub>6</sub> Mo <sub>7</sub> O <sub>2</sub> ·4H <sub>2</sub> O	54	µg/L
Resazurin	0.3	mg/L
Yeast extract	1.2	mg/L

### 3.2.3. Chemical analysis

Total solids (TS) and VS were assessed according to Standard Methods for the examination of water and wastewater (Association and Association, 1995). Soluble and total chemical oxygen demand (sCOD and tCOD, respectively), TAN and PO<sub>4</sub><sup>3-</sup>-P, were measured in triplicate using the kits LCK 114 (the same for sCOD and tCOD), APC 303 and LCK 350 brand Hach Lange (Hach, USA). To measure soluble parameters such as sCOD, TAN, and PO<sub>4</sub><sup>3-</sup>-P, the samples were filtered through 0.45 µm syringe filters model CHROMAFIL Xtra PES-45/25 (Macherey-Nagel, Germany).

### 3.2.4. Analysis of soluble cations

Soluble cations were measured in the soluble phase at the beginning and end of the BMP using inductively coupled plasma mass spectrometry (ICP-MS), (PlasmaQuant MS, Analytik Jena AG, Germany). The metals measured were Na<sup>+</sup>, Ca<sup>2+</sup>, K<sup>+</sup>, Mg<sup>2+</sup>, Cu<sup>+2+</sup>, Fe<sup>2+/3+</sup> and Al<sup>3+</sup>. The samples for ICP-MS analysis, were prepared by acidifying 9.9 mL of samples using 0.1 mL of 69% HNO<sub>3</sub> (CAS No.: 7697-37-2, CARL ROTH ROTIPURAN®, Germany). The parameters used in ICP-MS to perform metals analysis are shown in Table 2. Although ICP-MS measures the total concentration of the analysed isotopes, the concentrations of the different cations are expressed with their oxidation state, except Fe and Cu, which are expressed as Fe<sup>+2/+3</sup> and Cu<sup>+2</sup> since their oxidation state cannot be determined with ICP-MS.

**Table 3.2.** Parameters used to determine cations using ICP-MS

Parameter	
RF power	1.30 [kW]
Measurement mode	Fe in H <sub>2</sub> mode, other elements in no gas mode
Acquisition time	~2 minutes
Solution uptake	4 mL
Cell gas flow	
Plasma flow	9 L/min
Auxiliary flow:	1.40 L/min
Pump rate	10 RPM
Stabilization delay	45 s
Calibration solutions	



IV-STOCK-35 and IV-STOCK-28 (Inorganic Ventures, The USA)  
 SRM 1640a - Trace Elements in Natural Water (NIST, The USA)

### 3.2.5. Speciation simulation using PHREEQC

A speciation simulation on PHREEQC version 3 (U.S. Geological Survey, USA) was conducted for the full-scale samples in BMP2, before performing the BMPs to assess the potential for spontaneous precipitation. TAN and  $\text{PO}_4^{3-}\text{-P}$  were considered in the precipitation reaction, however, the soluble organic matter was not considered in the simulation. MINTEQ.DAT database was used and the struvite reaction ( $\text{MgNH}_4\text{PO}_4 \cdot 6\text{H}_2\text{O} = \text{Mg}^{2+} + \text{PO}_4^{3-} + \text{NH}_4^+ + 6\text{H}_2\text{O}$ ) with  $\log_k -13.15$  and  $\Delta H 23.62$  kcal as thermodynamic constants was added to the model since it was not present in the database (Bhuiyan et al., 2007). The input data for the simulation are shown in Table 3.3. The simulations were run with the average value of the parameters measured in the sludge samples characterisation and ICP-MS measurements. Saturation indexes (SIs) were used to compare the samples, in which a positive index means that the minerals would precipitate.

**Table 3.3.** Input data for speciation simulation with PHREEQC.

Measurement	THP-WAS <sub>f</sub>	WAS <sub>f</sub>	Blank
Temperature [°C]	35	35	35
Pressure [atm]	1	1	1
pH	7.4	7.4	7.4
Alkalinity as [mg/L] of $\text{HCO}_3^-$ added	726.5	726.5	726.5
$\text{PO}_4^{3-}$ [mg/L]	230	177	151
$\text{NH}_4^+$ [mg-N/L]	1,315	1,247	1,149
Na <sup>+</sup> [mg/L]	421.9	413.1	400.49
$\text{Ca}^{2+}$ [mg/L]	24.7	19.6	17.5
$\text{K}^+$ [mg/L]	381.5	370.4	313.3
$\text{Mg}^{2+}$ [mg/L]	3.3	0.9	0.9
$\text{Cu}^+$ * [mg/L]	0.0	0.1	0.0
$\text{Fe}^{2+}$ * [mg/L]	6.5	3.4	4.0
$\text{Al}^{3+}$ [mg/L]	0.0	0.1	0.0

\* Considering that ICP-MS does not allow to measure the cations oxidation states, the lower oxidation state was chosen to resemble anaerobic conditions.

### 3.2.6. Analysis of results

The specific degree of solubilisation (SDOS) describes the solubilisation of TAN and  $\text{PO}_4^{3-}\text{-P}$  of (i-th compound) per mass of VS in the initial substrate, and it is defined in equation (3.2)

(Pavez-Jara et al., 2023). SDOS was analysed at the beginning and end of the BMP2 (full-scale samples) using the soluble concentration of nutrients and cations measured. For assessing this parameter, the soluble concentration of specific compounds in the Blank sample (no substrate added) was subtracted from the soluble concentration, and this was divided by the VS concentration of the initial substrate in the bottle. The results are expressed in the mass of the  $i$ -th compound solubilised per mass of VS in the initial substrate.

$$i\text{-SDOS} = \frac{C_{i,j} - C_{i,\text{Blank}}}{IC_j} \quad (3.2),$$

Where:

$i\text{-SDOS}$  = Specific degree of solubilisation of the  $i$ -th parameter (nutrients and cations).

$C_{i,j}$  = Soluble concentration of the  $i$ -th parameter in the  $j$ -th sample.

$C_{i,\text{Blank}}$  = Soluble concentration of the  $i$ -th parameter Blank sample.

$IC_j$  = VS concentration (homogenous) of the  $i$ -th substrate in the  $j$ -th sample, before AD.

$i = \text{PO}_4^{3-}\text{-P}$  and TAN.

$j = \text{THP-WAS}_f$  and  $\text{WAS}_f$ .

Single-factor ANOVA with a confidence level of 95% was used to evaluate the significance of differences between the different samples. Also, mean difference tests with the same level of significance as ANOVA were used when comparing two samples' averages.

### 3.3. Results and discussion

#### 3.3.1. Organic matter solubilisation and CH<sub>4</sub> production during lab-scale BMP.

Figure 3.1-a shows sCOD concentration during the BMP1 tests, from the figure it can be observed that all samples decreased sCOD concentration during AD, as expected from the degradation of organics. Furthermore, an increased THP temperature also increased the sCOD solubilisation, as previously reported in the literature (Appels et al., 2010; Bougrier et al., 2008; Haug et al., 1978; Li and Noike, 1992; Valo et al., 2004). It is important to stress that the increment of sCOD at the initial day of THP200<sub>i</sub> was more noticeable more pronounced than in the samples of THP160 and THP120. The increment in sCOD on the initial day in THP200<sub>i</sub> was likely due to temperature-induced carbohydrates degradation or dehydration, which is reported to happen around 200 °C (Pineda-Gómez et al., 2014; Shogren, 1992; Wilson and Novak, 2009). A sharp decrease in sCOD THP200<sub>i</sub> after day 10 may have been caused by the sudden start of VFA conversion, which delayed CH<sub>4</sub> production. A reason for delayed CH<sub>4</sub> production could be a possible toxicity of the high temperature-produced melanoidins or TAN on methanogens, during BMP1 lag phase (Capson-Tojo et al., 2020; Seyed et al., 2021; Zhou et al., 2015). Also, the sample THP200<sub>i</sub> showed significantly higher recalcitrant sCOD (sCOD at the day 30), which in full-scale AD processes will remain in the reject water. Figure 3.1-b shows the cumulative CH<sub>4</sub> production in the measured samples during the 30 days AD. The endogenous CH<sub>4</sub> production of the inoculum (Blank<sub>i</sub>) was not subtracted to evidence kinetic CH<sub>4</sub> production directly; therefore, to assess the BMP directly the blank sample must be subtracted according to the indications raised by Holliger et al. (2016). The BMP values reached  $135 \pm 22$ ,  $143 \pm 13$ ,  $156 \pm 36$  and  $154 \pm 16$  N-mL CH<sub>4</sub>/g COD for WAS, THP120, THP160, and THP200<sub>i</sub> showing that the higher THP temperature and COD solubilisation did not significantly increase the BMP1. COD solubilisation and anaerobic biodegradability are correlated in THP at reduced temperatures (Appels et al., 2010; Pinnekamp, 1988; Stuckey and McCarty, 1984), which was not the case for THP200<sub>i</sub>, where the additional solubilised COD did not seem to increase the biodegradability. Additionally, THP200<sub>i</sub> showed a lag phase of around 10 days, which indicated that the THP conditions caused the formation of inhibitory compounds for methanogenesis. Consequently, in the case of THP200<sub>i</sub> the decrease in sCOD observed in the day 12 (Figure 3.1-a) corresponded to an increase in the CH<sub>4</sub> production rate (Figure 3.1-b), which indicated the anaerobic conversion of organics .

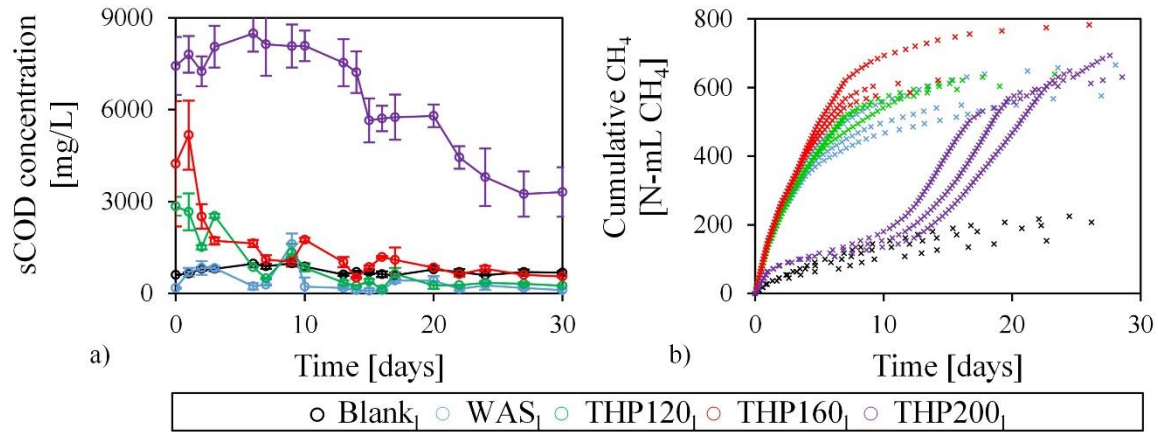


**Figure 3.1.** a) Cumulative CH<sub>4</sub> production during BMP1 test; b) sCOD in the measured samples during BMP1.

### 3.3.2. Nutrients release during lab-scale BMP

Figure 3.2-a and Figure 3.2-b show TAN and PO<sub>4</sub><sup>3-</sup>-P concentrations measured throughout the BMP1 tests in WAS<sub>I</sub> and THP-treated WAS<sub>I</sub> at 120°C, 160°C and 200°C. Figure 3.2-a shows that the increased temperature during the pre-treatment increased the initial TAN concentrations of the BMP1 test. The increased initial TAN concentrations in the THP-treated substrates corresponded to the TAN released likely by deamination of the organic N present in the substrates. Proteins deamination due to THP, including its temperature dependence, has been reported in literature (Pavez-Jara et al., 2023; Wilson and Novak, 2009).

TAN concentration at the end of the BMP tests reached 1.5, 1.7, 1.7, and 1.9 g TAN/L, for WAS<sub>I</sub>, THP120<sub>I</sub>, THP160<sub>I</sub> and THP200<sub>I</sub>, respectively. Furthermore, the positive slopes in a linear data fitting during the BMP1 (Figure 3.2-a) showed that TAN increased during the BMP test. Figure 3.2-a also shows that in the case of THP200<sub>I</sub>, TAN concentration increased during the first 10 days, and decreased afterwards likely due to precipitation of TAN-P-based minerals. The moment of the change in the TAN trend matched the end of the lag phase of CH<sub>4</sub> production. The CH<sub>4</sub> production, and corresponding VFA consumption, likely increased the pH in the sample bottles. It has been previously reported that increased pH favours the precipitation of several minerals such as struvite (Saidou et al., 2009; Tansel et al., 2018). Precipitation can also be observed from the parallel decrease in PO<sub>4</sub><sup>3-</sup>-P concentration (Figure 3.2-b). Furthermore, the increasing TAN concentration during the lag phase of CH<sub>4</sub> production, may be an indication that the toxic compounds created during (high-temperature) THP affect

greatly the methanogenesis rather than hydrolysis or fermentation reactions, causing deammonification.

Figure 3.2-b shows  $\text{PO}_4^{3-}\text{-P}$  concentration over time in the analysed samples. Also these measurements show increased  $\text{PO}_4^{3-}\text{-P}$  solubilisation at higher pre-treatment temperatures. Based on initial  $\text{PO}_4^{3-}\text{-P}$  concentrations shown in Figure 3.2-b the harsh conditions exerted by THP likely caused dephosphorylation of organics present in the WAS. High-temperature-induced dephosphorylation has already been observed in other proteinaceous solutions (Belec and Jenness, 1962; Grewal et al., 2018; van Boekel, 1999). During the BMP1 tests,  $\text{PO}_4^{3-}\text{-P}$  concentrations increased rapidly in the initial days followed by a sudden reduction, and fluctuating values throughout the BMP test. Averaging the concentrations during each assay showed an increase with the temperature; 338, 501, 511, 562 and 631 mg  $\text{PO}_4^{3-}\text{-P/L}$  in the case of Blank<sub>1</sub>, WAS<sub>1</sub>, THP120<sub>1</sub>, THP160<sub>1</sub> and THP200<sub>1</sub>, respectively.  $\text{PO}_4^{3-}\text{-P}$  concentration fluctuations indicate the complex interactions between the release and precipitation of  $\text{PO}_4^{3-}\text{-P}$  in the bulk liquid.  $\text{PO}_4^{3-}\text{-P}$  precipitation will be influenced by pH and available cations that may precipitate at current conditions; varying cations availability and changing pH could explain the non-steady behaviour of  $\text{PO}_4^{3-}\text{-P}$ . In all tests, the final  $\text{PO}_4^{3-}\text{-P}$  concentrations were higher than the concentration at the beginning of the tests. It is interesting to stress that THP200<sub>1</sub> exhibited a significantly higher  $\text{PO}_4^{3-}\text{-P}$  concentration compared to the other THP treated samples after incubation.

Figure 3.2-c shows TAN concentrations versus  $\text{PO}_4^{3-}\text{-P}$  concentrations during the BMP tests. Figure 3.2-c shows a weak correlations between the concentrations of TAN and  $\text{PO}_4^{3-}\text{-P}$  during AD in all the samples analysed. The weak correlation in nutrients concentrations showed that the solubilisation/release and precipitation of nutrients did not occurred at the same time during AD. Therefore, the concentrations of the final nutrients were likely more related to secondary reactions such as precipitation with species in solution than digestion time.

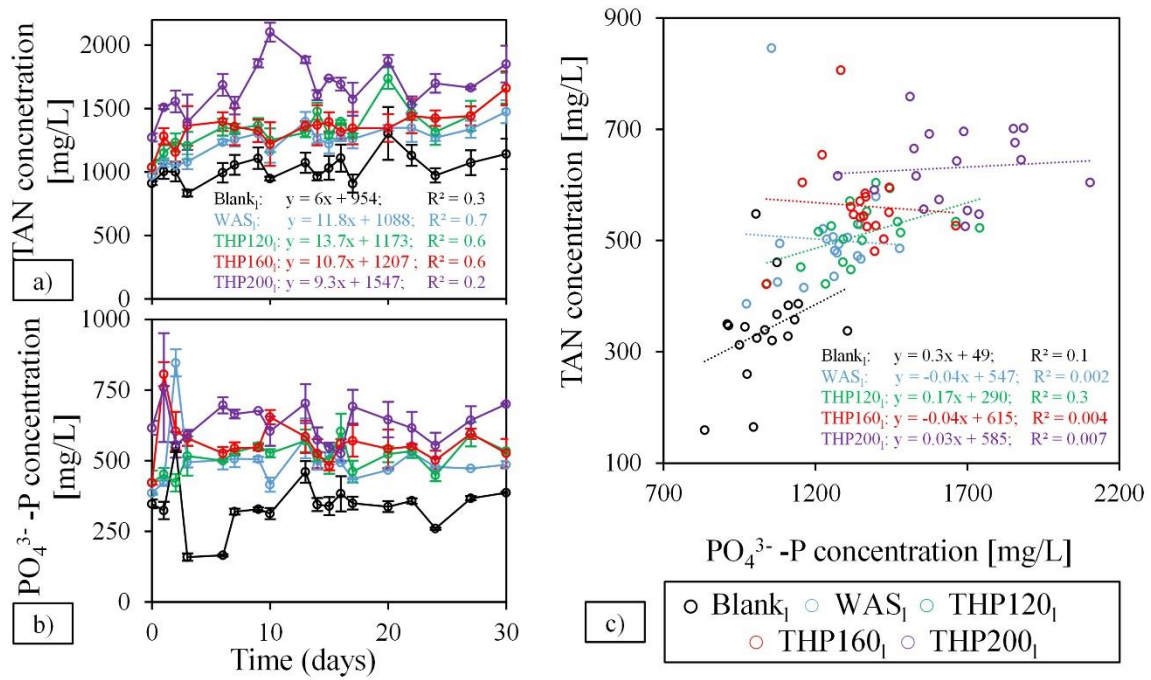


**Figure 3.2.** a) Release of  $\text{PO}_4^{3-}\text{-P}$  over time, during the BMP-1; b) Release of TAN over time, during the BMP1; c) correlation between TAN and  $\text{PO}_4^{3-}\text{-P}$  during BMP-1.

### 3.3.3. $\text{PO}_4^{3-}\text{-P}$ precipitation with soluble cations during AD.

To assess the possible precipitation of  $\text{PO}_4^{3-}\text{-P}$ -based minerals during AD, additional tests were performed using THP and WAS<sub>f</sub> sampled from a full-scale installation using THP. Figure 3.3-a shows  $\text{PO}_4^{3-}\text{-P}$  concentrations and  $\text{PO}_4^{3-}\text{-P}$ -SDOS at the beginning and end of the BMP2 tests performed with full-scale WAS<sub>f</sub>, THP-WAS<sub>f</sub> and Blank<sub>f</sub> samples.  $\text{PO}_4^{3-}\text{-P}$ -SDOS was chosen to remove the influence of the inoculum in the analysis and have a tool to compare results between different substrates. As shown in Figure 3.3-a, before AD, WAS<sub>f</sub> contained less  $\text{PO}_4^{3-}\text{-P}$  compared to THP-WAS<sub>f</sub> sludge, which is in line with the earlier results (Figure 3.2-b). The higher concentrations of  $\text{PO}_4^{3-}\text{-P}$  in THP-WAS<sub>f</sub> samples showed that the full-scale pre-treatment by itself releases the  $\text{PO}_4^{3-}\text{-P}$  present in the solid phase of WAS<sub>f</sub>, likely via temperature-induced dephosphorylation.  $\text{PO}_4^{3-}\text{-P}$  release during THP is related to the release of biomass' cytoplasmic content into the bulk liquid during exposure to high temperature and pressure and steam explosion, as mentioned by Barber (2016b). Furthermore, an important extent of the released  $\text{PO}_4^{3-}\text{-P}$  found in WAS<sub>f</sub> and THP-WAS<sub>f</sub> samples could originate from poly-P, released by phosphate accumulating organisms (PAOs). Under AD conditions the PAOs release  $\text{PO}_4^{3-}\text{-P}$ , consuming the VFA, which are common intermediates during the AD process and have likely been present (Mavinic et al., 1998; Mino et al., 1998).

In Figure 3.3-a, the sampling points after AD (+AD) show that WAS<sub>f</sub> significantly increased its PO<sub>4</sub><sup>3-</sup>-P-SDOS by 150 % during the AD process (from 1.4 mg PO<sub>4</sub><sup>3-</sup>-P /g VS to 3.5 mg PO<sub>4</sub><sup>3-</sup>-P /g VS). PO<sub>4</sub><sup>3-</sup>-P release during AD was likely caused by a combination of WAS<sub>f</sub> degradation and release of PO<sub>4</sub><sup>3-</sup>-P by PAOs. Conversely, after AD, THP-WAS<sub>f</sub> samples decreased their PO<sub>4</sub><sup>3-</sup>-P-SDOS by 9.7% (from 4.2 to 3.8 mg PO<sub>4</sub><sup>3-</sup>-P /g VS). The decrease of PO<sub>4</sub><sup>3-</sup>-P -SDOS after AD indicated that PO<sub>4</sub><sup>3-</sup>-P could have precipitated in minerals such as calcite, vivianite, struvite or other phosphate-based-cation precipitates, which commonly occur during AD (Bolzonella et al., 2012; Kecskéssová et al., 2020a; Li et al., 2019).

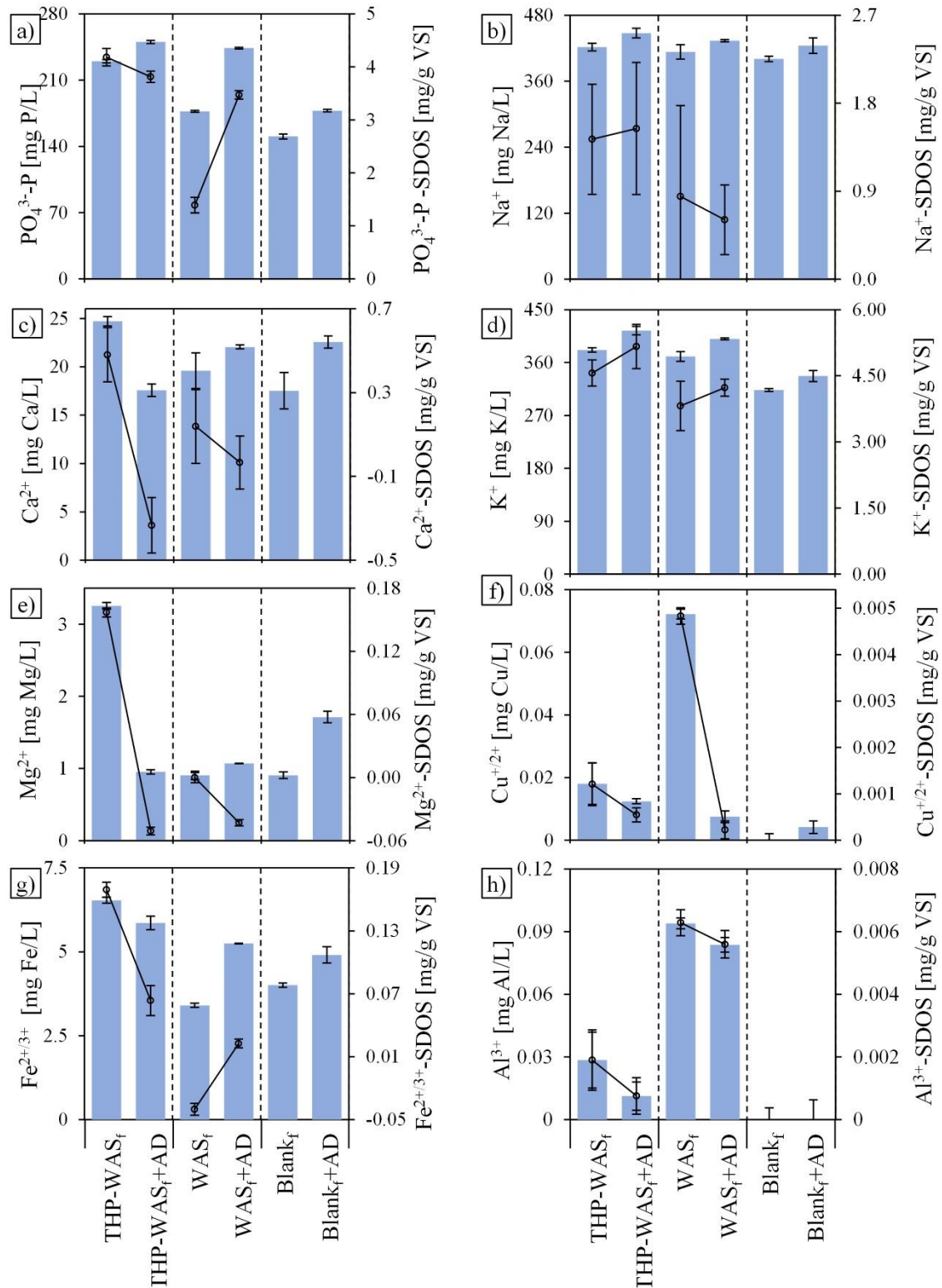


**Figure 3.3.** Concentration and SDOS before and after BMP2 digestion of a) PO<sub>4</sub><sup>3--</sup>P; b) Soluble Na<sup>+</sup>; c) Soluble Ca<sup>2+</sup>; d) Soluble K<sup>+</sup>; e) Soluble Mg<sup>2+</sup>; f) Soluble Cu<sup>+/2+</sup>; g) Soluble Fe<sup>2+/3+</sup>; h) Soluble Al<sup>3+</sup>, in the analysed samples.



Uncontrolled precipitation of  $\text{PO}_4^{3-}$ -P-based materials and the subsequent pipe-clogging/scaling are common phenomena in AD processes, associated mainly with struvite ( $\text{MgNH}_3\text{PO}_4 \cdot 6\text{H}_2\text{O}$ ) formation (Maqueda et al., 1994; Williams, 1999). Nonetheless, other minerals can precipitate alongside struvite. Besides  $\text{Mg}^{2+}$  and TAN,  $\text{PO}_4^{3-}$ -P can react with several other polyvalent cations, such as  $\text{Ca}^{2+}$  and  $\text{Fe}^{2+/3+}$ . The precipitates produced depend on the oversaturation of reactants ( $\text{PO}_4^{3-}$ -P, metal cations or TAN), pH, and ion strength of the bulk liquid (Cheng et al., 2015; Crutchik and Garrido, 2011; Drenkova-Tuhtan et al., 2016; Van Wazer and Callis, 1958). Figures 3.3-b, c, d, e, f, g and h show the concentrations and SDOS of different cations that are likely to precipitate with  $\text{PO}_4^{3-}$ -P under AD conditions. All measured elements except for  $\text{Al}^{3+}$  were present in the culture medium of the BMP test, and thus a background concentration of these elements was always measured. As shown in Figure 3.3, the SDOSs before AD of  $\text{Na}^+$ ,  $\text{Ca}^{2+}$ ,  $\text{K}^+$ ,  $\text{Mg}^{2+}$  and  $\text{Fe}^{2+/3+}$  were higher in  $\text{WAS-THP}_f$  samples compared to  $\text{WAS}_f$ . The increased concentration of soluble cations before AD indicates that THP by itself increased their solubilisation, likely due to the disruption of  $\text{WAS}_f$  cells' cytoplasm during the steam explosion. Figure 3.3 also shows that the cations  $\text{Ca}^{2+}$ ,  $\text{Mg}^{2+}$  and  $\text{Fe}^{2+/3+}$  decreased their SDOS after the BMP tests in  $\text{THP-WAS}_f$  and  $\text{WAS}_f$  samples.  $\text{Ca}^{2+}$  and  $\text{Mg}^{2+}$  are known to precipitate with  $\text{PO}_4^{3-}$ -P, and/or TAN and form different minerals such as hydroxyapatite, amorphous Ca-P, and struvite among others (Battistoni et al., 1997; Cunha et al., 2018; Schott et al., 2022; Tervahauta et al., 2014).

In the case of  $\text{WAS}_f$  samples,  $\text{Fe}^{2+/3+}$ -SDOS increased after AD, which could be attributed to substrate degradation and further release of structural  $\text{Fe}^{2+/3+}$  (Jefferson et al., 2001; Wood and Tchobanoglous, 1975). The negative  $\text{Fe}^{2+/3+}$ -SDOS observed in  $\text{WAS}_f$  samples before AD shows that some  $\text{Fe}^{2+/3+}$  likely precipitated or was bound to  $\text{WAS}_f$  before AD.

In the case of  $\text{Na}^+$  and  $\text{K}^+$  (monovalent cations), the mean differences analysis before and after the AD did not show statistical differences, with P-values equal to 0.769 and 0.895 in the case of  $\text{Na}^+$ , and 0.4439 and 0.2916 in the case of  $\text{K}^+$  for  $\text{WAS}_f$  and  $\text{THP-WAS}_f$  samples, respectively. These results suggest that  $\text{Na}^+$  and  $\text{K}^+$  as monovalent cations interacted to a lower extent with the ions in solution to form precipitates.

In the case of  $\text{Cu}^{+/2+}$  and  $\text{THP-WAS}_f$  the statistical analysis of its SDOS showed no differences before and after the BMP2 in with a P-value = 0.079 in a mean difference analysis.  $\text{Cu}^{+/2+}$  is likely reduced during AD (from  $\text{Cu}^{2+}$  to  $\text{Cu}^+$ ) and it probably behaved as a monovalent cation. Conversely,  $\text{Cu}^{+/2+}$  -SDOS decreased drastically in  $\text{WAS}$  samples before and after AD. In this

context, it is important to stress that the  $\text{Cu}^{+2+}$  concentration before AD was noticeably higher in the case of WAS compared to THP-WAS<sub>f</sub>. The mechanisms probably involve uptake and interaction with the EPS matrix of WAS during AD (Fermoso et al., 2009; Zhang et al., 2014). The lower  $\text{Cu}^{+2+}$  solubilisation before AD in THP-WAS<sub>f</sub> samples compared to WAS<sub>f</sub> may have also been a consequence of the interaction of  $\text{Cu}^{+2+}$  with the particulate organic matter formed during THP (Legros et al., 2017). Furthermore,  $\text{Al}^{3+}$ -SDOS showed no statistical differences in the samples analysed with P-value= 0.152 and 0.121 for THP-WAS<sub>f</sub> and WAS<sub>f</sub>, respectively. The low concentrations of  $\text{Al}^{3+}$  found in the soluble phase, likely obeyed to the high affinity capacity of this cation with humic substances and negatively charged particles (Dempsey et al., 1984; Elkins and Nelson, 2002), which most likely formed flocs.

#### **3.3.4. Modelling of potential P-based precipitates**

In order to assess the precipitation of the studied cations with the  $\text{PO}_4^{3-}$ -P present, a precipitation model was computed using PhreeqC. The saturation indexes (SIs) of the  $\text{PO}_4^{3-}$ -P-based species are shown in Figure 3.4. The simulation was conducted for the situation at the beginning of BMP2, since it is expected that the equilibrium precipitation reactions are faster than the biochemical degradation reactions occurring during AD (Bouropoulos and Koutsoukos, 2000; Le Corre et al., 2007). According to Figure 3.4, SIs of all  $\text{PO}_4^{3-}$ -P-based species were negative, meaning that these are not oversaturated and will remain in solution at least at the initial conditions of the BMP2.  $\text{Na}^+$  and  $\text{K}^+$  did not interact with  $\text{PO}_4^{3-}$ -P; nonetheless, they could have precipitated with other cations forming non-P-based minerals which are shown in the supplementary material. The general trend showed increased SIs in THP-WAS<sub>f</sub> samples compared to WAS<sub>f</sub> (closer to zero), confirming that THP increases the conditions for precipitation of  $\text{PO}_4^{3-}$ -P-based minerals. It is important to stress that the data were measured only at the beginning of AD, thus it is expected that more  $\text{PO}_4^{3-}$ -P and cations are released due to degradation processes during AD and thus might increase the SIs. Furthermore, the increased TAN concentration in the THP-treated samples (as shown in Figure 3.1), moves the equilibrium towards the products stimulating precipitation of TAN-based minerals, such as struvite. Also, elevated TAN concentrations may increase the pH within the anaerobic digesters, which might increase even more the SIs during AD

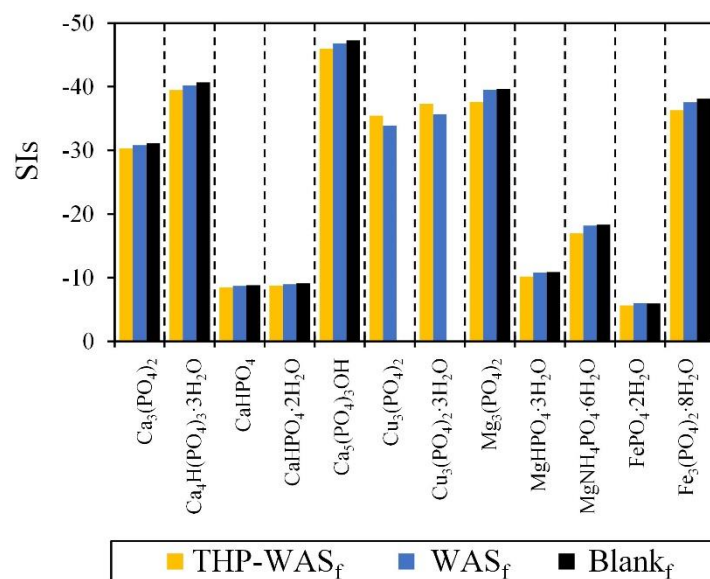


**Figure 3.4.** Saturation indexes for P-based compounds formed in the analysed samples, based on PhreeqC simulation. The absence of bars means that the compounds are not formed in that particular sample.

### 3.4. Concussions

The pre-treatment conditions during THP of WAS caused temperature-induced dephosphorylation and deamination of nutrients, leading to direct release of  $\text{PO}_4^{3-}\text{-P}$  and TAN. Direct nutrients release increased with the increased THP temperature.

Concentrations of nutrients during AD, particularly  $\text{PO}_4^{3-}\text{-P}$ , are more influenced by precipitation reactions than AD reaction time. THP temperature increments increased final nutrients concentrations, which can reach reject water in full-scale.

In full-scale THP-WAS samples, AD reduced  $\text{PO}_4^{3-}\text{-P-SDOS}$  as well as polyvalent cations' SDOS, evidencing that polyvalent cation likely precipitated to form  $\text{PO}_4^{3-}\text{-P-cations}$  or  $\text{PO}_4^{3-}\text{-P-TAN-cations}$  minerals. Since THP increases the solubilisation of polyvalent cation and TAN, it increases the proclivity to have spontaneous precipitation during AD.

### **3.5. List of abbreviations**

AD: anaerobic digestion.

BMP: biochemical methane potential.

EBPR: enhanced biological phosphorous removal.

ICP-MS: inductively coupled plasma mass spectrometry.

PAO: phosphate-accumulating organisms.

PAOs: phosphate accumulating organisms.

sCOD: soluble chemical oxygen demand.

SDOS: specific degree of solubilisation.

SIs: saturation indexes.

TAN: total ammoniacal nitrogen.

tCOD: total chemical oxygen demand.

THP: thermal hydrolysis process

TS: total solids.

VFA: volatile fatty acids.

VS: volatile solids.

WAS: waste activated sludge.

WWTPs: wastewater treatment plants.

### 3.6. References

- Abel-Denee, M., Abbott, T. and Eskicioglu, C. 2018. Using mass struvite precipitation to remove recalcitrant nutrients and micropollutants from anaerobic digestion dewatering centrate. *Water Research* 132, 292-300.
- Abma, W.R., Driessen, W., Haarhuis, R. and van Loosdrecht, M.C.M. 2010. Upgrading of sewage treatment plant by sustainable and cost-effective separate treatment of industrial wastewater. *Water Science and Technology* 61(7), 1715-1722.
- Appels, L., Baeyens, J., Degrève, J. and Dewil, R. 2008. Principles and potential of the anaerobic digestion of waste-activated sludge. *Progress in Energy and Combustion Science* 34(6), 755-781.
- Appels, L., Degrève, J., Van der Bruggen, B., Van Impe, J. and Dewil, R. 2010. Influence of low temperature thermal pre-treatment on sludge solubilisation, heavy metal release and anaerobic digestion. *Bioresource Technology* 101(15), 5743-5748.
- Association, A.P.H. and Association, A.W.W. (1995) Standard methods for the examination of water and wastewater, pp. [1000]-[1000].
- Baeten, J.E., Batstone, D.J., Schraa, O.J., van Loosdrecht, M.C.M. and Volcke, E.I.P. 2019. Modelling anaerobic, aerobic and partial nitrification-anammox granular sludge reactors - A review. *Water Research* 149, 322-341.
- Barat, R., Bouzas, A., Martí, N., Ferrer, J. and Seco, A. 2009. Precipitation assessment in wastewater treatment plants operated for biological nutrient removal: A case study in Murcia, Spain. *Journal of Environmental Management* 90(2), 850-857.
- Barber, W. 2016a. Thermal hydrolysis for sewage treatment: a critical review. *Water Research* 104, 53-71.
- Barber, W.P.F. 2016b. Thermal hydrolysis for sewage treatment: A critical review. *Water Research* 104, 53-71.
- Battistoni, P., Fava, G., Pavan, P., Musacco, A. and Cecchi, F. 1997. Phosphate removal in anaerobic liquors by struvite crystallization without addition of chemicals: Preliminary results. *Water Research* 31(11), 2925-2929.
- Belec, J. and Jenness, R. 1962. Dephosphorization of Casein by Heat Treatment. I. In Caseinate Solutions. *Journal of Dairy Science* 45(1), 12-19.
- Bhuiyan, M.I.H., Mavinic, D.S. and Beckie, R.D. 2007. A SOLUBILITY AND THERMODYNAMIC STUDY OF STRUVITE. *Environmental Technology* 28(9), 1015-1026.
- Bolzonella, D., Cavinato, C., Fatone, F., Pavan, P. and Cecchi, F. 2012. High rate mesophilic, thermophilic, and temperature phased anaerobic digestion of waste activated sludge: A pilot scale study. *Waste Management* 32(6), 1196-1201.
- Bougrier, C., Delgenès, J.P. and Carrère, H. 2007. Impacts of thermal pre-treatments on the semi-continuous anaerobic digestion of waste activated sludge. *Biochemical Engineering Journal* 34(1), 20-27.
- Bougrier, C., Delgenès, J.P. and Carrère, H. 2008. Effects of thermal treatments on five different waste activated sludge samples solubilisation, physical properties and anaerobic digestion. *Chemical Engineering Journal* 139(2), 236-244.
- Bouropoulos, N.C. and Koutsoukos, P.G. 2000. Spontaneous precipitation of struvite from aqueous solutions. *Journal of Crystal Growth* 213(3), 381-388.
- Brunner, G. 2009. Near critical and supercritical water. Part I. Hydrolytic and hydrothermal processes. *The Journal of Supercritical Fluids* 47(3), 373-381.
- Capson-Tojo, G., Moscoviz, R., Astals, S., Robles, Á. and Steyer, J.P. 2020. Unraveling the literature chaos around free ammonia inhibition in anaerobic digestion. *Renewable and Sustainable Energy Reviews* 117, 109487.

- Cheng, X., Chen, B., Cui, Y., Sun, D. and Wang, X. 2015. Iron(III) reduction-induced phosphate precipitation during anaerobic digestion of waste activated sludge. *Separation and Purification Technology* 143, 6-11.
- Cichy, B., Kuźdżał, E. and Krztoń, H. 2019. Phosphorus recovery from acidic wastewater by hydroxyapatite precipitation. *Journal of Environmental Management* 232, 421-427.
- Crutchik, D. and Garrido, J.M. 2011. Struvite crystallization versus amorphous magnesium and calcium phosphate precipitation during the treatment of a saline industrial wastewater. *Water Science and Technology* 64(12), 2460-2467.
- Cunha, J.R., Schott, C., van der Weijden, R.D., Leal, L.H., Zeeman, G. and Buisman, C. 2018. Calcium addition to increase the production of phosphate granules in anaerobic treatment of black water. *Water Research* 130, 333-342.
- Dempsey, B.A., Ganho, R.M. and O'Melia, C.R. 1984. The Coagulation of Humic Substances by Means of Aluminum Salts. *Journal AWWA* 76(4), 141-150.
- Devos, P., Filali, A., Grau, P. and Gillot, S. 2023. Sidestream characteristics in water resource recovery facilities: a critical review. *Water Research*, 119620.
- Devos, P., Haddad, M. and Carrère, H. 2021. Thermal Hydrolysis of Municipal sludge: Finding the Temperature Sweet Spot: A Review. *Waste and Biomass Valorization* 12(5), 2187-2205.
- Drenkova-Tuhtan, A., Schneider, M., Mandel, K., Meyer, C., Gellermann, C., Sextl, G. and Steinmetz, H. 2016. Influence of cation building blocks of metal hydroxide precipitates on their adsorption and desorption capacity for phosphate in wastewater—A screening study. *Colloids and Surfaces A: Physicochemical and Engineering Aspects* 488, 145-153.
- Dwyer, J., Starrenburg, D., Tait, S., Barr, K., Batstone, D.J. and Lant, P. 2008. Decreasing activated sludge thermal hydrolysis temperature reduces product colour, without decreasing degradability. *Water research* 42(18), 4699-4709.
- Elkins, K.M. and Nelson, D.J. 2002. Spectroscopic approaches to the study of the interaction of aluminum with humic substances. *Coordination Chemistry Reviews* 228(2), 205-225.
- Farhoosh, R. 2022. New insights into the kinetic and thermodynamic evaluations of lipid peroxidation. *Food Chemistry* 375, 131659.
- Fermoso, F.G., Bartacek, J., Jansen, S. and Lens, P.N.L. 2009. Metal supplementation to UASB bioreactors: from cell-metal interactions to full-scale application. *Science of The Total Environment* 407(12), 3652-3667.
- Figdore, B.A., David Stensel, H. and Winkler, M.-K.H. 2018. Bioaugmentation of sidestream nitrifying-denitrifying phosphorus-accumulating granules in a low-SRT activated sludge system at low temperature. *Water Research* 135, 241-250.
- Ghosh, S., Lobanov, S. and Lo, V.K. 2019. An overview of technologies to recover phosphorus as struvite from wastewater: advantages and shortcomings. *Environmental Science and Pollution Research* 26(19), 19063-19077.
- Grewal, M.K., Huppertz, T. and Vasiljevic, T. 2018. FTIR fingerprinting of structural changes of milk proteins induced by heat treatment, deamidation and dephosphorylation. *Food Hydrocolloids* 80, 160-167.
- Haug, R.T., Stuckey, D.C., Gossett, J.M. and McCarty, P.L. 1978. Effect of thermal pretreatment on digestibility and dewaterability of organic sludges. *Journal (Water Pollution Control Federation)*, 73-85.
- Holliger, C., Alves, M., Andrade, D., Angelidaki, I., Astals, S., Baier, U., Bougrier, C., Buffière, P., Carballa, M. and De Wilde, V. 2016. Towards a standardization of biomethane potential tests. *Water Science and Technology*, wst2016336.

- Holm-Nielsen, J.B., Al Seadi, T. and Oleskowicz-Popiel, P. 2009. The future of anaerobic digestion and biogas utilization. *Bioresource Technology* 100(22), 5478-5484.
- Jefferson, B., Burgess, J.E., Pichon, A., Harkness, J. and Judd, S.J. 2001. Nutrient addition to enhance biological treatment of greywater. *Water Research* 35(11), 2702-2710.
- Joss, A., Salzgeber, D., Eugster, J., König, R., Rottermann, K., Burger, S., Fabijan, P., Leumann, S., Mohn, J. and Siegrist, H. 2009. Full-Scale Nitrogen Removal from Digester Liquid with Partial Nitritation and Anammox in One SBR. *Environmental Science & Technology* 43(14), 5301-5306.
- Kecskésóvá, S., Imreová, Z., Martonka, M. and Drtil, M. 2020a. Chemical dissolution of struvite precipitates in pipes from anaerobic sludge digestion. *Chemical Papers*, 1-8.
- Kecskésóvá, S., Imreová, Z., Martonka, M. and Drtil, M. 2020b. Chemical dissolution of struvite precipitates in pipes from anaerobic sludge digestion. *Chemical Papers* 74(8), 2545-2552.
- Krishnamoorthy, N., Dey, B., Unpaprom, Y., Ramaraj, R., Maniam, G.P., Govindan, N., Jayaraman, S., Arunachalam, T. and Paramasivan, B. 2021. Engineering principles and process designs for phosphorus recovery as struvite: A comprehensive review. *Journal of Environmental Chemical Engineering* 9(5), 105579.
- Lackner, S., Gilbert, E.M., Vlaeminck, S.E., Joss, A., Horn, H. and van Loosdrecht, M.C.M. 2014. Full-scale partial nitritation/anammox experiences – An application survey. *Water Research* 55, 292-303.
- Le Corre, K.S., Valsami-Jones, E., Hobbs, P. and Parsons, S.A. 2007. Kinetics of Struvite Precipitation: Effect of the Magnesium Dose on Induction Times and Precipitation Rates. *Environmental Technology* 28(12), 1317-1324.
- Legros, S., Levard, C., Marcato-Romain, C.-E., Guiesse, M. and Doelsch, E. 2017. Anaerobic Digestion Alters Copper and Zinc Speciation. *Environmental Science & Technology* 51(18), 10326-10334.
- Li, L., Pang, H., He, J. and Zhang, J. 2019. Characterization of phosphorus species distribution in waste activated sludge after anaerobic digestion and chemical precipitation with  $\text{Fe}^{3+}$  and  $\text{Mg}^{2+}$ . *Chemical Engineering Journal* 373, 1279-1285.
- Li, Y.-Y. and Noike, T. 1992. Upgrading of anaerobic digestion of waste activated sludge by thermal pretreatment. *Water Science and Technology* 26(3-4), 857-866.
- Maqueda, C., Pérez Rodríguez, J.L. and Lebrato, J. 1994. Study of struvite precipitation in anaerobic digesters. *Water Research* 28(2), 411-416.
- Marti, N., Bouzas, A., Seco, A. and Ferrer, J. 2008. Struvite precipitation assessment in anaerobic digestion processes. *Chemical Engineering Journal* 141(1), 67-74.
- Mavinic, D.S., Koch, F.A., Hall, E.R., Abraham, K. and Niedbala, D. 1998. Anaerobic Co-Digestion of Combined Sludges from a Bnr Wastewater Treatment Plant. *Environmental Technology* 19(1), 35-44.
- Mino, T., van Loosdrecht, M.C.M. and Heijnen, J.J. 1998. Microbiology and biochemistry of the enhanced biological phosphate removal process. *Water Research* 32(11), 3193-3207.
- Monballiu, A., Desmidt, E., Ghyselbrecht, K. and Meesschaert, B. 2018. Phosphate recovery as hydroxyapatite from nitrified UASB effluent at neutral pH in a CSTR. *Journal of Environmental Chemical Engineering* 6(4), 4413-4422.
- Musvoto, E.V., Wentzel, M.C. and Ekama, G.A. 2000. Integrated chemical–physical processes modelling—II. simulating aeration treatment of anaerobic digester supernatants. *Water Research* 34(6), 1868-1880.
- Ochs, P., Martin, B., Germain-Cripps, E., Stephenson, T., van Loosdrecht, M. and Soares, A. 2023. Techno-economic analysis of sidestream ammonia removal technologies:



- Biological options versus thermal stripping. *Environmental Science and Ecotechnology* 13, 100220.
- Ortega-Martínez, E., Chamy, R. and Jeison, D. 2021. Thermal pre-treatment: Getting some insights on the formation of recalcitrant compounds and their effects on anaerobic digestion. *Journal of Environmental Management* 282, 111940.
- Pavez-Jara, J.A., van Lier, J.B. and de Kreuk, M.K. 2023. Accumulating ammoniacal nitrogen instead of melanoidins determines the anaerobic digestibility of thermally hydrolyzed waste activated sludge. *Chemosphere* 332, 138896.
- Pineda-Gómez, P., Angel-Gil, N.C., Valencia-Muñoz, C., Rosales-Rivera, A. and Rodríguez-García, M.E. 2014. Thermal degradation of starch sources: Green banana, potato, cassava, and corn - Kinetic study by non-isothermal procedures. *Starch/Staerke* 66(7-8), 691-699.
- Pinnekamp, J. (1988) *Water Pollution Research and Control* Brighton, pp. 97-108, Elsevier.
- Rahman, M.M., Salleh, M.A.M., Rashid, U., Ahsan, A., Hossain, M.M. and Ra, C.S. 2014. Production of slow release crystal fertilizer from wastewaters through struvite crystallization – A review. *Arabian Journal of Chemistry* 7(1), 139-155.
- Saidou, H., Korchef, A., Ben Moussa, S. and Ben Amor, M. 2009. Struvite precipitation by the dissolved CO<sub>2</sub> degasification technique: Impact of the airflow rate and pH. *Chemosphere* 74(2), 338-343.
- Schott, C., Cunha, J.R., van der Weijden, R.D. and Buisman, C. 2022. Phosphorus recovery from pig manure: Dissolution of struvite and formation of calcium phosphate granules during anaerobic digestion with calcium addition. *Chemical Engineering Journal* 437, 135406.
- Seyedi, S., Venkiteshwaran, K. and Zitomer, D. 2021. Current status of biomethane production using aqueous liquid from pyrolysis and hydrothermal liquefaction of sewage sludge and similar biomass. *Reviews in Environmental Science and Bio/Technology* 20(1), 237-255.
- Shogren, R.L. 1992. Effect of moisture content on the melting and subsequent physical aging of cornstarch. *Carbohydrate Polymers* 19(2), 83-90.
- Stuckey, D.C. and McCarty, P.L. 1984. The effect of thermal pretreatment on the anaerobic biodegradability and toxicity of waste activated sludge. *Water Research* 18(11), 1343-1353.
- Tansel, B., Lunn, G. and Monje, O. 2018. Struvite formation and decomposition characteristics for ammonia and phosphorus recovery: A review of magnesium-ammonia-phosphate interactions. *Chemosphere* 194, 504-514.
- Tervahauta, T., van der Weijden, R.D., Flemming, R.L., Hernández Leal, L., Zeeman, G. and Buisman, C.J.N. 2014. Calcium phosphate granulation in anaerobic treatment of black water: A new approach to phosphorus recovery. *Water Research* 48, 632-642.
- Valo, A., Carrère, H. and Delgenès, J.P. 2004. Thermal, chemical and thermo-chemical pre-treatment of waste activated sludge for anaerobic digestion. *Journal of Chemical Technology & Biotechnology: International Research in Process, Environmental & Clean Technology* 79(11), 1197-1203.
- van Boekel, M.A.J.S. 1999. Heat-induced deamidation, dephosphorylation and breakdown of caseinate. *International Dairy Journal* 9(3), 237-241.
- van Lier, J.B., Tilche, A., Ahring, B.K., Macarie, H., Moletta, R., Dohanyos, M., Hulshoff Pol, L.W., Lens, P. and Verstraete, W. 2001. New perspectives in anaerobic digestion. *Water Science and Technology* 43(1), 1-18.
- Van Loosdrecht, M., Hooijmans, C., Brdjanovic, D. and Heijnen, J. 1997. Biological phosphate removal processes. *Applied microbiology and biotechnology* 48, 289-296.

- Van Wazer, J.R. and Callis, C.F. 1958. Metal complexing by phosphates. *Chemical Reviews* 58(6), 1011-1046.
- Williams, S. 1999. Struvite Precipitation in the Sludge Stream at Slough Wastewater Treatment Plant and Opportunities for Phosphorus Recovery. *Environmental Technology* 20(7), 743-747.
- Wilson, C.A. and Novak, J.T. 2009. Hydrolysis of macromolecular components of primary and secondary wastewater sludge by thermal hydrolytic pretreatment. *Water research* 43(18), 4489-4498.
- Wood, D.K. and Tchobanoglous, G. 1975. Trace Elements in Biological Waste Treatment. *Journal (Water Pollution Control Federation)* 47(7), 1933-1945.
- Zhang, Z., Zhou, Y., Zhang, J. and Xia, S. 2014. Copper (II) adsorption by the extracellular polymeric substance extracted from waste activated sludge after short-time aerobic digestion. *Environmental Science and Pollution Research* 21(3), 2132-2140.
- Zhou, Y., Schideman, L., Zheng, M., Martin-Ryals, A., Li, P., Tommaso, G. and Zhang, Y. 2015. Anaerobic digestion of post-hydrothermal liquefaction wastewater for improved energy efficiency of hydrothermal bioenergy processes. *Water Science and Technology* 72(12), 2139-2147.



# 4.

## **Role of the composition of humic substances formed during thermal hydrolysis process on struvite precipitation in reject water from anaerobic digestion\***

---

\* Based on Pavez-Jara, J., et al., Role of the composition of humic substances formed during thermal hydrolysis process on struvite precipitation in reject water from anaerobic digestion. Journal of Water Process Engineering, 2024. 59: p. 104932.

## Abstract

Thermal hydrolysis process (THP) is a widely used pre-treatment method in the anaerobic digestion (AD) of waste municipal sewage sludge. A post AD dewatering step of the digestate produces a liquid stream called reject water. THP increases the concentration of humic substances (HSs) and nutrients in the produced reject water. Struvite precipitation is a widely used technique to remove and (potentially) recover  $\text{PO}_4^{3-}$ -P and the corresponding amount of total ammoniacal nitrogen from reject water. The chemical characteristics of the THP-produced HSs influence reaction yields and morphology of struvite. In our current study, struvite batch precipitation experiments were conducted at different pHs, and different concentrations of HSs, consisting of either melanoidins or humic acids. Our results showed that at pH 6.5 struvite precipitation was severely retarded. However, increased concentrations of melanoidins at pH 6.5 enhanced struvite precipitation. Batch experiments conducted at pH 7.25 and 8 with increased melanoidins concentrations showed  $\text{PO}_4^{3-}$ -P precipitation yields over 86%. Humic acids negatively impacted struvite precipitation at all analysed pH values, presumably because of  $\text{Mg}^{2+}$  complexation. Morphological analysis showed that the presence of both HSs affected Feret diameters, aspect ratio, and cleavage pattern of struvite. Also, HSs rendered coloured crystals. Overall, our results showed that struvite precipitation is affected by HSs intrinsic characteristics, affecting yield, morphology, and colour of the formed precipitates.

#### 4.1. Introduction

Pre-treatment technologies for waste municipal sewage sludge prior to anaerobic digestion (AD) in wastewater treatment plants (WWTPs) are implemented to enhance energy efficiency, reduce costs and residues, and sanitize AD digestates (Appels et al., 2011; Carrere et al., 2010). The thermal hydrolysis process (THP) is widely used in full-scale AD pre-treatments installations (Sahu et al., 2022), using different configurations such as SUSTEC® (Netherlands), CAMBI® (CAMBI, Norway), Lysotherm® (Eliquo Technologies, Germany), Exelys™, and Bio Thelis™ (Veolia, France). In all mentioned THP technologies, primary sludge, waste activated sludge, or a combination of both are exposed to elevated temperatures (160-180°C) for a defined period of time to enhance the anaerobic digestibility and digestate dewaterability, to reduce pathogen concentrations, and to shorten the AD solids retention time (Barber, 2016; Gahlot et al., 2022). Nonetheless, the use of high temperatures during THP alters the chemical composition of the sludge matrixes, producing a particular type of humic substances (HSs) known as melanoidins via the Maillard reaction (Dwyer et al., 2008).

Melanoidins are coloured compounds, consisting of polymerised aromatic groups, and result from a series of reactions between reducing sugars and amino groups present in proteins (Bork et al., 2022; Ellis, 1959). The Maillard reaction already occurs at room temperature, but is pronounced at higher temperatures (Wang et al., 2011) such as those occurring during THP. Melanoidins can be classified based on their pH-dependent solubility as a result of their variable isoelectric point in the same way as HSs (Migo et al., 1993). The pH-dependent solubility of melanoidins allows us to classify them, like HSs, as fulvic acids, humic acids, and humins (Taguchi and Sampei, 1986). In addition, melanoidins behave as polydentate ligands, complexing cations in solution, due to the presence of negatively charged ketone and hydroxyl groups in their structure (Gomyo and Horikoshi, 1976; Rufián-Henares and de la Cueva, 2009). Also, under AD conditions melanoidins may behave as recalcitrant substances, in the same manner as the rest of HSs (Azman et al., 2017; Ortega-Martínez et al., 2021). The AD recalcitrance and partially soluble character of melanoidins might lead to problems in the AD-downstream processes, particularly during the treatment of reject water after digestate-dewatering (Ngo et al., 2021; Zhang et al., 2018).

During AD, nutrients are usually released from degraded substrates, thus the reject water contains elevated concentrations of total ammoniacal nitrogen (TAN) and  $\text{PO}_4^{3-}\text{-P}$ . In various WWTPs, TAN and  $\text{PO}_4^{3-}\text{-P}$  are removed before the reject water is recirculated to the WWTPs' headworks. In The Netherlands, several full-scale WWTPs apply struvite precipitation and

subsequent partial nitritation/anammox (PN/A) to remove  $\text{PO}_4^{3-}\text{-P}$  and TAN (Abma et al., 2010; Marti et al., 2010; Taddeo et al., 2018; Vlaeminck et al., 2012).

Struvite precipitation is a chemical process in which  $\text{Mg}^{2+}$  reacts with  $\text{PO}_4^{3-}\text{-P}$ , water, and TAN to form a mineral, which precipitates, and can be separated from the liquid solution via sedimentation. The struvite stoichiometric reaction is shown in Equation 4.1 (Le Corre et al., 2009). Struvite precipitation is a two-step process until an equilibrium is reached: nucleation and crystal growth (Nielsen, 1969). Nucleation is a first-order phase transition in which small embryos of a new solid phase are created in a large volume of the previous unstable phase (De Yoreo and Vekilov, 2003). Crystals growth is the step in which molecules aggregate to the previously created nuclei. The crystal growth step can also be accompanied by agglomeration, in which, small crystals merge to create bigger aggregates (Galbraith et al., 2014).



The struvite precipitation process is pH dependent and requires strict control of the reactants, to ensure that the added amount of  $\text{Mg}^{2+}$  reacts with the  $\text{PO}_4^{3-}\text{-P}$  in solution. However, when it comes to struvite precipitation in reject water, TAN is generally not monitored since it is commonly in excess compared to  $\text{PO}_4^{3-}\text{-P}$ . The more-than-stoichiometric TAN concentration in reject water shifts the equilibrium towards the products formation, thereby enhancing precipitation (Equation 4.1). The struvite precipitation process is currently commercially available at full-scale with brand names, such as Airprex® (Centrisys-CNP, USA), PHOSPAQ™ (Paques, Netherlands) and Pearl® (Ostara, Canada). The application of the struvite precipitation process in wastewater treatment provides a triple benefit: 1) it removes  $\text{PO}_4^{3-}\text{-P}$  and TAN from reject water, reducing the nutrient load in the mainstream treatment; 2) it reduces maintenance in the reject water pipelines and sludge dewatering equipment due to undesired precipitation and clogging; and 3) it produces a renewable slow-release fertiliser (de-Bashan and Bashan, 2004). The use of struvite as fertilizer relies on its low solubility in water, which allows for a slow nutrient release, while it prevents leaching into underground water bodies (Münch and Barr, 2001).

The THP-AD recalcitrant HSs affect the struvite precipitation processes (Munir et al., 2017), although the exact mechanisms are yet not fully understood. Chemical properties inherent to the HSs, such as pH-dependent solubility and complexation properties, may interfere with the precipitation process and may affect the struvite characteristics. To the knowledge of the

authors the literature addresses HSs as a set of compounds with similar characteristics and not considering the singularities among them. In our present work, we investigated the influence of HSs as melanoidins and humic acids on the struvite crystallisation process, evaluating the effects on the yields of nutrients precipitated, and the morphology of the crystals produced. The results were used to build a conceptual model which considers the influence of specific characteristics of HSs on the struvite precipitation process.



## 4.2. Materials and methods

### 4.2.1. Analytical measurements

The ultraviolet absorbance at 254 nm (UVA 254) and colour were measured using a UV-Vis spectrophotometer (Genesys 10S, Thermo Scientific, USA) in quartz and plastic cuvettes of 1 cm path length, respectively. Colour was measured at 475 nm using a 500 mg Pt-Co/L colour reference solution (Certipur® Merck, Germany). UVA 254 and colour measurements were expressed in 1/cm and mg Pt-Co/L, respectively. The concentrations of  $\text{PO}_4^{3-}\text{-P}$ , TAN, total organic carbon (TOC), and  $\text{Mg}^{2+}$  were determined using Hach Lange kits (Hach, Germany: LCK 350, LCK 303, LCK 386, and LCK 326, respectively). The spectrophotometer model DR3900 (Hach, Germany) was used to read the kits. Specific ultraviolet absorbance (SUVA) was calculated as the ratio of UVA 254 in 1/m to the concentration of TOC in mg/L (Edzwald and Van Benschoten 1990). Each sample was measured in triplicate, error bars are used to indicate the standard deviation of the measurements.

To evaluate the level of significance between the differences of the samples, single-factor ANOVA plus Tukey's HSD at 95% confidence were used. Additionally, a two-tailed single sample t-test at 95% confidence was used to compare experimental results with stoichiometric values.

### 4.2.2. Struvite precipitation tests

Struvite crystallisation tests were performed in triplicate using a 0.5 L Jar test device (VELP Scientifica, Italy), at a mixing speed of 160 rpm for one hour at  $20\pm 1^\circ\text{C}$ , following the procedure described by Li et al. (2019). The pH was measured online and manually controlled by adding 5 M NaOH. The volume of added NaOH was considered negligible, as it was less than 1% of the total reaction volume. The term HSs refers to the melanoidins and humic acids used in our present study. The experimental design is shown in Table 4.1, where the samples were named after the concentration and type of HSs present, including: i) No-HSs, absence of HSs; ii) MEL-1, melanoidins 1 g TOC/L; iii) MEL-2, melanoidins 2 g TOC/L; iv) HA-1, humic acid 1 g TOC/L; i) HA-2, humic acid 2 g TOC/L. Table 4.2 shows humic acid and melanoidins stock solutions' preparation and characterisation. The reagents' concentrations in the crystallisation tests were 15mM, 66.45mM and 15mM for  $\text{Mg}^{2+}$ , TAN and  $\text{PO}_4^{3-}\text{-P}$ , respectively. The nutrients and HSs concentrations were chosen to resemble typical values of reject water from WWTPs that aim for biological nutrient removal (BNR), having phosphate

accumulating organisms in the waste activated sludge (Bergmans et al., 2014; De Vrieze et al., 2016; Gupta et al., 2015; Li et al., 2023; Pastor et al., 2008; Pavez-Jara et al., 2023). The reagents were added as  $\text{NaH}_2\text{PO}_4 \cdot \text{H}_2\text{O}$  (CAS: 10049-21-5, Sigma-Aldrich, Germany),  $\text{NH}_4\text{Cl}$  (CAS: 12125-02-9, Merck, Germany) and  $\text{MgCl}_2$  (CAS: 7786-30-3, Sigma-Aldrich, Germany). After the crystallisation experiments,  $\text{PO}_4^{3-}\text{-P}$  and TAN were measured in the solution, and in the crystals formed. The soluble concentrations were measured directly using the Hach-Lange kits described in section 2.1. The nutrients in the crystals were measured by dissolving 0.1 g of the precipitated solids in 5 mL of 1M  $\text{HNO}_3$  (Merck, Germany) (Warmadewanthi and Liu, 2009), and then diluting the solution 100 times in demineralised water before measuring with the respective kits.

**Table 4.1.** Experimental design of crystallisation tests at different pH and HSs concentrations.

Run (Triplicate)	pH	Melanoidins concentration g TOC/L	Humic acid concentration g TOC/L
1	6.50	0	0
2	7.25	0	0
3	8.00	0	0
4	6.50	1	0
5	7.25	1	0
6	8.00	1	0
7	6.50	2	0
8	7.25	2	0
9	8.00	2	0
10	6.50	0	1
11	7.25	0	1
12	8.00	0	1
13	6.50	0	2
14	7.25	0	2
15	8.00	0	2

#### 4.2.3. Solubility analysis of solubility of HSs at different pHs

HSs can be characterised based on their humic acid fraction (HAF) and fulvic acid fraction (FAF), which were measured as described by Klavins et al. (1999), using the method described by Zahmatkesh et al. (2016). The commercial humic acid used in our present study was obtained from humic acid sodium salt (CAS: 1415-93-6, Sigma-Aldrich, Germany), and a stock solution of melanoidins was prepared according to Dwyer et al. (2008). A characterisation of the stock solutions is shown in Table 4.2. HAF and FAF in HSs, were measured by decreasing the pH to 2 using 5 M  $\text{HCl}$ , followed by separation of the precipitate using a Microspin 12

centrifuge (Biosan, Latvia) at 14,000 rpm (11,500 rcf) for 20 min. TOC was measured in both the original samples and the supernatant after acidification and centrifugation. In addition, solubility tests were performed at pH levels of 6.5, 7.25, and 8, corresponding to the pH levels used in the crystallization experiments. The precipitated fraction was separated using the aforementioned methodology. Duplicate experiments were conducted, and the results are presented as the percentage of TOC that is soluble and particulate at the experiment pHs.

**Table 4.2.** Characterisation of the stock solutions of HSs used in the experiments.

HSs stock solutions	UVA 254 (1/cm)	Colour (g Pt-Co/L)	TOC (g TOC/L)	Preparation method
Melanoidins	605 ± 33	239 ± 33	24 ± 2	Autoclaving glucose 0.25 M, glycine 0.25 M, and NaHCO <sub>3</sub> 0.5 M at 121°C for 3 hours.
Humic acid	297 ± 17	183 ± 11	3.6 ± 0.2	Suspending 20 g/L of humic acid sodium salt in demineralised water.

#### 4.2.4. Microscopy and particle size distribution analysis (PSD)

Struvite samples produced during the crystallization experiments were filtered through a 1.2 µm filter and dried to a constant weight in a vacuum desiccator at 20 ± 1°C and -600 mbar. Digital Microscope (Keyence VHX-5000, Belgium) and an environmental scanning electron microscope (ESEM) model QUANTA FEG 650 (FEI, USA) were used to capture images of the produced struvite at different magnifications. The software of the digital microscope was utilized to measure the particle size distribution (PSD) of the crystals in the images, including the minimum and maximum Feret diameters. The aspect ratio was determined as the ratio of the maximum to minimum Feret diameters of each crystal. An aspect ratio of 1 means that the maximum and minimum Feret diameters are equal (perfect circle/sphere), and larger aspect ratios indicate elongated shapes. The results were plotted as "box and whisker" plots, with the boxes indicating the quartiles and the whiskers indicating the maximum and minimum values. The median and average were represented by a horizontal line in the middle and an "X", respectively. Particles with a zero value for one of the Feret diameters in the images were excluded from the analysis and considered experimental errors.

#### 4.2.5. Shear rate-induced breakage in struvite crystals

To investigate the effect of humic acid and melanoidins on struvite breakage, crystallization experiments were performed under specific shear rates. A modular compact rheometer model

MRC 302 (Anton Paar GmbH, Austria) was used to conduct the experiments. Struvite crystallization tests were carried out in a measuring cup C-CC27/SS/AIR (Anton Paar GmbH, Austria) using a concentric cylinder CC27 (Anton Paar GmbH, Austria) at 20°C. The volume of the 5M NaOH solution, which was required to maintain the pH at 7.25 at the end of the reaction, was determined through preliminary experiments. The humic acid and melanoidins concentrations used in the experiments were the same as those in the struvite crystallization experiments described in section 2.2. The chosen shear rates for the experiments were 1-10-100-1000 1/s. The precipitates were analysed by measuring the minimum and maximum Feret diameters, and the aspect ratio was calculated using the method described in section 2.4.

#### **4.2.6. Complexation of reagents with HSs**

Solutions of 15 mM of  $Mg^{2+}$  and  $PO_4^{3-}$ -P with 0, 1 and 2 g TOC/L (No-HSs, MEL-1, MEL-2, HA-1 and HA-2) were prepared and filtered in triplicate using nominal pore 1 kDa ultrafiltration membranes (Ultracel® regenerated cellulose, Merck Millipore, Germany) in a 50 mL AMICON® stirred cell (Merck Millipore, Germany). During filtration, 10 mL of permeate were collected and colour, UVA 254 and  $Mg^{2+}$  or  $PO_4^{3-}$ -P (depending on the assay) were measured. The results were expressed as the percentage of the fraction of ions of  $Mg^{2+}$  or  $PO_4^{3-}$ -P in the permeate over the initial concentration in the entire solution. The fraction that passed the ultrafiltration membrane over the initial concentration was called  $Mg^{2+}$  or  $PO_4^{3-}$ -P fraction in the permeate ( $Mg^{2+}$ -FP or  $PO_4^{3-}$ -P-FP, respectively).

### 4.3. Results and discussion

#### 4.3.1. Characterisation of HSs solubility and results of complexation assays

The solubility of HSs and their complexes varies with the pH of the solution or suspension in which they are present (Garcia-Mina, 2006; Tipping and Ohnstad, 1984). Table 4.3 shows a solubility characterisation of the melanoidins and humic acid stock solutions used in our experiments. As shown in Table 4.3, melanoidins were completely soluble at all the pH values studied. Additionally, the melanoidins' structure contained 97% FAF, which is soluble at any pH (Klavins et al., 1999). On the other hand, the humic acid stock solution was less soluble than the melanoidin solution, and its solubility slightly decreased at lower pH values used in the experiments. As anticipated for humic acid, the FAF only amounted to 6.4% (soluble fraction at pH 2). SUVA results showed that the humic acids had a roughly three times higher degree of aromaticity than the melanoidins. In their study on natural freshwater, Kikuchi et al. (2017) found a positive correlation between SUVA and metal complexation in the case of Fe and Cu. Therefore, it is reasonable to expect that humic acid complexes metals to a greater extent than melanoidins.

**Table 4.3.** Solubility and aromaticity characterisation of the HSs used in our present study at the studied pHs.

Characteristic	Melanoidins stock	Humic acid stock
Solubility at pH 6.5	Soluble: $100 \pm 2$ % TOC	$87 \pm 1$ % TOC
Solubility at pH 7.25	Soluble: $100 \pm 2$ % TOC	$89 \pm 2$ % TOC
Solubility at pH 8	Soluble: $100 \pm 1$ % TOC	$91 \pm 2$ % TOC
Characterisation as HSs at pH 2 based on Klavins et al. (1999)	FAF: $97 \pm 2$ % TOC HAF: $3.4 \pm 0.1$ % TOC	FAF: $6.4 \pm 0.3$ % TOC HAF: $94 \pm 4$ % TOC
SUVA (L/m/mg TOC)	$2.5 \pm 0.2$	$8.0 \pm 0.6$

#### 4.3.2. Complexation of HSs with $Mg^{2+}$ and $PO_4^{3-}$ -P

The complexation of cations with HSs depends on the presence and density of cation binding sites present in HSs moieties, which are mainly associated with hydroxyl, and carboxylic groups (Stevenson, 1994). Figure 4.1 shows the results of  $Mg^{2+}$  and  $PO_4^{3-}$ -P complexation assays performed at 1 and 2 g TOC/L of HSs. TAN was not tested because it was present in

excess in the synthetic reject water. Expectedly, the complexation of  $\text{PO}_4^{3-}\text{-P}$  was not affected by the presence of melanoidins or humic acid at all pH levels studied, attributable to the negative charges of melanoidins, humic acid, and  $\text{PO}_4^{3-}\text{-P}$  repelling each other (Migo et al., 1997). However,  $\text{PO}_4^{3-}\text{-P}$  can form binary complexes with HSs in the presence of multivalent cations such as  $\text{Ca}^{2+}$  (Audette et al., 2020). Multivalent cation-mediated complexation was not tested in our study, but it is expected to occur in full-scale struvite precipitation installations, as AD reject water contains multiple multivalent cations (Ezebuio and Körner, 2017). Furthermore, in the assays without HSs only 92% of  $\text{PO}_4^{3-}\text{-P}$  passed through the ultrafiltration membranes, while in the samples containing HSs, more than 95% of the  $\text{PO}_4^{3-}\text{-P}$  reached the permeate. The observed differences were significant in all cases as shown by statistic tests (shown in the appendix, Table A4.1). The lower  $\text{PO}_4^{3-}\text{-P}$  concentration in the permeate likely can be attributed to the repulsion of the negatively charged regenerated cellulose ultrafiltration membrane (Weber et al., 2013) and the  $\text{PO}_4^{3-}\text{-P}$  anions. Nonetheless, and despite the abundant presence of negatively charged groups related to the melanoidins and humic acids in the solution, the available  $\text{Na}^+$  ions present in HSs solutions may have partly neutralised the negative  $\text{PO}_4^{3-}\text{-P}$  charges, allowing membranes passage.

Conversely to  $\text{PO}_4^{3-}\text{-P}$ ,  $\text{Mg}^{2+}$  was strongly complexed by HSs at all studied pH values (Figure 4.1-b).  $\text{Mg}^{2+}$  complexation increased with the increased TOC concentration in both melanoidins and humic acid solutions. HSs-cation complexation varies with the specific characteristics of the HSs present (Morales et al., 2005; Plavšić et al., 2006; Rufián-Henares and de la Cueva, 2009). Enhanced  $\text{Mg}^{2+}$  complexation may be associated with HSs aromaticity and the humic or fulvic acid character of the HSs used in our present study. Mantoura et al. (1978) found that in general, fulvic acids complexed cations to a lower extent compared to humic acids. In our present study, the FAF in the purchased humic acid was substantially lower than in the experimentally produced melanoidins solution (Table 4.3). Additionally, the SUVA in humic acid was around three times higher than the SUVA of melanoidins (Table 4.3), suggesting higher aromaticity and complexing capacity in humic acid. The complexation of  $\text{Mg}^{2+}$  with HSs was not affected by pH, and the p-values in a single-factor ANOVA at 95% confidence, comparing all used concentrations, were not statistically different, i.e., 0.51, 0.67, 0.99, 0.83, and 0.78 in the case of No-HSs, MEL-1, MEL-2, HA-1, and HA-2, respectively. This indifference to pH contradicts other studies that have found a clear correlation between pH and HSs complexation capacity (Bosire et al., 2016; Yan et al., 2015). However, our researched pH range of 6.5 – 8.0 was quite narrow and far from the theoretical neutralisation

pH of HSs, which is around pH 3.0-4.5 (Karim et al., 2013). The complexation of  $\text{Mg}^{2+}$  in reject water is of considerable importance for practice, since it would lower the degree of supersaturation of the struvite precipitation reaction (Equation 4.1 and Equation 4.2, respectively), and thus could hinder struvite formation.

Colour and UVA 254 were analysed to quantify the fraction of HSs that passed through a 1kDa ultrafiltration membrane (shown in appendix Table A4.2 and A3). Around 15 % of the colour and 38% of UVA 254 passed through the 1 kDa membrane in the case of MEL-1 and MEL-2, and 1% and 3% passed it in the case of HA-1 and HA-2, respectively. The lower fraction of colour and UVA 254 of humic acids in the 1kDa permeate compared to melanoidins at the same concentrations, evidenced that the humic acid in the solution had higher MW.

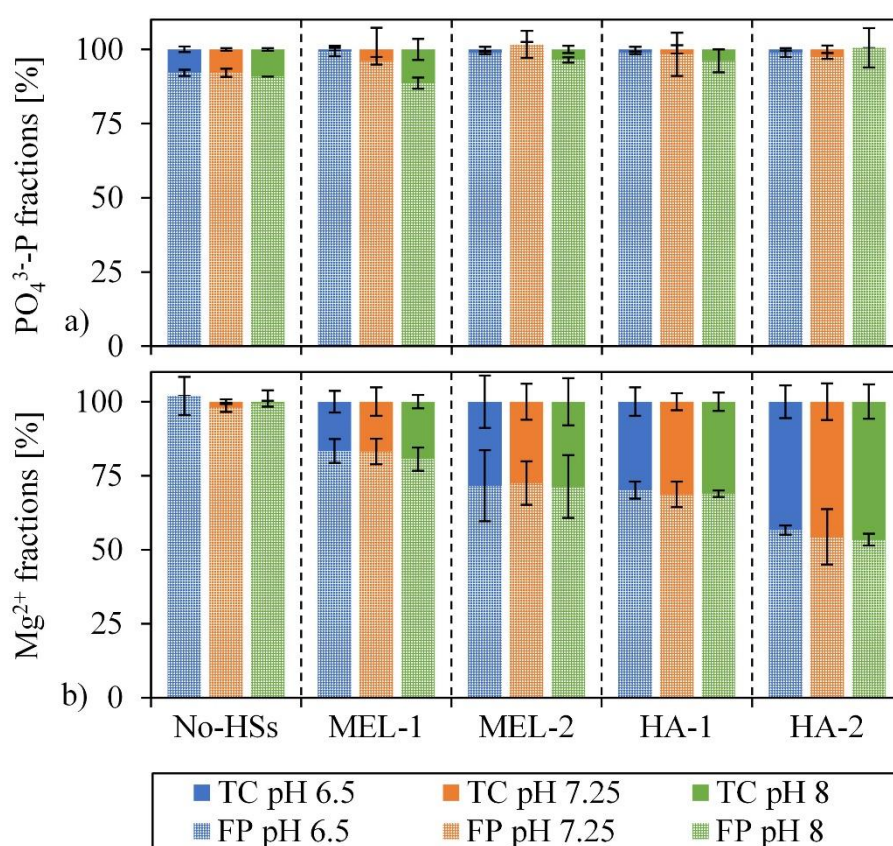


**Figure 4.1.** Complexation experiments using  $\text{PO}_4^{3-}\text{-P}$  and  $\text{Mg}^{2+}$  with an incremental concentration of melanoidins and humic acid; a)  $\text{PO}_4^{3-}\text{-P}$  fractions; b)  $\text{Mg}^{2+}$  fractions. “TC” represents total concentration and “FP” represents the fraction in the permeates.

#### 4.3.3. Nutrients mass balances

Figure 4.2 shows the levels of precipitated (P-) and soluble (S-) nutrients at the studied pH values and incremental concentrations of HSs. Our results indicated that an increase in pH led to an enhancement in struvite precipitation; molar ratios indeed confirmed the presence of struvite ( $Mg_{2+}:NH_4^+:PO_4^{3-} \approx 1$ ; appendix Figure A4.1). The enhanced struvite formation at pH 7.25 and 8 is attributed to the higher degree of supersaturation induced by the elevated pH. For struvite, the degree of supersaturation ( $\Omega$ ) is defined in Equation 4.2.

$$\Omega = \sqrt[3]{\frac{a_1 \cdot [Mg^{2+}] \cdot a_2 \cdot [NH_4^+] \cdot a_3 \cdot [PO_4^{3-}]}{K_{sp}}} \quad (4.2),$$

Where  $a_1$ ,  $a_2$ , and  $a_3$  represent the activity coefficients of  $Mg^{2+}$ ,  $NH_4^+$  and  $PO_4^{3-}$  and “[ ]” their molar concentrations, respectively;  $K_{sp}$  is the thermodynamic solubility product, which may vary between  $4.37 \cdot 10^{-14}$  to  $3.89 \cdot 10^{-10}$  depending on the method used for its determination (Bhuiyan et al., 2007). Our results showed that variations in pH affected the speciation of reagents, which in turn affects  $\Omega$  and the amount of produced struvite. Considering the speciation of the reagents in solution, Desmidt et al. (2013) found that the optimum range for struvite precipitation is at pH 8-10; which is consistent with the lower precipitate yields at pH 6.5 found in our study. Barber (2016) stated that the THP-AD-reject water tends to have a slight alkalic pH due to the elevated concentration of TAN, which may increase  $\Omega$ , promoting uncontrolled struvite precipitation.

We also examined the effect of HSs on struvite precipitation. The presence of melanoidins at pH 7.25 and 8 did not significantly alter the fraction of TAN and  $PO_4^{3-}$ -P in the precipitates. However, at pH 6.5 the incremental melanoidins concentrations resulted in a higher percentage of  $PO_4^{3-}$ -P in the precipitates, from 43% (No HSs) to 53 % and 55% in the case of MEL-1 and MEL-2. The ANOVA test at 95% confidence showed significant differences at pH 6.5 in the samples No-HSs, Mel-1 and Mel-2 samples (p-value= 0.0039), and Tukey HSD- test showed that the  $PO_4^{3-}$ -P measurements in MEL-1 and MEL-2 were equal (p-value=0.53) and significantly higher than No-HSs (p-value= 0.013 and p-value=0.004, respectively). At pH 6.5, MEL-1 and MEL-2 promoted struvite formation, presumably due to the addition of nucleation centres (seeding material), resulting from the partial solubility of melanoidins at lower pH values. Despite the high solubility of melanoidins (shown in Table 4.2) the impurities formed at decreased pH may act as seeding material and promote nucleation and further precipitation (Ariyanto et al., 2014; Battistoni et al., 2005; Le Corre et al., 2007; Mehta and Batstone, 2013).



Likely, the formed impurities had a colloidal nature and thus remained in suspension during sample centrifugation for assessing the solubility.

In contrast to melanoidins, humic acid hindered struvite precipitation (Figure 4.2) particularly at pH 6.5, in which only 6 % (HA-1) and 17 % (HA-2) of the  $\text{PO}_4^{3-}$ -P precipitated, compared to 43% in No-HSs. Also at pH 7.25 and 8, the presence of humic acid reduced precipitation; however, this effect was much less than at the lowest pH tested. Previous studies also have reported inhibitory effects of humic substances on struvite precipitation. For instance, Zhou et al. (2015) found inhibition in struvite formation caused by 40 mg/L HSs, using HSs containing  $\geq 90\%$  fulvic acid. Furthermore, Wei et al. (2019) also found that humic acid caused inhibition of struvite nucleation and moderately hindered crystals growth; the study suggests that  $\text{Mg}^{2+}$  complexation in the humic acid matrix might have caused the inhibition. Complexation of HSs and  $\text{Mg}^{2+}$  has already been reported in literature (Bosire et al., 2016; Zhao et al., 2016). Moreover, the experiments in our present work strongly suggested that HSs and particularly the humic acid –  $\text{Mg}^{2+}$  complexes, hindered struvite precipitation.

Finally, we assessed the mass balance of nutrients in each experiment and found that the discrepancy between supernatant plus precipitate was within 10% of the initial nutrient mass (mean difference t-test at 95% of confidence showed in Table A4.1 of appendix). Also, a single-factor ANOVA analysis at 95% of confidence, showed that all summed masses deviated slightly (p-values of  $1.52 \cdot 10^{-4}$  and  $3.28 \cdot 10^{-9}$  in the case of  $\text{PO}_4^{3-}$ -P and TAN, respectively). The small differences are attributed to the heterogeneity of suspended samples and the interference of the  $\text{PO}_4^{3-}$ -P measurement with humic substances. TAN mass was found to be slightly higher than the expected value, possibly due to deamination of glycine in the melanoidins stock solution under high-temperature conditions. Deamination of proteins caused by exposure to high temperatures has been described before. Wilson and Novak (2009) found ammonia production in thermal hydrolysis with bovine serum albumin already at  $130^\circ\text{C}$ , which increased with the reaction temperature.

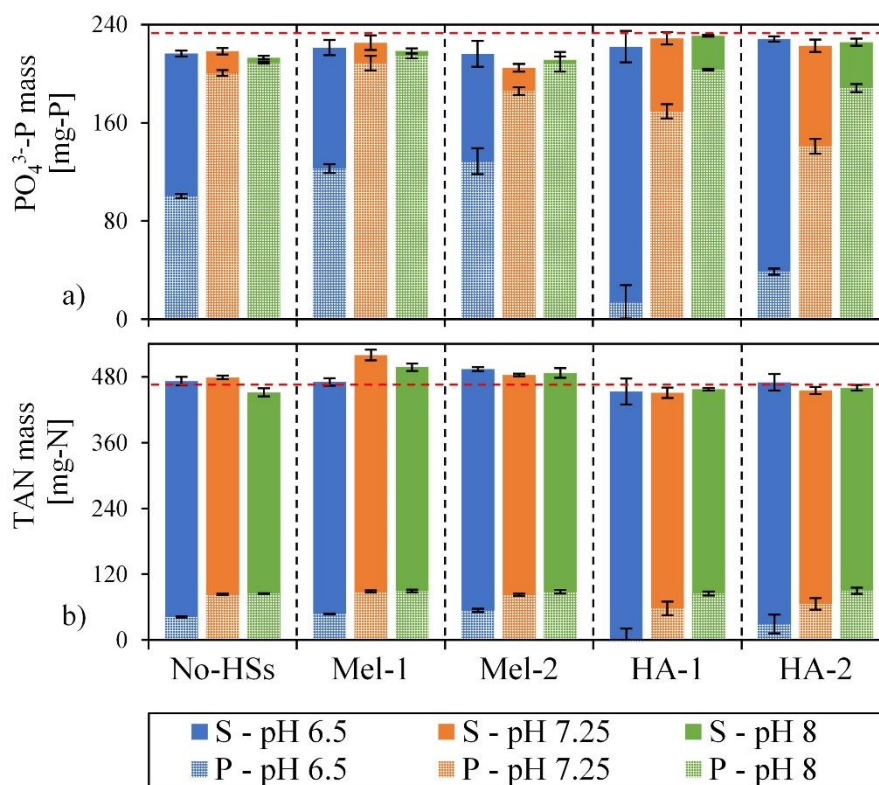


**Figure 4.2.** Nutrients mass balances at different concentrations of melanoidins and humic acids at different pH values. a)  $\text{PO}_4^{3-}$ -P mass; b) TAN mass. “P” represents the nutrient mass in the precipitates, and “S” is the mass in the supernatants; the red-dashed lines represent the stoichiometric mass of nutrients.

#### 4.3.4. PSD and morphology of the produced crystals

The PSD and morphology of the produced crystals in the presence of melanoidins at different pH values are presented in Figure 4.3. Crystals produced in presence of humic acid, could not be analysed, since humic acid precipitates clogged the filters, while the attached non-soluble humic particles influenced the crystal size (additional material, Figure A4.2). Crystallization experiments showed that in the absence of HSs (No-HSs), the size average and variability of crystals decreased with an increased pH. Minimum Feret diameters in No-HSs averaged  $53 \pm 36 \mu\text{m}$ ,  $50 \pm 27 \mu\text{m}$  and  $39 \pm 18 \mu\text{m}$  at pH 6.5, 7.25 and 8 respectively; and maximum Feret diameters averaged  $105 \pm 68 \mu\text{m}$ ,  $94 \pm 53 \mu\text{m}$  and  $88 \pm 43 \mu\text{m}$  at the same pH values, respectively. Increased pH resulted in smaller crystals, even though the mass balance showed a higher degree of TAN and  $\text{PO}_4^{3-}$ -P crystallisation under these conditions (Figure 4.1). Supersaturation is described to be positively correlated with nucleation (Mehta and Batstone, 2013), and it defines the size of crystals (Shaddel et al., 2019). In our present study, elevated

pH induced elevated supersaturation indexes, which led to the formation of more nuclei producing more and smaller crystals. Shaddel et al. (2019) described similar behaviour at pH 7.5, 8.5 and 9.5.

Furthermore, MEL-1 and MEL-2 solutions rendered smaller crystals compared to No-HSs, at all analysed pH values. However, the decrease in size with increasing pH was not consistent, and the largest crystals among MEL-1 were formed at pH 7.25, with average minimum and maximum Feret diameters of 39  $\mu\text{m}$  and 61  $\mu\text{m}$ , respectively. MEL-2 rendered decreased Feret diameters and higher size variability with increasing pH. The observed smaller Feret diameter of the formed crystals in presence of melanoidins, could jeopardize the separation of crystals and reject water in full scale struvite reactors. A low crystal diameter might lead to the need of different settling velocities in completely stirred systems or fluidised bed systems (Vasa and Pothanamkandathil Chacko, 2021). Also, small diameters are not efficient for secondary nucleation, which, according to Cayey and Estrin (Cayey and Estrin, 1967), only occurs with particles bigger than 220  $\mu\text{m}$ , due to their greater contact probabilities (Mullin, 2001).

Crystal morphology was expressed by its aspect ratio (Figure 4.3-c). The presence of melanoidins decreased the averaged aspect ratio regardless of the melanoidins concentration, compared with the No-HSs assays. The pH did not show a clear influence on the aspect ratio, except in MEL-2 where the crystals became less elongated with increased pH. Figure 4.4 shows pictures of the crystals formed under the different conditions studied. No-HSs samples returned semi-transparent crystals with elongated blade-like shapes. These elongated shapes are in line with the observed aspect ratio data (Figure 4.3-c). On the other hand, the addition of melanoidins, rendered more square-like shaped crystals with a distinctive brownish colour (Figure 4.4), indicating the presence of melanoidins either at the surface or incorporated throughout the crystals, following the hypotheses of Zhou et al. (2015) and Abel-Denee et al. (2018). After nucleation, crystals-growth may occur following 2 processes, i) growing atom by atom, and ii) by aggregation of smaller crystals into bigger ones (Galbraith et al., 2014). Melanoidins adsorbed on the struvite crystals during the growth process can be expected to interfere with both growth processes. This phenomenon was illustrated by the microscopic observations (Figure 4.4); the presence of melanoidins led to brownish crystals. The same processes are proposed for other HSs, albeit, due to their lower solubility, the effects might be more pronounced. HSs might either act as a “glue” to aggregate the smaller particles into bigger ones (Figure 4.6), or as a solid particle that hinders the aggregation process, decreasing the crystal size as described by Wei et al. (2019). The struvite growth process in presence of HSs

is likely driven by the nature of the HSs and the crystals shear stress-induced breakage during the crystallisation process.

Figure 4.5 shows a magnification of the crystals formed under the different applied conditions. In case of No-HSs, optic and ESEM microscopy showed that the increased pH caused so called “dendrites” formation in the crystal structure (Kobayashi, 1993; Lee, 2017). Dendrites are hierarchical structures, which grow far from the plane front in preferential direction, like a tree. Dendrites formation was observed in samples without HSs at elevated pH, likely due to the increased supersaturation index that produced more nuclei, from which the crystals grew from multiple sites (Glicksman and Lupulescu, 2004). Conversely, in the samples with melanoidins, optic microscopy showed homogenous pigmentation in struvite crystals, likely due to the high melanoidins’ solubility (Figure 4.5). In additional material, Figure A4.2 shows humic acid precipitates using optical microscopy and ESEM. Humic acid formed a compact cake on the filters when the crystals were separated from the supernatant. The cake was characterised by a compact rigid structure and the cake particles differed distinctly from the crystals formed in the solution. ESEM revealed that the compact and rigid cake was likely formed due to adhesive forces between humic acid and the formed crystals. Optical microscopy clearly revealed the brown-coloured crystals and the tight interaction of particulate-humic material in the struvite crystals (Additional material, Figure 4.A2). The presence of HSs led to smaller-sized struvite crystals, but results could not reveal whether HSs hindered the crystals' growth or increased the crystals weakness, inducing breakage of the struvite formed.

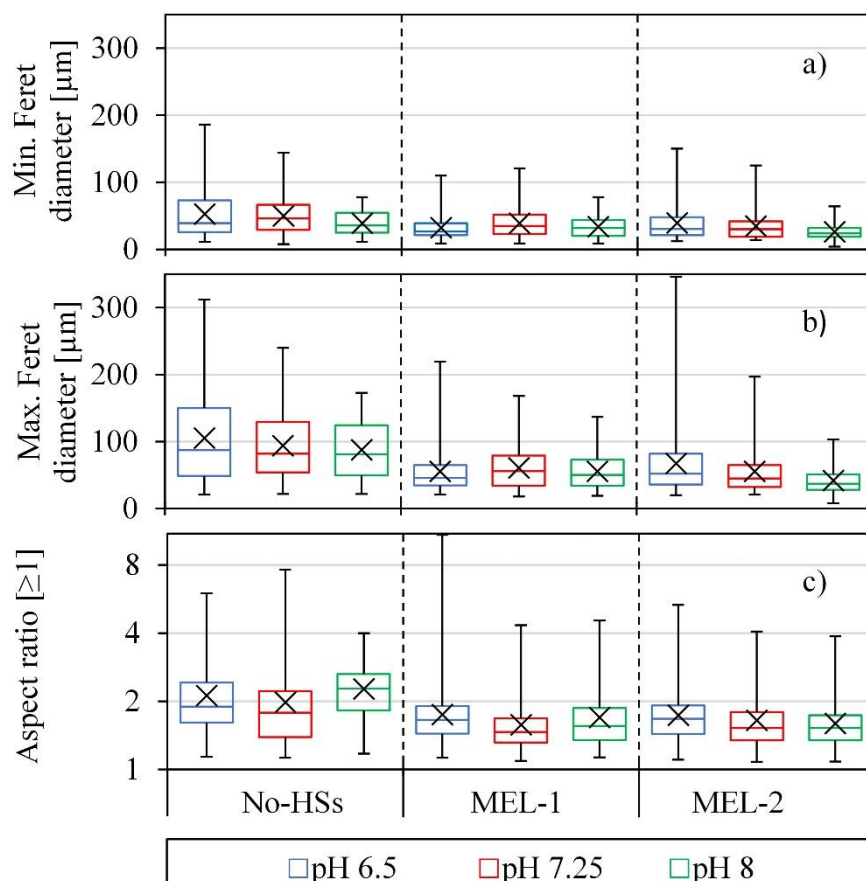


**Figure 4.3.** PSD analysis of the crystallisation experiments: a) Minimum Feret diameter; b) Maximum Feret diameter; c) Aspect ratio (logarithmic scale). HSs data are not shown, since precipitates could not be determined.

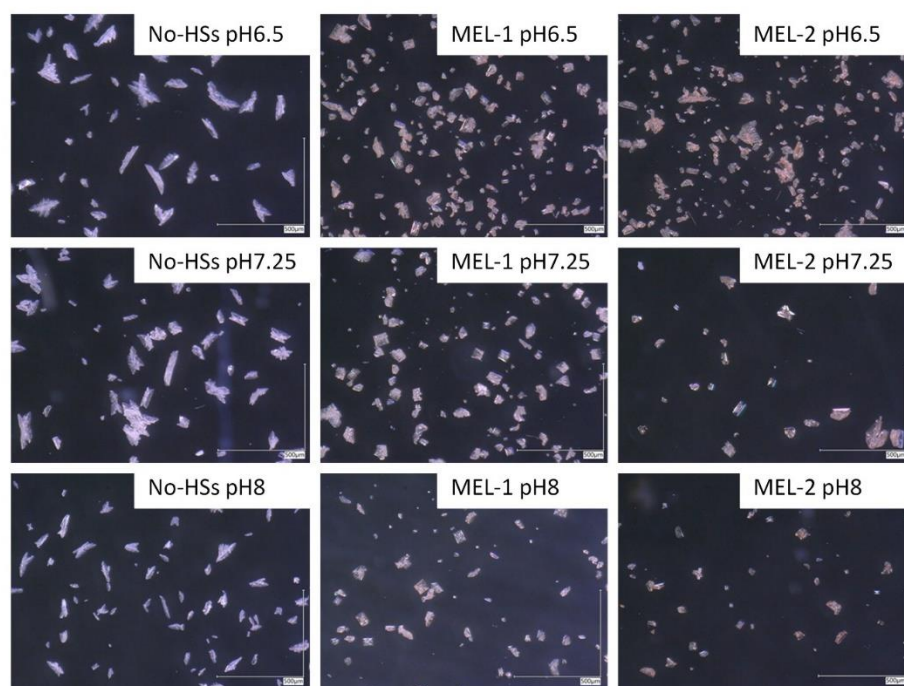


**Figure 4.4.** Struvite pictures in presence of melanoidins at different pH conditions.

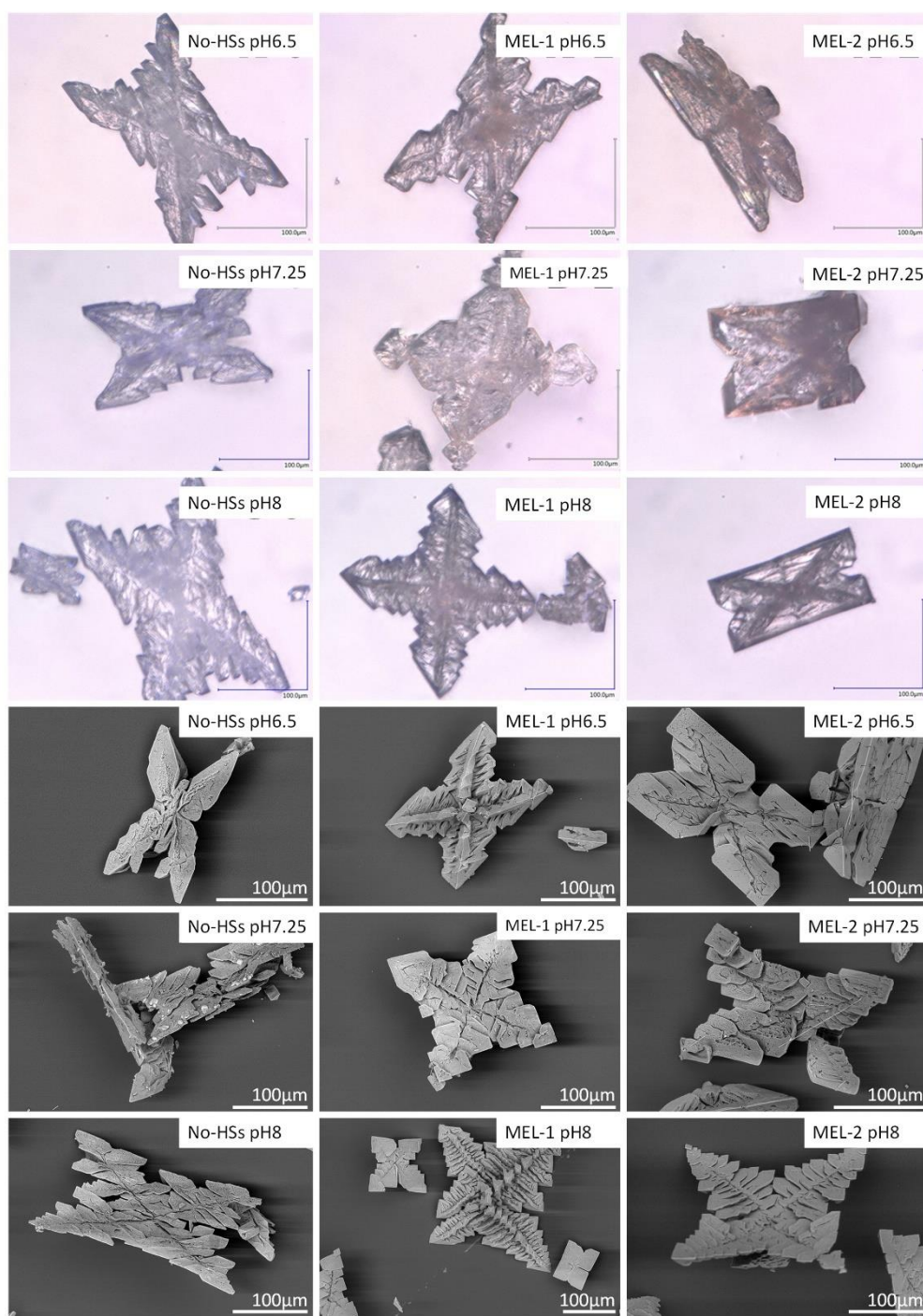


**Figure 4.5.** Optic microscopy and ESEM pictures of specific crystals formed in the presence of melanoidins at different pH conditions.

#### 4.3.5. Shear rate-induced breakage of the struvite produced.

Experiments at increasing shear rate were conducted to further research the stability of the formed crystals. We assumed that the stability is inverse to the susceptibility of struvite crystals to break (breakage), which can be a combination of abrasion and cleavage. The breakage of



formed crystals was indirectly measured by conducting struvite crystallization experiments in the presence of melanoidins and humic acid at various shear rates ranging from 1, 10, 100, to 1000 1/s. The experiments were performed at pH 7.25. HA-2 was not analysed, because the produced precipitate remained adhered to the filters and yielded a low quantity. Figures 4.6-a and b show the minimum and maximum Feret diameters of the formed struvite crystals at the different shear rates and HSs concentrations. The results showed that in the case of No-HSs, increased shear rate prevented the crystals to grow. No-HSs samples showed drastically reduced minimum and maximum Feret diameters, i.e., from  $91 \pm 108 \mu\text{m}$  to  $8 \pm 6 \mu\text{m}$  and  $227 \pm 207$  to  $22 \pm 12 \mu\text{m}$ , respectively, with increased shear stress during crystal formation, from 1 to 1000 1/s. Also, the occurrence of big crystals (represented in Figure 4.6 by upper whiskers) decreased, characterised by decreasing minimum and maximum Feret diameters from 742 to 13  $\mu\text{m}$  and 1159 to 24  $\mu\text{m}$ , at 1 and 1000 1/s, respectively. The aspect ratio of the crystals was not affected by the shear rate and crystal morphology remained mildly elongated.

Melanoidins prevented breakage of the crystals, and possibly led to aggregation of particles that might have been broken without melanoidin addition. The minimum and maximum Feret diameters increased with the melanoidins concentration, particularly at 10 1/s, and decreased with shear rate. However, the size reduction induced by the increased shear stress was less prominent in MEL-1 and MEL-2 than in No-HSs, referring to both maximum and minimum Feret diameters. Melanoidins also decreased the aspect ratio at increased concentration, possibly due to breakage of needle-shaped particles and subsequent aggregation in non-preferential directions.

HA-1 showed the smallest particle size among the studied HSs samples. These small particles were probably a mixture of struvite and humic acid, as shown in Additional material Figure A4.2. However, HA-1 did not show a clear trend regarding the size of maximum and minimum Feret diameters at shear rates of 10 and 100 1/s, while larger particles were formed at shear rates of 1 and 1000 1/s. The aspect ratio in HA-1 samples hardly changed with shear rate; nevertheless, the low values indicated the presence of rounded particles.



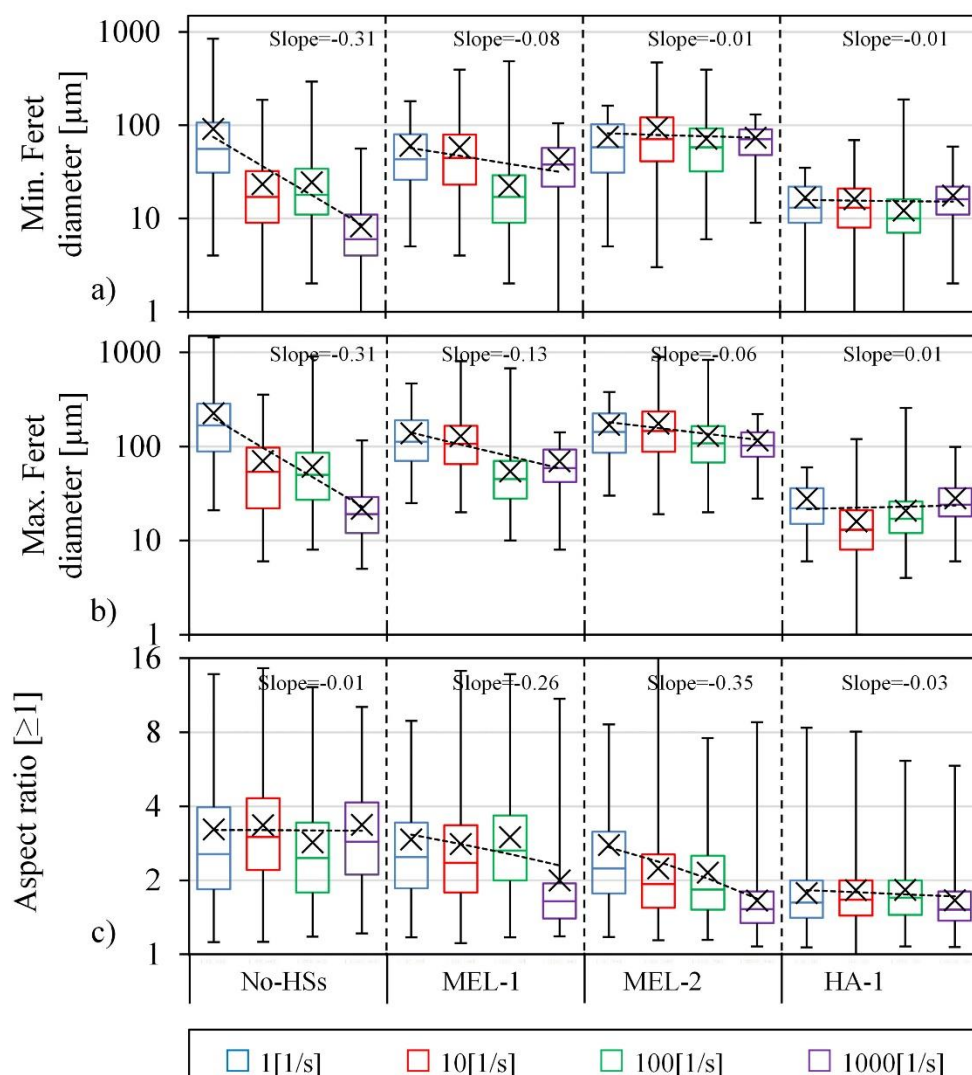


**Figure 4.6.** Particle size distribution of struvite crystals in shear rate breakage tests at different HSs concentrations. a) Minimum Feret diameter (logarithmic scale); b) Maximum Feret diameter (logarithmic scale); c) Aspect ratio. The dotted lines represent a linear data fitting between the measured average values and the logarithm of the shear rate.

The observed results clearly showed that HSs addition increased the stability of the struvite crystals and rendered particles with a smaller aspect ratio. Compared to samples without HSs, the resulting particles with melanoidin addition had larger Feret diameters, whereas they were smaller with HAs addition. These results suggest that there are differences in the adhesive forces of melanoidins and HAs on struvite crystals causing different degrees of breakage. Such forces are most likely size and shape-dependent, as described by Carvill (1993).

In the struvite-HSs interaction, two types of interactive forces play a prominent role. The struvite-struvite interactive forces have been described previously by Fromberg et al. (2020) as Van der Waals/electrostatic forces that are dependent on the distance between the crystals, as stated in the DLVO theory. In addition, the HSs-struvite forces are attributable to either adsorption as described by Zhang et al. (2016) and Wei et al. (2019), or to DLVO-related forces, causing adsorption of the particulate/colloidal organic matter on, or in, the crystals. The latter is more apparent for humic acid containing a particulate fraction of 11% (at pH 7.25), while melanoidins were fully soluble (Table 4.2). DLVO forces can be described by measuring zeta potential of the analysed suspensions, which is determined by the composition and ionic strength of the solution (Bhattacharjee, 2016; Fromberg et al., 2020; Zhang et al., 2023). HSs have a negative zeta potential, however, Rodrigues et al. (2009) found that the presence of  $Mg^{2+}$  was able to elevate the zeta potential of HSs solutions at pH 4, 7, and 9 and created molecular aggregates. Besides, struvite zeta potential is predominantly negative and tends to decrease with increasing pH and  $Mg^{2+}$  concentration (Bouropoulos and Koutsoukos, 2000; Fromberg et al., 2020). Considering that the zeta potentials of struvite and HSs are both negative, cations in solution ( $Mg^{2+}$  and  $NH_4^+$ ), likely facilitated the formation of HSs-embedded crystals. Figure 4.7 shows a schematic representation of the observed struvite crystal growth phenomena in the (non-) presence of HSs.

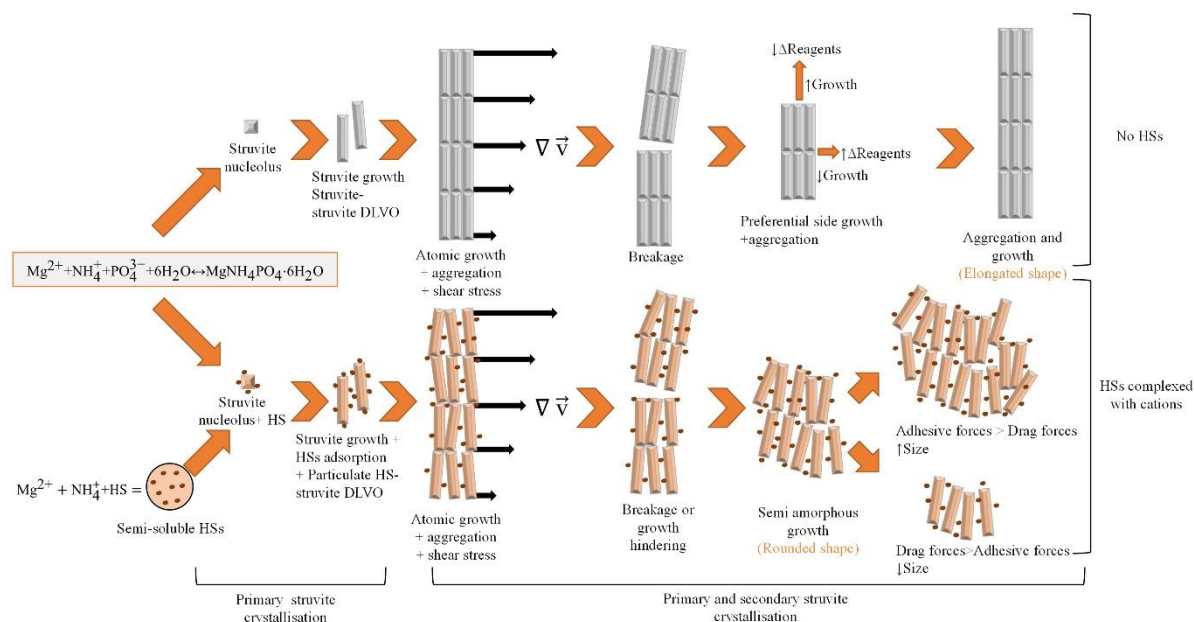


**Figure 4.7.** Comparison between struvite crystal growth and breakage in the presence of melanoidins and humic acid (light brown coloured), and absence of HSs (grey coloured). The scheme indicates crystal growth, aggregation and breakage or growth hindering, HSs-crystal adsorption and intercalation, as well as the role of DLVO and adhesive forces. Shear forces are represented as the divergence of velocity ( $\nabla \vec{v}$ ).

#### **4.3.6. Implications of THP-formed HSs on full-scale $\text{PO}_4^{3-}$ -P removal.**

The formation of HSs during THP through the Maillard reaction generates HSs with a wide range of molecular weights and solubilities (Dwyer et al., 2008; Liu et al., 2012), capable of forming complexes with cations in solution. Melanoidins present in the THP-reject water may complex  $\text{Mg}^{2+}$ , increasing the amount of  $\text{Mg}^{2+}$  salts required to achieve the desired  $\text{Mg}^{2+}/\text{PO}_4^{3-}$ -P molar ratio. Therefore, part of the  $\text{PO}_4^{3-}$ -P might not be removed due to  $\text{Mg}^{2+}$ -HSs chelation, or more  $\text{Mg}^{2+}$  salts may be needed to reach the desired concentration. Additionally, the colloidal or particulate fraction produced during THP may reach the struvite crystallisation reactors (Barber, 2016; Zhang et al., 2018), leading to intercalation in the struvite crystals, affecting their sizes and settling times. HSs-intercalated struvite may compromise adoption of struvite as a fertiliser, because of the non-conventional colour of the crystals. Moreover, the adsorbed and/or embedded HSs on, or in, the struvite crystal might contain other cations, such as heavy metals (Bianchi et al., 2008; Jansen et al., 1996; Yip et al., 2010), which might also compromise its use as fertiliser. The environmental implications of HSs and heavy metals in struvite is a subject of interest for further research. Furthermore, another observed consequence of THP pre-treatment is an increase in TAN concentration in anaerobic digesters (Jolis, 2008; Ochs et al., 2021). The increase in TAN concentration during AD also increases the reactors' pH; this increase is commonly moderate since the anaerobic process occurs in a pH range suitable for the microorganisms to grow (pH 7-8). The elevated TAN concentrations and the THP-induced pH increase might benefit struvite precipitation, since they both increase the supersaturation index and promote crystallisation.

#### 4.4. Conclusions

Our present study led to the following conclusions:

- Melanoidins moderately, and humic acid strongly complexed  $Mg^{2+}$ . The complexing capacity of HSs is related to the HSs origin, particularly the soluble fraction of HSs, and its aromaticity.
- Humic acid strongly hindered struvite formation, likely due to  $Mg^{2+}$  complexation. The struvite crystallisation inhibition was higher at pH 6.5 compared to pH 7.25 and 8.
- Melanoidins presence decreased the maximum and minimum Feret diameters and the aspect ratio of the formed struvite crystal. In addition, melanoidins enhanced the stability of struvite crystals towards breakage at elevated shear rates, particularly when exceeding 10 1/s. Conversely, humic acid did not affect the struvite crystal stability towards abrasion or breakage and reduced the Feret diameters and aspect ratio.
- Adsorption of HSs on, or in, the produced struvite resulted in an evident change in colour.

#### **4.1. List of abbreviations**

AD: anaerobic digestion.

ESEM: environmental scanning electron microscope.

FAF: fulvic acid fraction.

HA-1: experiments in presence of humic substances as humic acids in a concentration of 1 g/L of total organic carbon.

HA-2: experiments in presence of humic substances as humic acids in a concentration of 2 g/L of total organic carbon.

HAF: humic acid fraction.

HSs: humic substances.

MEL-1: experiments in presence of humic substances as melanoidins in a concentration of 1 g/L of total organic carbon.

MEL-2: experiments in presence of humic substances as melanoidins in a concentration of 2 g/L of total organic carbon.

No-HSs: experiments without the presence of humic substances.

PN/A: partial nitrification/anammox.

PSD: particle size distribution.

SUVA: specific ultraviolet absorbance.

TAN: total ammoniacal nitrogen.

THP: thermal hydrolysis process.

TOC: total organic carbon.

UVA 254: ultraviolet absorbance at 254 nm.

WWTPs: wastewater treatment plants.

## 4.2. References

- Abel-Denee, M., Abbott, T. and Eskicioglu, C. 2018. Using mass struvite precipitation to remove recalcitrant nutrients and micropollutants from anaerobic digestion dewatering centrate. *Water Research* 132, 292-300.
- Abma, W.R., Driessen, W., Haarhuis, R. and van Loosdrecht, M.C.M. 2010. Upgrading of sewage treatment plant by sustainable and cost-effective separate treatment of industrial wastewater. *Water Science and Technology* 61(7), 1715-1722.
- Appels, L., Lauwers, J., Degève, J., Helsen, L., Lievens, B., Willems, K., Van Impe, J. and Dewil, R. 2011. Anaerobic digestion in global bio-energy production: Potential and research challenges. *Renewable and Sustainable Energy Reviews* 15(9), 4295-4301.
- Ariyanto, E., Sen, T.K. and Ang, H.M. 2014. The influence of various physico-chemical process parameters on kinetics and growth mechanism of struvite crystallisation. *Advanced Powder Technology* 25(2), 682-694.
- Audette, Y., Smith, D.S., Parsons, C.T., Chen, W., Rezanezhad, F. and Van Cappellen, P. 2020. Phosphorus binding to soil organic matter via ternary complexes with calcium. *Chemosphere* 260, 127624.
- Azman, S., Khadem, A.F., Plugge, C.M., Stams, A.J.M., Bec, S. and Zeeman, G. 2017. Effect of humic acid on anaerobic digestion of cellulose and xylan in completely stirred tank reactors: inhibitory effect, mitigation of the inhibition and the dynamics of the microbial communities. *Applied Microbiology and Biotechnology* 101(2), 889-901.
- Barber, W. 2016. Thermal hydrolysis for sewage treatment: a critical review. *Water Research* 104, 53-71.
- Battistoni, P., Paci, B., Fatone, F. and Pavan, P. 2005. Phosphorus Removal from Supernatants at Low Concentration Using Packed and Fluidized-Bed Reactors. *Industrial & Engineering Chemistry Research* 44(17), 6701-6707.
- Bergmans, B.J.C., Veltman, A.M., Van Loosdrecht, M.C.M., Van Lier, J.B. and Rietveld, L.C. 2014. Struvite formation for enhanced dewaterability of digested wastewater sludge. *Environmental Technology* 35(5), 549-555.
- Bhattacharjee, S. 2016. DLS and zeta potential – What they are and what they are not? *Journal of Controlled Release* 235, 337-351.
- Bhuiyan, M., Mavinic, D. and Beckie, R. 2007. A solubility and thermodynamic study of struvite. *Environmental technology* 28(9), 1015-1026.
- Bianchi, V., Masciandaro, G., Giraldi, D., Ceccanti, B. and Iannelli, R. 2008. Enhanced Heavy Metal Phytoextraction from Marine Dredged Sediments Comparing Conventional Chelating Agents (Citric Acid and EDTA) with Humic Substances. *Water, Air, and Soil Pollution* 193(1-4), 323-333.
- Bork, L.V., Haase, P.T., Rohn, S. and Kanzler, C. 2022. Structural characterization of polar melanoidins deriving from Maillard reaction intermediates – A model approach. *Food Chemistry* 395, 133592.
- Bosire, G.O., Kgarebe, B.V. and Ngila, J.C. 2016. Experimental and Theoretical Characterization of Metal Complexation with Humic Acid. *Analytical Letters* 49(14), 2365-2376.
- Bouropoulos, N.C. and Koutsoukos, P.G. 2000. Spontaneous precipitation of struvite from aqueous solutions. *Journal of Crystal Growth* 213(3), 381-388.
- Carrere, H., Dumas, C., Battimelli, A., Batstone, D.J., Delgenes, J.P., Steyer, J.P. and Ferrer, I. 2010. Pretreatment methods to improve sludge anaerobic degradability: A review. *J. Hazard. Mater.* 183(1-3), 1-15.
- Carvill, J. (1993) *Mechanical Engineer's Data Handbook*. Carvill, J. (ed), pp. 146-171, Butterworth-Heinemann, Oxford.

- Cayey, N. and Estrin, J. 1967. Secondary nucleation in agitated, magnesium sulfate solutions. *Industrial & Engineering Chemistry Fundamentals* 6(1), 13-20.
- de-Bashan, L.E. and Bashan, Y. 2004. Recent advances in removing phosphorus from wastewater and its future use as fertilizer (1997–2003). *Water Research* 38(19), 4222-4246.
- De Vrieze, J., Smet, D., Klok, J., Colsen, J., Angenent, L.T. and Vlaeminck, S.E. 2016. Thermophilic sludge digestion improves energy balance and nutrient recovery potential in full-scale municipal wastewater treatment plants. *Bioresource Technology* 218, 1237-1245.
- De Yoreo, J.J. and Vekilov, P.G. 2003. Principles of Crystal Nucleation and Growth. *Reviews in Mineralogy and Geochemistry* 54(1), 57-93.
- Desmidt, E., Ghyselbrecht, K., Monballiu, A., Rabaey, K., Verstraete, W. and Meesschaert, B.D. 2013. Factors influencing urease driven struvite precipitation. *Separation and Purification Technology* 110, 150-157.
- Dwyer, J., Starrenburg, D., Tait, S., Barr, K., Batstone, D.J. and Lant, P. 2008. Decreasing activated sludge thermal hydrolysis temperature reduces product colour, without decreasing degradability. *Water research* 42(18), 4699-4709.
- Ellis, G.P. (1959) *Advances in Carbohydrate Chemistry*. Wolfrom, M.L. (ed), pp. 63-134, Academic Press.
- Ezebuio, N.C. and Körner, I. 2017. Characterisation of anaerobic digestion substrates regarding trace elements and determination of the influence of trace elements on the hydrolysis and acidification phases during the methanisation of a maize silage-based feedstock. *Journal of Environmental Chemical Engineering* 5(1), 341-351.
- Fromberg, M., Pawlik, M. and Mavinic, D.S. 2020. Induction time and zeta potential study of nucleating and growing struvite crystals for phosphorus recovery improvements within fluidized bed reactors. *Powder Technology* 360, 715-730.
- Gahlot, P., Balasundaram, G., Tyagi, V.K., Atabani, A.E., Suthar, S., Kazmi, A.A., Štěpanec, L., Juchelková, D. and Kumar, A. 2022. Principles and potential of thermal hydrolysis of sewage sludge to enhance anaerobic digestion. *Environmental Research* 214, 113856.
- Galbraith, S.C., Schneider, P.A. and Flood, A.E. 2014. Model-driven experimental evaluation of struvite nucleation, growth and aggregation kinetics. *Water Research* 56, 122-132.
- Garcia-Mina, J.M. 2006. Stability, solubility and maximum metal binding capacity in metal–humic complexes involving humic substances extracted from peat and organic compost. *Organic Geochemistry* 37(12), 1960-1972.
- Glicksman, M.E. and Lupulescu, A.O. 2004. Dendritic crystal growth in pure materials. *Journal of Crystal Growth* 264(4), 541-549.
- Gomyo, T. and Horikoshi, M. 1976. On the Interaction of Melanoidin with Metallic Ions. *Agricultural and Biological Chemistry* 40(1), 33-40.
- Gupta, A., Novak, J.T. and Zhao, R. 2015. Characterization of organic matter in the thermal hydrolysis pretreated anaerobic digestion return liquor. *Journal of Environmental Chemical Engineering* 3(4, Part A), 2631-2636.
- Jansen, S., Paciolla, M., Ghabbour, E., Davies, G. and Varnum, J.M. 1996. The role of metal complexation in the solubility and stability of humic acid. *Materials Science and Engineering: C* 4(3), 181-187.
- Jolis, D. 2008. High-Solids Anaerobic Digestion of Municipal Sludge Pretreated by Thermal Hydrolysis. *Water Environment Research* 80(7), 654-662.
- Karim, S., Okuyama, Y. and Aoyama, M. 2013. Separation and characterization of the constituents of compost and soil humic acids by two-dimensional electrophoresis. *Soil Science and Plant Nutrition* 59(2), 130-141.

- Kikuchi, T., Fujii, M., Terao, K., Jiwei, R., Lee, Y.P. and Yoshimura, C. 2017. Correlations between aromaticity of dissolved organic matter and trace metal concentrations in natural and effluent waters: A case study in the Sagami River Basin, Japan. *Science of The Total Environment* 576, 36-45.
- Klavins, M., Eglite, L. and Serzane, J. 1999. Methods for analysis of aquatic humic substances. *Critical Reviews in Analytical Chemistry* 29(3), 187-193.
- Kobayashi, R. 1993. Modeling and numerical simulations of dendritic crystal growth. *Physica D: Nonlinear Phenomena* 63(3), 410-423.
- Le Corre, K.S., Valsami-Jones, E., Hobbs, P., Jefferson, B. and Parsons, S.A. 2007. Struvite crystallisation and recovery using a stainless steel structure as a seed material. *Water Research* 41(11), 2449-2456.
- Le Corre, K.S., Valsami-Jones, E., Hobbs, P. and Parsons, S.A. 2009. Phosphorus Recovery from Wastewater by Struvite Crystallization: A Review. *Critical Reviews in Environmental Science and Technology* 39(6), 433-477.
- Lee, D.N. 2017. Orientations of dendritic growth during solidification. *Metals and Materials International* 23(2), 320-325.
- Li, B., Huang, H.M., Boiarkina, I., Yu, W., Huang, Y.F., Wang, G.Q. and Young, B.R. 2019. Phosphorus recovery through struvite crystallisation: Recent developments in the understanding of operational factors. *Journal of Environmental Management* 248, 109254.
- Li, X., Liu, C., Xie, H., Sun, Y., Xu, S. and Liu, G. 2023. Nitrogen removal of thermal hydrolysis-anaerobic digestion liquid: A review. *Chemosphere* 320, 138097.
- Liu, X., Wang, W., Gao, X., Zhou, Y. and Shen, R. 2012. Effect of thermal pretreatment on the physical and chemical properties of municipal biomass waste. *Waste Management* 32(2), 249-255.
- Mantoura, R., Dickson, A. and Riley, J. 1978. The complexation of metals with humic materials in natural waters. *Estuarine and Coastal Marine Science* 6(4), 387-408.
- Marti, N., Pastor, L., Bouzas, A., Ferrer, J. and Seco, A. 2010. Phosphorus recovery by struvite crystallization in WWTPs: Influence of the sludge treatment line operation. *Water Research* 44(7), 2371-2379.
- Mehta, C.M. and Batstone, D.J. 2013. Nucleation and growth kinetics of struvite crystallization. *Water Research* 47(8), 2890-2900.
- Migo, V.P., Del Rosario, E.J. and Matsumura, M. 1997. Flocculation of melanoidins induced by inorganic ions. *Journal of Fermentation and Bioengineering* 83(3), 287-291.
- Migo, V.P., Matsumura, M., Del Rosario, E.J. and Kataoka, H. 1993. The effect of pH and calcium ions on the destabilization of melanoidin. *Journal of Fermentation and Bioengineering* 76(1), 29-32.
- Morales, F.J., Fernández-Fraguas, C. and Jiménez-Pérez, S. 2005. Iron-binding ability of melanoidins from food and model systems. *Food Chemistry* 90(4), 821-827.
- Mullin, J.W. (2001) *Crystallization*, Elsevier.
- Münch, E.V. and Barr, K. 2001. Controlled struvite crystallisation for removing phosphorus from anaerobic digester sidestreams. *Water Research* 35(1), 151-159.
- Munir, M.T., Li, B., Boiarkina, I., Baroutian, S., Yu, W. and Young, B.R. 2017. Phosphate recovery from hydrothermally treated sewage sludge using struvite precipitation. *Bioresource Technology* 239, 171-179.
- Ngo, P.L., Udugama, I.A., Gernaey, K.V., Young, B.R. and Baroutian, S. 2021. Mechanisms, status, and challenges of thermal hydrolysis and advanced thermal hydrolysis processes in sewage sludge treatment. *Chemosphere* 281, 130890.
- Nielsen, A.E. 1969. Nucleation and growth of crystals at high supersaturation. *Kristall und Technik* 4(1), 17-38.



- Ochs, P., Martin, B.D., Germain, E., Stephenson, T., van Loosdrecht, M. and Soares, A. 2021. Ammonia removal from thermal hydrolysis dewatering liquors via three different deammonification technologies. *Science of The Total Environment* 755, 142684.
- Ortega-Martínez, E., Chamy, R. and Jeison, D. 2021. Thermal pre-treatment: Getting some insights on the formation of recalcitrant compounds and their effects on anaerobic digestion. *Journal of Environmental Management* 282, 111940.
- Pastor, L., Marti, N., Bouzas, A. and Seco, A. 2008. Sewage sludge management for phosphorus recovery as struvite in EBPR wastewater treatment plants. *Bioresource Technology* 99(11), 4817-4824.
- Pavez-Jara, J.A., van Lier, J.B. and de Kreuk, M.K. 2023. Effects of thermal hydrolysis process-generated melanoidins on partial nitrification/anammox in full-scale installations treating waste activated sludge. *Journal of Cleaner Production* 432.
- Plavšić, M., Čosović, B. and Lee, C. 2006. Copper complexing properties of melanoidins and marine humic material. *Science of The Total Environment* 366(1), 310-319.
- Rodrigues, A., Brito, A., Janknecht, P., Proença, M.F. and Nogueira, R. 2009. Quantification of humic acids in surface water: effects of divalent cations, pH, and filtration. *Journal of Environmental Monitoring* 11(2), 377-382.
- Rufián-Henares, J.A. and de la Cueva, S.P. 2009. Antimicrobial Activity of Coffee Melanoidins—A Study of Their Metal-Chelating Properties. *Journal of Agricultural and Food Chemistry* 57(2), 432-438.
- Sahu, A.K., Mitra, I., Kleiven, H., Holte, H.R. and Svensson, K. (2022) *Clean Energy and Resource Recovery*. An, A., Tyagi, V., Kumar, M. and Cetecioglu, Z. (eds), pp. 405-422, Elsevier.
- Shaddel, S., Ucar, S., Andreassen, J.-P. and Østerhus, S.W. 2019. Engineering of struvite crystals by regulating supersaturation – Correlation with phosphorus recovery, crystal morphology and process efficiency. *Journal of Environmental Chemical Engineering* 7(1), 102918.
- Stevenson, F.J. (1994) *Humus chemistry: genesis, composition, reactions*, John Wiley & Sons.
- Taddeo, R., Honkanen, M., Kolppo, K. and Lepistö, R. 2018. Nutrient management via struvite precipitation and recovery from various agroindustrial wastewaters: Process feasibility and struvite quality. *Journal of Environmental Management* 212, 433-439.
- Taguchi, K. and Sampei, Y. 1986. The formation, and clay mineral and CaCO<sub>3</sub> association reactions of melanoidins. *Organic geochemistry* 10(4-6), 1081-1089.
- Tipping, E. and Ohnstad, M. 1984. Aggregation of aquatic humic substances. *Chemical Geology* 44(4), 349-357.
- Vasa, T.N. and Pothanamkandathil Chacko, S. 2021. Recovery of struvite from wastewaters as an eco-friendly fertilizer: Review of the art and perspective for a sustainable agriculture practice in India. *Sustainable Energy Technologies and Assessments* 48, 101573.
- Vlaeminck, S., De Clippeleir, H. and Verstraete, W. 2012. Microbial resource management of one-stage partial nitrification/anammox. *Microbial biotechnology* 5(3), 433-448.
- Wang, H.-Y., Qian, H. and Yao, W.-R. 2011. Melanoidins produced by the Maillard reaction: Structure and biological activity. *Food Chemistry* 128(3), 573-584.
- Warmadewanthi and Liu, J.C. 2009. Recovery of phosphate and ammonium as struvite from semiconductor wastewater. *Separation and Purification Technology* 64(3), 368-373.
- Weber, F., Koller, G., Schennach, R., Bernt, I. and Eckhart, R. 2013. The surface charge of regenerated cellulose fibres. *Cellulose* 20(6), 2719-2729.
- Wei, L., Hong, T., Cui, K., Chen, T., Zhou, Y., Zhao, Y., Yin, Y., Wang, J. and Zhang, Q. 2019. Probing the effect of humic acid on the nucleation and growth kinetics of struvite by constant composition technique. *Chemical Engineering Journal* 378, 122130.

- Wilson, C.A. and Novak, J.T. 2009. Hydrolysis of macromolecular components of primary and secondary wastewater sludge by thermal hydrolytic pretreatment. *Water Research* 43(18), 4489-4498.
- Yan, M., Lu, Y., Gao, Y., Benedetti, M.F. and Korshin, G.V. 2015. In-Situ Investigation of Interactions between Magnesium Ion and Natural Organic Matter. *Environmental Science & Technology* 49(14), 8323-8329.
- Yip, T.C.M., Yan, D.Y.S., Yui, M.M.T., Tsang, D.C.W. and Lo, I.M.C. 2010. Heavy metal extraction from an artificially contaminated sandy soil under EDDS deficiency: Significance of humic acid and chelant mixture. *Chemosphere* 80(4), 416-421.
- Zahmatkesh, M., Spanjers, H., Toran, M.J., Blázquez, P. and van Lier, J.B. 2016. Bioremoval of humic acid from water by white rot fungi: exploring the removal mechanisms. *AMB Express* 6(1), 118.
- Zhang, Q., Vlaeminck, S.E., DeBarbadillo, C., Su, C., Al-Omari, A., Wett, B., Pümpel, T., Shaw, A., Chandran, K., Murthy, S. and De Clippeleir, H. 2018. Supernatant organics from anaerobic digestion after thermal hydrolysis cause direct and/or diffusional activity loss for nitrification and anammox. *Water Research* 143, 270-281.
- Zhang, Q., Zhao, S., Ye, X. and Xiao, W. 2016. Effects of organic substances on struvite crystallization and recovery. *Desalination and Water Treatment* 57(23), 10924-10933.
- Zhang, Y., Gu, K., Zhao, K., Deng, H. and Hu, C. 2023. Enhancement of struvite generation and anti-fouling in an electro-AnMBR with Mg anode-MF membrane module. *Water Research* 230, 119561.
- Zhao, C., Tang, C.Y., Li, P., Adrian, P. and Hu, G. 2016. Perfluorooctane sulfonate removal by nanofiltration membrane—the effect and interaction of magnesium ion / humic acid. *Journal of Membrane Science* 503, 31-41.
- Zhou, Z., Hu, D., Ren, W., Zhao, Y., Jiang, L.-M. and Wang, L. 2015. Effect of humic substances on phosphorus removal by struvite precipitation. *Chemosphere* 141, 94-99.

### 4.3. Appendix chapter 4

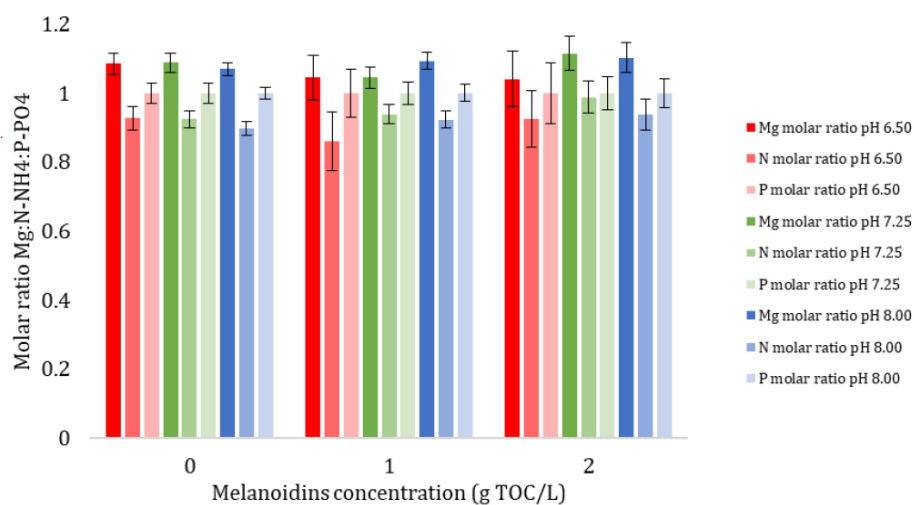


**Figure A4.1:** Molar ratio in struvite precipitation experiments with melanoidins

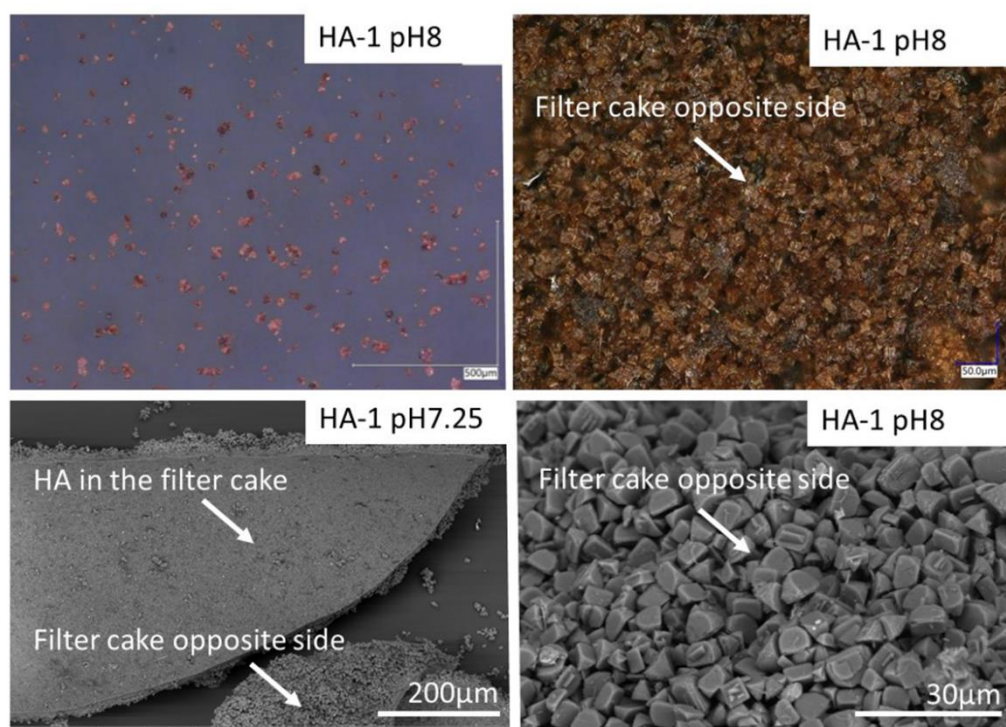


**Figure A4.2:** Optic microscopy and ESEM pictures of crystals formed in the presence of humic acid.

**Table A4.1.** p-values in two-tailed t-tests comparing the mass balances of the  $\text{PO}_4^{3-}\text{-P}$  and TAN with their theoretical concentrations. The values with a star represent the p-value  $\geq \alpha=0.05$ , meaning that the values fit the mass balance.

Sample	pH	$\text{PO}_4^{3-}\text{-P}$ total	TAN Total
No-HSs	pH 6.5	0.007	0.235*
	pH 7.25	0.011	0.017
	pH 8	0.002	0.094*
MEL-1	pH 6.5	0.090*	0.274*
	pH 7.25	0.170*	0.010
	pH 8	0.008	0.014
MEL-2	pH 6.5	0.117*	0.005
	pH 7.25	0.004	0.006
	pH 8	0.028	0.053*
HA-1	pH 6.5	0.294*	0.483*
	pH 7.25	0.329*	0.122*
	pH 8	0.063*	0.035
HA-2	pH 6.5	0.077*	0.626*
	pH 7.25	0.081*	0.120*
	pH 8	0.056*	0.225*

**Table A4.2.** Colour and UVA 254 in complexation assays of  $\text{PO}_4^{3-}\text{-P}$ .

Colour initial mg Pt-Co/L					
Assay pH	No-HSs	MEL-1	MEL-2	HA-1	HA-2
pH 6.5	0	10,439 $\pm$ 95	20,587 $\pm$ 190	49,874 $\pm$ 1140	101,064 $\pm$ 1316
pH 7.25	0	10,165 $\pm$ 435	20,148 $\pm$ 251	51,848 $\pm$ 1316	101,064 $\pm$ 1011
pH 8	0	9,726 $\pm$ 251	19,270 $\pm$ 251	52,507 $\pm$ 658	102,380 $\pm$ 3949
Colour permeate mg Pt-Co/L					
Assay pH	No-HSs	MEL-1	MEL-2	HA-1	HA-2
pH 6.5	0	2,211 $\pm$ 380	2,774 $\pm$ 24	621 $\pm$ 24	868 $\pm$ 24
pH 7.25	0	2,046 $\pm$ 190	2,829 $\pm$ 71	539 $\pm$ 63	1060 $\pm$ 71
pH 8	0	2,156 $\pm$ 343	2,829 $\pm$ 41	553 $\pm$ 24	1156 $\pm$ 24
UVA 254 initial 1/cm					
Assay pH	No-HSs	MEL-1	MEL-2	HA-1	HA-2
pH 6.5	0	26.1 $\pm$ 0.2	51.5 $\pm$ 0.6	82.5 $\pm$ 0.2	164.1 $\pm$ 2.0
pH 7.25	0	25.1 $\pm$ 0.2	50.5 $\pm$ 0.9	84.1 $\pm$ 0.2	164.9 $\pm$ 1.5
pH 8	0	25.2 $\pm$ 0.2	50.3 $\pm$ 0.5	80.3 $\pm$ 1.0	167.5 $\pm$ 0.6
UVA 254 permeate 1/cm					

Assay pH	No-HSs	MEL-1	MEL-2	HA-1	HA-2
pH 6.5	0	10.0 ± 0.2	19.2 ± 0.1	2.70 ± 0.03	4.8 ± 0.1
pH 7.25	0	10.1 ± 0.2	19.7 ± 0.1	2.81 ± 0.03	5.10 ± 0.04
pH 8	0	9.8 ± 0.2	19.70 ± 0.01	2.7 ± 0.1	5.1 ± 0.1

**Table A4.3.** Colour and UVA 254 in complexation assays of  $\text{Mg}^{2+}$ .

Colour initial mg PT-Co/L					
Assay pH	No-HSs	MEL-1	MEL-2	HA-1	HA-2
pH 6.5	0	10,145 ± 884	19,911 ± 187	63,697 ± 1316	137,048 ± 3313
pH 7.25	0	9,874 ± 117	20,344 ± 187	64,135 ± 760	133,976 ± 4560
pH 8	0	10,213 ± 117	20,452 ± 649	63,697 ± 2373	133,537 ± 3313
Colour permeate mg Pt-Co/L					
Assay pH	No-HSs	MEL-1	MEL-2	HA-1	HA-2
pH 6.5	0	1,650 ± 47	3,463 ± 124	256 ± 24	400 ± 12
pH 7.25	0	1,731 ± 62	3,598 ± 124	221 ± 21	400 ± 43
pH 8	0	1,664 ± 35	3,625 ± 124	290 ± 31	434 ± 43
UVA 254 initial 1/cm					
Assay pH	No-HSs	MEL-1	MEL-2	HA-1	HA-2
pH 6.5	0	25.2 ± 0.4	51.5 ± 0.9	61.1 ± 1.0	128.5 ± 1.0
pH 7.25	0	24.8 ± 0.4	51.2 ± 1.2	63.5 ± 0.2	130.1 ± 1.4
pH 8	0	26.2 ± 0.5	51.3 ± 1.6	65.5 ± 1.8	133.3 ± 0.6
UVA 254 permeate 1/cm					
Assay pH	No-HSs	MEL-1	MEL-2	HA-1	HA-2
pH 6.5	0	9.4 ± 0.1	20.0 ± 0.4	1.635 ± 0.004	2.980 ± 0.008
pH 7.25	0	9.4 ± 0.1	20.3 ± 0.4	1.711 ± 0.002	2.8 ± 0.1
pH 8	0	9.3 ± 0.1	19.9 ± 0.6	1.946 ± 0.002	2.9 ± 0.1





# 5.

## **Effects of thermal hydrolysis process-generated melanoidins on partial nitrification/anammox in full-scale installations treating waste activated sludge\***

---

\* Based on Pavez-Jara, J.A., J.B. van Lier, and M.K. de Kreuk, Effects of thermal hydrolysis process-generated melanoidins on partial nitrification/anammox in full-scale installations treating waste activated sludge. *Journal of Cleaner Production*, 2023. 432: p. 139767.



## Abstract

Thermal hydrolysis process (THP) is a well-established anaerobic digestion (AD) pre-treatment technology. Despite the THP benefits the pre-treatment increases the concentrations of nutrients and melanoidins in the digestate reject water after dewatering. The increased concentrations of nutrients and melanoidins formed during THP-AD can impact downstream processes, such as struvite precipitation and partial nitrification/anammox (PN/A). In our present work, six full-scale PN/A influents and effluents were sampled in The Netherlands (4 with THP and 2 without THP). Full-scale samples were characterised and the stoichiometric  $O_2$  consumption and melanoidins chelated to trace elements were analysed. The results showed that THP increased the concentration of total ammoniacal nitrogen (TAN), chemical oxygen demand (COD), total organic carbon (TOC), UVA 254 and colour, which are indicators of melanoidins occurrence. THP furthermore decreased the stoichiometric  $NO_3^-$ -N production from the PN/A reaction in effluents. The disparity between stoichiometric and measured  $NO_3^-$ -N in the THP-using plants was explained by the proliferation of denitrifiers. Moreover, denitrification improved the N removal efficiency due to the consumption of the stoichiometrically-produced  $NO_3^-$ -N. Also, the stoichiometric  $O_2$  consumption increased in the plants using THP, reaching up to 56% of the  $O_2$  used for partial oxidation of TAN. Trace elements analysis revealed that the plants with elevated concentrations of melanoidins in the effluent showed a high percentage of chelated multivalent cations, particularly transition metals such as Fe. Kendall correlation coefficient analysis showed that the chelation of multivalent cations was correlated mainly with colour occurrence in the reject waters. Overall, the results indicated that in PN/A systems using THP-AD increased  $O_2$  consumption and trace elements availability should be considered during the process design.

## 5.1. Introduction

Anaerobic digestion (AD) is a well-established technology to diminish the amount of excess sludge from wastewater treatment plants (WWTPs) and to recover biochemical energy as biogas (Appels et al., 2008). During AD of primary and secondary sludges, hydrolysis of particulate matter determines the overall conversion rate of the process, and is thus considered the “rate-limiting step” (Appels et al., 2008; Pavlostathis and Giraldo-Gomez, 1991; Tiehm et al., 2001). Hydrolysis acceleration has been reached at both lab-scale and full-scale by the application of pre-treatments on the AD substrates (Appels et al., 2008; Hendriks and Zeeman, 2009). Thermal hydrolysis process (THP) is the most widespread pre-treatment for AD; it has become commercially available in Norway in the 1990s, and has since expanded to the rest of the world (Devos et al., 2023; Kor-Bicakci and Eskicioglu, 2019; Ødeby et al., 1996). During THP, the AD substrates’ temperature is increased to 140-170 °C for around 20-30 min, followed by a sudden decrease in pressure (and temperature), which causes cell disruption and cytoplasmic content release (Ringoot et al., 2012). The use of THP-AD has demonstrated advantages such as reduced pathogens concentrations in AD effluents, increased anaerobic biodegradability, and improved mixing and dewaterability of the AD-digestates (Barber, 2016). Despite the evident advantages of THP, it has been observed that this pre-treatment increases nutrient concentrations and leads to the formation of recalcitrant compounds (Dwyer et al., 2008b).

THP-AD systems are characterised by increased total ammoniacal nitrogen (TAN) concentrations as a consequence of increased solubilisation and biodegradability of proteins (Bougrier et al., 2008; Li and Noike, 1992). The increased nutrients solubilisation in THP-AD can lead to negative effects in the AD process, such as free ammonia nitrogen (FAN) inhibition and spontaneous struvite precipitation (Barber, 2016; Yuan et al., 2012). Additionally, elevated nutrients concentrations can affect AD downstream processes as follows: 1) Increased  $\text{Mg}^{2+}$  requirements in struvite precipitation due to increased  $\text{PO}_4^{3-}$  concentrations, which may increase  $\text{PO}_4^{3-}$  recovery, and 2) Increased  $\text{O}_2$  requirements to convert elevated TAN concentrations into  $\text{N}_2$  in mainstream conventional nitrification-denitrification processes or a partial nitrification-anammox (PN/A) process in the reject water line. Furthermore, Zhang et al. (2020b) observed that  $\text{PO}_4^{3-}$  increased along with the THP pre-treatment temperature and with reaction times shorter than 30 minutes.  $\text{PO}_4^{3-}$  release can be attributed to the disintegration of phosphate-accumulating organisms (PAOs) present in waste activated sludge (WAS) from WWTPs using enhanced biological phosphorous removal (Coats et al., 2011; Qiu et al., 2019).

Also, the presence of living PAOs during AD can lead to increased  $\text{PO}_4^{3-}$  concentrations as a result of their VFA uptake accompanied by  $\text{PO}_4^{3-}$  release (Flores-Alsina et al., 2016; Wang et al., 2016). However,  $\text{PO}_4^{3-}$  solubility in the AD reactors' digestates depends on the cationic load among other factors (e.g. pH and reagent concentrations), which determine the precipitation of P-based minerals (Flores-Alsina et al., 2016). In increasing numbers of full-scale installations, soluble  $\text{PO}_4^{3-}$  in AD reject water is removed using the struvite precipitation process, in which  $\text{Mg}^{2+}$  is added at mildly elevated pH. However, during struvite precipitation other P-based minerals can co-precipitate with different metals such as  $\text{Al}^{3+}$ ,  $\text{Ca}^{2+}$ , and  $\text{Fe}^{2+/3+}$  (Becker et al., 2019; Fischer et al., 2011).

In addition to the increased nutrients concentrations, THP leads to the formation of melanoidins, which are coloured polymers from the Maillard reaction (Dwyer et al., 2008b; Penaud et al., 2000). Melanoidins are formed when carbohydrates and proteins are exposed to high temperatures, leading to polymerisation reactions and thus increased molecular weight and a higher degree of aromaticity (Hodge, 1953; Wang et al., 2011). Like humic substances (HSs) and irrespective their anthropogenic origin, melanoidins can be classified as fulvic acids, humic acids and humins, depending on their pH-dependent solubility (L. Malcolm, 1990; McDonald et al., 2004; Migo et al., 1993). Melanoidins furthermore behave as polydentate ligands, chelating ions in solution in the same way as conventional HSs. The complexing effect of HSs has been widely used in agriculture to chelate nutrients, and promote their slow release (El-sayed et al., 2017; Morales et al., 2005). As a result of the complex chemical composition of THP-formed melanoidins, part of these compounds cannot be anaerobically biodegraded, and reach the AD downstream processes.

After THP-AD, the reject water contains an elevated concentration of nutrients, which is increasingly removed prior conveying the reject water to the headworks of the WWTP to safeguard its proper functioning. A common option to remove TAN in reject waters is the PN/A process, which is less expensive compared to the traditional nitrification/denitrification process in the WWTP's mainstream. Compared to nitrification/denitrification, PN/A requires 50-60 % less  $\text{O}_2$  consumption and it does not require any organic matter as electron donor for the ultimate denitrification step (Fux and Siegrist, 2004). The PN/A process was discovered and further developed in the 1990s and has been growing thenceforth to reach over a hundred full-scale plants operating in 2014 (Lackner et al., 2014). As the name suggests, PN/A reactors work in a dynamic equilibrium between two main microbial populations: 1) aerobic ammonium oxidising organisms (AOO) and 2) anoxic ammonium oxidisers (anammox) (Gilbert et al.,

2013; Lotti et al., 2014a). In a simplified way, AOO use  $O_2$  to convert  $NH_4^+$  into  $NO_2^-$ , and anammox microorganisms oxidise  $NH_4^+$  using  $NO_2^-$  to produce  $N_2$ . After the  $N_2$  concentration reaches saturation in the liquid,  $N_2$  is stripped to the gas phase (Baeten et al., 2019; Strous et al., 1998; Van Hulle et al., 2010). Since modern PN/A systems comprise only one single-step reactor, AOO and anammox microorganisms coexist in a delicate equilibrium, conducting their metabolic reactions in parallel (Lackner et al., 2014). Moreover, PN/A reactors treating reject waters from the AD process, make beneficial use of the high TAN concentrations, high temperature (30-35°C), and low organics concentrations (Joss et al., 2009). However, THP modifies the properties of reject water and the subsequent PN/A process' influent. Furthermore, organics formed during THP-AD can cause diffusional limitation on the AOO, hindering the PN/A process (Zhang et al., 2018b). Also, the THP-formed organic matter in reject water may imbalance the microbial populations in PN/A, leading to the growth of heterotrophs (Wang et al., 2020). In addition, the heterotrophic degradation of THP-produced melanoidins using  $O_2$  might lead to elevated  $O_2$  uptake rates in the PN/A reactors. Furthermore, the melanoidin's-mediated cations complexation may cause a scarcity of available trace elements, which might hinder the growth of the PN/A microbial populations.

In our present work, we researched the observed performance differences between PN/A reactors treating reject waters from anaerobic digesters fed with THP pre-treated sludge versus and digesters fed with non-pre-treated sludge. To better understand the impact of THP pre-treatment on the PN/A process, the biomass, nutrients, organics, and soluble cations were characterised and compared between the PN/A reactors treating either THP-treated sludge reject water or reject water without pre-treatment. In addition, stoichiometric calculations were performed to assess the aerobic/anoxic biodegradability of the (semi)recalcitrant organics produced during THP (melanoidins), using different final electron acceptors. The latter, permits analysis of whether denitrification occurred as a possible N-removal pathway. Finally, trace elements complexation assays were conducted to investigate trace metals availability and the possible occurrence of microbial growth factors limitations in the full-scale PN/A reactors.

## 5.2. Methodology

### 5.2.1. Sampling campaign in full-scale PN/A reactors

Influent and effluent from side stream PN/A processes treating AD-reject water were sampled in six WWTPs, all located in the Netherlands. The PN/A effluent samples included homogenous samples containing liquid broth and biomass. Only one sample was taken, and the measured values correspond to that sampling moment. The locations and some process characteristics of the studied WWTPs are shown in Table 5.1. After the sampling, the biomass and reject waters were stored separately at 4°C for further analysis.

**Table 5.1.** Characteristics of the WWTPs sampled in our study.

	<b>Sluisjesdijk (SLU)</b>	<b>Olburgen (OLB)</b>	<b>Tilburg (TIL)</b>	<b>Hengelo (HEN)</b>	<b>Apeldoorn (APE)</b>	<b>Amersfoort (AME)</b>
<b>THP system (if applies)</b>	No THP	No THP	CAMBI®	CAMBI®	TURBOTE C® SUSTEC	LYSOTE RM® ELIQUO WATER & ENERGY BV
<b>PN/A system</b>	Two steps SHARON/ANA MMOX®	CANNO N®	ANAMM OX®	NAS- ONE® COLSEN	DEMON®	DEMON ®
<b>Influent origin</b>	Municipal AD reject water sampled after struvite precipitation.	Combined anaerobically treated potato starch wastewater + municipal AD reject	Municipal AD reject water sampled after struvite precipitation.	Municipal AD reject water sampled after struvite precipitation.	Municipal AD reject water sampled after struvite precipitation.	Municipal AD reject water sampled after struvite precipitation.

		water sampled after struvite precipitation.				
--	--	---	--	--	--	--

### 5.2.2. Chemical analysis

True colour was determined in 0.45 µm filtered samples, using filters CHROMAFIL Xtra PES-45/25 (Macherey-Nagel, Germany). The absorbance was measured at 475 nm using a Platinum-Cobalt colour standard solution (Hazen 500, Certipur® Merck, Germany) with a concentration of 500 mg Pt-Co/L, in a Genesys 10S UV-Vis spectrophotometer (Thermo Scientific, USA), using 1 cm pathway plastic cuvettes. UVA 254 was measured in filtered samples in the same spectrophotometer as true colour at 254 nm using 1 cm pathway quartz cuvettes. The results are expressed in mg Pt-Co/L and 1/cm in the case of T. colour and UVA 254, respectively. Specific ultraviolet absorbance (SUVA) was calculated as the quotient among UVA 254 in metres, and total organic carbon (TOC) in mg/L.

Total and volatile solids (TS and VS, respectively) were measured according to Standard methods for the examination of water and wastewater (Rice et al., 2012), when measuring TS and VS in granular biomass, the samples were first crushed to homogenise them. Chemical oxygen demand (COD), TOC, ortho and total phosphate ( $\text{PO}_4^{3-}\text{-P}$  and TP, respectively), TAN,  $\text{NO}_2\text{-N}$ ,  $\text{NO}_3\text{-N}$ , and total-N (TN) were measured with the Hach Lange kits LCK114, LCK386, LCK350, APC303, LCK342, LCK340 and LCK338, respectively (Hach, USA). Electroconductivity (EC) was measured with a probe LF 413T IDS (Xylem, Germany). Volatile fatty acids (VFA) were measured using gas chromatography coupled with a flame ionisation detector (FID-GC) (Shimadzu GC 14B, Japan) following the description of (Ceron-Chafla et al., 2020). The samples were measured in triplicate, and the error bars' length in the results represents two times the standard deviation among the measurements.

### 5.2.3. Metals concentration measurements in the analysed PN/A reactors

The soluble concentrations of B, Na, Mg, Al, K, Ca, Mn, Fe, Co, Ni, Cu, Zn, Mo and Cd in the studied samples were measured using ICP-MS (PlasmaQuant MS, Analytik Jena AG,

Germany). The samples for ICP-MS analysis were prepared acidifying 9.9 mL of 0.22  $\mu\text{m}$  filtered samples using 0.1 mL of  $\text{HNO}_3$  69% (CAS No.: 7697-37-2, CARL ROTH ROTIPURAN®, Germany). The parameters used in the ICP-MS device are shown in additional information. ICP-MS measures the total concentration of the analysed isotopes, thus the concentrations of the measured cations are expressed without their oxidation state, although they are likely ionised in solution.

#### **5.2.4. Melanoidins-metals complexation assays using ultrafiltration**

Bioavailability of trace elements is a complicated parameter to measure. However, we assumed that the non-bound metals were more bioavailable than the complexed ones. To measure the complexation of multiple metals with melanoidins at the same time, the full-scale samples were fractionated using crossflow ultrafiltration membranes to reject the high molecular weight compounds that behave as multidentate ligands. The membranes used to conduct the fractionation were a nominal 0.5  $\mu\text{m}$  glass fibre filter Advantec GC-50 (Frisenette, Denmark) and a 1 kDa Ultracel® regenerated cellulose membrane (Merck Millipore, USA). The fractionation was conducted using an Amicon® stirred cell Model 8010 (Merck Millipore, USA) at  $21 \pm 2$  °C using Ar gas at 2.8 bar to induce the trans-membrane pressure, and 600 rpm stirring speed to minimise the cake/gel layer formation. After the micro- and ultra-filtrations, the samples were characterised, measuring COD, TOC, Colour, UVA 254 (supplementary material Figure A5.1) and metals concentrations in both fractions. Metals in the analysed samples were measured using ICP-MS. The results are expressed as concentration, and as the quotient of the concentration of each cation in the 1kDa permeate over the concentration in the 0.5  $\mu\text{m}$  permeate.

#### **5.2.5. Biomass specific substrates conversion rates**

To measure the microbial activity in the analysed PN/A reactors, we measured specific ammonium oxidising activity (SAOA), specific anammox activity (SAA) and specific denitrifying activity (SDA) in batch tests. The culture media used to measure the microbial activities are shown in supplementary information. In all the specific activity measurements, flocs and granules were taken as homogeneously as possible from the samples to resemble the full-scale conditions. Furthermore, to avoid possible inhibition from the melanoidins/substrate still present in the sample broths, the PN/A biomass was rinsed before performing the activity tests. The rinsing was performed using the same culture medium in which the respective activity was measured without adding the respective substrates. The biomass was rinsed three

times doubling the samples' volume, followed by soft centrifugation at 3,500 rpm for 10 minutes, in a centrifuge model Heraeus Labofuge 400 (Thermo Fisher Scientific, USA). Since the analysed samples contained granular biomass, the solids concentration could not be determined beforehand, and was estimated based on previous tests before conducting the activity measurement. After each activity measurement was completed, the biomass used was crushed and the actual VS concentration was measured and used to calculate the activity value in gN/gVS/day.

SAOA was measured respirometrically at  $35 \pm 1^\circ\text{C}$  in a 120 mL stirred and sealed reaction chamber, connected to a dissolved oxygen (DO) probe model FDO® 925 (WTW, Germany) (additional material, Figure A5.1). Initially, the vessel containing the culture medium without substrate was magnetically stirred keeping the upper valve open (valve 1 in Figure A5.1, additional material) to allow air exchange and reach DO saturation. After DO reached the saturation concentration, the previously rinsed PN/A biomass was added to the reaction chamber, which was filled with the culture medium without substrate, and the upper valve was closed. A 20X concentrated TAN solution was added to the culture medium through the lower valve (valve 2 in Figure A5.1, additional material) to start the reaction. The reaction was stopped when the DO concentration reached 3 mg O<sub>2</sub>/L, and the maximum slope of the DO depletion curve was transformed stoichiometrically to N consumed per day, per VS, and was used as the activity indicator.

SAA and SDA were determined manometrically using an Oxytop® IS system (WTW, Germany) in triplicate, measuring the overpressure generated by the N<sub>2</sub> produced as a result of the anammox and/or denitrification reactions. SAA and SDA were determined using sealed bottles with 200 mL of reaction volume and around 130 mL of headspace. The exact volume of each bottle was determined in advance. In the same way as in all the activity measurements, the biomass was washed with their respective culture medium without substrate to remove the residual reject water that might interfere with the measurements. Before starting the measurements, the culture medium without substrate and the biomass were flushed for 1 minute with Ar gas, and the samples were placed on a stirring plate and warmed until they reached 35°C in a temperature-controlled incubator. After the constant temperature was reached, the inner pressure was equalised to atmospheric, and the concentrated substrate(s) were added with a syringe. The moles of N<sub>2</sub> produced were calculated using the ideal gas law, Henry's constant at 35 °C (for dissolved N<sub>2</sub>) and a correction factor from Antoine's law at 35°C, which considers that 5.54 % of the total pressure in the headspace corresponds to water vapour. After the



specific activity was completed, the headspace gas composition was measured, and the biomass was crushed to take homogenous samples for VS measurement. The specific activity measurement was considered as the maximum slope of the N<sub>2</sub> production curve over the mass of biomass (VS) and time.

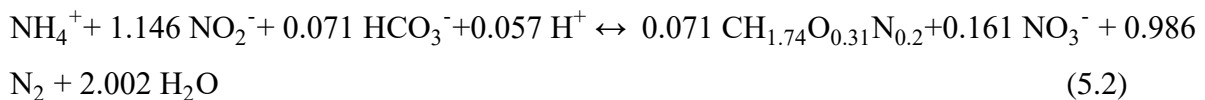
### 5.2.6. Stoichiometric calculations

Stoichiometric NO<sub>3</sub><sup>-</sup>-N productions in the reactors analysed were calculated according to Equation 5.3, based on the anammox conversion reaction reported by Lotti et al. (2014b).

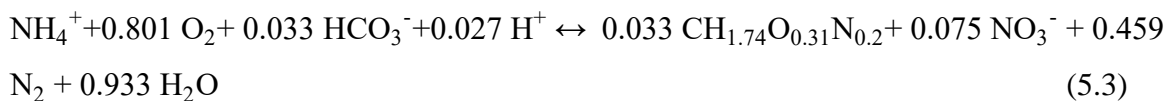
Partial nitritation:



Anammox:



Partial nitritation and anammox:



Equation 5.4 shows the theoretical NO<sub>3</sub><sup>-</sup>-N that should be found in the PN/A reactors effluents, based on TAN concentrations and the stoichiometric calculations shown in Equation 5.3.

$$\text{NO}_3^- \text{-N}_{\text{theoretical}} = 0.075 \frac{\text{g NO}_3^- \text{-N}}{\text{g TAN}} (\text{TAN}_{\text{influent}} - \text{TAN}_{\text{effluent}}) \quad (5.4)$$

If it is assumed that the overall volume in the influent and effluent are equal, the NO<sub>3</sub><sup>-</sup>-N produced can be calculated as the difference between the concentration in the effluent and the influent, as shown in Equation 5.5.

$$\text{NO}_3^- \text{-N}_{\text{produced}} = (\text{NO}_3^- \text{-N}_{\text{effluent}} - \text{NO}_3^- \text{-N}_{\text{influent}}) \quad (5.5)$$

To calculate the required amount of electrons to denitrify NO<sub>3</sub><sup>-</sup>-N to N<sub>2</sub>, Equation 5.6 was used. In the case of TIL and HEN the NO<sub>3</sub><sup>-</sup>-N concentration in the effluent was slightly lower than in the influent thus the variation in those cases was considered equal to zero to avoid negative values.

Denitrification:



From Equation 5.6 the organic matter (COD) that can be oxidised using  $\text{NO}_3^-$ -N as final electron acceptor was calculated, and it is shown in Equation 5.7.

$$\frac{\text{COD}}{\text{NO}_3^- \text{-N}} = 2.857 \frac{\text{g COD}}{\text{g NH}_3^- \text{-N}} \text{NO}_3^- \text{-N}_{\text{produced}} \quad (5.7)$$

To quantify the (extra)oxygen consumptions in the analysed reactors, the indexes shown in Equations 5.8, 5.9 and 5.10 were calculated. Equation 5.8 shows The  $\text{NO}_3^-$ -N used to oxidise organic matter present in the PN/A reactors via denitrification, expressed as COD according to Equation 5.7. Equation 5.9 shows the  $\text{O}_2$  used to oxidise organic matter present in the PN/A reactors. Finally, Equation 5.10 shows the  $\text{O}_2$  used to partially oxidise TAN.

$$\text{NO}_3^- \text{-N}_{\text{Ox-OM}} \left( \frac{\text{g O}_2}{\text{L}} \right) = 2.857 \frac{\text{g O}_2}{\text{g NO}_3^- \text{-N}} \left( \text{NO}_3^- \text{-N}_{\text{theoretical}} - \text{NO}_3^- \text{-N}_{\text{produced}} \right) \quad (5.8)$$

$$\text{O}_{2\text{OM}} \left( \frac{\text{g O}_2}{\text{L}} \right) = (\text{COD}_{\text{influent}} - \text{COD}_{\text{effluent}}) - \text{NO}_3^- \text{-N}_{\text{Ox-OM}} \quad (5.9)$$

$$\text{O}_{2\text{TAN}} \left( \frac{\text{g O}_2}{\text{L}} \right) = 1.831 (\text{TAN}_{\text{influent}} - \text{TAN}_{\text{effluent}}) + 3.43 (\text{NO}_2^- \text{-N}_{\text{effluent}} - \text{NO}_2^- \text{-N}_{\text{influent}}) \quad (5.10)$$

### 5.2.7. Data analysis

The Kendall rank correlation coefficient was used to find the correlation between specific measured parameters. This non-parametric index is recommended for small datasets such as the one in our present study, which was only seven points (Field, 2013). The plotted points only correspond to the correlation coefficients that were significantly different to zero at 95% of confidence.

Principal component analysis (PCA) was computed as a dimensionality reduction method when analysing the trace element concentrations of the analysed WWTPs. To reduce the influence of the naturally different concentrations of the different metals, each set of measured metal concentration was z-scored (average=0 and standard deviation=1) before the PCA analysis. The PCA was conducted with the function PCA in MATLAB R2019a, and the results are shown in biplots.

### 5.3. Results and discussion

#### 5.3.1. PN/A streams chemical characterisation

Table 5.2 shows the (bio)chemical characterisation of the PN/A influent and effluent of the studied WWTPs. Measurements were grouped into descriptors of organic matter (COD, TOC, T. colour and UVA 254), nutrients ( $\text{PO}_4^{3-}\text{-P}$ , TP, TAN,  $\text{NO}_2^-\text{-N}$ ,  $\text{NO}_3^-\text{-N}$ , and TN), and conversion capacities (SAOA, SAA and SDA). As shown in Table 5.2, the WWTP in which THP was implemented (TIL, AME, APE and HEN) showed higher values of COD and TOC in the influents compared with the plants not using THP. Furthermore, the PN/A effluents showed a reduction in the concentration of COD and TOC compared to the influents. The reduction in COD and TOC contents was likely caused by the partial oxidation of the organics in the influents by a heterotrophic consortium of microorganisms, which used the organic matter as carbon and energy sources. In addition, UVA 254 and T. colour followed COD and TOC trends indicating that part of the degraded organics during PN/A corresponded to aromatic and coloured compounds, such as melanoidins. The negligible VFA concentrations in both influent and effluent of the PN/A confirmed that the organic matter in the PN/A reactors did not comprise these AD-intermediates. The occurrence of melanoidins was likely caused by THP before AD as reported by various studies (Barber, 2016; Dwyer et al., 2008b; Zhang et al., 2020a).

Non-VFA COD concentrations remained very high in the sludge reject water, indicating that the melanoidins in the PN/A influents were recalcitrant under anaerobic conditions. However, results from our present study clearly indicated that melanoidins were partly biodegradable when exposed to aerobic/anoxic conditions in the PN/A reactors. Apparently, the presence of  $\text{O}_2$  and/or oxygenated nitrogen compounds like  $\text{NO}_3^-$  and  $\text{NO}_2^-$  as the final electron acceptor is of importance to achieve oxidation of these organic compounds. The increased reduction-oxidation (redox) potential under aerobic/anoxic conditions renders a higher potential energy to be harvested by the microorganisms compared to the use of solely organics as final electron acceptors under anaerobic conditions (Aghababaie et al., 2015). Moreover, SUVA increased in the effluents of the PN/A reactors compared to the influents except for the OLB full scale reactor, indicating that effluent organics were characterised by higher aromaticity compared to the influents. The higher aromaticity in the effluents can be explained by microbial preferential consumption of the less aromatic compounds in the influents. Moreover, electrical conductivity

decreased in the effluent of all the analysed full-scale plants due to total N removal during the PN/A process.

In contrast to TAN and total N concentrations,  $\text{PO}_4^{3-}\text{-P}$  and TP concentrations did not show clear removal trends in the analysed full-scale plants. In fact,  $\text{PO}_4^{3-}\text{-P}$  and TP showed highly variable concentrations in the studied influents and effluents, ranging from only 2.9 mg P/L ( $\text{PO}_4^{3-}\text{-P}$  in OLB's influent) to 175 mg P/L (TP in APE's effluent). Besides,  $\text{PO}_4^{3-}\text{-P}$  and TP concentrations in the effluents varied independently from the influents' concentrations, increasing in the samples from SLU-S, SLU-A, AME, APE, and OLB. The variable  $\text{PO}_4^{3-}\text{-P}$  concentrations in influent and effluent might be attributed to the presence and activity of PAOs in PN/A reactors. PAOs consume organics (mainly VFA) and release  $\text{PO}_4^{3-}\text{-P}$  under anaerobic conditions, which may have occurred when aeration ceased in the PN/A reactors. In contrast, PAOs accumulate  $\text{PO}_4^{3-}\text{-P}$  under oxic/anoxic conditions, decreasing the  $\text{PO}_4^{3-}\text{-P}$  concentration in the reactor broth (Sato et al., 1992; van Loosdrecht et al., 1997). To the best of our knowledge, the possible occurrence of simultaneous N and P removal in full-scale PN/A reactors is thus far not reported and needs further research. However, some studies have successfully applied simultaneous P and N removal in lab-scale (Ma et al., 2020; Xu et al., 2019; Zhang et al., 2018a). In addition, the  $\text{PO}_4^{3-}\text{-P}$  /TP ratio increased in the effluent of all studied PN/A plants except for HEN, where the concentrations of  $\text{PO}_4^{3-}\text{-P}$  and TP decreased distinctly in the effluent. The change in the  $\text{PO}_4^{3-}\text{-P}$  /TP ratio might be related to melanoidins oxidation with subsequent  $\text{PO}_4^{3-}\text{-P}$  release. The difference between soluble  $\text{PO}_4^{3-}\text{-P}$  and TP concentrations likely corresponded to either  $\text{PO}_4^{3-}\text{-P}$  complexed to the HSs using cations for the chemical binding (Gerke, 1992), or the accumulation of organic-P from microbial metabolites/ debris. Additionally, TAN was the predominant N species in the studied PN/A plants' influents, which can be expected treating sludge reject water of the preceding AD process (Table 5.1). TAN removal efficiencies were exceeding 70% and  $\text{NO}_2^-\text{-N}$  was almost not present in all the PN/A effluents of the analysed plants, except for SLU-S. It should be noted that SLU consists of a two-step anammox process where a Sharon reactor is followed by the anammox reactor. Therefore, in SLU-S,  $\text{NO}_2^-\text{-N}$  and  $\text{NO}_3^-\text{-N}$  increased in the effluent due to TAN oxidation in the Sharon reactor (van Kempen et al., 2001). Also, TN concentrations varied following TAN concentrations, since TN was comprised to a large extent by TAN. Furthermore,  $\text{NO}_3^-$  occurred in the reactors' effluents as a reaction product, as expected from PN/A stoichiometric conversion (Lotti et al., 2014b). The difference between the sum of TAN,  $\text{NO}_2^-\text{-N}$ ,  $\text{NO}_3^-\text{-N}$  concentrations and the TN concentrations likely corresponded to the soluble

organic N fraction, which was a very small fraction. Soluble organic-N in PN/A influents and effluent likely corresponded to N that formed part of the melanoidins structure (Dwyer et al., 2008a; Zhang et al., 2020a).

SAOA, SAA and SDA were assessed to reveal the presence and abundance of the different N converting bacteria and their potential contribution to overall N conversion in the studied PN/A plants. As was expected, SLU-A and SLU-S presented the highest SAOA and SAA (Table 5.2), since the biomass in the two-step anammox process is largely dominated by one specific type of microorganisms in each reactor. Although denitrification is not pursued in PN/A systems, Table 5.2 shows that all the analysed plants showed SDA, which was around 25% of the SAA (except for OLB). Remarkably, SLU-A showed the highest SDA, evidencing the occurrence of denitrifiers in the SLU-A reactor; denitrifiers in SLU-A possibly converted  $\text{NO}_3^-$  into  $\text{N}_2$ , using organics from microbial decay as electron donor. SAOA was considerably higher compared to SAA in the full-scale plants not using THP. The relatively low SAOA in THP-fed PN/A plants is likely indicative of AOO inhibition caused by the melanoidins and colloidal material present in THP-reject water (Valenzuela-Heredia et al., 2022; Zhang et al., 2018b).

**Table 5.2.** Specific conversion rates related to SAOA, SAA, and SDA in the mixed liquor, and characterisation of the soluble chemical parameters measured in the studied WWTPs.

Microbial activity	SLU-S and SLU-A *			OLB		TIL		HEN		APE		AME	
SAOA (g N/g VS/day)	3.9 ± 1.2 (SLU-S)			2.4 ± 0.7		0.2 ± 0.1		0.9 ± 0.5		0.39 ± 0.02		1.10 ± 0.50	
SAA (g N/g VS/day)	1.43 ± 0.07 (SLU-A)			0.91 ± 0.07		0.56 ± 0.04		0.89 ± 0.07		0.89 ± 0.04		0.57 ± 0.08	
SDA (g N/g VS/day)	0.4 ± 0.1 (SLU-A)			0.12 ± 0.03		0.14 ± 0.07		0.23 ± 0.02		0.220 ± 0.013		0.13 ± 0.02	
Soluble parameters	Influent	SHARO N Effluent	ANAMM OX Effluent	Influent	Effluent	Influent	Effluent	Influent	Effluent	Influent	Effluent	Influent	Effluent
COD (mg COD/L)	470 ± 17	530 ± 3	314 ± 2	108 ± 2	71 ± 5	3,151 ± 5	821 ± 42	3,527 ± 20	1,874 ± 15	1,709 ± 31	811 ± 2	1,602 ± 18	1,168 ± 6
TOC (mg C/L)	130 ± 5	150 ± 8	107 ± 3	73 ± 4	67.8 ± 0.3	2,020 ± 20	296 ± 7	1203 ± 24	685 ± 12	528 ± 3	267 ± 5	506 ± 11	361 ± 10
True colour (mg Pt-Co/L)	236 ± 2	307 ± 9	281 ± 14	701 ± 2	63 ± 24	2,563 ± 91	1,261 ± 82	5,381 ± 55	4,891 ± 0	1,284 ± 67	1,400 ± 52	2,260 ± 157	2,563 ± 99

UVA 254 (1/cm)	1.075 ± 0.001	2.29 ± 0.04	1.617 ± 0.006	0.261 ± 0.002	0.212 ± 0.005	13.2 ± 0.2	5.1 ± 0.2	22.6 ± 0.2	17.41 ± 0.04	5.58 ± 0.05	4.94 ± 0.01	8.41 ± 0.05	8.04 ± 0.07
SUVA (m·L/mg C)	0.83 ± 0.03	1.52 ± 0.09	1.51 ± 0.04	0.36 ± 0.02	0.313 ± 0.008	0.66 ± 0.01	1.72 ± 0.07	1.88 ± 0.04	2.54 ± 0.05	1.06 ± 0.01	1.85 ± 0.04	1.66 ± 0.04	2.23 ± 0.06
VFA (mg COD/L)	17 ± 16	Not detected	Not detected	Not detected	Not detected	28 ± 7	6 ± 11	70 ± 23	61 ± 2	296 ± 1	16 ± 8	Not detected	Not detected
PO <sub>4</sub> <sup>3-</sup> (mg PO <sub>4</sub> <sup>3-</sup> -P/L) (% of total P)	21.9 ± 0.2 (97%)	27.9 ± 0.2 (91%)	28.3 ± 0.2 (87%)	2.94 ± 0.07 (99%)	18.4 ± 0.2 (99%)	102.6 ± 0.9 (78%)	57 ± 2 (85%)	107 ± 3 (91%)	23 ± 1 (79%)	33.40 ± 0.03 (91%)	172 ± 1 (99%)	29.7 ± 0.5 (92%)	51 ± 6 (97%)
TP mg (P/L)	22.7 ± 0.3	30.9 ± 0.3	32.3 ± 0.2	2.9 ± 0.7	18.61 ± 0.09	131 ± 3	66 ± 2	117 ± 2	29 ± 2	36.7 ± 0.6	175 ± 2	32.3 ± 0.5	52 ± 3
TAN (mg N/L)	1,190 ± 119	590 ± 20	55 ± 2	243 ± 19	21.9 ± 2	1,970 ± 134	101 ± 8	2,400 ± 40	199 ± 3	1,663 ± 20	204 ± 0	1,910 ± 10	580 ± 22
NO <sub>2</sub> <sup>-</sup> -N (mg N/L)	Not detected	664 ± 7	Not detected	9.76 ± 0.05	1.213 ± 0.006	Not detected	Not detected	Not detected	Not detected	Not detected	Not detected	0.126 ± 0.005	57 ± 2

NO <sub>3</sub> <sup>-</sup> -N (mg N/L)	Not detected	185 ± 22	73.2 ± 0.3	2.5 ± 0.2	23.2 ± 0.4	10.17 ± 0.05	4.0 ± 0.1	17.0 ± 0.4	14.1 ± 0.2	Not detect ed	Not detect ed	6.3 ± 0.2	18.4 ± 3
TN (mg N/L)	1,399 ± 13	1,222 ± 33	136 ± 1	281 ± 17	55 ± 1	2,048 ± 140	134 ± 5	2,553 ± 42	280 ± 4	1,548 ± 33	244 ± 23	2,205 ± 32	751 ± 32
EC (mS/cm)	10.45 ± 0.03	6.79 ± 0.01	1.746 ±0.03	6.35 ± 0.02	4.84 ±	13.50 ± 0.07	2.85 ± 0.01	14.94 ± 0.07	3.61 ± 0.02	13.70 ± 0.07	6.20 ± 0.03	13.54 ± 0.07	5.87 ± 0.03

\* SLU-S and SLU-A represent Sluisjesdijk Sharon and Anammox reactors, respectively.



### 5.3.2. Stoichiometry of the PN/A reaction and O<sub>2</sub> consumption

Following the PN/A reaction's stoichiometry 7.5% of TAN-N (molar base) is converted to NO<sub>3</sub><sup>-</sup>-N as an end-product (Lotti et al., 2014b). Consequently, a lower-than-stoichiometric NO<sub>3</sub><sup>-</sup>-N concentration in the PN/A effluents indicates NO<sub>3</sub><sup>-</sup> reduction. Denitrification and dissimilatory nitrate reduction to ammonia (DNRA) are recognised as the main mechanisms to reduce NO<sub>3</sub><sup>-</sup>. Since DNRA only occurs under strict reducing conditions (Pandey et al., 2020), we considered denitrification as the main pathway for NO<sub>3</sub><sup>-</sup>-N reduction in our present study. Moreover, SDA was observed in all the studied full-scale PN/A reactors (Table 5.2). The denitrification pathway is enhanced in zones of lower DO, or moderate oxidation-reduction potentials (Rambags et al., 2019), such as the inner part of granules, or in flocs if the aeration is stopped. The latter is prevalent in reactors with intermittent-aeration systems. Figure 5.1-a shows a comparison between the stoichiometric NO<sub>3</sub><sup>-</sup>-N production based on TAN conversion and the difference between the effluent and influent NO<sub>3</sub><sup>-</sup>-N measured values in mg N/L of each full-scale reactor. The stoichiometric NO<sub>3</sub><sup>-</sup>-N production was in line with the difference in TAN concentrations in influent and effluent (TAN conversion), which were distinctly higher in the plants using THP, as has been previously reported (Barber, 2016) and shown in Table 5.2. Also, the NO<sub>3</sub><sup>-</sup>-N produced in the PN/A step was close to zero in three out of four of the plants using THP, showing that denitrification consumed all the NO<sub>3</sub><sup>-</sup>-N generated in PN/A. Conversely, the plants not using THP (SLU and OLB) presented NO<sub>3</sub><sup>-</sup>-N concentrations close to the stoichiometric production. The proximity between the stoichiometric and measured NO<sub>3</sub><sup>-</sup>-N values indicated less prominence of denitrification in these full scale PN/A plants. Although considerable SDA values were assessed, the near absence of denitrification was likely due to lack of electron donors such as biodegradable organics. Increased denitrification may increase N<sub>2</sub>O formation and thus greenhouse gas emissions, as widely discussed in the literature (Gulhan et al., 2023; Kong et al., 2016; Ma et al., 2017; Massara et al., 2017; Ni and Yuan, 2015). Furthermore, the plants using THP removed more N than stoichiometrically possible via PN/A, indicating that organic matter in the influent was used as electron donor for denitrification. Partially biodegradable organics from THP may have a positive impact on the deammonification process, reducing the N-load to the mainstream nitrification-denitrification process of the WWTP.

The most important control parameter in PN/A systems is DO. Aeration must be controlled carefully to one hand, provide sufficient O<sub>2</sub> to partially oxidise TAN and, on the other hand, to avoid O<sub>2</sub> inhibition of the anammox microorganisms (Morales et al., 2015; Seuntjens et al.,

2018). The stoichiometric  $O_2$  demands to oxidise TAN in the influents were calculated and are shown in Figure 5.1-b. In the same way as  $NO_3^-$ -N production, the  $O_2$  demand followed TAN conversion in the influents, and was distinctly higher in the plants using THP due to the elevated TAN concentrations present in the influents. In addition to the required amount of  $O_2$  to convert the TAN into  $NO_2^-$ -N, an additional amount of  $O_2$  was used to oxidise the organics in the influents (numbers in brackets). The oxidation of organic compounds was likely performed using a combination of  $O_2$ ,  $NO_2^-$ -N and  $NO_3^-$ -N as final electron acceptors, as explained previously. From Figure 5.1-b, it can be observed that the additional  $O_2$  demand can reach up to 56 % in the case of TIL, being distinctly higher in the plants using THP. The additional  $O_2$  demand increased the energy requirement of the PN/A reactors, which is primarily dependent on the influent TAN concentration (Deng et al., 2021). It should be noted that AD-reject water is commonly recirculated to the mainstream treatment process for further treatment. This means that in the absence of PN/A, the additional  $O_2$  demand would be otherwise spent in the secondary treatment. However, our results clearly showed that the  $O_2$  demand to mineralise COD (as organics) must also be considered in the process design, even though PN/A systems are commonly designed to only consider the  $O_2$  needed to partially oxidise TAN. The additional  $O_2$  consumption might also affect the required  $O_2$  supply rate, giving additional restrictions to the aeration systems to reach the DO setpoints in the reactors. To verify the influence of THP on the  $O_2$  consumption rate, the  $O_2$  supply and consumption rates must be tested in full-scale reactors and the aeration adapted accordingly.

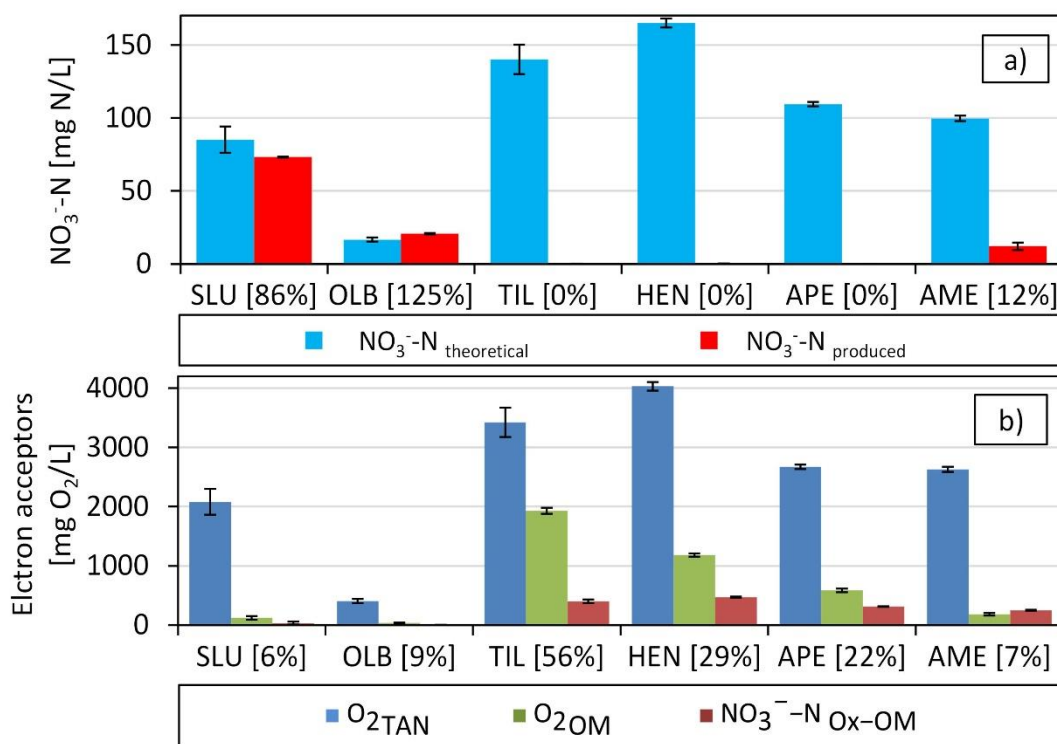


**Figure 5.1.** a) Stoichiometric versus measured  $\text{NO}_3^- \text{-N}$  production in the studied plants. The numbers in brackets represent the percentage of  $\text{NO}_3^- \text{-N}_{\text{measured}}$  over the stoichiometrically produced  $\text{NO}_3^- \text{-N}$ ; b) Electron acceptors per litre of reactor used to oxidise the TAN and organics in the studied PN/A systems as shown in Equations 5.8, 5.9 and 5.10. The numbers in brackets represent the  $\text{O}_2$  used to oxidise organics, over  $\text{O}_2$  used to oxidise TAN.

### 5.3.3. PN/A streams trace elements characterisation and complexation assays

Most prevalent cations concentrations were measured in the soluble fraction of the influents and effluents of the studied PN/A reactors using ICP-MS. The cations concentrations are shown in Figure 5.2 (full data set available in additional information). It is important to stress that the concentrations of the measured cations differed in all the analysed plants, attributable to the very different treatments applied (Table 5.1) and the use of specific chemicals in treatment steps prior to PN/A. In some WWTPs, cations were added i) to control process variables such as pH ( $\text{Na}^+$  as  $\text{NaOH}$ ); ii) to coagulate/precipitate (in)organic matter ( $\text{Fe}^{3+}$  as  $\text{FeCl}_3$ ); iii) as reagents in previous processes such as  $\text{Mg}^{2+}$  in struvite precipitation (Abma et al., 2010; Driessen et al., 2020; Oosterhuis et al., 2014).

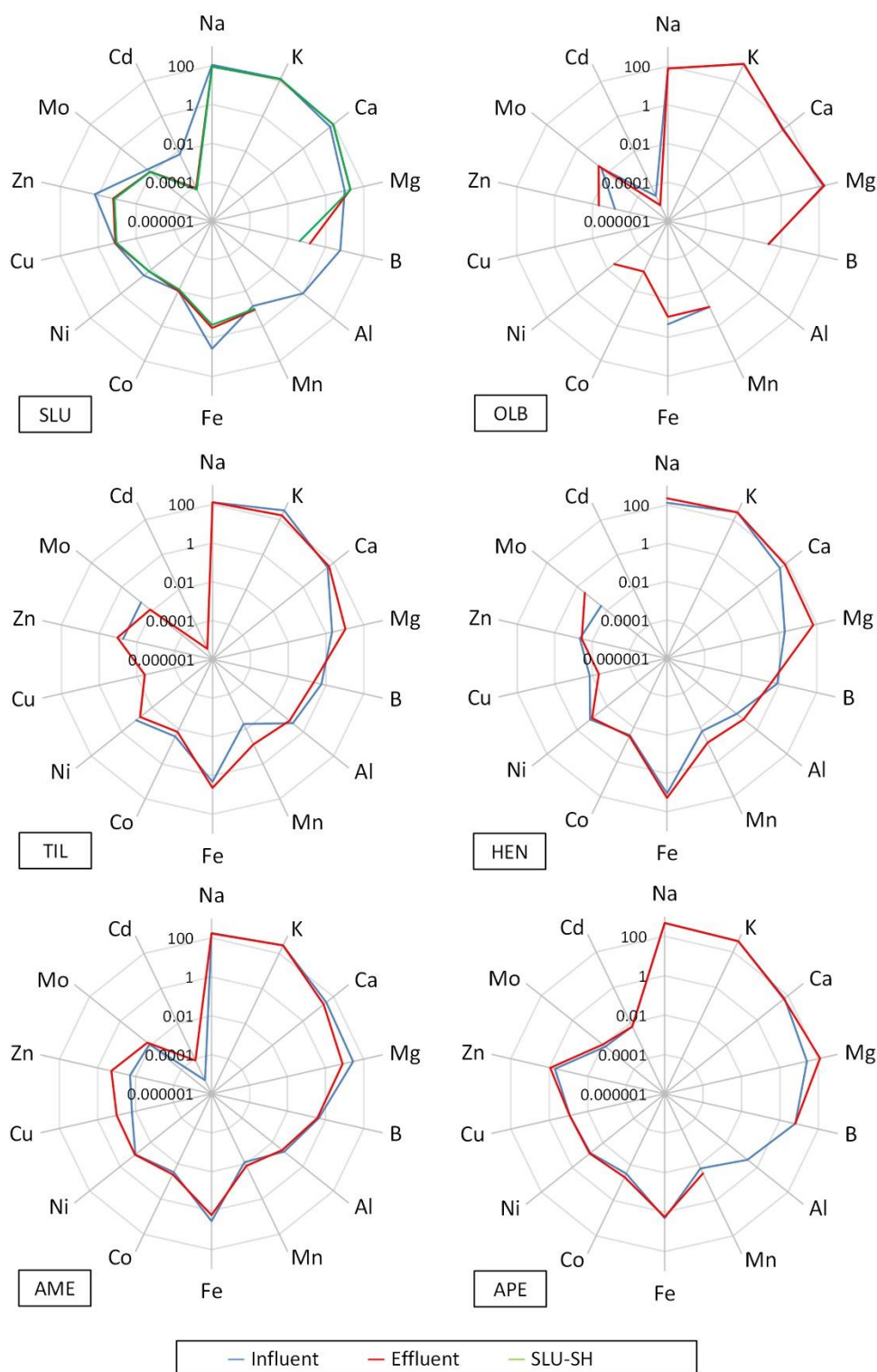


**Figure 5.2.** Cations characterisation in the PN/A step of the studied WWTPs. The units in the vertical axis are mg/L and the scale is logarithmic.

PCA was conducted as a dimensionality reduction technique to understand the behaviour of the cations present in the influents and effluents of the PN/A reactors analysed (Figure 5.3).

The variability explained in the two plotted components was 75.8 [%] in the case of the influents and 67.6 [%] in the case of the effluents. Among the influents samples (Figure 5.3-a) the data from AME and HEN were the most closely related with 0.04 [RAD] of angle difference among the vectors, followed by TIL with 0.32 [RAD] of difference with HEN. Besides, B, Al, Cu, Zn and Ca were clustered in the two plotted components, while the transition metals Fe, Co Ni and Mo were clustered only in the negative part of the first component. Figure 5.3-b shows that SLU-S, SLU-A and OLB behaved similarly, which do not use THP as pre-treatment. Also, HEN and TIL showed similar behaviour. The metals distribution was scattered within the biplot, not showing a clear trend among the metals groups.

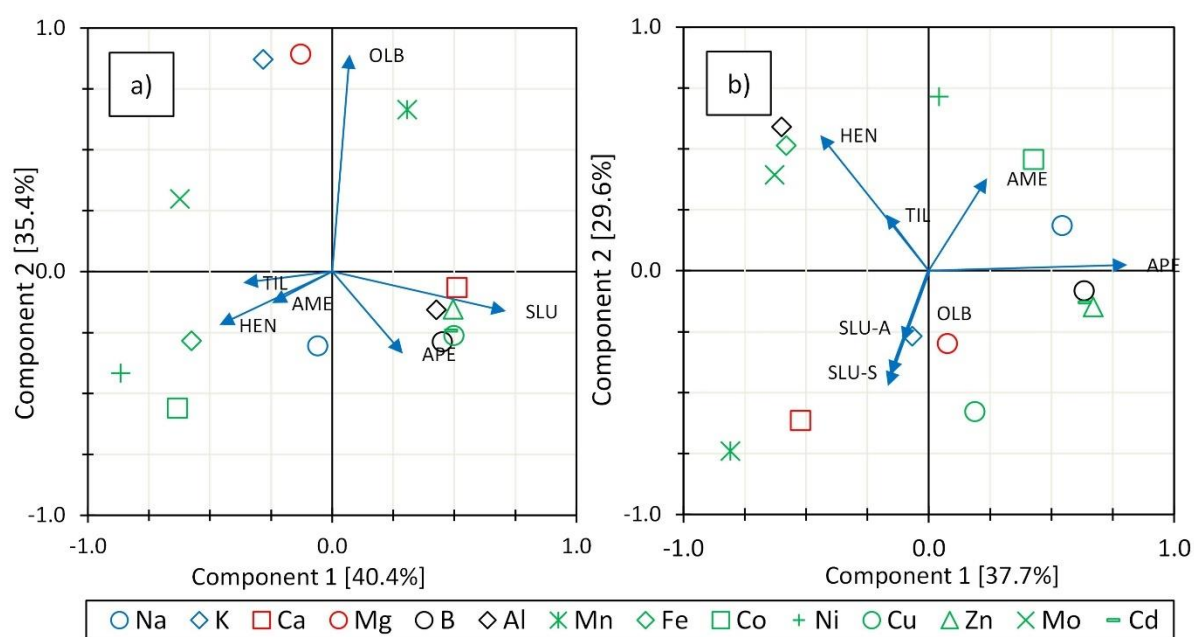


**Figure 5.3.** PCA of the cations analysed in PN/A reactors of the studied plants. Cations are clustered and indicated with different colours: blue= monovalent; red= divalent; black: trivalent (metalloids); multivalent (transition metals).

#### 5.3.4. Membrane separation of trace elements in PN/A effluents

HSs and melanoidins behave as multidentate ligands (Mantoura et al., 1978; Tipping, 2002). The metal complexing capacity of these organic compounds can eventually limit the bioavailability of trace elements and hinder microbial growth (anabolism) or substrate conversion capacities (catabolism). Complexation of cations is expected since melanoidins tend to have a negative charge at neutral pH due to the de dissociation of carboxylic and phenolic groups (Bekedam et al., 2008; Migo et al., 1993).

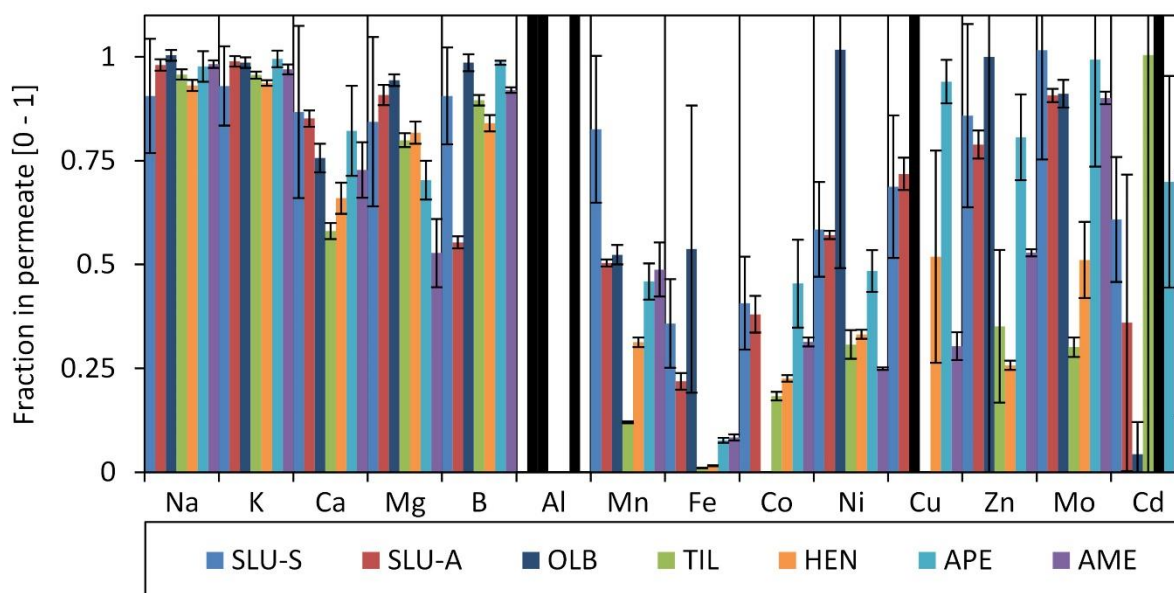
In the plants using THP a maximum of 17% of colour passed the ultrafiltration membrane, which was the case for the APE sample (additional material). The concentrations of trace elements showed a similar pattern as the THP effluent results shown in Figure 5.2. The observed high similarity in results was likely caused by the used membranes in the filtration processes having a similar pore size, viz. the dead-end filtration membrane had a pore size of 0.45  $\mu\text{m}$  (data in Figure 5.2) and the crossflow filtration membrane had a pore size of 0.5  $\mu\text{m}$  (Figure 5.4).

Figure 5.4 shows the cation fractions that were filtered using a 0.5  $\mu\text{m}$  pore size membrane and subsequently passed the 1kDa ultrafiltration membrane. A low value in the 1kDa-filtered fraction implies that the specific cation is to a great extent complexed to the melanoidins present in the broth of PN/A reactors. Results in Figure 5.4 show that Al was strongly complexed by the melanoidins in the broth, since Al was nearly absent in the 1 kDa permeate. Furthermore, Al was not found at all in three of the 0.5  $\mu\text{m}$  filtered effluents (Fig. 5, black bars), likely because it formed part of the solids and colloidal matrix and was thus rejected by the 0,5  $\mu\text{m}$  membrane. The binding capacity of Al with organics is widely reported in various concentrations and pHs (Tipping et al., 1988). Next to Al, Fe was the second element in place regarding the degree of complexation with melanoidins, showing an average of only 19% of the Fe fraction that passed the 1kDa membrane (Figure 5.4). Notably, compared to the THP equipped full-scale plants, larger Fe fractions in the 1 kDa permeates were measured in the plants not using THP, reaching 36%, 22% and 54% in the case of SLU-S, SLU-A and OLB, respectively. In all the plants using THP as pre-treatment and which were characterised by relatively high concentrations of organic matter (Table 5.2), the observed Fe complexation was considerable. The fractions that passed the 1 kDa membrane reached only 1%, 8%, 8%, and 2% in the case of TIL, AME, APE, and HEN, respectively (Figure 5.4). We, therefore, hypothesize that the effects of THP on Fe concentration in the 1kDa permeates was indicative for the complexation of this metal with the THP-created melanoidins. Fe commonly occurs in biological systems in oxidation states  $\text{Fe}^{2+}$  and  $\text{Fe}^{3+}$ , and the specific oxidation state mainly depends on the redox conditions (Pehkonen, 1995). After AD, Fe is expected to occur in reject waters in the reduced form ( $\text{Fe}^{2+}$ ). However, during struvite precipitation, which is commonly performed in airlift reactors, and in limitedly aerated PN/A reactors,  $\text{Fe}^{2+}$  is likely oxidised to  $\text{Fe}^{3+}$ . The  $\text{Fe}^{3+}$  ion strongly binds HSs, forming stable bonds with multidentate ligands, such as HSs and melanoidins (Srivastva, 2020). Fe is an important metal in the anammox heme proteins, which constitute up to 30% of the protein content and gives these microorganisms

their distinctive reddish colour (Ferousi et al., 2017; Kartal et al., 2012). In addition, Fe is involved in  $\text{NH}_4^+$  oxidation, being part of the ammonium-monooxygenase metalloenzyme. Ammonium-monooxygenase catalyses the conversion of  $\text{NH}_4^+$  to hydroxylamine (Gilch et al., 2009).

Also, Mn and Co were strongly complexed with melanoidins, and less than 50% of these metals passed through the 1 kDa membrane. Co is an essential nutrient for microbial growth involved in the N-cycle (Nicholas et al., 1964). Co has also shown positive effects on the anammox conversion capacity when dosed as a trace element (Li et al., 2020). Furthermore, Ni can be found in metalloproteins produced by some AOO, such as urease (Koper et al., 2004). However, Ni can be toxic if present in high concentrations, with IC<sub>50</sub> values of 6.0 mg Ni/L in solution (Kalkan Aktan et al., 2018) that were never reached in our present study.

The cations' complexation stability depends on many factors such as oxidation state, atomic radius and nature of the ligands; however, they follow the Irving–Williams series for divalent cations ( $\text{Mn} < \text{Fe} < \text{Co} < \text{Ni} < \text{Cu} > \text{Zn}$ ) (Irving and Williams, 1953). The complexation of specific trace elements that play a role in enzymatic cofactors may hinder both, microbial catabolism, and anabolism in PN/A biomass from full-scale installations using THP.



**Figure 5.4.** The fraction of the 0.5 µm filtered supernatant that passed the 1 kDa membrane. The black bars represent the absence of a specific cation in the 0.5 µm filtered supernatant.

### **5.3.5. Correlation analysis of cation complexation and organic matter in the PN/A reactors**

A correlation analysis was performed among the fraction of metals that passed the 1kDa membrane (non-complexed) and the melanoidins indicators such as COD, TOC, COL, and UVA254 in the 0.5  $\mu\text{m}$  fraction of PN/A. The Kendal correlation coefficient ( $\tau$ ) was calculated; this coefficient is employed for non-parametric correlations in small datasets, which was only seven data points in this case (Field, 2013). Also, a two-tailed ANOVA analysis at 95% of confidence was performed to analyse the correlation significance. Figure 5.5 shows significant correlations at 95% of confidence of  $\tau$  between the parameters, COD, TOC, COL, and UVA254, in the 0.5  $\mu\text{m}$  fraction, and the fraction of cations that passed the 1 kDa membrane. Figure 5.5. Significant correlation at 95% of confidence of Kendall correlation coefficient ( $\tau$ ) between the concentration of COD, TOC, COL, and UVA254 in the 0.5  $\mu\text{m}$  fraction, and the fraction of cations that passed through the 1 kDa membrane. A negative correlation coefficient means that the cation was more HSs-complexed and hence, less bioavailable. Figure 5.5 shows that the largest negative correlation was found between Fe and colour ( $\tau=0.90$ ). This highly negative correlation showed that the increased concentration of colour in the broth of PN/A reactors produced a higher extent of complexed Fe. Also, colour presented a negative correlation coefficient with Mn, Ni, and Zn ( $\tau=0.81$ ), which indicated a high complexation of these metals with HSs that caused colour occurrence. Furthermore, UVA 254 presented a significantly negative correlation coefficient with Ni and Zn, and TOC with Fe and Zn. Overall, colour in the PN/A effluents showed a significant negative correlation coefficient with the chelation of six multivalent cations (Ca, Mn, Fe, Ni, Zn and Mo). These results showed that the complexation of cations in the effluents of PN/A reactors was correlated with the melanoidins occurrence. Our present study proved that the complexation of cations with multidentate ligands occurred, which eventually may cause problems in full-scale PN/A reactors. However, current results did not prove any biomass growth/conversion-rate limitation as a consequence of trace elements scarcity. To identify the trace elements that indeed limit bioconversion, further research is needed in the field of trace elements availability in biological systems with high concentrations of polydentate ligands.



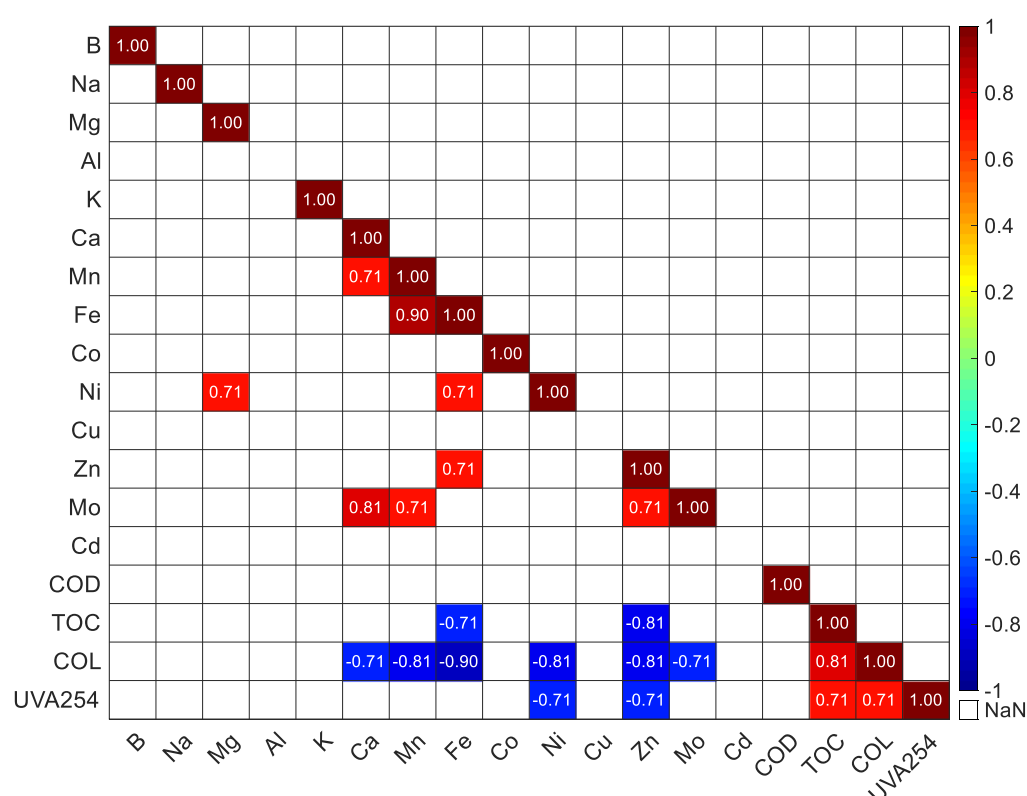


**Figure 5.5.** Significant correlation at 95% of confidence of Kendall correlation coefficient ( $\tau$ ) between the concentration of COD, TOC, COL, and UVA254 in the 0.5  $\mu\text{m}$  fraction, and the fraction of cations that passed through the 1 kDa membrane.

### 5.3.6. Significance of the results for full-scale installations using THP.

The increased TAN and melanoidin concentrations associated with AD-THP, demand optimized operational parameters and control strategies. In full-scale PN/A reactors that are not designed for elevated concentrations of organics and TAN, some modifications are required. DO control systems need to be adjusted to the elevated  $\text{O}_2$  consumption rate, due to the degradation of biodegradable organics. Fulfilling the increased  $\text{O}_2$  requirements could be reached by extending the aeration periods in intermittent aeration systems, or installing additional aeration systems. Also, the TAN conversion capacity likely needs to be increased, which can be attained by increasing the concentration of AOO in the reactors or extending the retention time in the reactors. Increase in AOO concentration may be reached by improving the liquid solids separation techniques as used in DEMON® systems (Izadi et al., 2021).

Elevated denitrification capacity in PN/A systems has the potential to enhance the N-removal efficiency from the reject waters. However, it also raises concerns regarding increased

greenhouse gas emissions, such as  $\text{N}_2\text{O}$ . Further studies are needed to understand  $\text{N}_2\text{O}$  emissions from the treatment of reject water from AD-THP-based systems.

Transition metals-melanoidins complexation was discussed as a side-effect of the use of reject water from a THP-AD system. Trace metals complexation might cause trace elements limitation in the PN/A microbial populations. Future research is needed to explore the effects of specific trace metal limitations and its implications for microbial PN/A populations. Full-scale mitigation strategies, such as trace elements addition to PN/A systems, may help to alleviate metals limitation in the case of PN/A systems working with high concentrations of melanoidins.

## 5.4. Conclusions

The analysis of the studied PN/A systems allowed us to draw the following conclusions:

- The use of THP as AD pre-treatment technique, increased COD, TOC, T. colour and UVA 254 in influents of PN/A systems, evidencing an increase in the concentrations of melanoidins in full-scale PN/A systems. The melanoidins in the PN/A influents were not fully recalcitrant under the aerobic/anoxic conditions, and were partly degraded during the PN/A step.
- The use of AD-THP increased the O<sub>2</sub> requirements in the PN/A reactors, which resulted in increased aeration requirements in full-scale installations. The additional O<sub>2</sub> was used to oxidise the elevated concentrations of TAN and non-recalcitrant melanoidins in PN/A influents.
- In WWTPs using AD-THP, NO<sub>3</sub><sup>-</sup>-N concentrations in PN/A effluents were lower than the stoichiometric values, attributable to the occurrence of heterotrophic denitrification. Denitrifying microorganisms using the organic matter in the reject waters as electron donors, increased the N-removal efficiency in PN/A systems treating AD-THP reject waters.
- The presence of melanoidins in the effluents of PN/A reactors increased the fraction of chelated Fe and other transition metals. The complexation of transition metals in PN/A effluents is mainly correlated with the presence and intensity of colour. The complexation of transition metals might cause trace metals limitation in the microbial populations of the PN/A systems.

## **5.5. List of abbreviations**

AD: anaerobic digestion.

AME: Amersfoort.

AOO: aerobic ammonium oxidising organisms.

APE: Apeldoorn.

COD: chemical oxygen demand.

DNRA: dissimilatory nitrate reduction to ammonia.

DO: dissolved oxygen.

EC: electroconductivity.

FAN: free ammonia nitrogen.

FID-GC: flame ionisation detector gas chromatography.

HEN: Hengelo.

HSs: humic substances.

OLB: Olburgen.

PCA: principal component analysis.

PN/A: partial nitrification/anammox.

SAA: specific anammox activity.

SAOA: specific ammonium oxidising activity.

SDA: specific denitrifying activity.

SLU: Sluisjesdijk.

SUVA: specific ultraviolet absorbance.

T. colour: True colour.

TAN: total ammoniacal nitrogen.

THP: thermal hydrolysis process.

TIL: Tilburg.

TN: total nitrogen.

TOC: total organic carbon.

TP: Total phosphorous.

TS: Total solids.

UVA 254: ultraviolet absorbance at 254 nm.

VFA: volatile fatty acids.

VS: volatile solids.

WAS: waste activated sludge.

WWTPs: wastewater treatment plants.

$\tau$ : Kendal correlation coefficient.

## 5.6. References

- Abma, W.R., Driessen, W., Haarhuis, R. and van Loosdrecht, M.C.M. 2010. Upgrading of sewage treatment plant by sustainable and cost-effective separate treatment of industrial wastewater. *Water Science and Technology* 61(7), 1715-1722.
- Aghababae, M., Farhadian, M., Jeihanipour, A. and Biria, D. 2015. Effective factors on the performance of microbial fuel cells in wastewater treatment – a review. *Environmental Technology Reviews* 4(1), 71-89.
- Appels, L., Baeyens, J., Degre, J. and Dewil, R. 2008. Principles and potential of the anaerobic digestion of waste-activated sludge. *Progress in Energy and Combustion Science* 34(6), 755-781.
- Baeten, J.E., Batstone, D.J., Schraa, O.J., van Loosdrecht, M.C.M. and Volcke, E.I.P. 2019. Modelling anaerobic, aerobic and partial nitrification-anammox granular sludge reactors - A review. *Water Research* 149, 322-341.
- Barber, W.P.F. 2016. Thermal hydrolysis for sewage treatment: A critical review. *Water Research* 104, 53-71.
- Becker, G.C., Wüst, D., Köhler, H., Lautenbach, A. and Kruse, A. 2019. Novel approach of phosphate-reclamation as struvite from sewage sludge by utilising hydrothermal carbonization. *Journal of Environmental Management* 238, 119-125.
- Bekedam, E.K., Roos, E., Schols, H.A., Van Boekel, M.A.J.S. and Smit, G. 2008. Low Molecular Weight Melanoidins in Coffee Brew. *Journal of Agricultural and Food Chemistry* 56(11), 4060-4067.
- Bougrier, C., Delgenès, J.P. and Carrère, H. 2008. Effects of thermal treatments on five different waste activated sludge samples solubilisation, physical properties and anaerobic digestion. *Chemical Engineering Journal* 139(2), 236-244.
- Campos, J., Garrido-Fernandez, J., Mendez, R. and Lema, J. 1999. Nitrification at high ammonia loading rates in an activated sludge unit. *Bioresource Technology* 68(2), 141-148.
- Ceron-Chafla, P., Kleerebezem, R., Rabaey, K., van Lier, J.B. and Lindeboom, R.E.F. 2020. Direct and Indirect Effects of Increased CO<sub>2</sub> Partial Pressure on the Bioenergetics of Syntrophic Propionate and Butyrate Conversion. *Environmental Science & Technology* 54(19), 12583-12592.
- Coats, E.R., Watkins, D.L. and Kranenburg, D. 2011. A Comparative Environmental Life-Cycle Analysis for Removing Phosphorus from Wastewater: Biological versus Physical/Chemical Processes. *Water Environment Research* 83(8), 750-760.
- Deng, Z., van Linden, N., Guillen, E., Spanjers, H. and van Lier, J.B. 2021. Recovery and applications of ammoniacal nitrogen from nitrogen-loaded residual streams: A review. *Journal of Environmental Management* 295, 113096.
- Devos, P., Filali, A., Grau, P. and Gillot, S. 2023. Sidestream characteristics in water resource recovery facilities: A critical review. *Water Research* 232, 119620.
- Driessen, W., Van Veldhoven, J.T.A., Janssen, M.P.M. and Van Loosdrecht, M.C.M. 2020. Treatment of sidestream dewatering liquors from thermally hydrolysed and anaerobically digested biosolids. *Water Practice and Technology* 15(1), 142-150.
- Dwyer, J., Kavanagh, L. and Lant, P. 2008a. The degradation of dissolved organic nitrogen associated with melanoidin using a UV/H<sub>2</sub>O<sub>2</sub> AOP. *Chemosphere* 71(9), 1745-1753.
- Dwyer, J., Starrenburg, D., Tait, S., Barr, K., Batstone, D.J. and Lant, P. 2008b. Decreasing activated sludge thermal hydrolysis temperature reduces product colour, without decreasing degradability. *Water Research* 42(18), 4699-4709.
- El-sayed, M.E., Abdelaal, W.A. and Ahmed, A.A. 2017. Effect of using treated drainage water by modified clay on some plant and soil properties. *Nat Sci* 15(12), 17-25.

- Ferousi, C., Lindhoud, S., Baymann, F., Kartal, B., Jetten, M.S.M. and Reimann, J. 2017. Iron assimilation and utilization in anaerobic ammonium oxidizing bacteria. *Current Opinion in Chemical Biology* 37, 129-136.
- Field, A. (2013) *Discovering statistics using IBM SPSS statistics*, sage.
- Fischer, F., Bastian, C., Happe, M., Mabillard, E. and Schmidt, N. 2011. Microbial fuel cell enables phosphate recovery from digested sewage sludge as struvite. *Bioresource Technology* 102(10), 5824-5830.
- Flores-Alsina, X., Solon, K., Kazadi Mbamba, C., Tait, S., Gernaey, K.V., Jeppsson, U. and Batstone, D.J. 2016. Modelling phosphorus (P), sulfur (S) and iron (Fe) interactions for dynamic simulations of anaerobic digestion processes. *Water Research* 95, 370-382.
- Fux, C. and Siegrist, H. 2004. Nitrogen removal from sludge digester liquids by nitrification/denitrification or partial nitritation/anammox: environmental and economical considerations. *Water Science and Technology* 50(10), 19-26.
- Gerke, J. 1992. Orthophosphate and organic phosphate in the soil solution of four sandy soils in relation to pH-evidence for humic-Fe-(AL-) phosphate complexes. *Communications in Soil Science and Plant Analysis* 23(5-6), 601-612.
- Gilbert, E.M., Müller, E., Horn, H. and Lackner, S. 2013. Microbial activity of suspended biomass from a nitritation–anammox SBR in dependence of operational condition and size fraction. *Applied Microbiology and Biotechnology* 97(19), 8795-8804.
- Gilch, S., Meyer, O. and Schmidt, I. 2009. A soluble form of ammonia monooxygenase in *Nitrosomonas europaea*. 390(9), 863-873.
- Graaf, A.v.d., Bruijn, P.d., Robertson, L., Jetten, M. and Kuenen, J. 1996. Autotrophic growth of anaerobic ammonium-oxidizing micro-organisms in a fluidized bed reactor. *Microbiology-Reading* 142(8), 2187-2196.
- Gulhan, H., Cosenza, A. and Mannina, G. 2023. Modelling greenhouse gas emissions from biological wastewater treatment by GPS-X: The full-scale case study of Corleone (Italy). *Science of The Total Environment* 905, 167327.
- Hendriks, A.T.W.M. and Zeeman, G. 2009. Pretreatments to enhance the digestibility of lignocellulosic biomass. *Bioresource Technology* 100(1), 10-18.
- Hodge, J.E. 1953. Dehydrated Foods, Chemistry of Browning Reactions in Model Systems. *Journal of Agricultural and Food Chemistry* 1(15), 928-943.
- Irving, H. and Williams, R. 1953. 637. The stability of transition-metal complexes. *Journal of the Chemical Society (Resumed)*, 3192-3210.
- Izadi, P., Izadi, P. and Eldyasti, A. 2021. Towards mainstream deammonification: Comprehensive review on potential mainstream applications and developed sidestream technologies. *Journal of Environmental Management* 279, 111615.
- Joss, A., Salzgeber, D., Eugster, J., König, R., Rottermann, K., Burger, S., Fabijan, P., Leumann, S., Mohn, J. and Siegrist, H. 2009. Full-Scale Nitrogen Removal from Digester Liquid with Partial Nitritation and Anammox in One SBR. *Environmental Science & Technology* 43(14), 5301-5306.
- Kalkan Aktan, C., Uzunhasanoglu, A.E. and Yapsakli, K. 2018. Speciation of nickel and zinc, its short-term inhibitory effect on anammox, and the associated microbial community composition. *Bioresource Technology* 268, 558-567.
- Kartal, B., van Niftrik, L., Keltjens, J.T., Op den Camp, H.J.M. and Jetten, M.S.M. (2012) *Advances in Microbial Physiology*. Poole, R.K. (ed), pp. 211-262, Academic Press.
- Kong, Q., Wang, Z.-b., Niu, P.-f. and Miao, M.-s. 2016. Greenhouse gas emission and microbial community dynamics during simultaneous nitrification and denitrification process. *Bioresource Technology* 210, 94-100.

- Koper, T.E., El-Sheikh, A.F., Norton, J.M. and Klotz, M.G. 2004. Urease-Encoding Genes in Ammonia-Oxidizing Bacteria. *Applied and Environmental Microbiology* 70(4), 2342-2348.
- Kor-Bicakci, G. and Eskicioglu, C. 2019. Recent developments on thermal municipal sludge pretreatment technologies for enhanced anaerobic digestion. *Renewable and Sustainable Energy Reviews* 110, 423-443.
- L. Malcolm, R. 1990. The uniqueness of humic substances in each of soil, stream and marine environments. *Analytica Chimica Acta* 232, 19-30.
- Lackner, S., Gilbert, E.M., Vlaeminck, S.E., Joss, A., Horn, H. and van Loosdrecht, M.C.M. 2014. Full-scale partial nitrification/anammox experiences – An application survey. *Water Research* 55, 292-303.
- Li, J., Chen, X., Liu, W. and Tao, Y. 2020. Biostimulation of a marine anammox bacteria-dominated bioprocess by Co(II) to treat nitrogen-rich, saline wastewater. *Science of The Total Environment* 749, 141489.
- Li, Y.-Y. and Noike, T. 1992. Upgrading of Anaerobic Digestion of Waste Activated Sludge by Thermal Pretreatment. *Water Science and Technology* 26(3-4), 857-866.
- Lotti, T., Kleerebezem, R., Hu, Z., Kartal, B., Jetten, M.S.M. and van Loosdrecht, M.C.M. 2014a. Simultaneous partial nitrification and anammox at low temperature with granular sludge. *Water Research* 66, 111-121.
- Lotti, T., Kleerebezem, R., Lubello, C. and van Loosdrecht, M.C.M. 2014b. Physiological and kinetic characterization of a suspended cell anammox culture. *Water Research* 60, 1-14.
- Ma, C., Jensen, M.M., Smets, B.F. and Thamdrup, B. 2017. Pathways and Controls of N<sub>2</sub>O Production in Nitrification–Anammox Biomass. *Environmental Science & Technology* 51(16), 8981-8991.
- Ma, H., Xue, Y., Zhang, Y., Kobayashi, T., Kubota, K. and Li, Y.-Y. 2020. Simultaneous nitrogen removal and phosphorus recovery using an anammox expanded reactor operated at 25 °C. *Water Research* 172, 115510.
- Mantoura, R.F.C., Dickson, A. and Riley, J.P. 1978. The complexation of metals with humic materials in natural waters. *Estuarine and Coastal Marine Science* 6(4), 387-408.
- Massara, T.M., Malamis, S., Guisasola, A., Baeza, J.A., Noutsopoulos, C. and Katsou, E. 2017. A review on nitrous oxide (N<sub>2</sub>O) emissions during biological nutrient removal from municipal wastewater and sludge reject water. *Science of The Total Environment* 596-597, 106-123.
- McDonald, S., Bishop, A.G., Prenzler, P.D. and Robards, K. 2004. Analytical chemistry of freshwater humic substances. *Analytica Chimica Acta* 527(2), 105-124.
- Migo, V.P., Matsumura, M., Del Rosario, E.J. and Kataoka, H. 1993. The effect of pH and calcium ions on the destabilization of melanoidin. *Journal of Fermentation and Bioengineering* 76(1), 29-32.
- Morales, F.J., Fernández-Fraguas, C. and Jiménez-Pérez, S. 2005. Iron-binding ability of melanoidins from food and model systems. *Food Chemistry* 90(4), 821-827.
- Morales, N., Val del Río, A., Vázquez-Padín, J.R., Gutiérrez, R., Fernández-González, R., Icaran, P., Rogalla, F., Campos, J.L., Méndez, R. and Mosquera-Corral, A. 2015. Influence of dissolved oxygen concentration on the start-up of the anammox-based process: ELAN®. *Water Science and Technology* 72(4), 520-527.
- Ni, B.-J. and Yuan, Z. 2015. Recent advances in mathematical modeling of nitrous oxides emissions from wastewater treatment processes. *Water Research* 87, 336-346.
- Nicholas, D.J.D., Fisher, D.J., Redmond, W.J. and Osborne, M. 1964. A cobalt requirement for nitrogen fixation, hydrogenase, nitrite and hydroxylamine reductases in *clostridium pasteurianum*. *Nature* 201(4921), 793-795.



- Ødeby, T., Netteland, T. and Solheim, O.E. 1996 Thermal Hydrolysis as a Profitable Way of Handling Sludge. Hahn, H.H., Hoffmann, E. and Ødegaard, H. (eds), pp. 401-409, Springer Berlin Heidelberg, Berlin, Heidelberg.
- Oosterhuis, M., Ringoot, D., Hendriks, A. and Roeleveld, P. 2014. Thermal hydrolysis of waste activated sludge at Hengelo Wastewater Treatment Plant, The Netherlands. *Water Science and Technology* 70(1), 1-7.
- Pandey, C.B., Kumar, U., Kaviraj, M., Minick, K.J., Mishra, A.K. and Singh, J.S. 2020. DNRA: A short-circuit in biological N-cycling to conserve nitrogen in terrestrial ecosystems. *Science of The Total Environment* 738, 139710.
- Pavlostathis, S. and Giraldo-Gomez, E. 1991. Kinetics of anaerobic treatment: a critical review. *Critical Reviews in Environmental Science and Technology* 21(5-6), 411-490.
- Pehkonen, S. 1995. Determination of the oxidation states of iron in natural waters. A review. *Analyst* 120(11), 2655-2663.
- Penaud, V., Delgenès, J.-P. and Moletta, R. 2000. Characterization of Soluble Molecules from Thermochemically Pretreated Sludge. *Journal of Environmental Engineering* 126(5), 397-402.
- Qiu, G., Zuniga-Montanez, R., Law, Y., Thi, S.S., Nguyen, T.Q.N., Eganathan, K., Liu, X., Nielsen, P.H., Williams, R.B.H. and Wuertz, S. 2019. Polyphosphate-accumulating organisms in full-scale tropical wastewater treatment plants use diverse carbon sources. *Water Research* 149, 496-510.
- Rambags, F., Tanner, C.C. and Schipper, L.A. 2019. Denitrification and anammox remove nitrogen in denitrifying bioreactors. *Ecological Engineering* 138, 38-45.
- Rice, E.W., Baird, R.B., Eaton, A.D. and Clesceri, L.S. (2012) Standard methods for the examination of water and wastewater, American Public Health Association Washington, DC.
- Ringoot, D., Kleiven, H. and Panter, K. 2012 Energy efficient thermal hydrolysis with steam explosion, pp. 1-8.
- Rongsayamanont, C., Limpiyakorn, T., Law, B. and Khan, E. 2010. Relationship between respirometric activity and community of entrapped nitrifying bacteria: implications for partial nitrification. *Enzyme and Microbial Technology* 46(3-4), 229-236.
- Rustrian, E., Delgenes, J., Bernet, N. and Moletta, R. 1997. Nitrate reduction in acidogenic reactor: influence of wastewater COD/N-NO<sub>3</sub> ratio on denitrification and acidogenic activity. *Environmental technology* 18(3), 309-315.
- Sánchez, O., Martí, M.C., Aspé, E. and Roeckel, M. 2001. Nitrification rates in a saline medium at different dissolved oxygen concentrations. *Biotechnology letters* 23(19), 1597-1602.
- Satoh, H., Mino, T. and Matsuo, T. 1992. Uptake of Organic Substrates and Accumulation of Polyhydroxyalkanoates Linked with Glycolysis of Intracellular Carbohydrates under Anaerobic Conditions in the Biological Excess Phosphate Removal Processes. *Water Science and Technology* 26(5-6), 933-942.
- Seuntjens, D., Carvajal-Arroyo, J.M., Ruopp, M., Bunse, P., De Mulder, C.P., Lochmatter, S., Agrawal, S., Boon, N., Lackner, S. and Vlaeminck, S.E. 2018. High-resolution mapping and modeling of anammox recovery from recurrent oxygen exposure. *Water Research* 144, 522-531.
- Srivastva, A.N. (2020) Stability and Applications of Coordination Compounds, BoD–Books on Demand.
- Strous, M., Heijnen, J.J., Kuenen, J.G. and Jetten, M.S.M. 1998. The sequencing batch reactor as a powerful tool for the study of slowly growing anaerobic ammonium-oxidizing microorganisms. *Applied Microbiology and Biotechnology* 50(5), 589-596.
- Tiehm, A., Nickel, K., Zellhorn, M. and Neis, U. 2001. Ultrasonic waste activated sludge disintegration for improving anaerobic stabilization. *Water Research* 35(8), 2003-2009.

- Tipping, E. (2002) Cation binding by humic substances, Cambridge University Press.
- Tipping, E., Woof, C., Backes, C.A. and Ohnstad, M. 1988. Aluminium speciation in acidic natural waters: Testing of a model for al-humic complexation. *Water Research* 22(3), 321-326.
- Valenzuela-Heredia, D., Panatt, C., Belmonte, M., Franchi, O., Crutchik, D., Dumais, J., Vázquez-Padín, J.R., Lesty, Y., Pedrouso, A., Val del Río, Á., Mosquera-Corral, A. and Campos, J.L. 2022. Performance of a two-stage partial nitrification-anammox system treating the supernatant of a sludge anaerobic digester pretreated by a thermal hydrolysis process. *Chemical Engineering Journal* 429, 131301.
- Van Hulle, S.W.H., Vandeweyer, H.J.P., Meesschaert, B.D., Vanrolleghem, P.A., Dejans, P. and Dumoulin, A. 2010. Engineering aspects and practical application of autotrophic nitrogen removal from nitrogen rich streams. *Chemical Engineering Journal* 162(1), 1-20.
- van Kempen, R., Mulder, J.W., Uijterlinde, C.A. and Loosdrecht, M.C.M. 2001. Overview: full scale experience of the SHARON® process for treatment of rejection water of digested sludge dewatering. *Water Science and Technology* 44(1), 145-152.
- van Loosdrecht, M.C.M., Hooijmans, C.M., Brdjanovic, D. and Heijnen, J.J. 1997. Biological phosphate removal processes. *Applied Microbiology and Biotechnology* 48(3), 289-296.
- Wang, H.-Y., Qian, H. and Yao, W.-R. 2011. Melanoidins produced by the Maillard reaction: Structure and biological activity. *Food Chemistry* 128(3), 573-584.
- Wang, R., Li, Y., Chen, W., Zou, J. and Chen, Y. 2016. Phosphate release involving PAOs activity during anaerobic fermentation of EBPR sludge and the extension of ADM1. *Chemical Engineering Journal* 287, 436-447.
- Wang, W., Xie, H., Wang, H., Xue, H., Wang, J., Zhou, M., Dai, X. and Wang, Y. 2020. Organic compounds evolution and sludge properties variation along partial nitrification and subsequent anammox processes treating reject water. *Water Research* 184, 116197.
- Xu, X., Qiu, L., Wang, C. and Yang, F. 2019. Achieving mainstream nitrogen and phosphorus removal through Simultaneous partial Nitrification, Anammox, Denitrification, and Denitrifying Phosphorus Removal (SNADPR) process in a single-tank integrative reactor. *Bioresource Technology* 284, 80-89.
- Yuan, Z., Pratt, S. and Batstone, D.J. 2012. Phosphorus recovery from wastewater through microbial processes. *Current Opinion in Biotechnology* 23(6), 878-883.
- Zhang, D., Feng, Y., Huang, H., Khunjar, W. and Wang, Z.-W. 2020a. Recalcitrant dissolved organic nitrogen formation in thermal hydrolysis pretreatment of municipal sludge. *Environment International* 138, 105629.
- Zhang, M., Qiao, S., Shao, D., Jin, R. and Zhou, J. 2018a. Simultaneous nitrogen and phosphorus removal by combined anammox and denitrifying phosphorus removal process. *Journal of Chemical Technology & Biotechnology* 93(1), 94-104.
- Zhang, Q., Vlaeminck, S.E., DeBarbadillo, C., Su, C., Al-Omari, A., Wett, B., Pümpel, T., Shaw, A., Chandran, K., Murthy, S. and De Clippeleir, H. 2018b. Supernatant organics from anaerobic digestion after thermal hydrolysis cause direct and/or diffusional activity loss for nitrification and anammox. *Water Research* 143, 270-281.
- Zhang, T., He, X., Deng, Y., Tsang, D.C.W., Yuan, H., Shen, J. and Zhang, S. 2020b. Swine manure valorization for phosphorus and nitrogen recovery by catalytic-thermal hydrolysis and struvite crystallization. *Science of The Total Environment* 729, 138999.

5.7. Appendix chapter 5

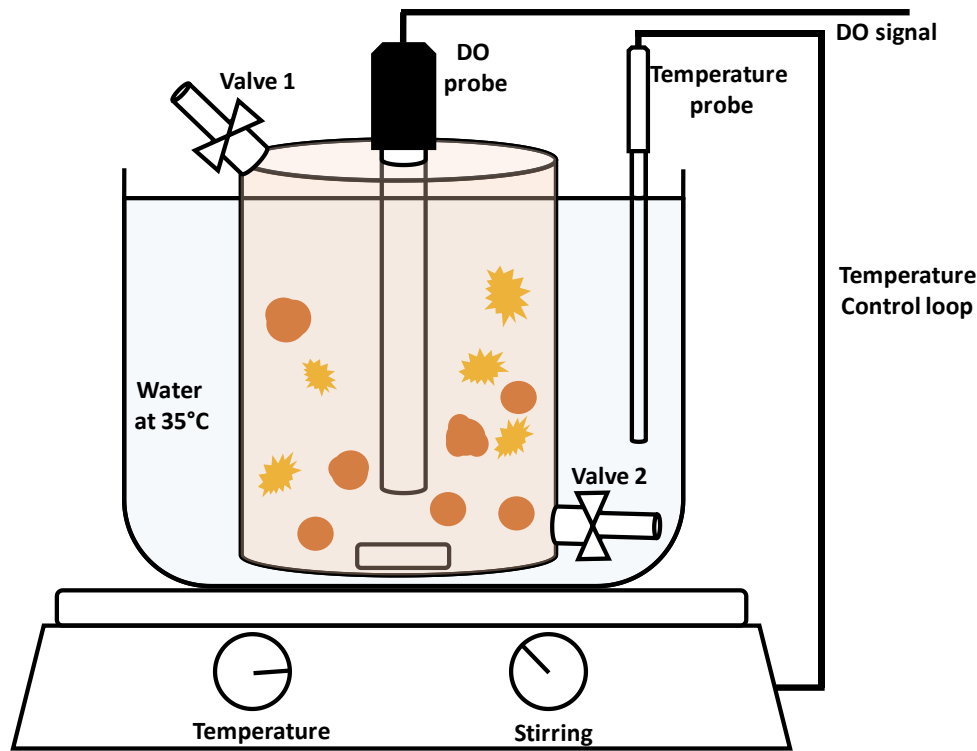


Figure A5.1. Scheme of the respirometric system to measure SAOA.

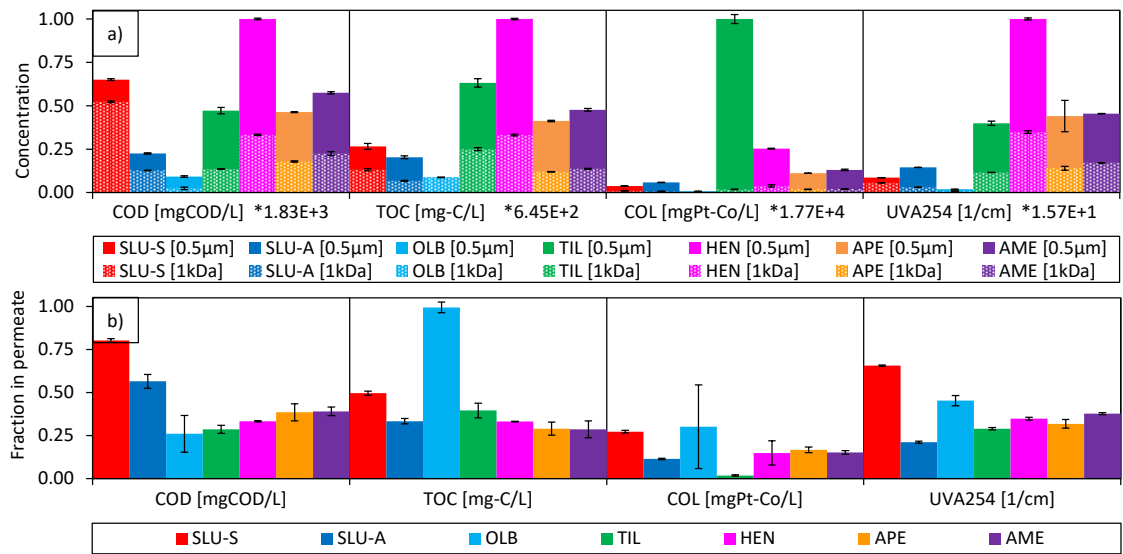


Figure A5.2: Melanoidins indicators in effluents of PN/A reactors in the membrane filtration experiments: a) concentrations in 0.5 µm (solid colour) and 1 kDa membranes (dotted bars). The vertical number is dimensionless; b) Fraction of the melanoidins indicator that passed the 1kDa fraction over 0.5 µm fraction.

Table A5.2. Parameters used to determine cationic isotopes using ICP-MS.

Parameter	
RF power	1.30 [kW]
Measurement mode	Fe in H <sub>2</sub> mode, other elements in no gas mode
Acquisition time	~2 minutes
Solution uptake	4 mL
Cell gas flow	
Plasma flow	9 L/min
Auxiliary flow:	1.40 L/min
Pump rate	10 RPM
Stabilization delay	45 s
Calibration solutions	
IV-STOCK-35 and IV-STOCK-28 (Inorganic Ventures, The USA)	
SRM 1640a - Trace Elements in Natural Water (NIST, The USA)	

**Table A5.3.** Composition of the culture media of SAOA, SAA and SDA.

SAOA was adapted from Campos et al. (1999), Sánchez et al. (2001) and (Rongsayamanont et al., 2010)		
Substrate	Concentration in the medium	Concentration in stock (20X)
NH <sub>4</sub> Cl	306 mg/L (80 mg N/L)	6.113 g/L (1.6 g N/L)
Mineral medium I	Concentration in the medium	Concentration in stock (100X)
KH <sub>2</sub> PO <sub>4</sub>	250 mg/L	25 g/L
MgSO <sub>4</sub>	60 mg/L	6 g/L
NaCl	1000 mg/L	100 g/L
Mineral medium II	Concentration in the medium	Concentration in stock (10X)
NaHCO <sub>3</sub>	5 g/L	50 g/L
Trace elements solution	Concentration in the medium	Concentration in stock (1000X)
FeSO <sub>4</sub> ·7H <sub>2</sub> O	2.7 mg/L	2.7 g/L
MnCl <sub>2</sub> ·4H <sub>2</sub> O	0.1 mg/L	100 mg/L

CoCl <sub>2</sub> ·6H <sub>2</sub> O	0.024 mg/L	24 mg/L
NiCl <sub>2</sub> ·6H <sub>2</sub> O	0.024 mg/L	24 mg/L
CuCl <sub>2</sub> ·2H <sub>2</sub> O	0.017 mg/L	17 mg/L
ZnCl <sub>2</sub>	0.068 mg/L	68 mg/L
Na <sub>2</sub> MoO <sub>4</sub>	0.024 mg/L	24 mg/L
SAA adapted from Graaf et al. (1996)		
Substrates	Concentration in the medium	Concentration in stock (100X)
(NH <sub>4</sub> ) <sub>2</sub> SO <sub>4</sub>	377mg/L (80 mg N/L)	37.7 g/L
NaNO <sub>2</sub>	394mg/L (80 mg N/L)	39.4 g/L
Mineral medium I	Concentration in the medium	Concentration in stock (100X)
KHCO <sub>3</sub>	500 mg/L	50 g/L
KH <sub>2</sub> PO <sub>4</sub>	27.2 mg/L	2.72 g/L
Mineral medium II	Concentration in the medium	Concentration in stock (100X)
MgSO <sub>4</sub> ·7H <sub>2</sub> O	300 mg/L	30 g/L
Mineral medium III	Concentration in the medium	Concentration in stock (100X)
CaCl <sub>2</sub> ·2H <sub>2</sub> O	180 mg/L	18 g/L
Trace elements solution I	Concentration in the medium	Concentration in stock (1000X)
EDTA	5 mg/L	5 g/L
FeSO <sub>4</sub>	5 mg/L	5 g/L
Trace elements solution II	Concentration in the medium	Concentration in stock (1000X)
EDTA	15 mg/L	15 g/L
ZnSO <sub>4</sub> ·7H <sub>2</sub> O	0.43 mg/L	0.43 g/L
CoCl <sub>2</sub> ·6H <sub>2</sub> O	0.24 mg/L	0.24 g/L
MnCl <sub>2</sub> ·4H <sub>2</sub> O	0.99 mg/L	0.99 g/L
CuSO <sub>4</sub> ·5H <sub>2</sub> O	0.25 mg/L	0.25 g/L
NaMoO <sub>4</sub> ·2H <sub>2</sub> O	0.22 mg/L	0.22 g/L
NiCl <sub>2</sub> ·6H <sub>2</sub> O	0.19 mg/L	0.19 g/L

NaSeO <sub>4</sub> ·10H <sub>2</sub> O	0.21 mg/L	0.21 g/L
H <sub>3</sub> BO <sub>4</sub>	0.014 mg/L	0.014 g/L
SDA adapted from Rustrian et al. (1997)		
Substrates	Concentration in the medium	Concentration in stock (100X)
NaCH <sub>2</sub> COOH·3H <sub>2</sub> O	637.8 mg/L (300 mg COD/L)	63.78 g/L (30 g COD/L)
NaNO <sub>3</sub>	182.13 mg NaNO <sub>3</sub> /L (30 mg N/L)	18.213 g NaNO <sub>3</sub> /L (3 g N/L)
Mineral medium	Concentration in the medium	Concentration in stock (100X)
Peptone	50 mg/L	5 g/L
Yeast extract	50 mg/L	5 g/L
NH <sub>4</sub> Cl	38 mg/L	3.8 g/L
MgSO <sub>4</sub> ·7H <sub>2</sub> O	600 mg/L	60 g/L
CaCl <sub>2</sub> ·2H <sub>2</sub> O	70 mg/L	7 g/L
EDTA	100 mg/L	10 g/L
KH <sub>2</sub> PO <sub>4</sub>	50 mg/L	5 g/L
K <sub>2</sub> HPO <sub>4</sub>	90 mg/L	9 g/L
Trace elements solution	Concentration in the medium	Concentration in stock (500X)
FeCl <sub>3</sub> ·6H <sub>2</sub> O	3 mg/L	1.5 g/L
HBO <sub>3</sub>	0.3 mg/L	150 mg/L
CUSO <sub>4</sub> ·5H <sub>2</sub> O	0.06 mg/L	30 mg/L
KI	0.06 mg/L	30 mg/L
MnCl <sub>2</sub> ·4H <sub>2</sub> O	0.24 mg/L	120 mg/L
Na <sub>2</sub> MoO <sub>4</sub> ·2H <sub>2</sub> O	0.12 mg/L	60 mg/L
ZnSO <sub>4</sub> ·7H <sub>2</sub> O	0.24 mg/L	120 mg/L
CoCl <sub>2</sub> ·6H <sub>2</sub> O	0.3 mg/L	150 mg/L

**Table A5.4.** Cations characterisation in the PN/A step of the studied WWTPs.

	SLU-S and SLU-A			OLB		TIL		HEN		APE		AME	
Cation soluble concentration	Influent	SHARON Effluent	ANAMM OX Effluent	Influent	Effluent	Influent	Effluent	Influent	Effluent	Influent	Effluent	Influent	Effluent
B ( $\mu\text{g/L}$ )	5,858 $\pm$ 51	147 $\pm$ 32	42 $\pm$ 2	216 $\pm$ 1	206 $\pm$ 4	577 $\pm$ 6	223 $\pm$ 5	772 $\pm$ 93	387 $\pm$ 1	6,237 $\pm$ 74	6,219 $\pm$ 95	434 $\pm$ 3	373.2 $\pm$ 0.8
Na ( $\mu\text{g/L}$ )	109,821 $\pm$ 4,309	89,861 $\pm$ 1331	89,089 $\pm$ 1,251	79,548 $\pm$ 1,391	77,936 $\pm$ 1,330	127,010 $\pm$ 601	127,883 $\pm$ 412	132,546 $\pm$ 3,081	222,246 $\pm$ 4,947	471,870 $\pm$ 7,000	478,507 $\pm$ 19,923	178,795 $\pm$ 1,619	170,318 $\pm$ 3,251

Mg (µg/L)	9,910 ± 2,383	19,567 ± 136	20,052 ± 884	159,6 83 ± 3,361	185,1 56 ± 2,449	2,11 3 ± 89	10,7 56 ± 450	1,94 9 ± 9	64,5 12 ± 580	25,357 ± 2,437	123,117 ± 2,749	28,3 74 ± 358	7,94 7 ± 2,36 4
Al (µg/L)	945 ± 1637	Not detected	Not detected	Not detect ed	Not detect ed	198 ± 9	121 ± 11	44 ± 9	125 ± 21	232 ± 7	Not detected	58 ± 4	44 ± 12
K (µg/L)	133,869 ± 6,482	125,561 ± 1,038	130,196 ± 1,281	1,026, 034 ± 8,779	1,049, 392 ± 12,02 7	342, 126 ± 1,54 3	179, 513 ± 1,91 1	285, 386 ± 9,08 0	281, 734 ± 2,04 7	405,597 ± 6,899	409,091 ± 6,463	283, 845 ± 2,13 1	286, 114 ± 3,07 0
Ca (µg/L)	59,168 ± 17,742	93,435 ± 611	94,326 ± 1,100	42,32 2 ± 2,456	38,09 3 ± 2,168	39,4 27 ± 1,29 5	48,4 23 ± 3,22 4	33,7 39 ± 669	73,0 13 ± 1,40 8	60,599 ± 467	54,615 ± 3,058	33,9 71 ± 1,50 8	22,9 82 ± 1,48 1



Mn (µg/L)	72 ± 92	115 ± 2	102.4 ± 0.6	82 ± 2	82.2 ± 1.0	5.0 ± 0.7	74.4 ± 0.8	17 ± 11	75 ± 1	16 ± 1	30.3 ± 0.8	7.8 ± 0.2	13 ± 2
Fe (µg/L)	3,690 ± 4,370	320 ± 26	223 ± 5	210 ± 31	87 ± 27	2,092 ± 80	4,374 ± 76	11,100 ± 1,113	18,942 ± 457	2,067 ± 11	1,795 ± 42	3,471 ± 57	1,682 ± 67
Co (µg/L)	10 ± 1	9.7 ± 0.3	8.1 ± 0.4	Not detected	0.8 ± 0.2	26.2 ± 0.3	14.5 ± 0.7	27.9 ± 0.8	32.5 ± 0.5	30.9 ± 0.3	49 ± 2	28.9 ± 0.8	39.6 ± 0.7
Ni (µg/L)	31 ± 7	13.9 ± 0.1	13.9 ± 0.3	2.7 ± 0.1	3.6 ± 0.5	108.5 ± 1.7	60 ± 2	132 ± 3	100 ± 5	65 ± 1	72.5 ± 0.9	98.5 ± 0.9	105.1 ± 0.4

Cu (µg/L)	131 ± 76	125 ± 2	109 ± 2	Not detect ed	Not detect ed	Not dete cted	3.9 ± 0.6	13.6 ± 0.3	4 ± 1	86 ± 1	88 ± 5	15 ± 1	97 ± 1
Zn (µg/L)	1,519 ± 214	162 ± 3	139.3 ± 0.7	1 ± 1	5 ± 5	55 ± 2	108 ± 19	45 ± 2	36.1 ± 0.1	513 ± 2	890 ± 247	19 ± 3	187 ± 1
Mo (µg/L)	17.7 ± 0.6	11.8 ± 0.4	11.66 ± 0.07	25.2 ± 0.2	37.5 ± 0.8	52.7 ± 0.8	13 ± 2	24 ± 2	303 ± 8	6.93 ± 0.04	10.40 ± 0.05	11.9 ± 0.2	16.4 ± 0.1
Cd (µg/L)	6.4 ± 0.3	0.08 ± 0.02	0.06 ± 0.02	0.03 ± 0.03	0.01 ± 0.01	Not dete cted	0.00 4 ± 0.00 3	Not dete cted	Not dete cted	6.24 ± 0.02	6.23 ± 0.05	0.01 ± 0.01	0.08 ± 0.03



# 6.

## Outlook and perspectives

In this thesis, the effects of thermal hydrolysis process (THP) pre-treatment on waste activated sludge (WAS) were examined including the consequences for downstream anaerobic digestion of WAS and the treatment of digestate reject water. In this research, WAS characteristics before and after THP pre-treatment were assessed, following the topical introduction in **Chapter 1**. The effects of the physicochemical WAS transformations are discussed in the course of the subsequent research chapters (Chapters 2-5). Predominantly, the physical transformations involve the release and solubilisation of organics (**Chapter 2** and **Chapter 3**), a change in particle size, and a reduction in viscosity during THP (Barber, 2016b; Bougrier et al., 2006; Dwyer et al., 2008b; Feng et al., 2015; Feng et al., 2014; Higgins et al., 2017; Laurent et al., 2011; Ngo et al., 2021; Ngo et al., 2023; Sapkaite et al., 2017). Additionally, the chemical reactions occurring during THP include the solubilisation of organically bound cations and nutrients (**Chapter 3**), as well as melanoidins formation (**Chapter 2**, **Chapter 3**, and **Chapter 5**) (Barber, 2016a; Cao et al., 2023; Jin et al., 2023; Laurent et al., 2011; Park and Kim, 2015). In this Chapter, the research findings from this thesis are summarised, and the main conclusions are drawn. Also, future research directions are proposed based on the obtained results.

### **6.1. Side reactions during THP of WAS**

Maillard and caramelisation reactions are the most relevant chemical side reactions during THP of WAS that may constrain the downstream processing of both sludge and reject waters. During the Maillard and caramelisation reactions the formation of (semi)recalcitrant organics occurs, which may interfere with chemical and biochemical conversions during anaerobic digestion (AD) and in the downstream processes. Caramelisation reactions occur at higher temperatures than the Maillard reaction and can be easily avoided by decreasing THP temperature (Dwyer et al., 2008b; Wilson and Novak, 2009). Notably, the Maillard reactions occur even at room temperature (Benzing-Purdie et al., 1985; van Boekel, 2001), thus, its occurrence during THP of WAS is practically unavoidable. However, as well as the caramelisation reaction, the Maillard reaction is temperature dependent and the formation of melanoidins can be reduced by decreasing the THP temperature. Also, the soluble concentration of the Maillard reaction products may be reduced decreasing the pH, or by the addition of polyvalent cations which may mitigate their negative effects in biochemical conversions (Liang et al., 2009; Migo et al., 1993).

### **6.2. AD (semi-)recalcitrant melanoidins formation and total ammoniacal nitrogen (TAN) release during THP**

**Chapter 2** focused on the effects of THP of WAS on AD, and the (enhanced) release and uptake of TAN, melanoidins and organics. Also, the possible inhibition of acetotrophic methanogenic consortia in the presence of THP was explored. Results in **Chapter 2** showed that THP enhanced the solubilisation of WAS, while the concentration of aromatic compounds (melanoidins) increased as forecasted in **Chapter 1**, creating partially AD-digestible organics. The biodegradable fraction of the melanoidins corresponded to low molecular weight compounds, associated to the protein-like fraction of humic substances. The biodegradability of low molecular weight aromatic compounds has been previously studied, and despite the possible inhibitory effects of these compounds on the AD process, they are biodegradable, which is particularly true for the sugar dehydration products (Monlau et al., 2014). The possible inhibitory effects of these low molecular weight aromatic compounds might be overcome by acclimatising the growing biomass, e.g., by applying long biomass retention times. A similar strategy was followed by others, acclimatising the anaerobic sludge to phenolic compounds in anaerobic membrane bioreactors (Barrios-Martinez et al., 2006; Garcia Rea et al., 2022). **Chapter 2** also showed that the produced melanoidins did not cause acute inhibition on acetotrophic methanogens. However, the THP enhanced TAN release and led to increased TAN concentrations, strongly inhibiting the acetotrophic methanogenic consortia. The possible change in methanogenic populations, due to the THP-increased concentrations of melanoidins or TAN, was not explored in this thesis. Previous research about the influence of elevated TAN concentration on methanogenic populations suggests that the hydrogenotrophic pathway might be enhanced at the expense of direct acetoclastic methanogenesis (Tian et al., 2018; Wang et al., 2015; Wang et al., 2022).

Considering that THP aims to increase the hydrolysed WAS fraction, as well as the hydrolysis rate during AD, it is important that the products of the side reactions during THP do not impact the hydrolysis rate. It is widely known from the literature that humic substances (such as melanoidins) may hinder hydrolysis during AD (Fernandes et al., 2015; Huang et al., 2021; Yap et al., 2018). The actual mechanisms how humic substances hinder hydrolysis is not fully clear. Fernandes et al. (2015) hypothesised that hydrolytic enzymes bind to specific moieties of humic substances. As above mentioned, THP produces humic substances in the form of melanoidins, and despite their increased concentrations, THP is reported to increase the hydrolysis rate, allowing shorter retention times during AD (Barber, 2016a). Considering the unavoidable production of melanoidins during THP, and the observed evident increase in WAS digestion when THP is applied as pre-treatment, the formed melanoidins apparently, do not exert a

distinct inhibitory effect. Further research is required to find the optimum operational parameters that increase the concentration of digestible products, without compromising the enzymatic hydrolytic capacity. Also, more research is needed to elucidate the role of monovalent and multivalent cations, which are solubilised during THP, on both the hydrolysis rate and extent of hydrolysis. Literature results suggest that the multivalent cations play an important role in mitigating the negative effects of humic substances on the hydrolysis rate (Azman et al., 2015).

### **6.3. Release and precipitation of nutrients during THP and AD**

The during THP solubilised inorganics play an important role in both, the complexation with organics, and precipitation reactions. Precipitation reactions are particularly relevant, when WAS originating from enhances biological phosphorous removal (EBPR) is digested rendering elevated concentrations of  $\text{PO}_4^{3-}\text{-P}$  during AD (Van Loosdrecht et al., 1997). **Chapter 3** discussed the role of temperature-induced dephosphorylation and deamination during THP of EBPR WAS, leading to solubilisation of  $\text{PO}_4^{3-}\text{-P}$  and TAN. This, non-AD-mediated nutrients release, increased with increasing THP temperature. Results showed that TAN and  $\text{PO}_4^{3-}\text{-P}$  concentrations during AD were not correlated. TAN increase was associated to the degradation of organics, while  $\text{PO}_4^{3-}\text{-P}$  concentrations were governed by precipitation with multivalent cations. Based on these results it could be inferred that increased THP temperatures (160-200°C) would render a higher degree of nutrients solubilisation, compared to THP at 140-160°C. The solubilised nutrients could be partially removed by precipitation reactions before AD. The latter approach might be an effective strategy to minimise the negative effects of solubilised inorganics during AD and downstream processes, such as, non-controlled precipitation, incrustation or TAN inhibition (**Chapter 2**). In this regard,  $\text{PO}_4^{3-}\text{-P}$  removal is particularly of importance, considering that during AD,  $\text{PO}_4^{3-}\text{-P}$  may precipitate with multivalent cations in solution (**Chapter 3**), potentially leading to uncontrolled precipitation and thus incrustation (Langerak et al., 1999; Soler-Cabezas et al., 2018). Uncontrolled precipitation resulting from THP may lead to increased maintenance during AD. Uncontrolled precipitation is also expected during the THP processes that use large contact areas, such as Lysotherm®, which would distinctly increase maintenance costs.

### **6.4. Effects of different humic substances released during THP on struvite precipitation**

Research in **Chapter 4** explored the effects of synthetic humic acids and melanoidins on struvite precipitation, being implemented as a technology for controlled removal of TAN and  $\text{PO}_4^{3-}\text{-P}$  from reject water. Results in **Chapter 4** showed that melanoidins moderately complexed  $\text{Mg}^{2+}$ , whereas humic acids formed strong complexes with  $\text{Mg}^{2+}$ . The ability of the tested humic substances to form these complexes was found to be related to the origin of the humic substances (HSs), particularly the fraction of particulate/colloidal HSs and their aromaticity. It is known that melanoidins and humic acids, despite having a different origin, are classified in the same manner and do have the same properties (Ćosović et al., 2010; Ikan et al., 1990). A possible explanation for the differences in complexation between humic acids and melanoidins could be attributed to a reduced number of hydroxyl and ketone/carboxyl groups, due to dehydration reactions, which produce part of the Maillard reaction intermediates (Klavins et al., 1999). The reduced number of hydroxyl and ketone/carboxyl functional groups in melanoidins may result in less active sites that can complex the multivalent cations in solution. More research is needed to better understand the chemical differences between naturally formed humic acids and melanoidins, as well as the complexation of these with different cations.

The differences in effects between melanoidins and humic acids were evident from the results since humic acids hindered struvite precipitation to a higher extent and yielded less precipitates compared to melanoidins. Also, humic acid was not fully soluble under the tested pH conditions, which also might have hindered struvite crystal growth, especially at low pH values, when humic acid is less soluble. The pH played a crucial role during struvite precipitation, inhibiting struvite crystallization at pH 6.5, compared to pH 7.25 and 8. In relation to full-scale process operation, struvite precipitation should be performed at about neutral pH, having the least chemical (alkaline) addition. The complexation of  $\text{Mg}^{2+}$  and the hindrance of struvite formation in presence of humic acids and melanoidins, may force operators to increase the  $\text{Mg}^{2+}/\text{PO}_4^{3-}\text{-P}$  ratio, as well as the medium pH, which could result in increased process costs.

Furthermore, the presence of melanoidins showed a noticeable impact on the struvite crystals morphology. Melanoidins reduced both the maximum and minimum Feret diameters and the aspect ratio of the formed struvite crystals. This decrease in crystal size may force technology providers to redesign the precipitation and/or settling unit if THP-AD is used. Additionally, melanoidins enhanced the stability of struvite crystals, making them more resistant to breakage at higher shear rates, especially when exceeding 10 1/s. In contrast, humic acid did not



substantially affect the stability or abrasion of struvite crystals and even led to a decrease in Feret diameters and aspect ratio.

Furthermore, the microscopic analysis described in **Chapter 4** showed that the presence of HSs coloured the produced struvite. This change in colour may have unknown consequences if the product is used as a fertiliser. In The Netherlands, struvite is not used as a fertiliser and there is hardly a market for it, due to the wide availability of alternative and/or chemical low cost fertilisers (Timmerman and Hoving, 2016). However, outside The Netherlands, struvite precipitation and recovery, could be a viable alternative to cope with P-based fertiliser's scarcity (González et al., 2021; Münch and Barr, 2001; Muys et al., 2021; Vries et al., 2016). The multivalent cations chelating properties of THP-produced melanoidins may also increase the concentration of heavy metals in struvite, and thus in the soil, if the struvite from a THP-AD installations is used. More research is needed to understand the possible chelation of heavy metals. However, it is expected that solubilised heavy metals, which are multivalent cations, might be incorporated in struvite when THP is used as pretreatment.

### **6.5. Effects of the increased TAN concentrations and melanoidins on the PN/A process**

In **Chapter 5** experiments are discussed researching the influence of THP on the partial nitrification and anammox (PN/A) process on digestate reject water. The reject water samples were obtained from full-scale operating installations. In line with the results found in **Chapters 2** and **Chapter 3**, the application of THP as pre-treatment increased the concentrations of TAN and melanoidins in the full-scale reject water stream. Increased melanoidins concentrations were concomitantly observed with increased TAN, chemical oxygen demand (COD), total organic carbon (TOC), true colour (T. colour) and ultraviolet absorbance at 254 nm (UVA 254) in influents of the PN/A reactors. Values of these parameters were distinctly lower in the PN/A effluents. All these parameters indicated the presence of melanoidins, and can be used in full-scale installations to quantify melanoidins occurrence. This is particularly true for the spectrophotometric methods, which are easy to use and implement at full-scale sites. The soluble melanoidins in the PN/A influents were partially oxidised during the PN/A step. The partial heterotrophic oxidation of the THP-produced melanoidins increased the O<sub>2</sub> requirements during the PN/A step. Additional O<sub>2</sub> was also required for the increased partial nitrification capacity, to oxidise the elevated TAN concentrations. The additional O<sub>2</sub> that is needed to oxidise melanoidins must be considered when designing a PN/A process, otherwise, it may cause conversion rate limitations in ammonium oxidation. The operational costs of additional

O<sub>2</sub> to oxidise the elevated TAN and organics (biodegradable melanoidins) during the PN/A step must be taken into account when using THP, since it comprises an important part of the operational costs (Volcke et al., 2005), which is proportional to the oxygen uptake rate (Humbird et al., 2017).

Furthermore, in the wastewater treatment plants (WWTPs) using THP, NO<sub>3</sub><sup>-</sup>-N concentrations in PN/A effluents were lower than the stoichiometric values, attributable to the occurrence of denitrification, which increased the N-removal efficiency. However, increased denitrification during PN/A could concomitantly increase atmospheric N<sub>2</sub>O emissions, contributing to greenhouse gas emissions (Domingo-Félez et al., 2014; Kampschreur et al., 2009). N<sub>2</sub>O emissions during nitrification/ denitrification and PN/A processes are currently being studied (e.g. Mampaey et al. (2019)). The possible role of THP-produced organics in N<sub>2</sub>O production is yet not known and needs to be researched. If THP pre-treatment indeed increases N<sub>2</sub>O emissions, it is important to adequately amend operational strategies to minimise them, reducing environmentally negative effects.

Moreover, the presence of melanoidins in the effluents of PN/A reactors increased the fraction of chelated Fe<sup>2+/3+</sup> and other transition metals. Transition metals work as trace elements for both the anabolism and catabolism of PN/A biomass (Ferousi et al., 2017; Gilch et al., 2009; Kartal et al., 2012; Koper et al., 2004; Nicholas et al., 1964), and their scarcity could have detrimental effects on the process. If trace elements limitation of PN/A biomass would indeed occur, further research is needed to assess which metals are limiting, and whether it affects anabolism and/or catabolism of the (de)nitrifying biomass and/or anammox.

## **6.6. Effect on the WWTPs final effluent quality**

In addition to the effects of the THP-side reactions mentioned above, the production of melanoidins can impact the final effluent that is discharged to the receiving water body. Firstly, there is an aesthetic effect because the coloured character of the melanoidins. Also, to the best knowledge of the authors, thus far, there are no long-term toxicity experiments being conducted on the impact of THP-produced melanoidins on the receiving water bodies, and the possible accumulation of these. Additionally, elevated melanoidins concentrations may increase the concentration of (semi) recalcitrant N and P which is simultaneously discharged to the receiving water body (Dwyer et al., 2008a; He et al., 2011; Li and Brett, 2013; Zhang et al., 2020). Discharge of nutrients-containing melanoidins may hamper reaching the more stringent nutrients discharge criteria. More research is needed to elucidate the fate of the

anthropogenically generated humic substances during THP in the environment, and the discharge of nutrients and ions that these contain.

### 6.7. Overall conclusions

- The chapters in this thesis showed that THP processes enhanced solubilization of digestible organics from WAS, leading to an overall increase in the anaerobic digestibility. In addition, elevated TAN concentration were observed, as well as the formation of melanoidins. The presence of melanoidins during AD did not exert any toxicity to, or inhibition of, the methanogenic biomass. Conversely, elevated TAN concentrations led to acetotrophic methanogenesis inhibition.
- AD-THP of WAS coming from EBPR systems resulted in the release of  $\text{PO}_4^{3-}\text{-P}$  and TAN, influencing nutrient concentrations during anaerobic digestion. Elevated THP temperatures increased final nutrient concentrations, in the digestate which slightly increased the saturation indexes (SIs) of minerals that can precipitate during AD. The use of THP elevated SIs mainly due to elevated nutrients concentration.
- HA over melanoidins exhibited higher degrees of complexation with  $\text{Mg}^{2+}$ , negatively affecting the struvite precipitation and crystallisation process. While HA strongly hindered the formation of struvite crystals, both melanoidins and HA altered the crystal characteristics including its colour, but enhanced the crystal stability against breakage.
- AD-THP increased COD, TOC, T. colour, and UVA 254 in PN/A influents, which indicate the presence of AD-recalcitrant melanoidins. Increased concentrations of melanoidins and TAN increased  $\text{O}_2$  requirements in full-scale PN/A reactors. The mineralisation of biodegradable organics in the PN/A influents due to denitrification may increase the release of greenhouse gasses. Furthermore, melanoidins in PN/A influents increased chelation of transition metals, potentially causing trace metal limitations on the PN/A biomass.

### 6.8. Recommendations

- Insights from this current research may lead to cost-effective optimization of THP-AD processes beyond biogas production at full-scale. Traditionally, THP operational parameters have focused on maximizing  $\text{CH}_4$  production for energy recovery. However, as results indicate, a more integrated approach is needed, also incorporating operation and maintenance costs associated with sludge handling and reject water treatment in the WWTP. Such approach must also consider i) elevated TAN concentrations in AD and

reject water, ii) oxidation of organics formed during THP in the PN/A step, and iii) potential trace element supplementation due to chelation of transition metals with melanoidins.

- In full-scale applications, increased maintenance due to AD uncontrolled precipitation needs to be considered, while assessing the feasibility of THP projects, along with resulting changes in excess sludge dewaterability and polymer consumption during dewatering processes. Furthermore, while considering  $\text{PO}_4^{3-}$ -P recovery via struvite precipitation, THP implementation results in elevated  $\text{Mg}^{2+}$  requirements. Moreover, changes in crystal morphology and colour must be considered.
- On a scientific level, assessing changes in AD microbial populations, due to increased concentrations of melanoidins and TAN, would be an interesting follow-up research line. Particularly relevant is the impact on methanogens, where acetotrophic and hydrogenotrophic populations may respond differently to toxicants. Research should also explore the trade-off between THP-induced hydrolysis and melanoidins formation. The latter may hinder microbial hydrolysis during THP-AD. Additionally, the role of THP-solubilized and released cations in subsequent treatment processes requires consideration.
- It is recommended to conduct scientific research on struvite precipitation, exploring the mechanisms influencing crystal formation and crystal growth, in the presence of different HSs. Strategies that facilitate crystal growth and stabilize crystal structures should be developed to enhance operational efficiency. Furthermore, if struvite recovery is indeed feasible, the fate of heavy metals and emerging contaminants in the formed crystals should be investigated in all details.
- With regard to PN/A systems, which are impacted by THP-AD, future research should focus on developing strategies to optimize aeration for partially oxidising TAN and the biodegradable organic compounds, while preventing greenhouse gas emissions ( $\text{N}_2\text{O}$ ) related to denitrification. Furthermore, fundamental research should consider the impact of (possible) trace elements limitation, due to the chelation of melanoidins and transition metals. Regarding the latter research, the primary focus should be to elucidate which element(s) cause(s) possible limitation, while identifying the affected metabolic processes.

## **6.9. List of abbreviations**

AD: anaerobic digestion.

COD: chemical oxygen demand.

EBPR: enhanced biological phosphorous removal.

HSs: humic substances.

PN/A: partial nitrification and anammox.

SI: saturation index.

T. colour: true colour.

TAN: total ammoniacal nitrogen.

THP: thermal hydrolysis process.

TOC: total organic carbon.

UVA 254: ultraviolet absorbance at 254 nm.

WAS: waste activated sludge.

WWTPs: wastewater treatment plants.

## 6.10. References

- Azman, S., Khadem, A.F., Zeeman, G., Van Lier, J.B. and Plugge, C.M. 2015. Mitigation of Humic Acid Inhibition in Anaerobic Digestion of Cellulose by Addition of Various Salts. *Bioengineering* 2(2), 54-65.
- Barber, W. 2016a. Thermal hydrolysis for sewage treatment: A critical review. *Water research* 104, 53-71.
- Barber, W.P.F. 2016b. Thermal hydrolysis for sewage treatment: A critical review. *Water Research* 104, 53-71.
- Barrios-Martinez, A., Barbot, E., Marrot, B., Moulin, P. and Roche, N. 2006. Degradation of synthetic phenol-containing wastewaters by MBR. *Journal of Membrane Science* 281(1), 288-296.
- Benzing-Purdie, L.M., Ripmeester, J.A. and Ratcliffe, C.I. 1985. Effects of temperature on Maillard reaction products. *Journal of Agricultural and Food Chemistry* 33(1), 31-33.
- Bougrier, C., Albasi, C., Delgenès, J.P. and Carrère, H. 2006. Effect of ultrasonic, thermal and ozone pre-treatments on waste activated sludge solubilisation and anaerobic biodegradability. *Chemical Engineering and Processing: Process Intensification* 45(8), 711-718.
- Cao, X., He, R. and Jia, M. 2023. Characterization of melanoidins in thermal hydrolysis sludge and effects on dewatering performance. *Environmental Research* 239, 117226.
- Ćosović, B., Vojvodić, V., Bošković, N., Plavšić, M. and Lee, C. 2010. Characterization of natural and synthetic humic substances (melanoidins) by chemical composition and adsorption measurements. *Organic Geochemistry* 41(2), 200-205.
- Domingo-Félez, C., Mutlu, A.G., Jensen, M.M. and Smets, B.F. 2014. Aeration Strategies To Mitigate Nitrous Oxide Emissions from Single-Stage Nitrification/Anammox Reactors. *Environmental Science & Technology* 48(15), 8679-8687.
- Dwyer, J., Kavanagh, L. and Lant, P. 2008a. The degradation of dissolved organic nitrogen associated with melanoidin using a UV/H<sub>2</sub>O<sub>2</sub> AOP. *Chemosphere* 71(9), 1745-1753.
- Dwyer, J., Starrenburg, D., Tait, S., Barr, K., Batstone, D.J. and Lant, P. 2008b. Decreasing activated sludge thermal hydrolysis temperature reduces product colour, without decreasing degradability. *Water Research* 42(18), 4699-4709.
- Feng, G., Guo, Y. and Tan, W. 2015. Effects of thermal hydrolysis temperature on physical characteristics of municipal sludge. *Water Science and Technology* 72(11), 2018-2026.
- Feng, G., Liu, L. and Tan, W. 2014. Effect of Thermal Hydrolysis on Rheological Behavior of Municipal Sludge. *Industrial & Engineering Chemistry Research* 53(27), 11185-11192.
- Fernandes, T.V., van Lier, J.B. and Zeeman, G. 2015. Humic Acid-Like and Fulvic Acid-Like Inhibition on the Hydrolysis of Cellulose and Tributyrin. *BioEnergy Research* 8(2), 821-831.
- Ferousi, C., Lindhoud, S., Baymann, F., Kartal, B., Jetten, M.S.M. and Reimann, J. 2017. Iron assimilation and utilization in anaerobic ammonium oxidizing bacteria. *Current Opinion in Chemical Biology* 37, 129-136.
- García Rea, V.S., Egerland Bueno, B., Cerqueda-García, D., Muñoz Sierra, J.D., Spanjers, H. and van Lier, J.B. 2022. Degradation of p-cresol, resorcinol, and phenol in anaerobic membrane bioreactors under saline conditions. *Chemical Engineering Journal* 430, 132672.
- Gilch, S., Meyer, O. and Schmidt, I. 2009. A soluble form of ammonia monooxygenase in *Nitrosomonas europaea*. 390(9), 863-873.
- González, C., Fernández, B., Molina, F., Camargo-Valero, M.A. and Peláez, C. 2021. The determination of fertiliser quality of the formed struvite from a WWTP. *Water Science and Technology* 83(12), 3041-3053.

- He, Z., Olk, D.C. and Cade-Menun, B.J. 2011. Forms and Lability of Phosphorus in Humic Acid Fractions of Hord Silt Loam Soil. *Soil Science Society of America Journal* 75(5), 1712-1722.
- Higgins, M.J., Beightol, S., Mandahar, U., Suzuki, R., Xiao, S., Lu, H.-W., Le, T., Mah, J., Pathak, B., DeClippeleir, H., Novak, J.T., Al-Omari, A. and Murthy, S.N. 2017. Pretreatment of a primary and secondary sludge blend at different thermal hydrolysis temperatures: Impacts on anaerobic digestion, dewatering and filtrate characteristics. *Water Research* 122, 557-569.
- Huang, F., Liu, H., Wen, J., Zhao, C., Dong, L. and Liu, H. 2021. Underestimated humic acids release and influence on anaerobic digestion during sludge thermal hydrolysis. *Water Research* 201, 117310.
- Humbird, D., Davis, R. and McMillan, J.D. 2017. Aeration costs in stirred-tank and bubble column bioreactors. *Biochemical Engineering Journal* 127, 161-166.
- Ikan, R., Dorsey, T. and Kaplan, I.R. 1990. Characterization of natural and synthetic humic substances (melanoidins) by stable carbon and nitrogen isotope measurements and elemental compositions. *Analytica chimica acta* 232, 11-18.
- Jin, M., Liu, H., Deng, H., Xiao, H., Liu, S. and Yao, H. 2023. Dissociation and removal of alkali and alkaline earth metals from sewage sludge flocs during separate and assisted thermal hydrolysis. *Water Research* 229, 119409.
- Kampschreur, M.J., Poldermans, R., Kleerebezem, R., van der Star, W.R.L., Haarhuis, R., Abma, W.R., Jetten, M.S.M. and van Loosdrecht, M.C.M. 2009. Emission of nitrous oxide and nitric oxide from a full-scale single-stage nitrification-anammox reactor. *Water Science and Technology* 60(12), 3211-3217.
- Kartal, B., van Niftrik, L., Keltjens, J.T., Op den Camp, H.J.M. and Jetten, M.S.M. (2012) *Advances in Microbial Physiology*. Poole, R.K. (ed), pp. 211-262, Academic Press.
- Klavins, M., Eglite, L. and Serzane, J. 1999. Methods for Analysis of Aquatic Humic Substances. *Critical Reviews in Analytical Chemistry* 29(3), 187-193.
- Koper, T.E., El-Sheikh, A.F., Norton, J.M. and Klotz, M.G. 2004. Urease-Encoding Genes in Ammonia-Oxidizing Bacteria. *Applied and Environmental Microbiology* 70(4), 2342-2348.
- Langerak, E.P.A.v., Beekmans, M.M.H., Beun, J.J., Hamelers, H.V.M. and Lettinga, G. 1999. Influence of phosphate and iron on the extent of calcium carbonate precipitation during anaerobic digestion. *Journal of Chemical Technology & Biotechnology* 74(11), 1030-1036.
- Laurent, J., Casellas, M., Carrère, H. and Dagot, C. 2011. Effects of thermal hydrolysis on activated sludge solubilization, surface properties and heavy metals biosorption. *Chemical Engineering Journal* 166(3), 841-849.
- Li, B. and Brett, M.T. 2013. The influence of dissolved phosphorus molecular form on recalcitrance and bioavailability. *Environmental Pollution* 182, 37-44.
- Liang, Z., Wang, Y., Zhou, Y. and Liu, H. 2009. Coagulation removal of melanoidins from biologically treated molasses wastewater using ferric chloride. *Chemical Engineering Journal* 152(1), 88-94.
- Mampaey, K.E., Spérandio, M., van Loosdrecht, M.C.M. and Volcke, E.I.P. 2019. Dynamic simulation of N<sub>2</sub>O emissions from a full-scale partial nitrification reactor. *Biochemical Engineering Journal* 152, 107356.
- Migo, V.P., Matsumura, M., Del Rosario, E.J. and Kataoka, H. 1993. The effect of pH and calcium ions on the destabilization of melanoidin. *Journal of Fermentation and Bioengineering* 76(1), 29-32.
- Monlau, F., Sambusiti, C., Barakat, A., Quéméneur, M., Trably, E., Steyer, J.P. and Carrère, H. 2014. Do furanic and phenolic compounds of lignocellulosic and algae biomass

- hydrolyzate inhibit anaerobic mixed cultures? A comprehensive review. *Biotechnology Advances* 32(5), 934-951.
- Münch, E.V. and Barr, K. 2001. Controlled struvite crystallisation for removing phosphorus from anaerobic digester sidestreams. *Water Research* 35(1), 151-159.
- Muys, M., Phukan, R., Brader, G., Samad, A., Moretti, M., Haiden, B., Pluchon, S., Roest, K., Vlaeminck, S.E. and Spiller, M. 2021. A systematic comparison of commercially produced struvite: Quantities, qualities and soil-maize phosphorus availability. *Science of The Total Environment* 756, 143726.
- Ngo, P.L., Udugama, I.A., Gernaey, K.V., Young, B.R. and Baroutian, S. 2021. Mechanisms, status, and challenges of thermal hydrolysis and advanced thermal hydrolysis processes in sewage sludge treatment. *Chemosphere* 281, 130890.
- Ngo, P.L., Young, B.R., Brian, K. and Baroutian, S. 2023. New insight into thermal hydrolysis of sewage sludge from solubilisation analysis. *Chemosphere* 338, 139456.
- Nicholas, D.J.D., Fisher, D.J., Redmond, W.J. and Osborne, M. 1964. A cobalt requirement for nitrogen fixation, hydrogenase, nitrite and hydroxylamine reductases in *clostridium pasteurianum*. *Nature* 201(4921), 793-795.
- Park, S. and Kim, M. 2015. Innovative ammonia stripping with an electrolyzed water system as pretreatment of thermally hydrolyzed wasted sludge for anaerobic digestion. *Water Research* 68, 580-588.
- Sapkaite, I., Barrado, E., Fdz-Polanco, F. and Pérez-Elvira, S.I. 2017. Optimization of a thermal hydrolysis process for sludge pre-treatment. *Journal of Environmental Management* 192, 25-30.
- Soler-Cabezas, J.L., Mendoza-Roca, J.A., Vincent-Vela, M.C., Luján-Facundo, M.J. and Pastor-Alcañiz, L. 2018. Simultaneous concentration of nutrients from anaerobically digested sludge centrate and pre-treatment of industrial effluents by forward osmosis. *Separation and Purification Technology* 193, 289-296.
- Tian, H., Fotidis, I.A., Kissas, K. and Angelidaki, I. 2018. Effect of different ammonia sources on acetoclastic and hydrogenotrophic methanogens. *Bioresource Technology* 250, 390-397.
- Timmerman, M. and Hoving, I.E. 2016 Purifying manure effluents with duckweed, Wageningen UR Livestock Research.
- van Boekel, M.A.J.S. 2001. Kinetic aspects of the Maillard reaction: a critical review. *Food / Nahrung* 45(3), 150-159.
- Van Loosdrecht, M., Hooijmans, C., Brdjanovic, D. and Heijnen, J. 1997. Biological phosphate removal processes. *Applied microbiology and biotechnology* 48, 289-296.
- Volcke, E.I.P., Van Hulle, S.W.H., Donckels, B.M.R., van Loosdrecht, M.C.M. and Vanrolleghem, P.A. 2005. Coupling the SHARON process with Anammox: Model-based scenario analysis with focus on operating costs. *Water Science and Technology* 52(4), 107-115.
- Vries, S.d., Postma, R., Scholl, L.v., Blom-Zandstra, G., Verhagen, J. and Harms, I. 2016 Economic feasibility and climate benefits of using struvite from the Netherlands as a phosphate (P) fertilizer in West Africa, Wageningen Plant Research, Wageningen.
- Wang, H., Fotidis, I.A. and Angelidaki, I. 2015. Ammonia effect on hydrogenotrophic methanogens and syntrophic acetate-oxidizing bacteria. *FEMS Microbiology Ecology* 91(11), fiv130.
- Wang, Z., Wang, S., Hu, Y., Du, B., Meng, J., Wu, G., Liu, H. and Zhan, X. 2022. Distinguishing responses of acetoclastic and hydrogenotrophic methanogens to ammonia stress in mesophilic mixed cultures. *Water Research* 224, 119029.



- Wilson, C.A. and Novak, J.T. 2009. Hydrolysis of macromolecular components of primary and secondary wastewater sludge by thermal hydrolytic pretreatment. *Water Research* 43(18), 4489-4498.
- Yap, S.D., Astals, S., Lu, Y., Peces, M., Jensen, P.D., Batstone, D.J. and Tait, S. 2018. Humic acid inhibition of hydrolysis and methanogenesis with different anaerobic inocula. *Waste Management* 80, 130-136.
- Zhang, D., Feng, Y., Huang, H., Khunjar, W. and Wang, Z.-W. 2020. Recalcitrant dissolved organic nitrogen formation in thermal hydrolysis pretreatment of municipal sludge. *Environment International* 138, 105629.

## Acknowledgements

The people I would like to express my gratitude are the following:

1. To my supervisors, Merle and Jules, for their guidance, support, criticism and patience throughout this journey. Also, for all the work and non-work related discussions, they always enlighten me in one or another way.
2. To the members of my thesis committee, for accepting the invitation to be part of it, and for reading this manuscript. I would also like to express my gratitude to David Jeison, who I met during my bachelor and has helped me to guide my career ever since.
3. To ANID PFCHA/DOCEXT 72170548, TU Delft, STOWA, Paques BV, Water Authorities from The Netherlands (Waterschap de Dommel, Waterschap Vechtstromen, Waterschap Vallei en Veluwe and Waterschap Limburg). For the financial support to conduct the research.
4. To my colleagues/office-mates for their stimulating discussions and all the fun we had together, particularly while having lunch or coffees.
5. To all the lab technicians and support staff that made my life easier in the lab and helped me with all the formalities.
6. To the bachelor and master students that contributed making this work possible. I learned a lot from guiding your graduation processes.
7. To all the friends that this journey has brought me, they have been the support I have needed every time I have felt homesick, stressed or overwhelmed.
8. To my family in Chile, for their encouragement and understanding despite the distance.
9. To Nicole, the first person who believed that this could be possible and without hesitation hopped on in this endeavour. Without her support and love this thesis would not have been possible.

The following list shows the names of the people to which the acknowledgements refer, in alphabetical order:

**Point 1**

Jules  
Merle

**Point 2**

Prof.dr. A. Soares  
Prof.dr. D. Brdjanovic  
Prof.dr. D.A Jeison Nuñez  
Prof.dr. H. Carrere  
Prof.dr.ir. J. B. van Lier  
Prof.dr.ir. M. K. de Kreuk  
Prof.dr.ir. R. Dewil  
Prof.dr.ir. W. de Jong  
Rector Magnificus

**Point 3**

-

**Point 4**

Adrian  
Alexander  
Alexander  
André  
Andrea  
Anto  
Beatriz  
Bilal  
Bruno  
Carina  
Daniel  
Dhavissen  
Emiel  
Fauzul  
Gladis  
Guilherme  
Hongxiao

Iosif  
Jane  
Joana  
Joao  
Job  
Julian  
Lais  
Lenno  
Leon  
Luis  
Magela  
Maikon  
María  
Mona  
Niels  
Pamela  
Parastoo

Ralph  
Rifki  
Roberto  
Sabrina  
Sanne  
Sara  
Shreya  
Simon  
Simon  
Sofia  
Steef  
Tales  
Thomas  
Vale  
Victor  
Yana

**Point 5**

Armand  
Bokuretsion  
Bright  
David  
Helen  
Jan  
Jane

Jasper  
Louise  
Mariska  
Mohammed  
Patricia  
Riëlle  
Tamara

### **Point 6**

Divvay  
Jingdang  
Júlia  
Leslie  
Luke  
Quentin  
Raquel  
Sasha  
Sihan  
Widya  
Zhouyuan

### **Point 7**

Ale & Luzma  
Bruno & Fio  
Caro & Pedro  
Chio & Nacho  
Christos  
Cony & Chiri  
Coty & Samba  
David & Sole  
David Salas  
Diego & Maca  
Dori & Nico

Felipe B.  
Felipe L.  
Fran & Cona  
Francisco & Javi  
Gabriel & Alex  
Heather  
Ine & Marcelo  
Jaime & Caro  
Lore & Lucas  
Luchín & Pauli  
Mage & Sanne

Mona  
Nicol D.  
Pamela & Daniel  
Pato  
Paul & Jesu  
Seba  
Vane  
Victor

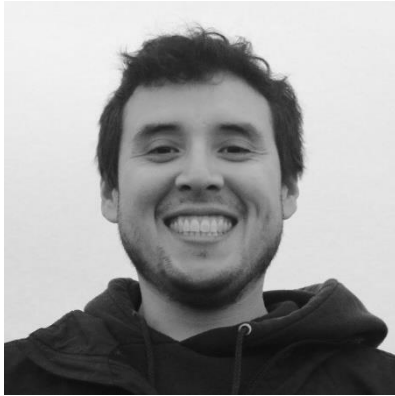
### **Point 8**

Elvira Solar Solar  
Mauricio Pavez Jara  
Patricia Jara Solar  
Waldo Pavez Del Sol  
Yannella Pavez Jara

### **Point 9**

Nicole Pereira Ríos

## About the applicant



Javier holds a bachelor's degree in engineering sciences and the title of Environmental Civil Engineer from Universidad de la Frontera, Chile, and a Master's degree in Engineering Sciences, with a specialization in Biotechnology from the same university. After he completed his Master's degree, he worked part-time as a researcher and as a project manager in the "Dirección de Innovación y Transferencia Tecnológica-UFRO". After two years working, he was awarded with a doctoral scholarship and started a PhD program at TU Delft, The Netherlands.

**List of publications**

Pavez, J., et al., Ultrafiltration of non-axenic microalgae cultures: Energetic requirements and filtration performance. *Algal Research*, 2015. **10**: p. 121-127.

Araneda, M., et al., Use of activated sludge biomass as an agent for advanced primary separation. *Journal of Environmental Management*, 2017. **192**: p. 156-162.

Ortega-Bravo, J.C., et al. Biogas Production from Concentrated Municipal Sewage by Forward Osmosis, Micro and Ultrafiltration. *Sustainability*, 2022. **14**, DOI: 10.3390/su14052629.

Pavez-Jara, J.A., J.B. van Lier, and M.K. de Kreuk, Accumulating ammoniacal nitrogen instead of melanoidins determines the anaerobic digestibility of thermally hydrolyzed waste activated sludge. *Chemosphere*, 2023. **332**: p. 138896.

Pavez-Jara, J.A., J.B. van Lier, and M.K. de Kreuk, Effects of thermal hydrolysis process-generated melanoidins on partial nitrification/anammox in full-scale installations treating waste activated sludge. *Journal of Cleaner Production*, 2023. **432**: p. 139767.

Pavez-Jara, J., et al., Role of the composition of humic substances formed during thermal hydrolysis process on struvite precipitation in reject water from anaerobic digestion. *Journal of Water Process Engineering*, 2024. **59**: p. 104932.